UNCLASSIFIED

AD NUMBER
AD504212
CLASSIFICATION CHANGES
TO: **UNCLASSIFIED**
FROM: **CONFIDENTIAL**
LIMITATION CHANGES
TO: **Approved for public release; distribution is unlimited.**
FROM: **Distribution authorized to U.S. Gov't. agencies and their contractors; Administrative/Operational Use; SEP 1969. Other requests shall be referred to Air Force Rocket Propulsion Lab., Edwards AFB, CA.**
AUTHORITY
AFRPL ltr 5 Feb 1986 ; AFRPL ltr 5 Feb 1986

THIS PAGE IS UNCLASSIFIED

THIS REPORT HAS BEEN DELIMITED
AND CLEARED FOR PUBLIC RELEASE
UNDER DOD DIRECTIVE 5200.20 AND
NO RESTRICTIONS ARE IMPOSED UPON
ITS USE AND DISCLOSURE.

DISTRIBUTION STATEMENT A

APPROVED FOR PUBLIC RELEASE;
DISTRIBUTION UNLIMITED.

AD 504 212

AUTHORITY: AFRPL ltr, 5 Feb 86

SECURITY MARKING

The classified or limited status of this report applies to each page, unless otherwise marked.
Separate page printouts MUST be marked accordingly.

CONFIDENTIAL

AFRPL-TR-69-189 [redacted]

AD 504212

(UNCLASSIFIED TITLE)

ADVANCED MANEUVERING PROPULSION TECHNOLOGY PROGRAM (SEVENTH QUARTERLY PROGRESS REPORT)

Rocketdyne
A Division of North American Rockwell Corporation
6633 Canoga Avenue
Canoga Park, California

Technical Report AFRPL-TR-69-189

September 1969

Group 4
Downgraded at 3-Year Intervals
Declassified After 12 Years

Air Force Rocket Propulsion Laboratory
Air Force Systems Command
United States Air Force
Edwards Air Force Base, California

CONFIDENTIAL

AFRPL-TR-69-189

(UNCLASSIFIED TITLE)

ADVANCED MANEUVERING PROPULSION TECHNOLOGY PROGRAM (SEVENTH QUARTERLY PROGRESS REPORT)

ROCKETDYNE
A Division of North American Rockwell Corporation
6633 Canoga Avenue
Canoga Park, California

Technical Report AFRPL-TR-69-189

September 1969

Group 4
Downgraded at 3-Year Intervals
Declassified After 12 Years

THIS MATERIAL CONTAINS INFORMATION AFFECTING THE NATIONAL DEFENSE OF THE UNITED STATES WITHIN THE MEANING OF THE ESPIONAGE LAWS, TITLE 18 U.S.C., SECTIONS 793 AND 794, THE TRANSMISSION OR REVELATION OF WHICH IN ANY MANNER TO AN UNAUTHORIZED PERSON IS PROHIBITED BY LAW.

In addition to security requirements which must be met, this document is subject to special export controls and each transmittal to foreign governments or foreign nationals may be made only with prior approval of AFRPL (RPPR/STINFO), Edwards, California, 93523.

Air Force Rocket Propulsion Laboratory
Air Force Systems Command
United States Air Force
Edwards Air Force Base, California

(U) FOREWORD

(U) This seventh quarterly report describes the progress made in the Advanced Maneuvering Propulsion Technology (AMPT) Program during the period of 1 May 1969 to 31 July 1969 and is submitted in accordance with the requirements of Contract F04611-67-C-0116, Part I, Item 1AB, Sequence No. B008 of Exhibit B.

(U) This publication was prepared by Rocketdyne, a division of North American Rockwell Corporation, as report R-7380-7, under the direction of R. R. Morin, Program Manager.

(U) Publication of this report does not constitute Air Force approval of the report's findings or conclusions. It is published only for the exchange and stimulation of ideas.

Robert L. Wiswell
AFRPL Program Manager
RPRES

(U) ABSTRACT

(U) The engine design and analysis task was continued with a detailed parametric analysis of thrust chamber temperature and pressure drop characteristics, the revision of the engine balance, and continued main oxidizer and turbine control valve design activity.

(U) The engine critical component task effort was primarily directed toward the completion of fabrication of the prototype channel-wall thrust chamber segment. Design of the main thrust chamber nozzle has been completed and design of the base closure and secondary engine nozzle simulator is nearing completion.

(U) Though testing of the main engine bearings and seals was initiated during the previous quarter, the effort was stopped temporarily because of operational problems and has been rescheduled to start September 1969.

(U) The basic analysis and design of the propellant feed system was completed during the previous quarter by both General Dynamics/Convair and Lockheed Missiles and Space Company.

CONTENTS

CONFIDENTIAL

ILLUSTRATIONS

TABLES

(U) INTRODUCTION

(C) The Advanced Maneuvering Propulsion System (AMPS) is a high-energy system utilizing LF_2/LH_2 propellants. A typical system is illustrated in Fig. 1 with some of the basic design parameters for the Advanced Development Program (ADP) together with some of the design variations which are being considered separately.

(C) The engine configuration (Fig. 2) utilizes concentric thrust chambers. The outer main thrust chamber (30,000 pounds of thrust) incorporates the toroïdal-aerodynamic spike design concept. The inner secondary thrust chamber (3300 pounds of thrust) is a bell-type design. The thrust chambers are fed from independent turbopumps which are driven by hot gases from each thrust chamber. Each thrust chamber can be throttled over a 9:1 thrust range, which gives the engine system an overall throttle ratio of 81:1. The normal mode of operation is for the thrust chambers to fire one at a time.

(C) The propellant feed system consists of the main propellant tankage; thermal conditioning and support structure; zero gravity expulsion system, fill, vent, feed, and drain lines; propellant management system; and a pressurization system. The 18,000-pound weight for the complete propulsion system, together with a 2000-pound payload (20,000 pounds total) is compatible with the present Titan IIID launch vehicle for polar orbit launches from the Western Test Range. A gimbal angle of ±10 degrees was selected to provide the capability for rapid turning maneuvers. System thermal design provides the capability of at least 14 days in orbit with no fluorine loss and with very little hydrogen loss, depending on the mission duty cycle.

(C) The Advanced Maneuvering Propulsion Technology (AMPT) Advanced Development Program consists of two phases. Phase I, the current program effort for a 31-month period, includes the following three tasks.

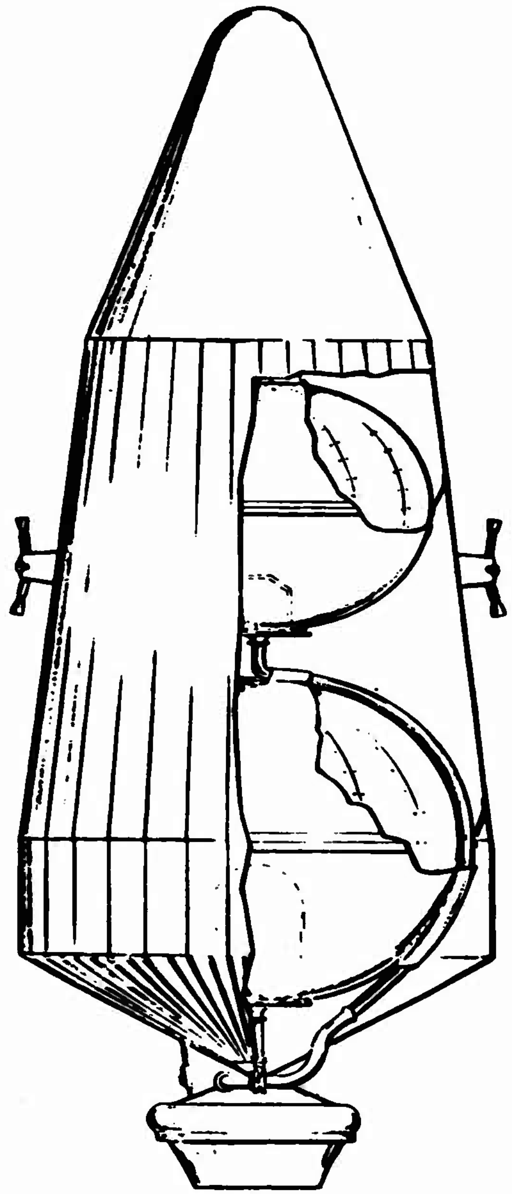

	DESIGN POINT FOR ADP	DESIGN VARIATIONS BEING CONSIDERED
PROPULSION SYSTEM WEIGHT, LB	18,000	10,000 TO 75,000
PAYLOAD WEIGHT, LB	2,000	1,000 TO 25,000
THRUST (MAXIMUM), LB	30,000	VARIATIONS WITH STAGE SIZE & APPLICATION
LAUNCH VEHICLE	TITAN III C WITHOUT TRANSTAGE	FAMILY OF LAUNCH VEHICLES
SPACE RESIDENCE TIME	14 DAYS (NO F_2 VENTING)	UP TO 180 DAYS
RESTARTS	30 MINIMUM	VARIATIONS WITH MISSION REQUIREMENTS
PAD HOLD CAPABILITY	• NO F_2 VENTING • H_2 VENTING & TOPPING	NEAR INSTANT LAUNCH READINESS
FLIGHT PLAN	• NO SUBORBITAL BURN • 100 NM, CIRCULAR POLAR ORBIT	DEPENDENT ON APPLICATION

CONFIDENTIAL

Figure 1. System Characteristics (U)

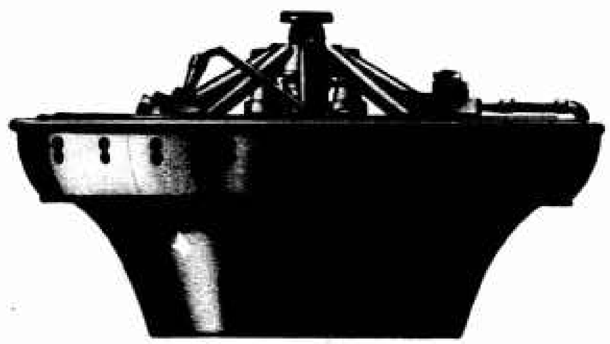

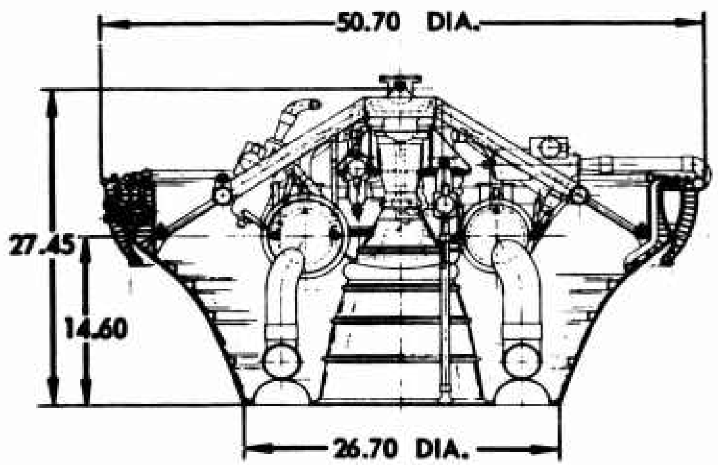

PARAMETER	MAIN ENGINE	SECONDARY ENGINE
THRUST, POUNDS	30,000	3,300
CHAMBER PRESSURE, PSIA	650	750
VACUUM SPECIFIC IMPULSE, SECONDS	460	457.5
MIXTURE RATIO, O/F	12:1	12:1
THROTTLE RATIO	9:1	9:1
AREA RATIO	60:1	60:1

CONFIDENTIAL

Figure 2. Engine System for Advanced Maneuvering Propulsion System (U)

CONFIDENTIAL

(C) Task I: Engine Analysis and Design

Task II: Engine Critical Component Demonstration Testing

Task III: Propellant Feed System Analysis and Design

(U) Effort on Tasks I and II was initiated 1 November 1967. Task III, being performed by two vehicle company subcontractors (General Dynamics/Convair and Lockheed Missiles and Space Company), was initiated 1 December 1967.

(U) SUMMARY

(C) This report presents a description of the work accomplished and the technical results obtained on the AMPT Program during the seventh quarterly period, 1 May 1969 through 31 July 1969. The major milestones for the Phase I program are shown in Fig. 3, and the basic program schedule is shown in Fig. 4.

(C) Task II milestones accomplished in the period were completions of the final design review of the prototype thrust chamber segment and the interim release of the main thrust chamber design. The Task III milestone of interim completion of the propellant feed system design and analysis was accomplished at the end of the last quarterly period.

(U) Significant accomplishments in each of the three major tasks are summarized below.

(U) 1. TASK I--ENGINE ANALYSIS AND DESIGN

(U) Work accomplished in Task I includes analysis and design effort for the engine system, thrust chamber, turbopumps, and engine controls. During this report period, a main engine system power balance and performance analysis was conducted to include various refinements and modifications which have been incorporated into the component designs. The analysis was performed for the limits of the thrust and mixture ratio operating range.

(U) In support of the main engine balance effort and future design effort, a detailed parametric analysis of the system temperature and pressure distribution characteristics was performed over the thrust and mixture ratio range for the current hardware configuration. All of the significant components in the thrust chamber assembly were included and appropriate graphs are presented for each.

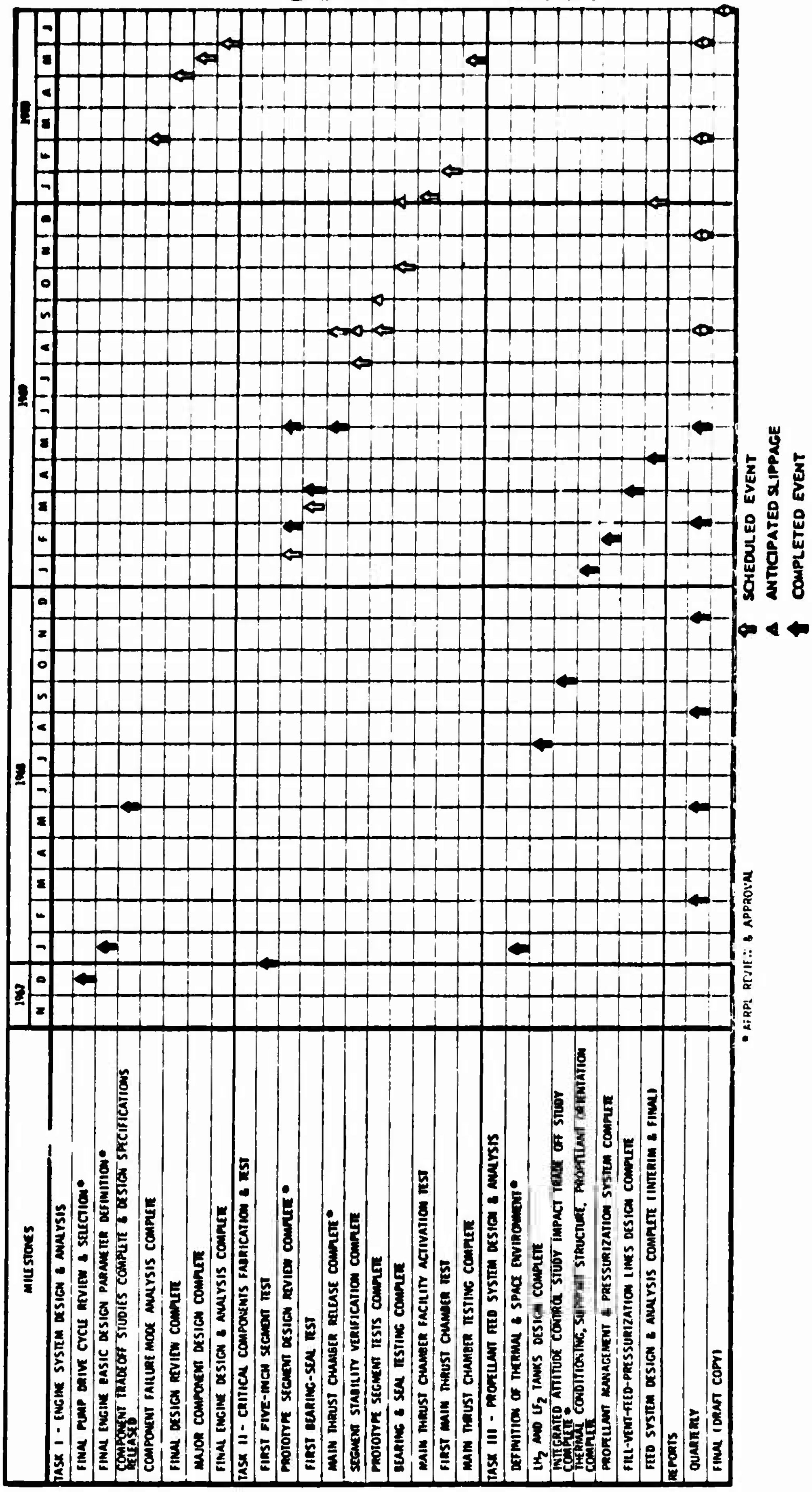

Figure 3. AMPT Program Milestones (U)

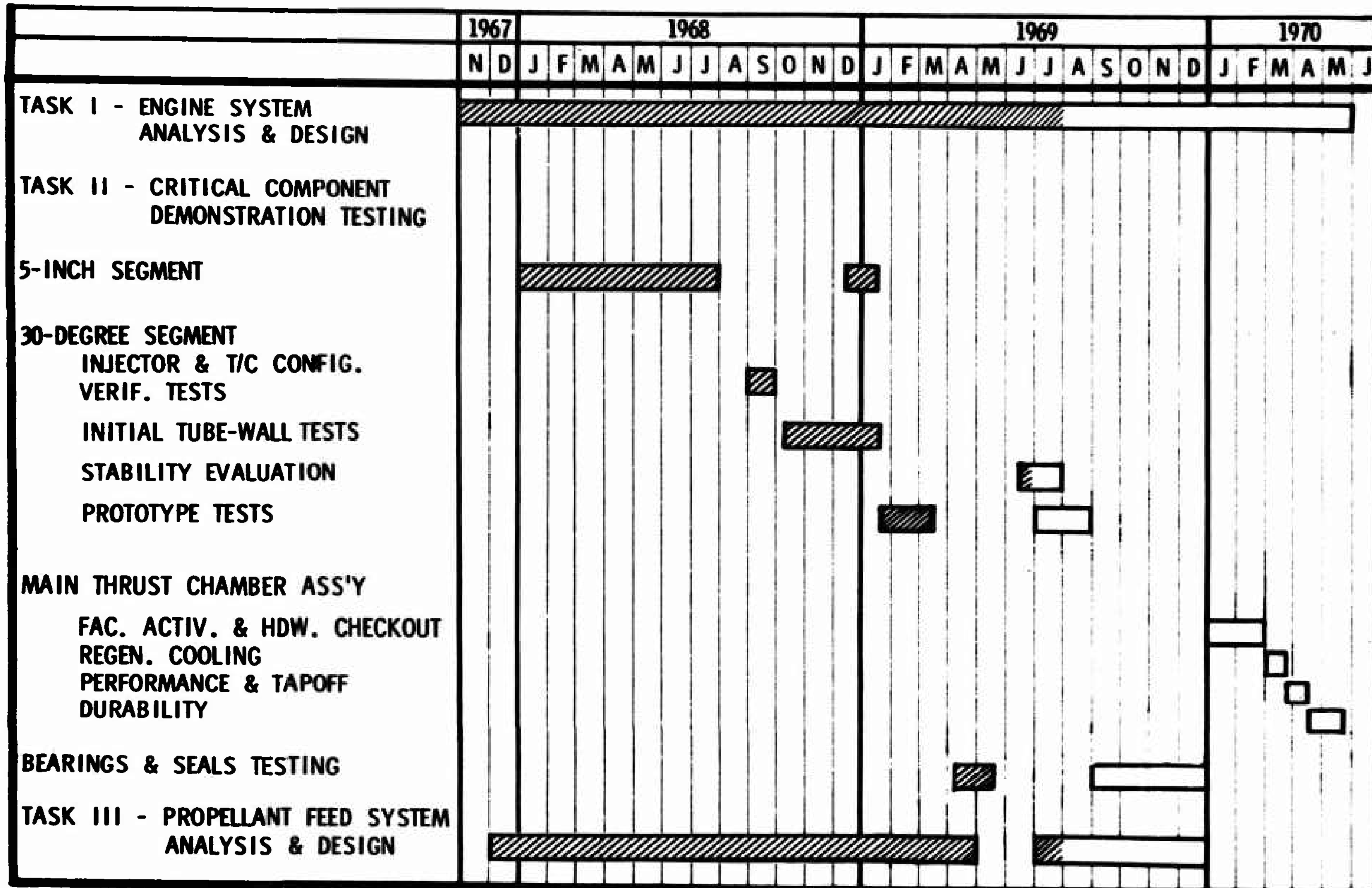

Figure 4. AMPT Phase I Program (U)

(U) The engine packaging effort was continued in parallel with the controls design effort so that available engine space versus controls component size could be considered in the final component designs. A preliminary packaging arrangement has been prepared based on current estimates of valve sizes.

(C) In support of the turbine control valve design effort currently in progress, a review of the criticality of internal leakage with respect to main and secondary engine operation was performed, and it was determined that in lieu of the previous requirement of 500 scim maximum, a maximum leakage of 5000 scim could be tolerated without influencing engine operation.

(U) During the report period, formal layout of the main engine oxidizer valve was initiated, the preliminary design of the main engine fuel turbine control valve was completed, and the secondary engine control system analysis also was completed.

(U) 2. TASK II--CRITICAL ENGINE COMPONENT DEMONSTRATION TESTING

(C) The critical engine components include segments of the main thrust chamber, complete main thrust chamber, and main and secondary engine LF_2 pump bearings and seals. The main engine thrust chamber development approach is shown in Fig. 5. The design philosophy of the approach is presented in Ref. 6 .

(C) During this report period, the primary effort in the area of main thrust chamber development was directed toward the fabrication of the 30-degree prototype channel-wall thrust chamber segment and injector. The fabrication of the contoured walls of the segment and the end plates has been completed and will be brazed together early in the next report period. The fabrication of the injector also has been completed. In addition, the preliminary manufacturing effort for the fabrication of the segments required for the 360-degree thrust chamber and fabrication of the nozzle assembly has been initiated.

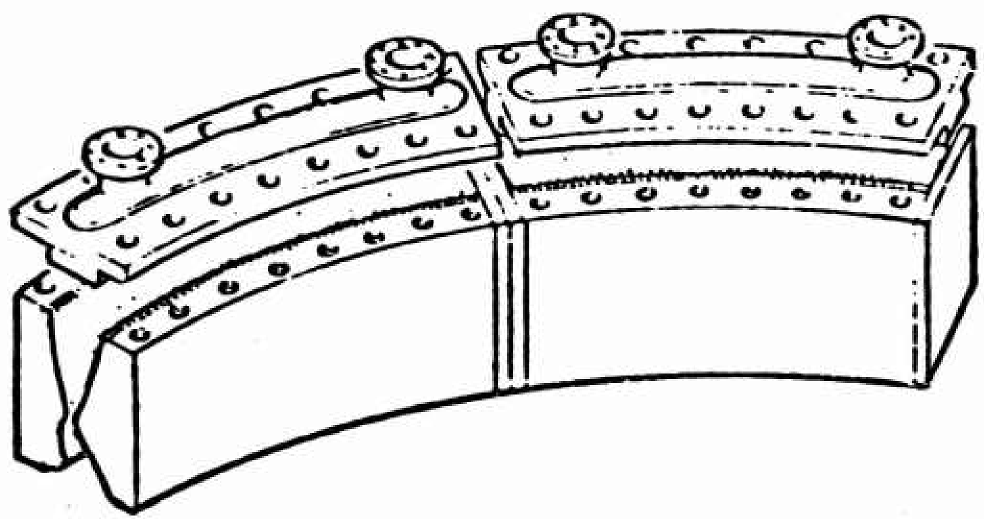

TWO 30-DEGREE THRUST CHAMBER SEGMENTS

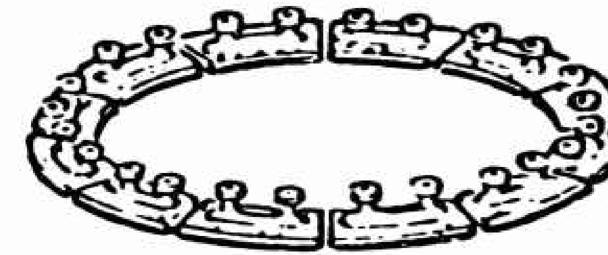

FULL SEGMENTED
INJECTOR AND MANIFOLD

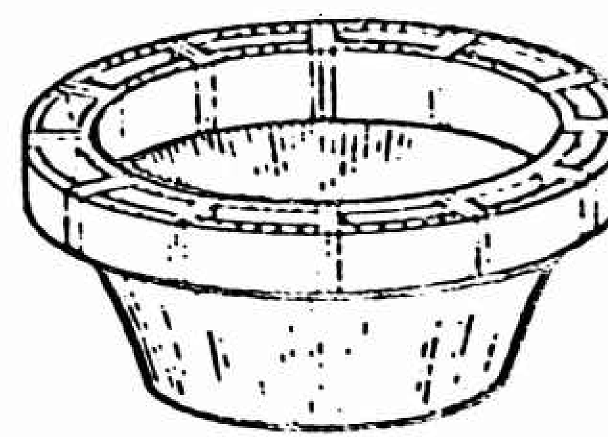

FULL SEGMENTED THRUST CHAMBER

Figure 5. AMPT Program Thrust Chamber and Injector Segments (U)

(C) A heat transfer analysis was performed to assess the reduction in heat load to the segment walls as a result of biasing the injected oxidizer to the outer periphery of the injector and also in support of the segment baffle (end plate) and nozzle extension design efforts. It was determined that the lowered coolant bulk temperature rise and local heat flux resulting from oxidizer biasing caused a reduction of approximately 150 F in the maximum gas-side wall temperature. The baffle and nozzle heat transfer analysis was completed.

(C) The segment stability test program was initiated during this report period. Utilizing the 30-degree water-cooled calorimeter thrust chamber segment and the 30-degree injector (U/N 3), one test was conducted for a duration of 3 seconds of an intended 5-second test. The test was terminated by a fire in the area of the facility oxidizer feed line. The fire appears to have originated in the facility oxidizer main valve. The investigation of the cause is still in process. A 1- to 2-week delay in the stability program is anticipated.

(C) During the second main oxidizer bearing and seal test performed during this quarter (and the fourth in the test series), a fire started at the intermediate seal and burned through the housing. The fire occurred after approximately 8.5 minutes of continuous operation and a total of approximately 10.5 minutes of accumulated operating time. The data indicate the most probable cause of failure was ignition of the Bearium B-10 intermediate seal segments because of excessive shaft deflection resulting in increased friction between the seal segments and the shaft mating ring. Design modifications to the seal have been incorporated and the reinitiation of the oxidizer bearing and seal test program has been scheduled for 1 September 1969.

(U) 3. TASK III--PROPELLANT FEED SYSTEM ANALYSIS AND DESIGN

(U) This task provides for analysis and design of an advanced propellant feed system to be integrated with the advanced engine design resulting from Tasks I and II. The task is being conducted by two selected vehicle subcontractors: General Dynamics/Convair and Lockheed Missiles and Space Company. The Task III schedule is shown in Fig. 6 .

(U) The propellant feed system basic analysis and design effort was completed by both subcontractors at the end of the previous quarterly period and the continued Task III effort was initiated late in this quarter (Fig. 6). The continued effort will include evaluation of technological advancements as related to AMPS, more detailed definition of the Phase II test configuration, design analysis for instant launch readiness, and a system malfunction and reliability analysis. Because this effort was started late in the quarterly period, no results are presented in this report but will be reported at the end of the next quarterly period.

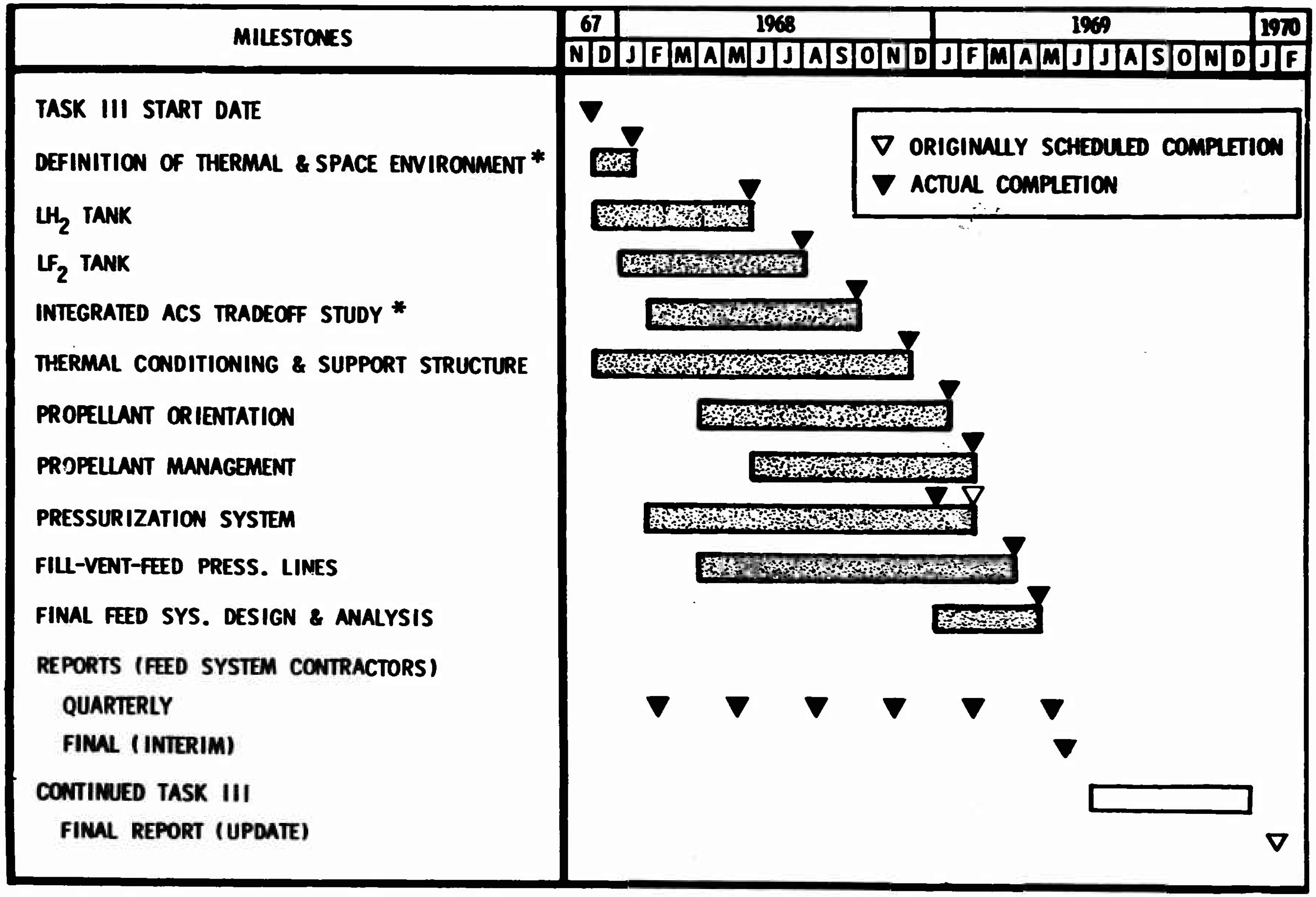

* AFRPL REVIEW & APPROVAL

Figure 6. Task III Schedule (U)

(U) TASK I--ENGINE SYSTEM DESIGN AND ANALYSIS

(U) Task I of the AMPT Program provides for design and analysis of the complete AMPS engine system. The subtasks in Task I include design and analysis efforts for the engine system, thrust chambers, turbopumps, and controls. The results obtained from the critical component testing (Task II) are to be used in applicable areas for the final engine system design.

(U) The Task I effort accomplished during this quarter included:

1. Update of main engine balance
2. Parametric analysis of complete thrust chamber temperature and pressure distribution characteristics
3. Continued effort on packaging of main and secondary engines
4. Turbine control valve leakage criticality
5. Continued effort on design of main engine oxidizer valve
6. Preliminary layout of main engine fuel turbine control valve
7. Completion of secondary engine analog model effort

(U) 1. MAIN ENGINE SYSTEM BALANCE

(C) A main engine system power balance and performance analysis was conducted to determine the effects of component modifications and experimental results that have occurred since the last engine system performance analysis was conducted for the turbine drive cycle selection studies. The recent system performance analysis was conducted for maximum and minimum thrust and for engine mixture ratios of 9:1 to 13:1. The system changes that were incorporated into the revised performance estimates are an accumulation of design modifications and refinements in the predicted operating characteristics of various components that have occurred in the past year.

(C) Some of the main engine component and system revisions have been discussed in detail in previous quarterly reports. However, the engine system power balance and performance estimates had not been updated to include these influences. A list of the accumulated changes that were included in this analysis is as follows:

1. Refinements in fuel and oxidizer turbine and pump efficiency estimates
2. Decrease in oxidizer turbine pressure ratio by the use of identical fuel and oxidizer turbines
3. Removal of cavitating venturis from propellant high-pressure feed system
4. Slight increase in theoretical values of c* and specific impulse from a revision in the heat of formation of HF
5. The change to a single-pass channel-wall chamber cooling circuit, resulting in a change to the coolant circuit pressure loss and bulk temperature rise, with a subsequent effect on fuel injector inlet and turbine drive gas inlet conditions and pump discharge pressure requirements.

(C) These changes or refinements in engine component design or operating characteristics were input to the computerized turbopump power balance and engine system performance analysis. The thrust chamber pressure losses, fuel injection temperature, and turbine inlet temperature values were obtained from the data presented in the subsequent section. The results of the main engine system performance analysis are shown in Table 1 for full thrust and minimum thrust operation over the intended range of mixture ratio. Some of the major operating conditions of the components also are presented.

TABLE 1

(U) MAIN ENGINE SYSTEM OPERATING PARAMETERS AND PERFORMANCE ESTIMATES

Engine Mixture Ratio	9:1		10:1		11:1		12:1		13:1	
Thrust, pounds	30K	3.33K	30K	3.33K	30K	3.33K	30K	3.33K	30K	3.33K
Total Oxidizer Flowrate, lb/sec	58.80	6.86	59.30	6.99	59.78	7.11	60.20	7.21	60.72	7.31
Total Fuel Flowrate, lb/sec	6.53	0.76	5.93	0.70	5.43	0.65	5.02	0.60	4.67	0.56
Injector Fuel Flowrate, lb/sec	5.11	0.727	4.71	0.67	4.37	0.62	4.06	0.57	3.82	0.53
Total Turbine Flowrate, lb/sec	1.428	0.035	1.22	0.030	1.06	0.028	0.952	0.023	0.854	0.021
Thrust Chamber Mixture Ratio	11.52	9.44	12.59	10.48	13.67	11.50	14.81	12.50	15.91	13.51
Fuel Injection Temperature, R	848	1490	938	1560	1018	1720	1088	1930	1158	2020
Fuel Pump Discharge Pressure, psia	2319	370	2217	358	2116	338	2033	335	1857	321
Oxidizer Pump Discharge Pressure, psia	887	102	887	102	888	103	889	103	890	103
Delivered Engine Specific Impulse, seconds	459.2	436.8	459.9	433.1	460.0	429.5	460.0	426.5	458.8	423.0

(U) 2. MAIN THRUST CHAMBER PRESSURE DROP AND COOLANT TEMPERATURE DISTRIBUTION

(C) A parametric analysis was conducted to determine predicted hydrogen pressure drop and temperature rise data for the various components of the current main thrust chamber configuration over the intended operating conditions. This analysis was based on the Task II experimental results from the chamber segment tests and the oxidizer mixture ratio bias injector and the other revisions or improvements in the design detail being incorporated into the prototype thrust chamber segment. The analysis was conducted for each of the thrust chamber subcomponents on a parametric basis to make the resulting data independent of any possible variations in future design or experimental results in other subcomponents in the thrust chamber assembly. In general, the method of analysis consisted of a detailed heat transfer analysis based on specific test points. The hydrodynamic analysis performed for interconnecting ducts and other subcomponents where no heat addition takes place was based on the design details for the 30-degree prototype segment assembly. The results of these detailed point design analyses were then extended on a parametric basis to cover the intended operating range with the use of scaling equations developed from the theoretical analysis.

(U) a. Chamber End Plate (Baffle)

(C) Heat transfer and fluid flow calculations were made for the baffle with the aid of a digital computer program where the cooling circuit is divided into increments. For each increment, an iteration procedure is followed to determine the heat flux from the combustion gas to the coolant, the resulting temperature profile, and the coolant change of state until they are compatible with the resulting friction and momentum pressure drop over the increment. This analysis was conducted for three operating chamber pressures (613, 222, and 74 psia) based on data

(C) obtained in solid-wall segment tests 014, 016, and 017. The heat flux data obtained from these tests were used to predict the heat flux profile, gas-side wall temperatures, coolant bulk temperature rise, and coolant pressure drop for the prototype chamber baffles operating at an engine mixture ratio of 12:1 and a coolant inlet temperature of 65 R. The results of the detailed analysis for these three engine operating points (P_c = 613, 222, and 74) were then used as the basis for an analytical scaling analysis to provide the same type of information over the entire engine system operating range. The scaling techniques were developed from the theoretical equations used in the analysis of the three basic operating points. These scaling methods were computerized to facilitate the rapid analysis of a wide range of parametric data. The computerized scaling methods also will make it very simple to evaluate the effects of newly acquired test data or design modifications. The results of the parametric analysis are shown in Fig. 7 through 9. The baffle coolant discharge temperature is shown in Fig. 7 versus chamber pressure for engine mixture ratios from 9:1 to 13:1. The bulk temperature rise of the coolant in the baffle is relatively insensitive to inlet pressure, and the curves shown in Fig. 7 are considered valid over a fairly wide range of coolant inlet pressures. The baffle coolant inlet versus exit pressure relationship is shown in Fig. 8 for each of the three selected operating chamber pressures and over the range of engine mixture ratios. The differences between the inlet and corresponding exit pressures are presented in Fig. 9 in the form of baffle pressure drop versus exit pressure. This latter curve presents the required information in a convenient form for the step-wise procedure of establishing the total system pressure drop, starting with the desired operating chamber pressure and backing through each component.

(U) b. Chamber Segment--Outer and Inner Body

(C) The thrust chamber segment outer and inner body heat transfer and fluid dynamics calculations also were based on test data obtained in solid-wall segment tests 014, 016, and 017. The detailed analysis performed for the three operating chamber pressures (613, 222, and 74 psia) assumed the most recent chamber design configuration with the oxidizer bias injector

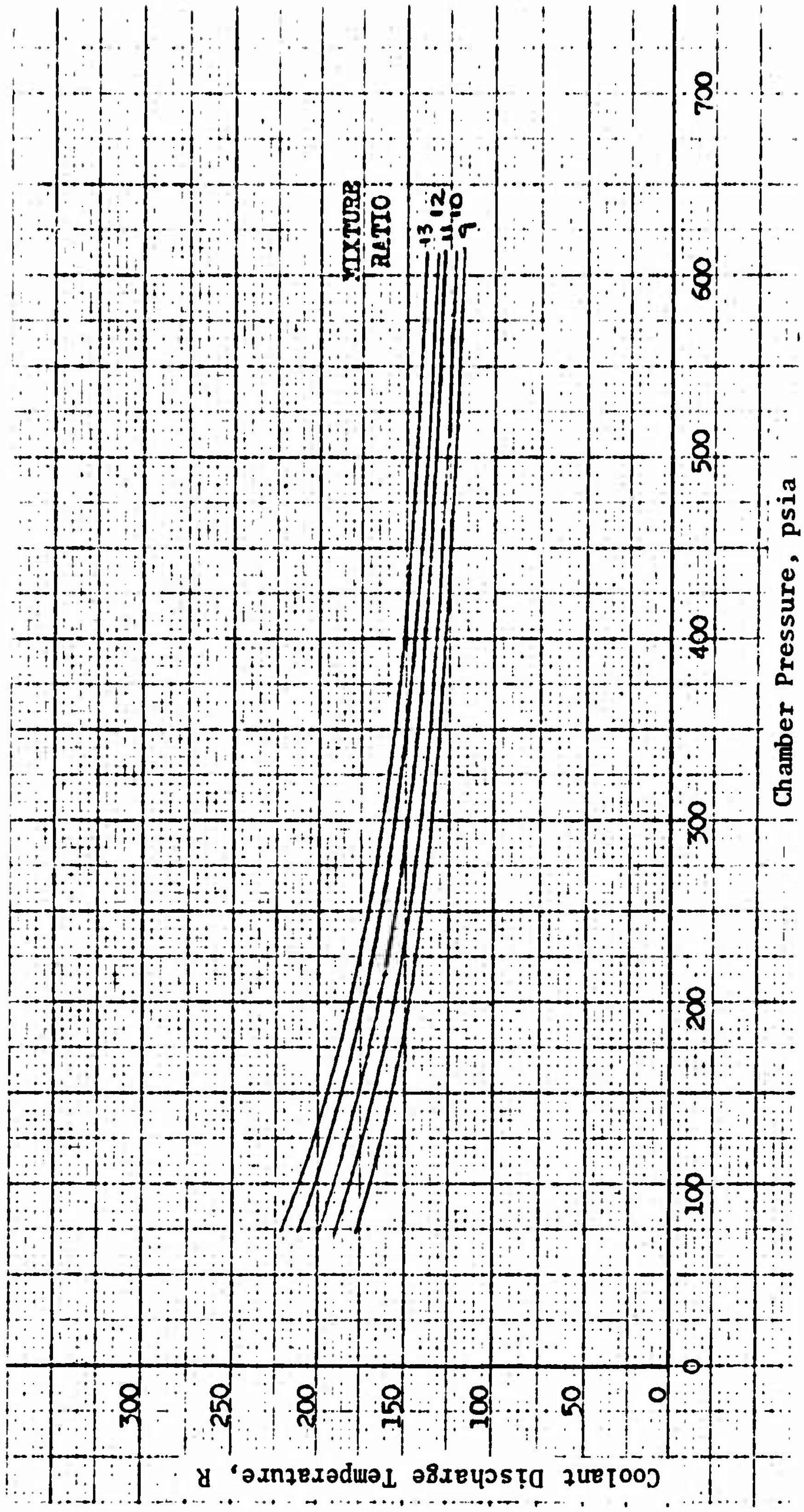

Figure 7. Baffle Coolant Discharge Temperature (U)

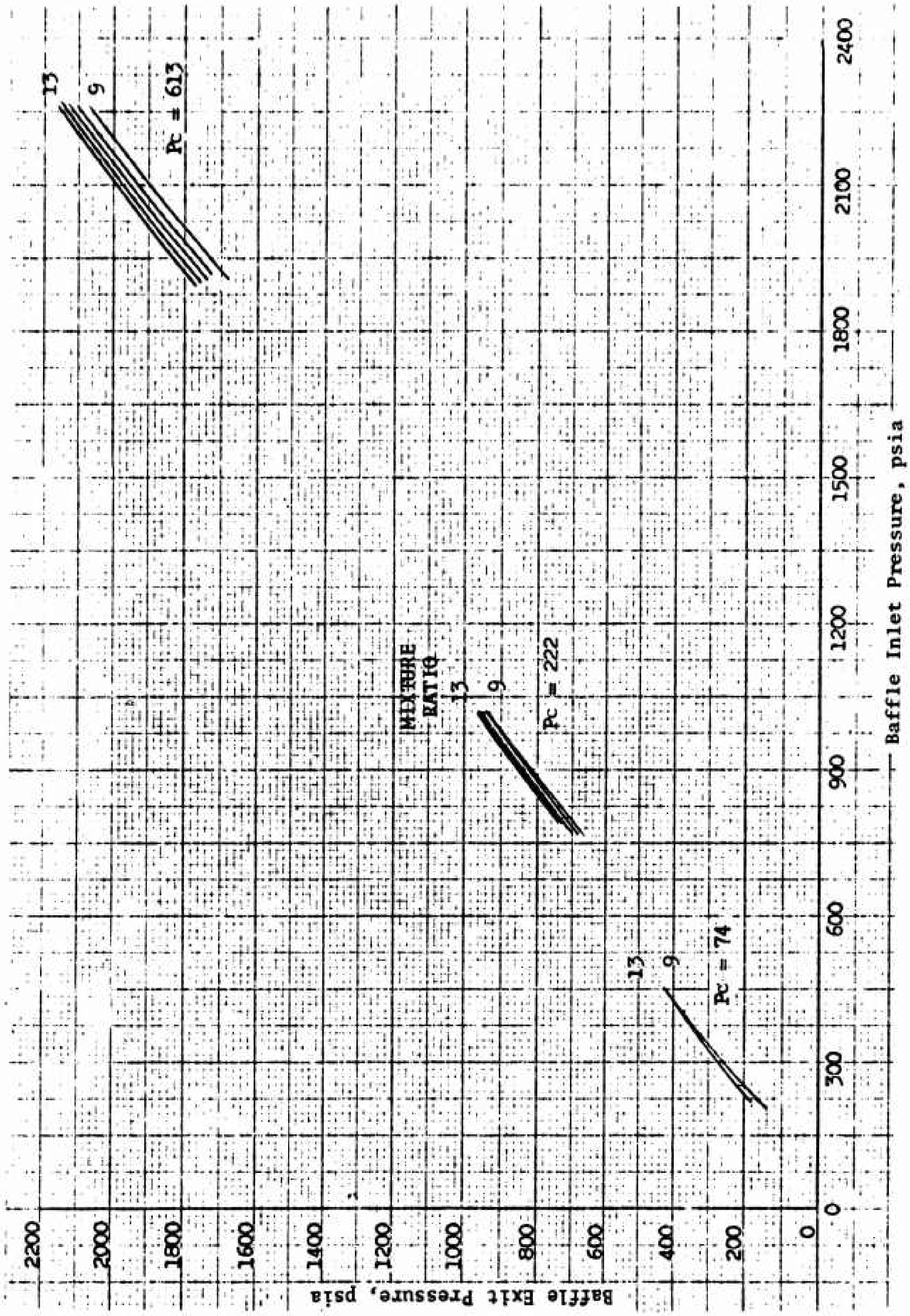

Figure 8. Baffle Coolant Pressures (U)

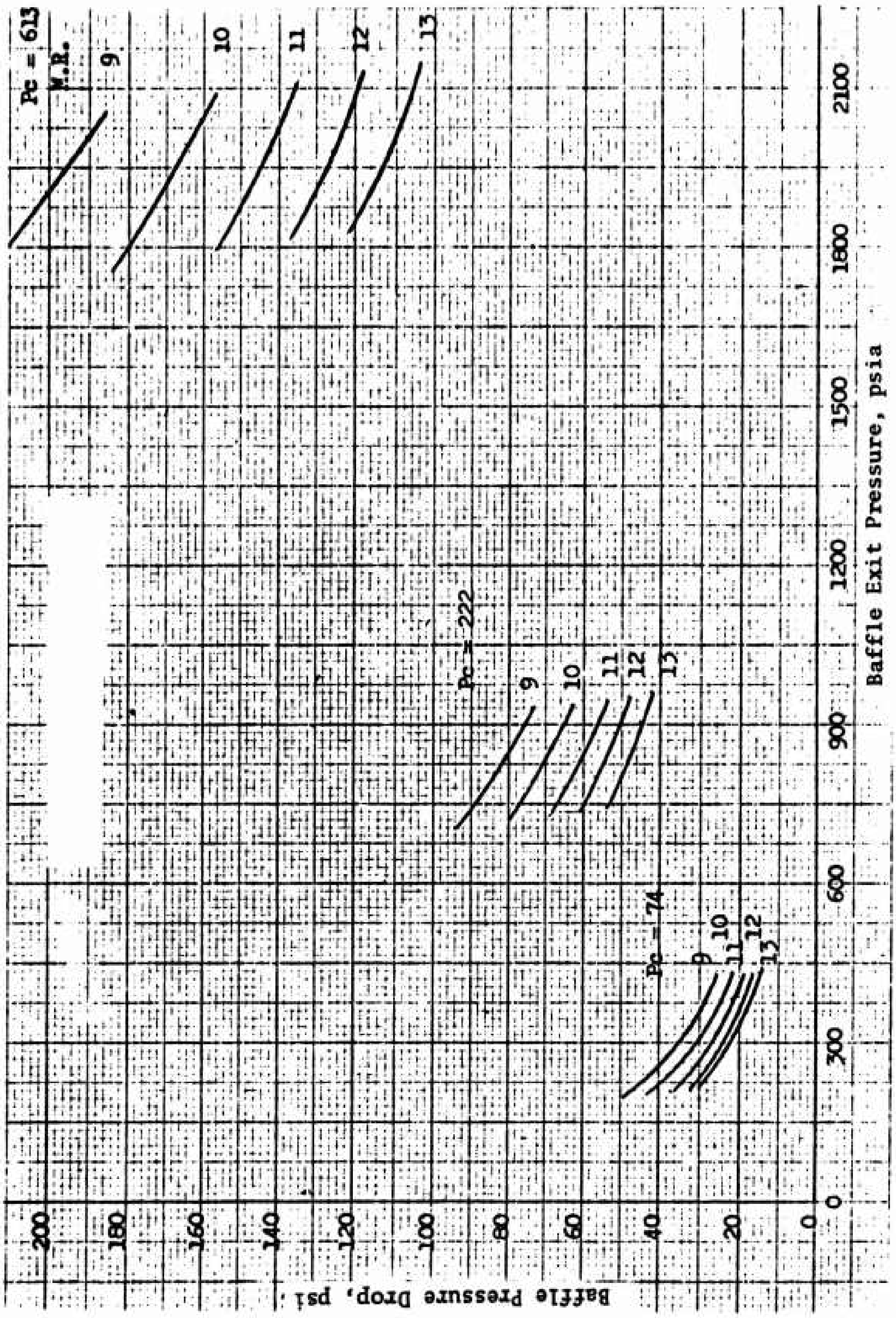

Figure 9. Baffle Coolant Pressure Drop (U)

(C) modification. The coolant enters the outer body and makes a single down-pass through the coolant channels. The coolant then crosses through the lower portion of the baffle to the inner body, which is cooled by a single up-pass, and the coolant is then transferred to the nozzle. The results of the detailed studies for the three operating chamber pressures were used to generate parametric data describing coolant temperature rise and exit pressure for a range of inlet temperature and pressure conditions for both the outer and inner bodies. The coolant discharge temperature versus operating chamber pressure is shown in Fig. 10 for mixture ratios of 9:1 to 13:1. The outer body coolant inlet temperatures were obtained from the baffle coolant discharge temperature (Fig. 7) and the outer body discharge temperature becomes the inner body inlet temperature for the corresponding chamber pressure and mixture ratio values.

(C) Chamber inner and outer body exit versus inlet pressure is shown in Fig. 11 for operating chamber pressures of 613, 222, and 74 psia and engine mixture ratios from 9:1 to 13:1. Inlet temperature for each engine mixture ratio is obtained from Fig. 7 and 10 for the outer and inner bodies, respectively. The pressure drop versus exit pressure is shown in Fig. 12 and 13 for the outer and inner bodies, respectively. Note that in the current cooling circuit, the outer body exit pressure is not equal to the inner body inlet pressure; an additional pressure drop occurs in the crossover duct within the lower portion of the baffle. Estimates of this crossover duct pressure loss are presented in the next section. The pressure losses shown for the outer body include all losses from the baffle exit to the entrance of the crossover duct. The pressure drop values shown for the inner body include all losses from the crossover duct exit to the exit of the inner body coolant channels. Heat addition was assumed to occur only in the coolant channels.

(U) c. Outer-to-Inner Body Crossover Duct

(U) The pressure losses that occur in the crossover duct between the outer body and inner body were estimated, based on the design configuration, for a range of engine fuel flowrates and for inlet conditions dictated

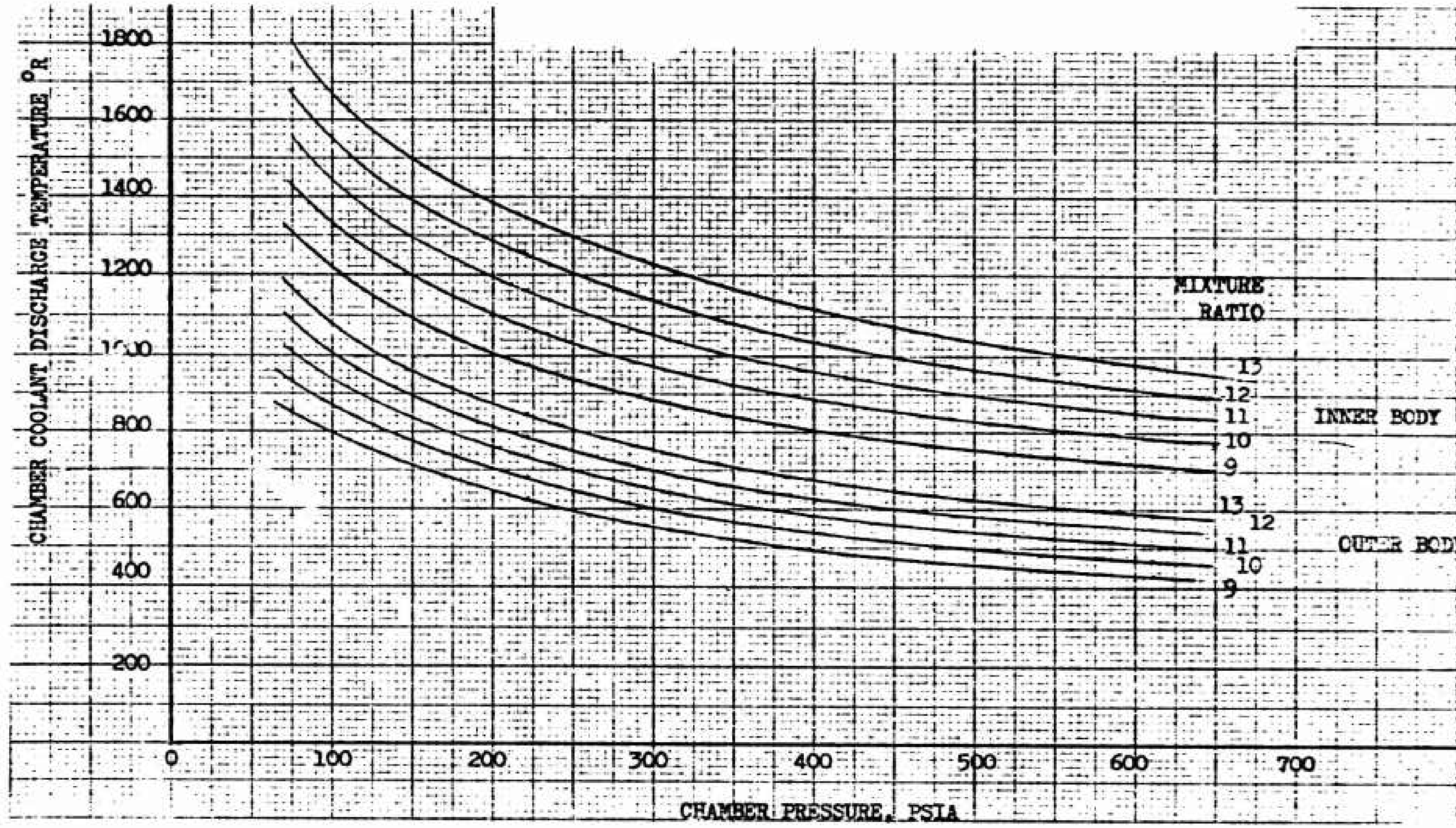

Figure 10. Channel-Wall Chamber Discharge Temperature (U)

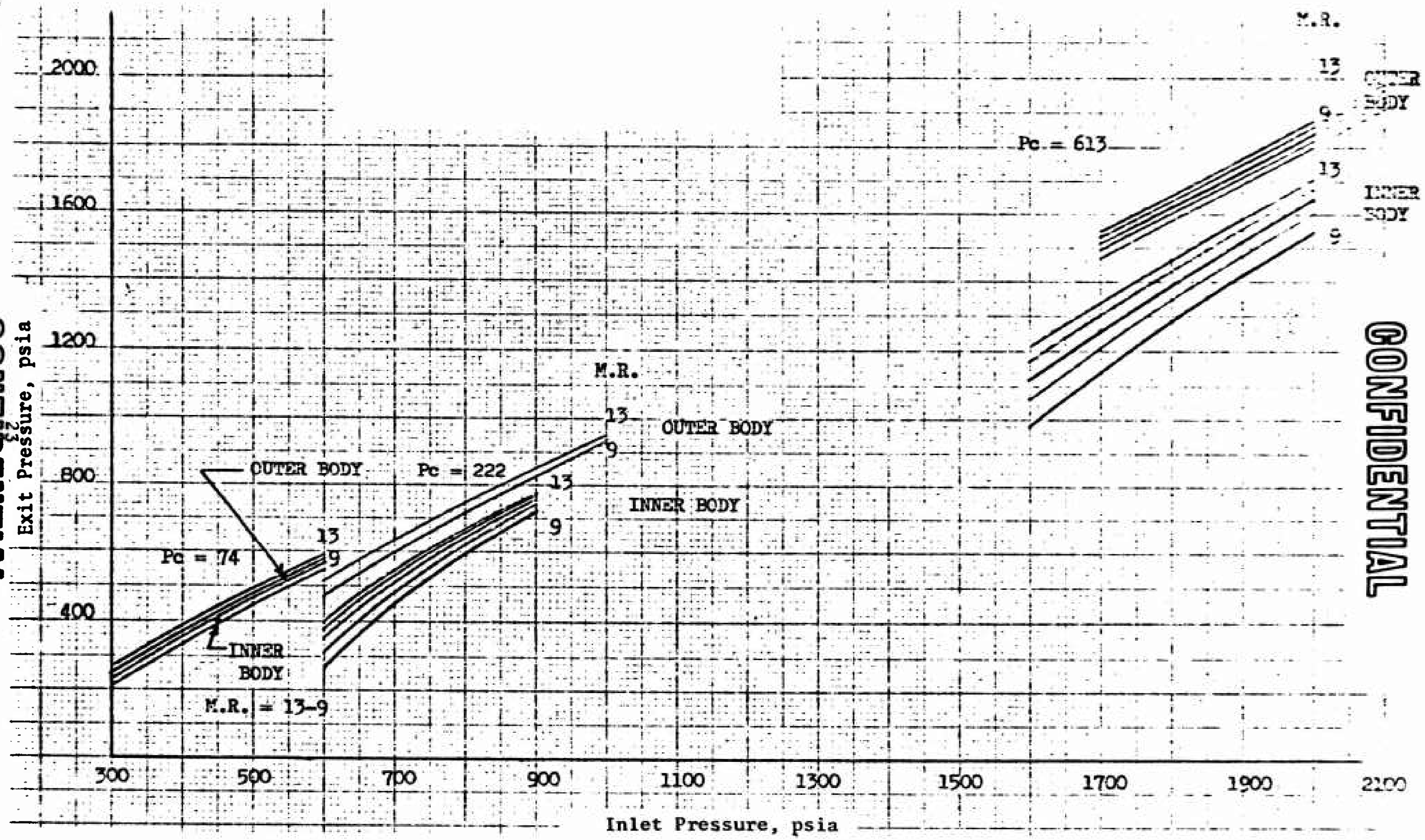

Figure 11. Chamber Inner and Outer Body Inlet/Exit Pressure Relationship (U)

CONFIDENTIAL

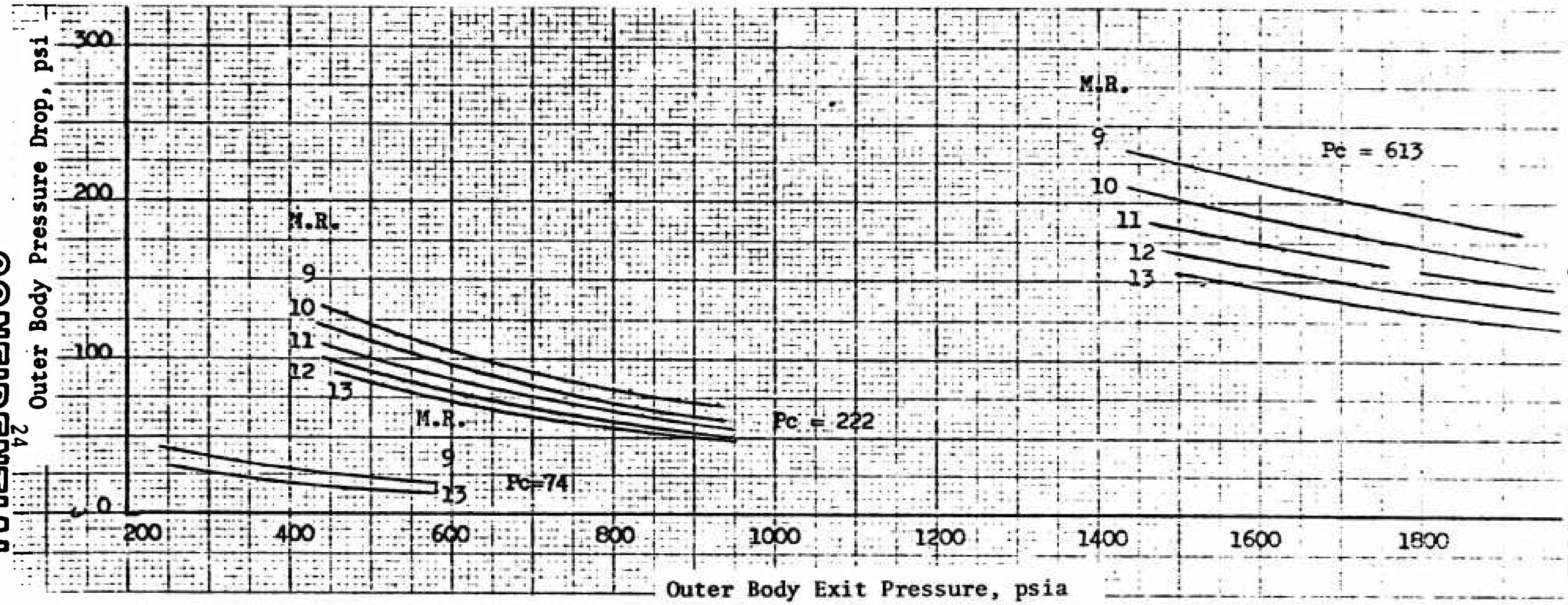

Figure 12. Outer Body Channel-Wall Chamber Pressure Drop (U)

CONFIDENTIAL

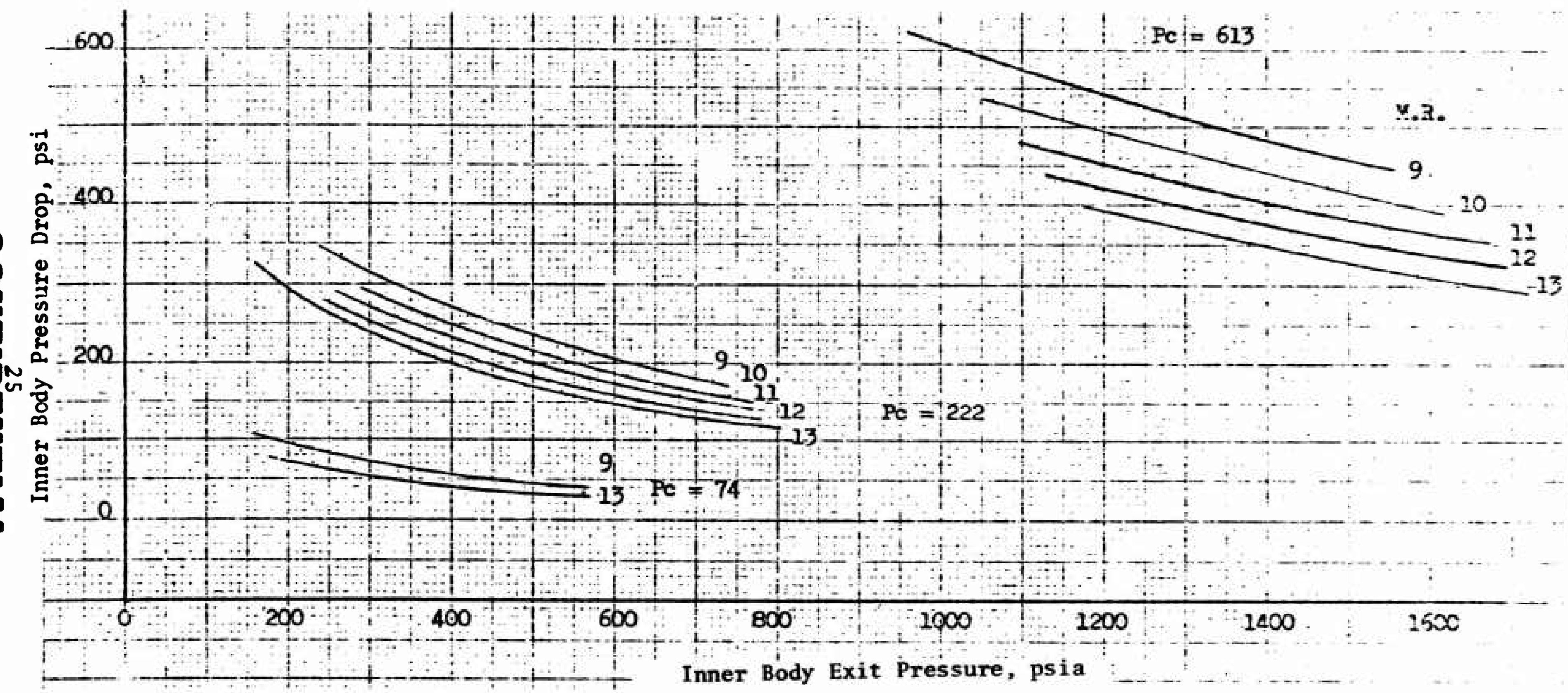

Figure 13. Inner Body Channel-Wall Chamber Pressure Drop (U)

CONFIDENTIAL

(U) by the outer body discharge flow conditions for the indicated values of operating chamber pressure and mixture ratio. These results are shown in Fig. 14 .

(U) d. Transfer From Inner Body Channels to Nozzle Tubes

(U) In the actual engine system design, the coolant will be transferred from the inner body channels to the nozzle tube bundle through a series of collection and distribution manifolds and transfer ducts. The total pressure loss incurred in this portion of the cooling circuit has been estimated versus engine system fuel flowrate for the transfer system inlet conditions (inner body discharge) dictated by the indicated operating chamber pressure and mixture ratio values. The results are shown in Fig. 15 .

(U) e. Nozzle Extension Tube Bundle

(C) Heat transfer and fluid flow calculations were conducted for the nozzle extension at specific operating points with the aid of a digital computer program. The cooling circuit is divided into increments, and heat flux, wall temperature, and coolant conditions are evaluated for each increment. The general method balances heat flux with the friction and momentum pressure drop over each increment. The nozzle cooling circuit considered in this analysis has the coolant entering the tube assembly in the upstream direction, at a location 6 inches (measured axially) from the leading edge of the nozzle extension and following the two-pass circuit illustrated in Fig. 16. The detailed analysis was conducted for preliminary estimates of nozzle tube bundle inlet conditions for operating chamber pressures of 650, 22, and 94 psia. These results were then scaled to cover a range of inlet pressures and for inlet temperatures predicted for the range of engine mixture ratios. Nozzle coolant inlet temperatures were obtained from the inner body exit temperatures (Fig. 10). The resulting nozzle coolant exit temperatures are shown in Fig. 17 as a function of operating chamber pressure and mixture ratio. Coolant inlet versus exit pressures and pressure drop versus exit pressures are shown in Fig. 18 and 19, respectively.

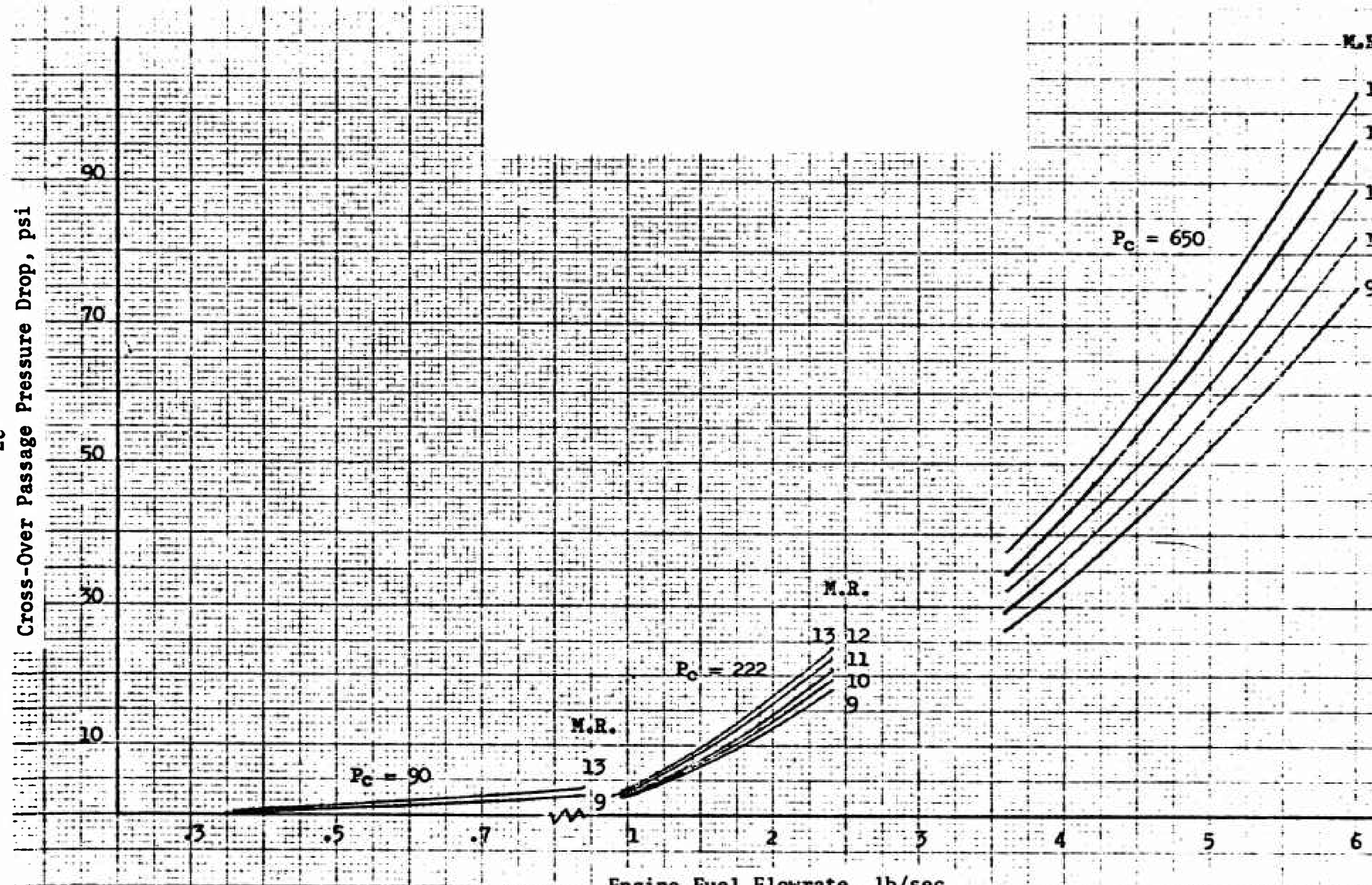

Figure 14. Inner Body-to-Outer Body Crossover Duct ΔP (U)

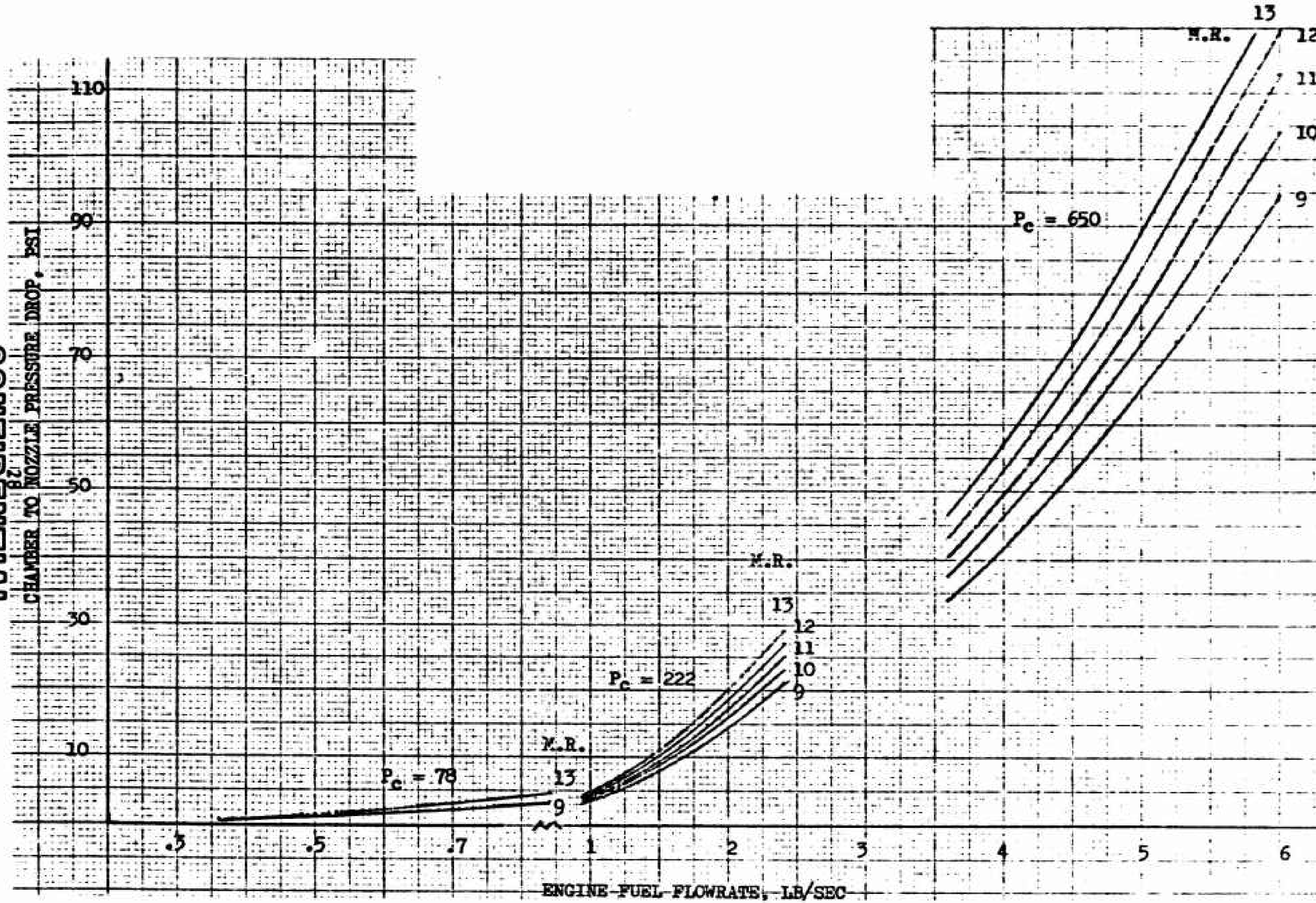

Figure 15. Coolant Pressure Drop From Inner Body Channels to Nozzle Tubes (U)

CONFIDENTIAL

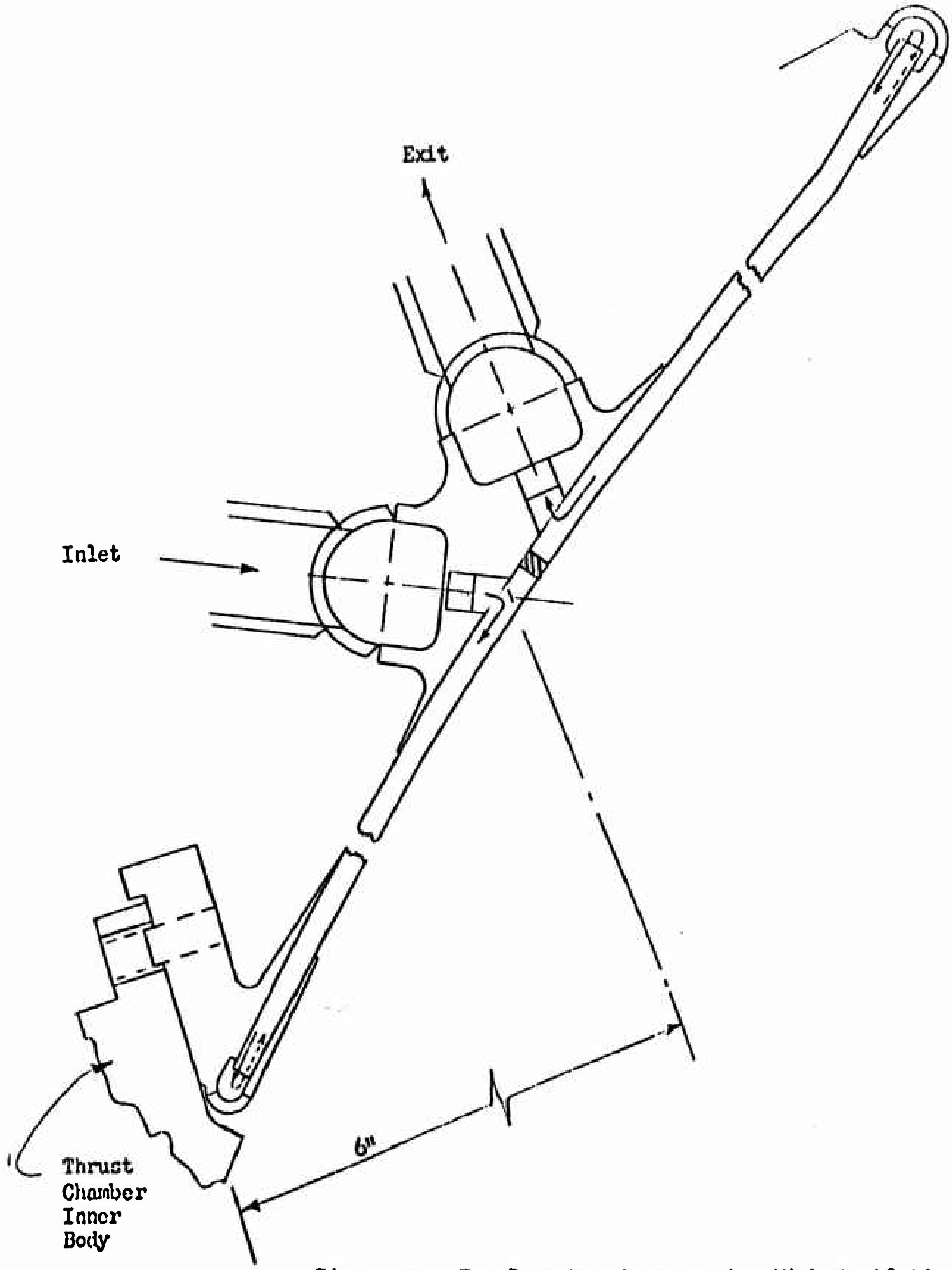

Figure 16. Two-Pass Nozzle Extension With Manifold Located 6 Inches (Axially) Downstream of Rear of Thrust Chamber Inner Body (U)

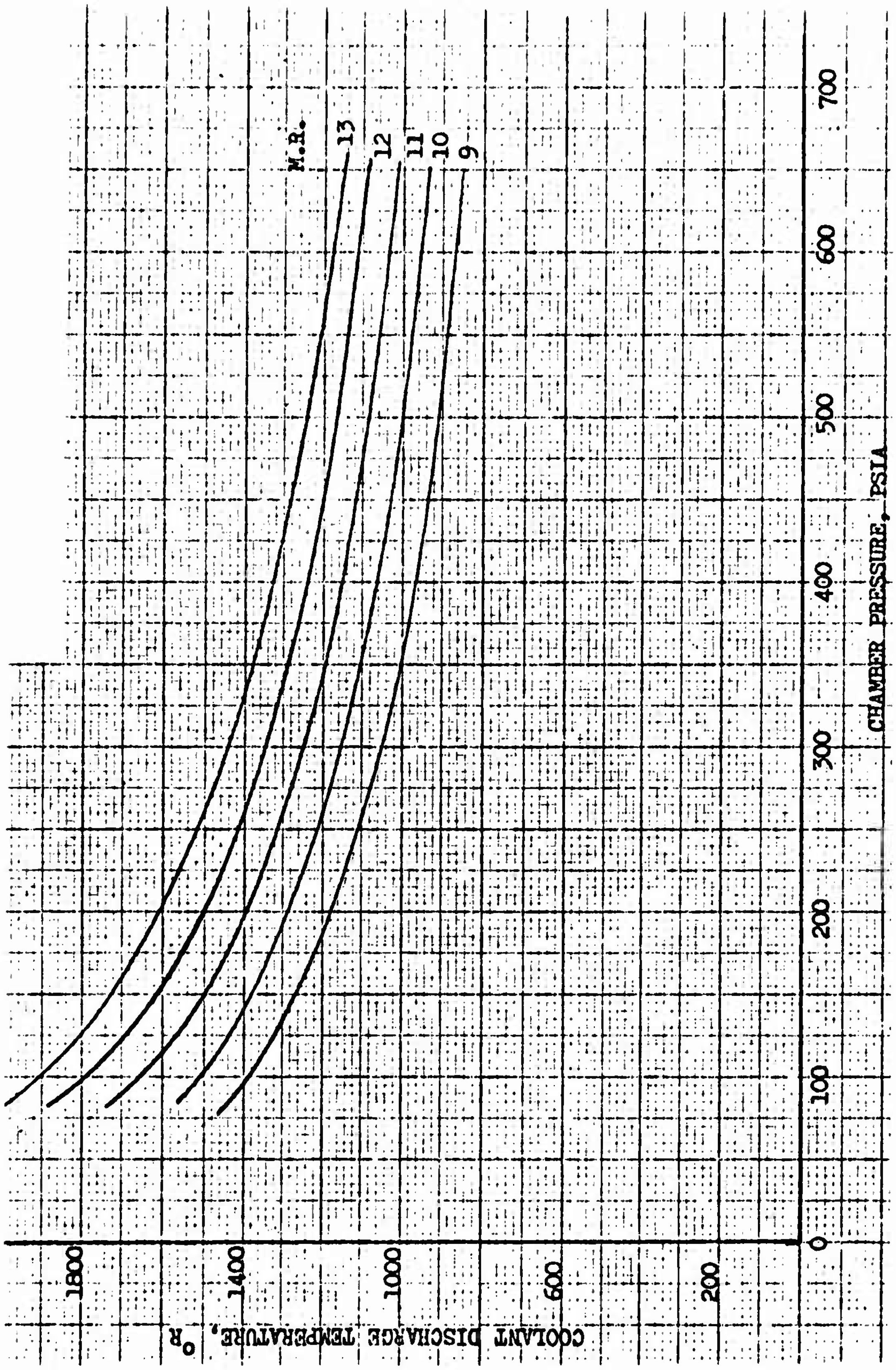

Figure 17. Chamber and Nozzle Coolant Discharge Temperature (U)

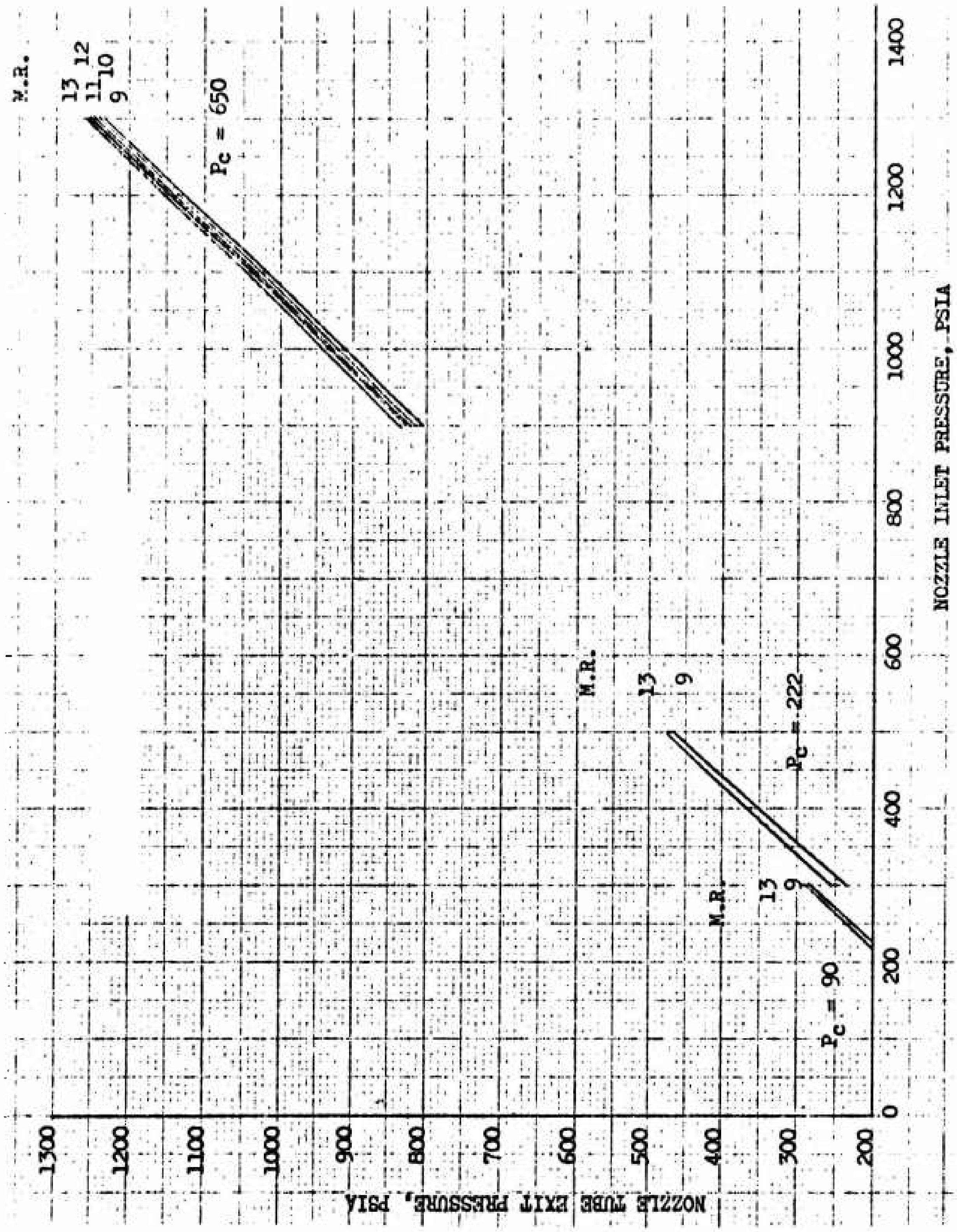

Figure 18. Nozzle Tube Inlet vs Exit Pressure (U)

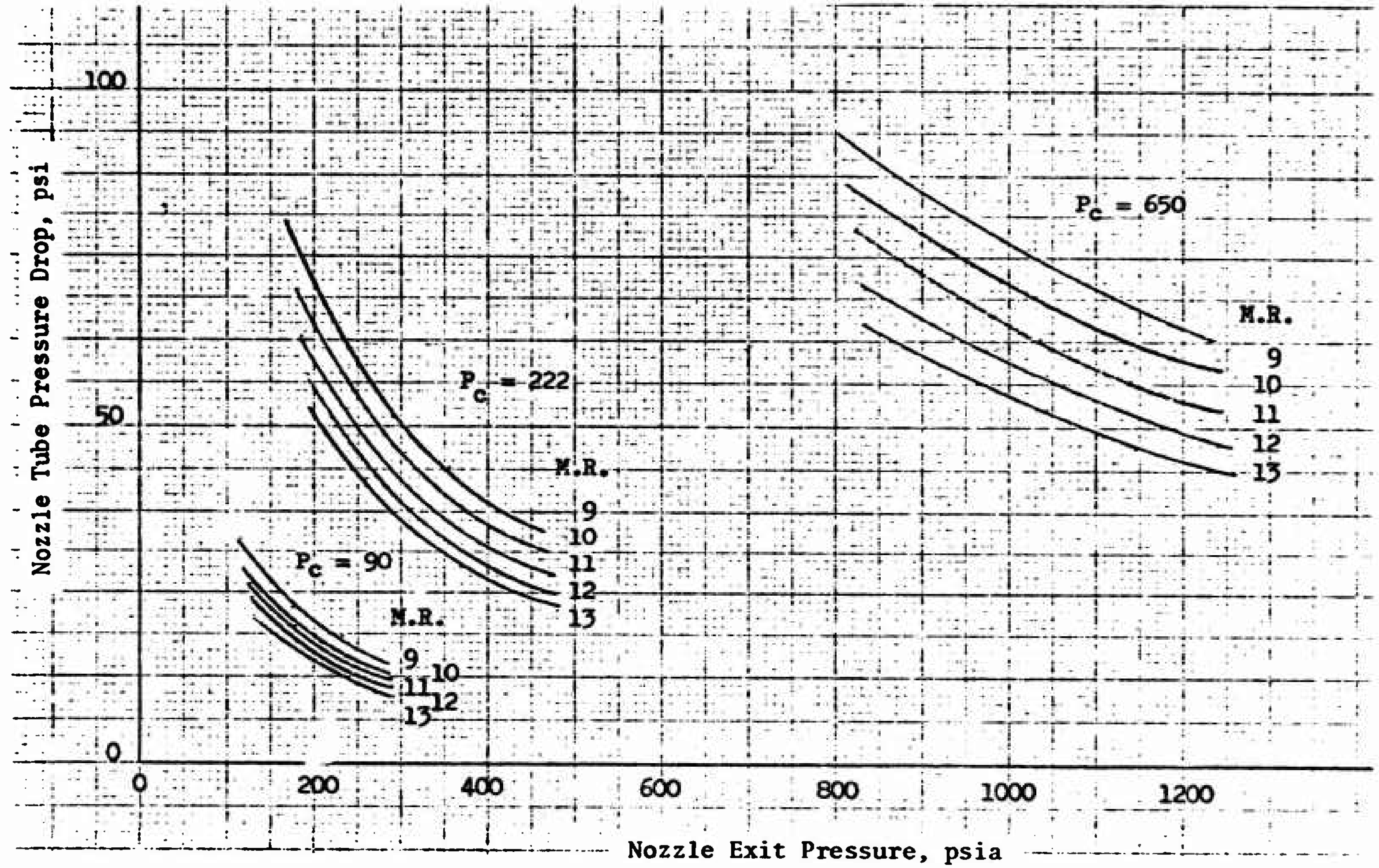

Figure 19. Nozzle Tube Pressure Drop vs Exit Pressure (Does Not Include Inlet or Exit Manifold) (U)

(U) f. Nozzle Exit Manifold and Return

(C) All of the heat addition that occurs in the nozzle is assumed to occur in the tube bundle; inlet and exit manifolds and ducting are considered to undergo a constant temperature flow process. However, the pressure loss estimates attributed to the nozzle exit manifold and the exit manifold-to-injector return ducting were separated in the parametric analysis because the turbine flow requirements are to be extracted from the nozzle exit manifold and a lower fuel flowrate will occur in the return ducting. The pressure drop versus flowrate relationship for these two thrust chamber components is shown in Fig. 20 and 21 for coolant temperature conditions corresponding to the indicated chamber pressure and mixture ratio values. The nozzle exit manifold is located adjacent to the inlet manifold and 12 return ducts carry the fuel up to each of the injector segments.

(U) g. Injector

(U) The fuel-side injector pressure drop predictions were based on the experimental test results obtained with the brazed face, U/N 1 injector segment. The experimental results were adjusted to account for the predicted fuel inlet temperatures that were determined from the parametric heat transfer and fluid flow analysis of the preceding thrust chamber components. The predicted fuel-side injector pressure drop values are shown in Fig. 22.

(U) h. Summary

(C) The determination of the engine system fuel-side pressure drop is actually an iterative procedure in that turbine power and flow requirements are dependent on the fuel pump discharge pressure requirements and available turbine drive gas inlet temperature, while coolant temperature rise and pressure losses are dependent on the total fuel flow (turbine and injector) through the chamber. Preliminary estimates of coolant pressure losses are made based on estimated propellant flows. These values are used in conjunction with the estimated coolant temperature rise to perform an engine

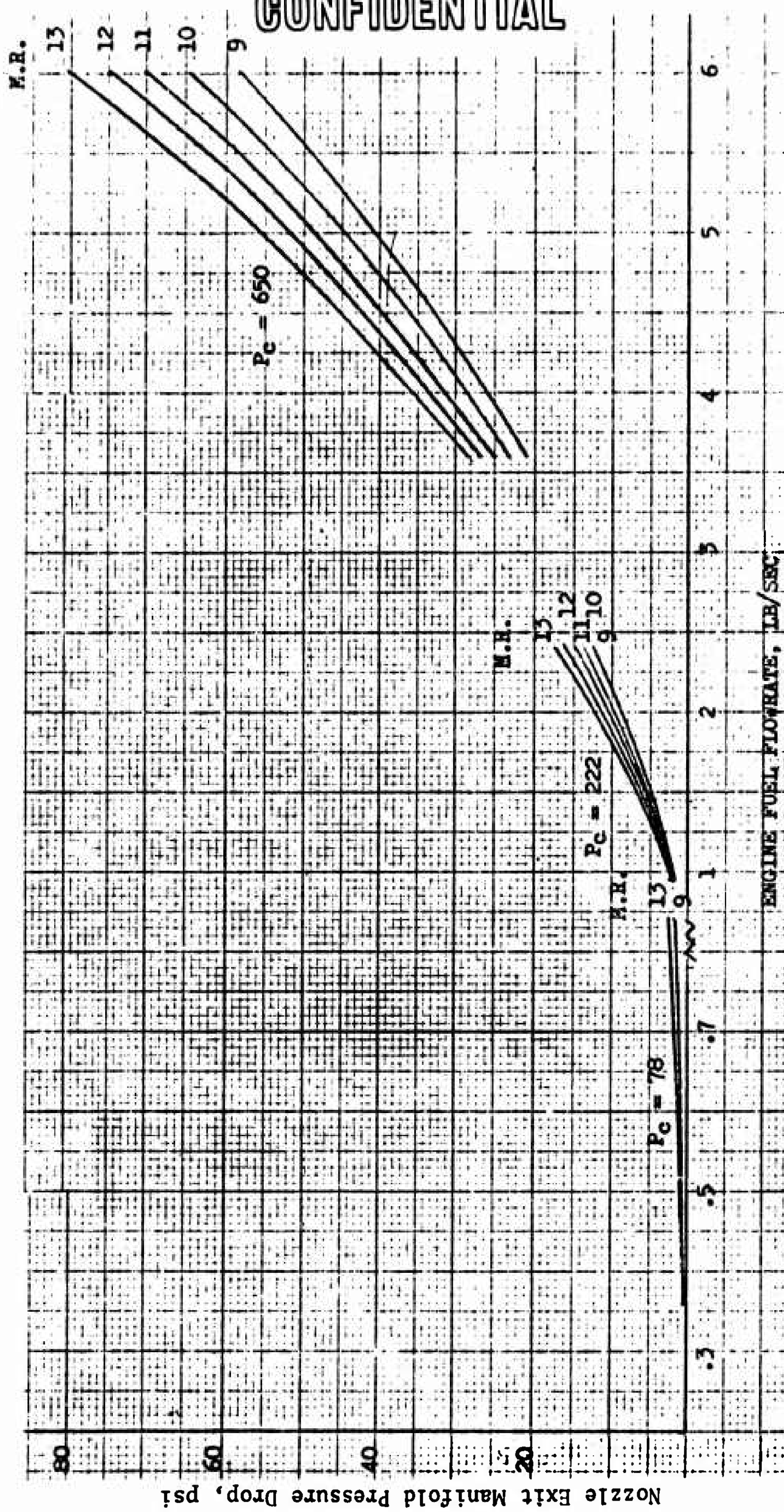

Figure 20. Nozzle Exit Manifold Pressure Drop vs Engine Fuel Flow (U)

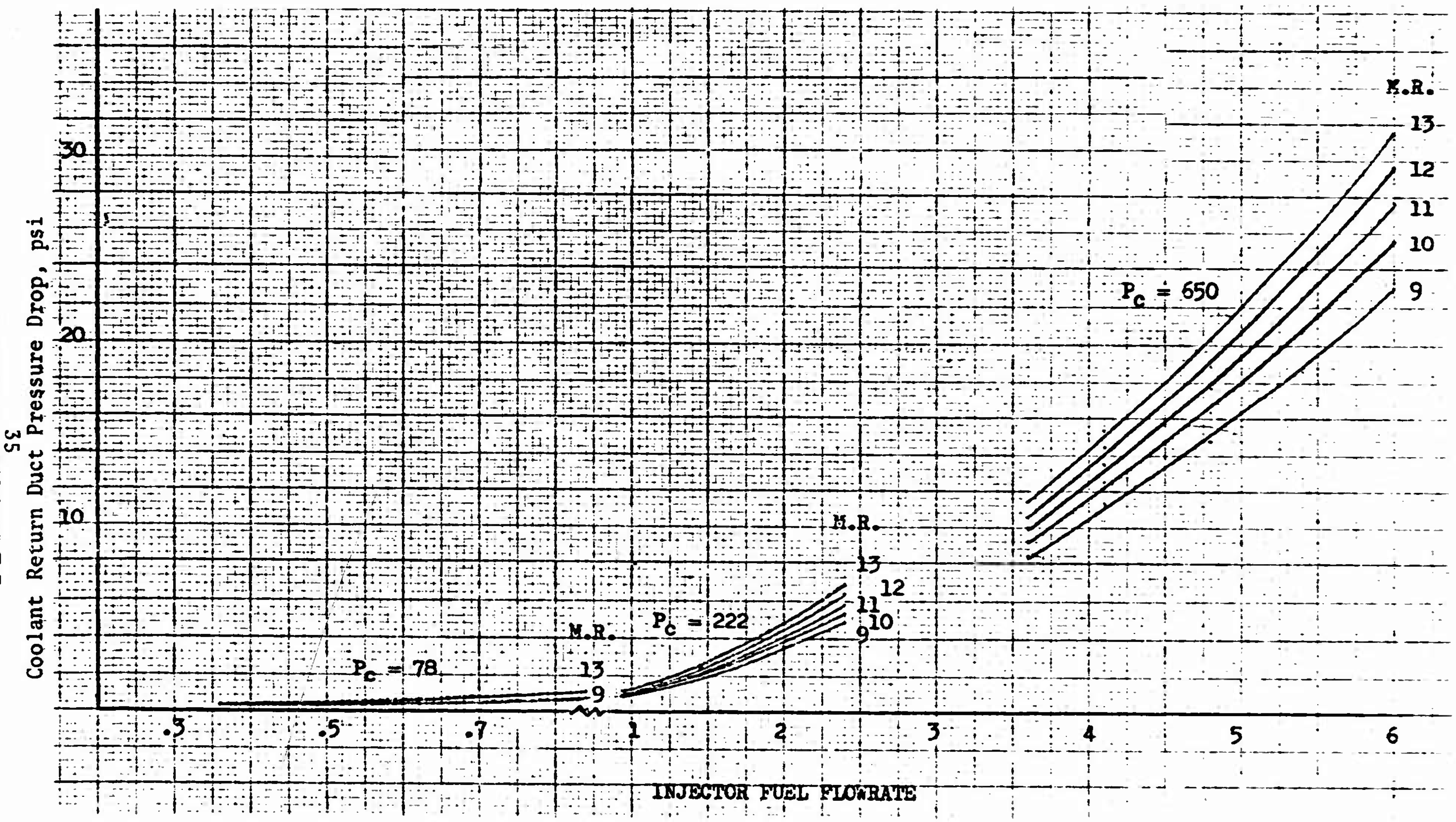

Figure 21. Pressure Drop for Coolant Return From Nozzle Exit Manifold to Injector vs Injector Flowrate (U)

CONFIDENTIAL

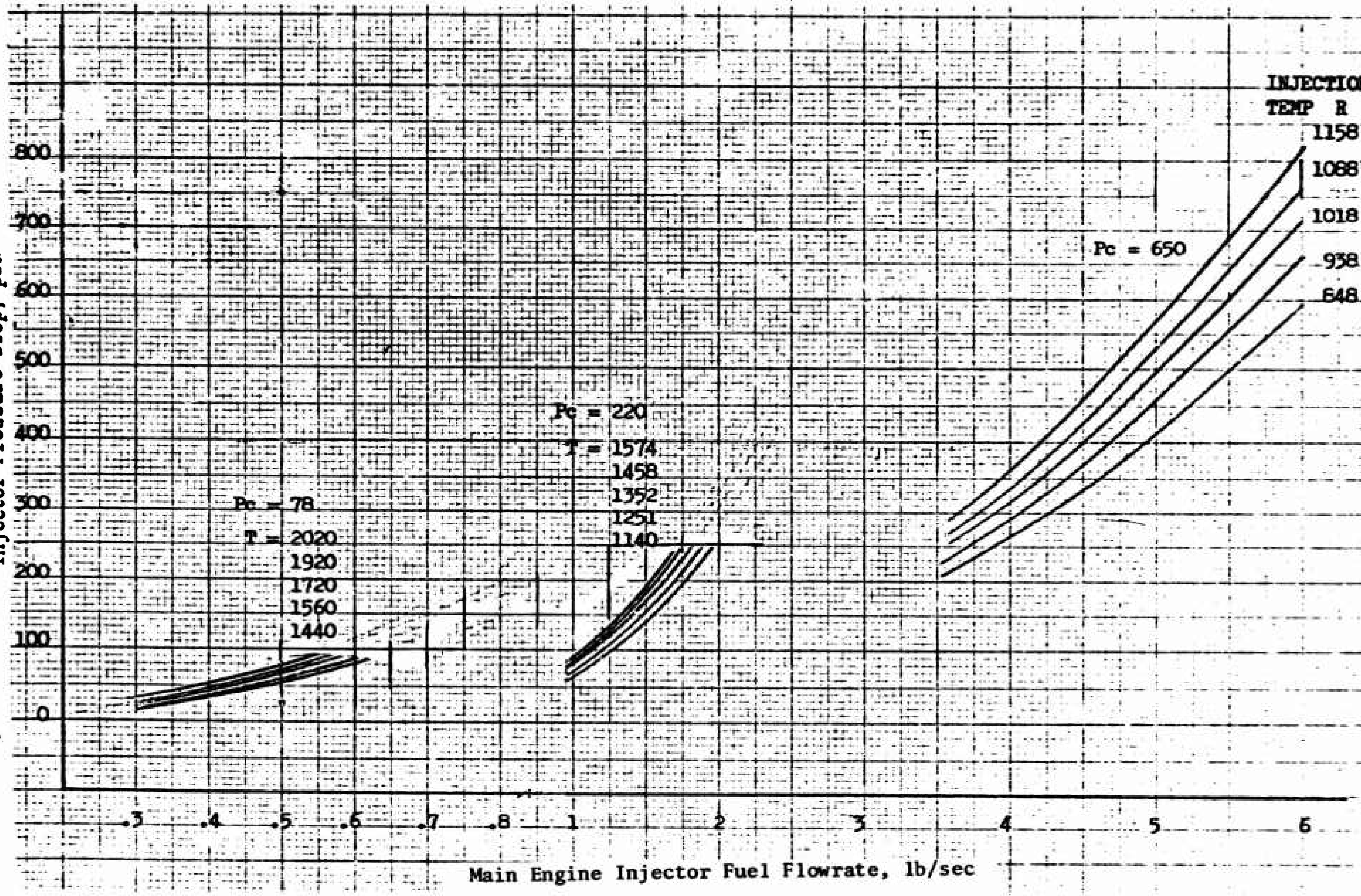

Figure 22. Main Engine Injector Pressure Drop (U)

(C) system power balance. This, then, provides refined propellant flowrates and permits refined estimates of the fuel-side pressure losses from the previously discussed curves for the thrust chamber components. Total system pressure losses are estimated by starting with the desired operating chamber pressure, then estimating injector and engine system propellant flowrates. The injector pressure drop is established first, and pressure losses are then determined for each component, working back to the pump discharge. The parametric data discussed in this report were used to establish the current estimates of coolant pressure drop and temperatures through the main engine thrust chamber assembly. The results are presented in Tables 2 and 3 for full thrust and minimum thrust and mixture ratios of 9:1 to 13:1. A summary of the pressure and temperature schedule through the thrust chamber for the nominal engine mixture ratio of 12:1 is shown in schematic form in Fig. 23.

(U) i. Engine Packaging

(C) Preliminary design configurations of the main propellant valves and the throttle control valves have been incorporated into the engine package. The main propellant valves are mounted vertically within the first and fourth quadrants of an engine package plan view, as shown in Fig. 24. The ducting leading to the turbopump inlets from the valves has been designed to function as a heat barrier in addition to directing the fluid flow. To enhance the ability of the ducts to resist heat flow, a suitable duct length was desired. In achieving this desired length, a design study was conducted, the results of which indicated that a relocation of the turbopumps would be advantageous. The turbopumps were repositioned by exchanging their former locations. Therefore, maintaining the existing propellant inlet interfaces from the vehicle greatly increased the overall duct lengths.

TABLE 2

(U) MAIN THRUST CHAMBER FUEL-SIDE PRESSURE DROP, FULL-THRUST OPERATION

Engine Mixture Ratio	9		10		11		12		13	
	ΔP	P_{inlet}	ΔP	P_{inlet}	ΔP	P_{inlet}	ΔP	P_{inlet}	ΔP	P_{inlet}
Injector	405	1055	385	1035	365	1015	335	985	320	970
Nozzle-to-Injector Transfer Duct	16	1071	15	1050	14	1029	13	998	12	982
Nozzle Exit Manifold	67	1138	62	1112	56	1085	52	1050	43	1025
Nozzle Tube Bundle	68	1206	64	1176	60	1145	56	1106	52	1077
Inner Body to Nozzle	110	1316	101	1277	92	1237	84	1190	77	1154
Inner Body	535	1851	504	1781	468	1705	450	1640	424	1578
Crossover Duct	63	1914	67	1848	72	1777	80	1720	87	1665
Outer Body	196	2110	180	2028	170	1947	159	1879	150	1715
Baffle	194	2304	175	2203	156	2103	142	2021	131	1846

CONFIDENTIAL

TABLE 3

(U) MAIN THRUST CHAMBER FUEL-SIDE PRESSURE DROP, MINIMUM-THRUST OPERATION

Engine Mixture Ratio	9		10		11		12		13	
	ΔP	P_{inlet}	ΔP	P_{inlet}	ΔP	P_{inlet}	ΔP	P_{inlet}	ΔP	P_{inlet}
Injector	90	168	90	168	90	168	90	168	85	163
Nozzle-to-Injector Transfer Duct	0.8		0.7		0.6		0.5		0.4	
Nozzle Exit Manifold	1	170	1	170	1	170	1	170	1	164
Nozzle Tube Bundle	27	197	25	195	24	194	22	192	21	185
Inner Body to Nozzle	2	199	2	197	2	196	2	194	2	187
Inner Body	100	299	95	292	89	287	84	278	79	266
Crossover Duct	2	301	2	294	2	289	1	279	1	267
Outer Body	39	240	37	331	35	324	33	312	32	299
Baffle	30	370	27	358	24	348	23	335	22	321

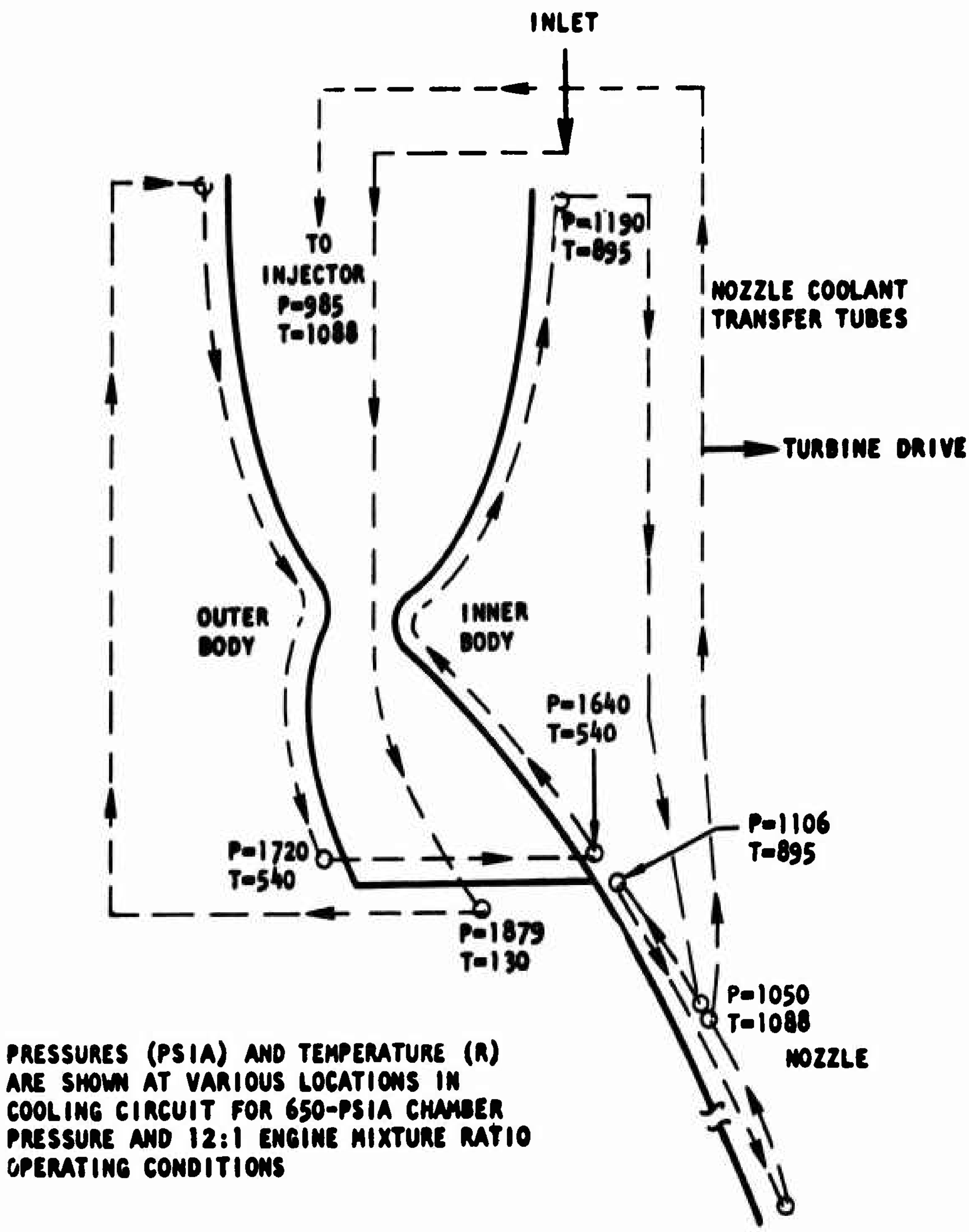

Figure 23. Main Engine Thrust Chamber Cooling Circuit (U)

CONFIDENTIAL

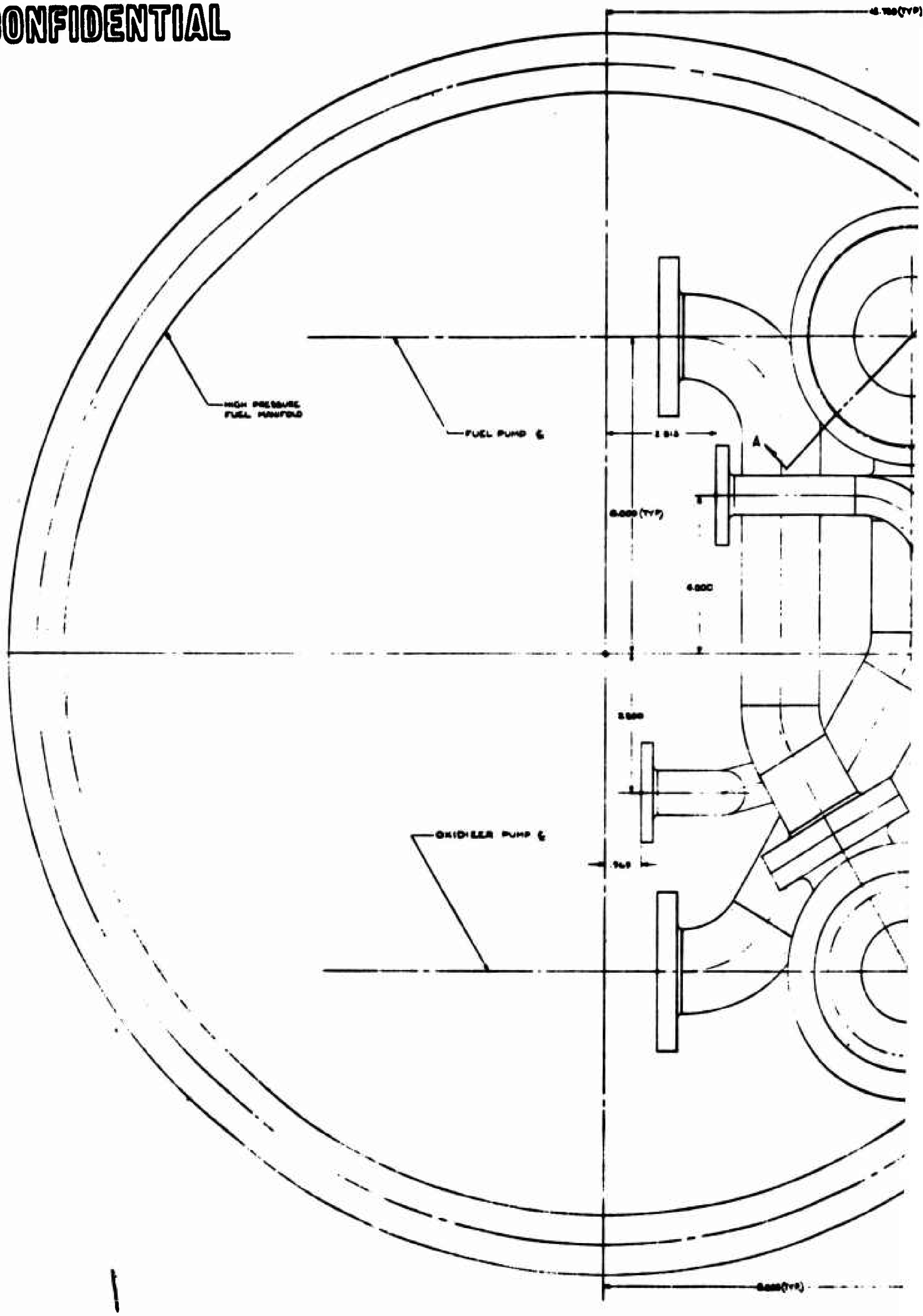

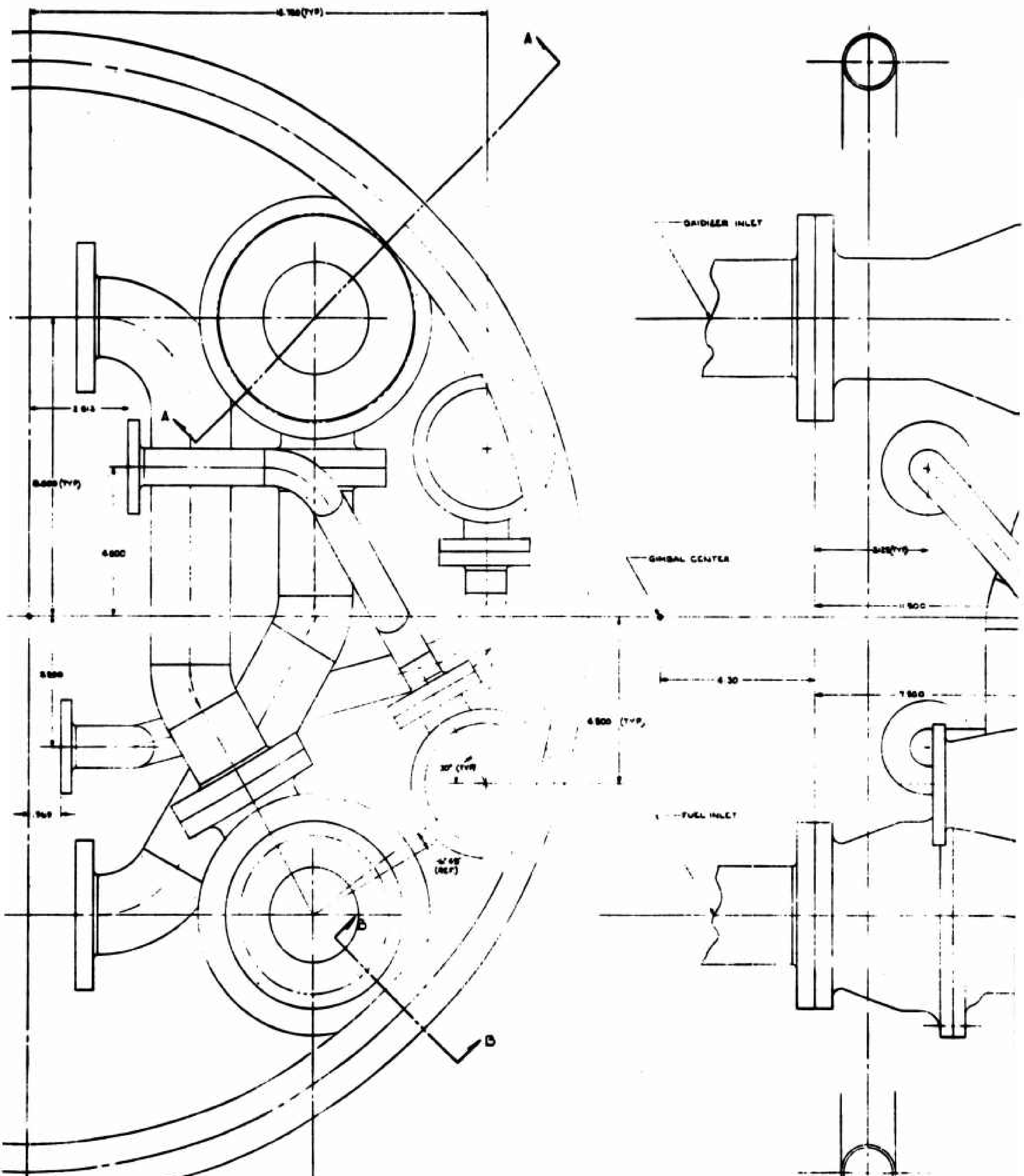

2

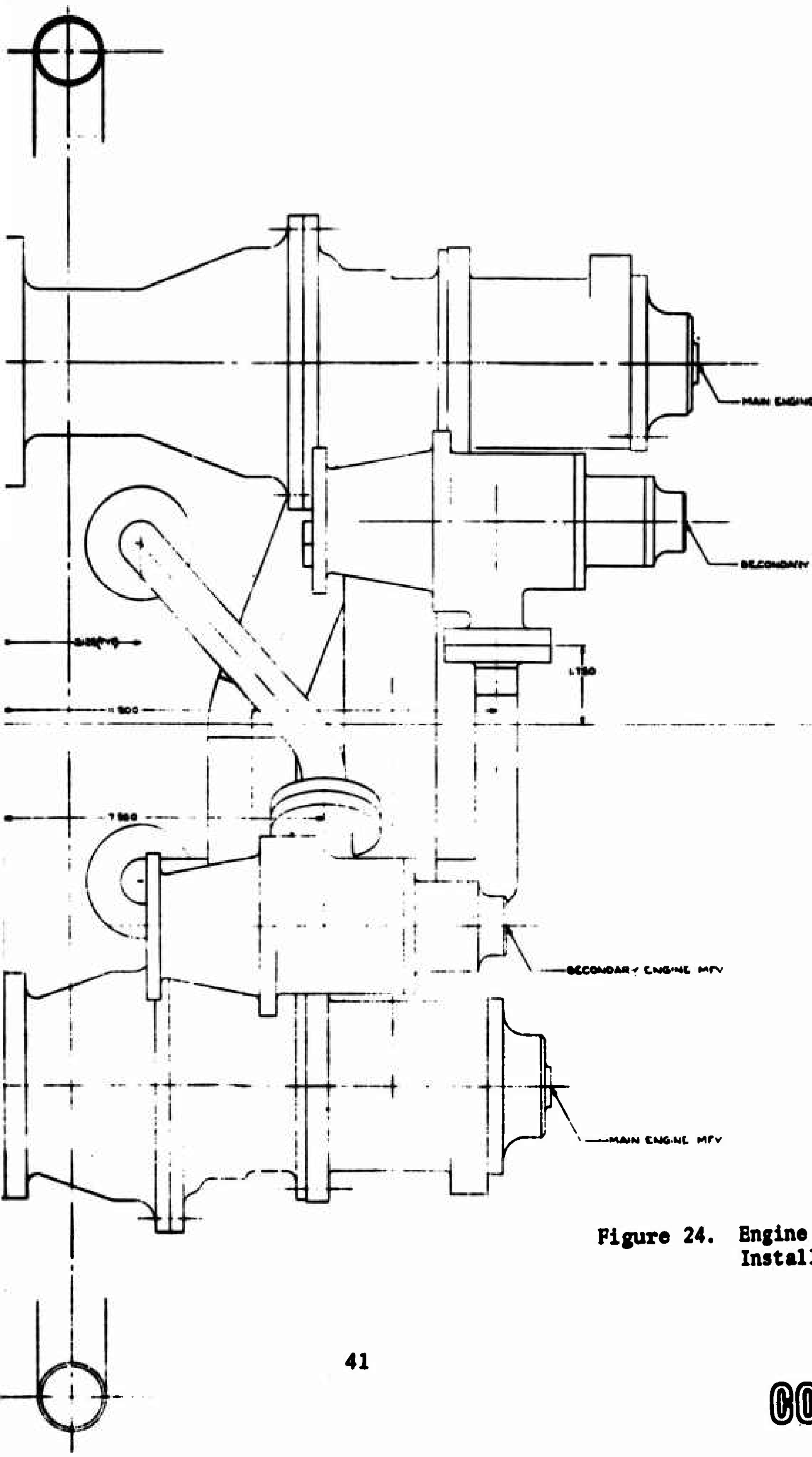

Figure 24. Engine Propellant Valve Installation (U)

3

(C) The valves will be mounted by low thermal conductive support structure minimizing the heat load into the valve. Detail layouts of the mounting structures and supports will be made as additional information (with respect to adjacent components and lines) is generated. Probable candidate materials to accomplish both functions is a composite structure of Rene' 41 and glass-reinforced epoxy resin.

(U) 3. TURBINE CONTROL VALVE LEAKAGE CRITICALITY

(C) The turbine control valve design specifications were established early in the Task I studies based on what was known at that time about engine system and component operating requirements. At that time, the maximum allowable leakage rate for the turbine control valve was specified as 500 standard cubic inches per minute (scim) of helium at 250-psia supply pressure. Recent design analysis studies on the turbine control valve have found this leakage requirement somewhat restrictive in design flexibility. It would have forced the design toward a poppet-type configuration and a relatively large valve envelope and greater engine packaging difficulty. A review of the preliminary turbine control valve design effort revealed this problem and it was decided to re-examine the turbine control valve leakage requirements based on the more detailed information presently available.

(C) A study of the main engine turbine control valves functions has indicated that valve through leakage is only critical during start and cutoff procedures and only on the oxidizer turbine control valve. The fuel turbine control valve is opened immediately after the start signal and the valve closing is the last function during the cutoff procedure; the main fuel valve is closed first. Therefore, leakage through the fuel turbine control valve (in the closed position) is not critical. The primary concern with the turbine control valve leakage is to avoid premature breakaway or rotation of the oxidizer pump before the oxidizer main valve is opened. Also, excessive turbine control valve leakage could cause a long oxidizer turbopump coast down time at cutoff. It is desirable to minimize this coast down time to avoid spinning the oxidizer pump at high rpm's without propellants in the pump.

(U) The results of the computerized engine start and cutoff model analysis were reviewed to obtain information that would aid in determining maximum allowable turbine control valve leakage and still avoid premature rotation of the oxidizer pump at start or long coast down times at engine cutoff.

(C) The engine start model results indicated that initial turbine inlet pressures to the oxidizer turbine are on the order of 5 psia. With this turbine inlet pressure, it would take approximately 0.006 lb/sec of hydrogen to break away the turbopump. The required starting torque was estimated by several methods including predicted bearing and seal friction loads from test experience, and data obtained from the turbine performance maps. The 0.006-lb/sec hydrogen flowrate is equivalent to an approximate helium leakage of 50,000 scim. Further analysis was performed to determine the influence of variations in turbine inlet pressure (or turbine control valve upstream pressure) and predicted turbopump starting torques. The results indicate that turbine control valve leakage rates of up to 50,000 scim of helium could be tolerated with no adverse effects during main engine start procedures.

(C) A similar type analysis was conducted to determine the criticality of the valve leakage with respect to the main engine cutoff. A review of the computer cutoff model analysis indicates that the oxidizer pump speed is reduced from its mainstage running speed to approximately 3000 rpm in a very short time, and this time is primarily controlled by the fact that the pump is loaded and producing a relatively high head during this period; leakage of relatively smaller turbine drive gas flowrates would not alter this pump speed/time profile. However, the coast time from 3000 rpm can be influenced by a continued (or leakage) flow of oxidizer turbine drive gas. This coast time was found to be a function of the turbopump rotating moment of inertia, the rolling friction and the leakage flowrates. A brief parametric study was conducted to determine the sensitivity of these parameters. It was found that for the estimated moment of inertia, and for rolling friction torques of approximately 2.0 in.-lb or greater, hydrogen leakage flows of 0.005 lb/sec and greater can be tolerated.

(C) These results indicate that turbine control valve leakage is not a critical item for the main engine system. Based on these findings, the design requirement value for the main engine turbine control valve leakage was increased to 5000 scim.

(C) A similar study was conducted for the secondary engine system. Because of the combustion chamber tapoff turbine drive gas system, turbine control valve leakage would not influence the cutoff operation. However, with the auxiliary helium turbine spin system used for a rapid engine start and the proposed start sequence, oxidizer turbine control valve leakage could cause premature rotation of the pump. Based on results from the cutoff model analysis and further analysis, it was found that leakage through this valve was even less critical than on the main engine. This is caused primarily by differences in the turbopump characteristics and the lower energy of the helium drive gas used during start.

(C) Therefore, leakage requirement specifications have been increased to 5000 scim on all of the turbine control valves.

(U) 4. MAIN ENGINE MAIN OXIDIZER VALVE ANALYSIS AND DESIGN

(C) Detailed definition of the valve design parameters was established for the valve poppet and seat to satisfy the cycle life and the 0.1-scim leakage requirement. These values are based on the review of results of previous oxidizer valve development programs and Rocketdyne experience on RPL-sponsored poppet and seat programs. Following are the design criteria established:

1. Radial motion of poppet relative to the seat with the poppet and seat in contact

    a. 0.001-inch maximum with cold-weldable materials

    b. 0.002-inch maximum with non-cold-weldable materials

(C) 2. Circumferential motion of the poppet relative to the seat with the poppet and seat in contact

a. 0.001-inch maximum with cold-weldable materials

b. 0.002-inch maximum with non-cold-weldable materials

3. Poppet and seat surface finish

a. 0.3-microinch arithmetic average

4. Poppet and seat flatness, including effects of seat installation loads, valve structural loads, and thermal effects

a. Flat within 10 microinches for a single-surface wave

b. Flat within 0.3 microinch for multiple-surface waves

5. Poppet and seat apparent stress under steady-state conditions

a. 500-psi minimum and 5000-psi maximum average stress

6. Sealing surface land width

a. An effective flat land width of 0.018 inch on a 3-inch diameter

(C) Formal layout of the main engine oxidizer valve was initiated using the above-listed detailed design parameters and is shown in Fig. 25. The seating material selected for the valve was titanium carbide. The seat closure will be welded instead of gasketed, and is flexure mounted. Metal-plated Naflex seals were selected for all sealing surfaces in the valve and at the valve interfaces. To reduce valve envelope requirements further, and to simplify the design, the final actuator design incorporates a single-acting pneumatic actuator to open the valve. Valve closing is provided by spring force and pressure difference across the poppet.

(U) 5. MAIN ENGINE TURBINE CONTROL VALVE ANALYSIS AND DESIGN

(C) The valving element for the main engine turbine control valve was reselected based on review of the preliminary design requirements for leakage and valve response. A ball-type valving element was selected as a result of

CONFIDENTIAL

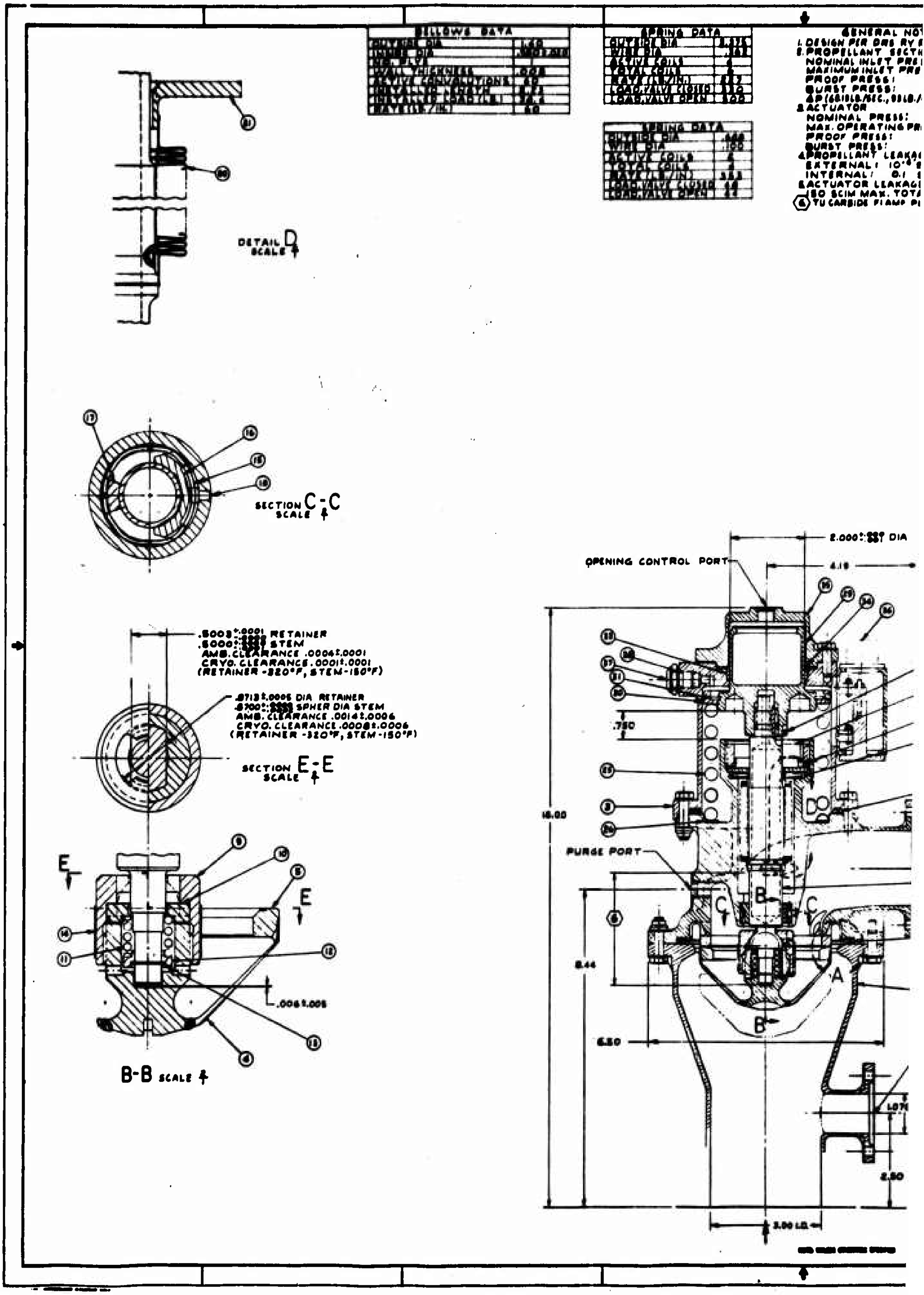

BELLOWS DATA	
OUTSIDE DIA	1.60
INSIDE DIA	[illegible]
NO. PLYS	[illegible]
WALL THICKNESS	.005
ACTIVE CONVOLUTIONS	40
INSTALLED LENGTH	[illegible]
INSTALLED LOAD (LB)	[illegible]
RATE (LB/IN)	60

SPRING DATA	
OUTSIDE DIA	[illegible]
WIRE DIA	[illegible]
ACTIVE COILS	4
TOTAL COILS	6
RATE (LB/IN)	[illegible]
LOAD, VALVE CLOSED	[illegible]
LOAD, VALVE OPEN	[illegible]

SPRING DATA	
OUTSIDE DIA	.468
WIRE DIA	.100
ACTIVE COILS	4
TOTAL COILS	6
RATE (LB/IN)	[illegible]
LOAD, VALVE CLOSED	[illegible]
LOAD, VALVE OPEN	[illegible]

GENERAL NOT
1. DESIGN PER DRG RY
2. PROPELLANT SECTI
NOMINAL INLET PRE
MAXIMUM INLET PRE
PROOF PRESS:
BURST PRESS:
ΔP (6.81 LB/SEC.,
3. ACTUATOR
NOMINAL PRESS:
MAX. OPERATING PR
PROOF PRESS:
BURST PRESS:
4. PROPELLANT LEAKA
EXTERNAL: 10^{-6}
INTERNAL: 0.1
5. ACTUATOR LEAKAG
150 SCIM MAX. TOT
6 TU CARBIDE FLAME P

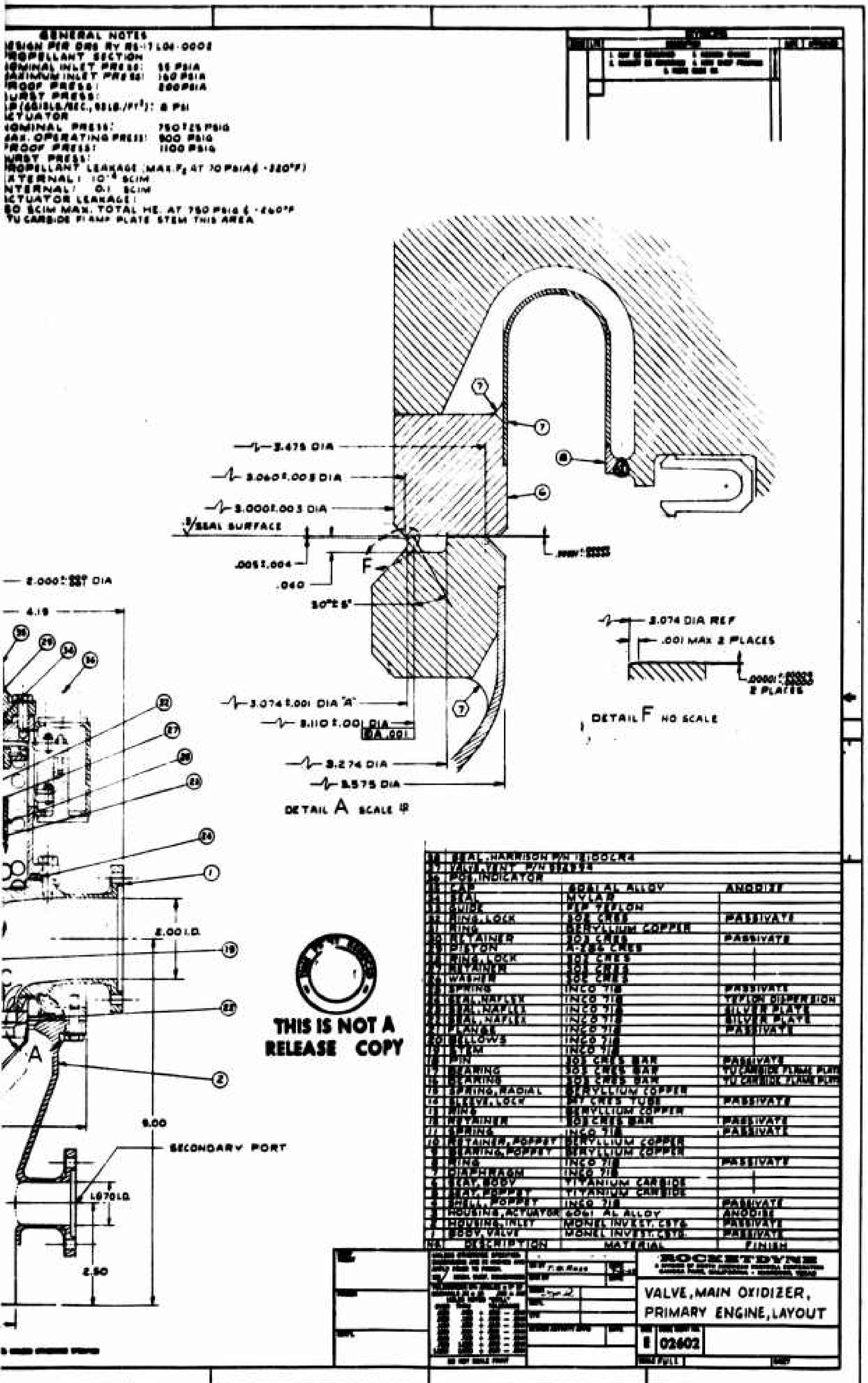

Figure 25. Main Engine Oxidizer Valve (U)

(C) new values established for internal leakage rate and valve response time (5000 scim and 1 second, respectively). These values are based on a more detailed analysis and their use will not result in any degradation in system performance.

(C) The preliminary layout of the turbine control valve incorporating the ball valving element is complete, as shown in Fig. 26. The valve has a single metal bellows seal on the upstream side. The electrically driven rotary actuator is directly coupled to the ball shaft to reduce the valve envelope. The design is currently being fitted into the engine system layout to check interface compatibility and to ensure the most efficient integration into the system, minimizing space requirements.

(C) The area versus thrust curve for the fuel turbine control valve is shown in Fig. 27 . This curve was prepared from earlier engine system data. An ideal thrust versus stroke curve was generated from control systems considerations and is shown in Fig. 28. The criterion applied to generate this curve was that control loop gain should be as constant as possible. The resulting linear characteristic curve has the disadvantage that a 1-percent nonlinearity of nominal thrust becomes a 9-percent nonlinearity at minimum thrust for a 9 to 1 throttling engine. An alternative is shown by the equal percentage curve, which has the property that a nonlinearity expressed as a percent of nominal is the same percentage of the current operating level, thus improving chances of maintaining a specified thrust accuracy over the entire thrust range. By combining both curves and eliminating thrust, an area versus stroke curve can be obtained. Additional refinements will be made to these data; however, the approach is to use the area versus stroke or rotation (ball-type valve) relationships thus generated to shape the ball passage in the turbine control valve design to achieve the required throttling characteristic.

CONFIDENTIAL

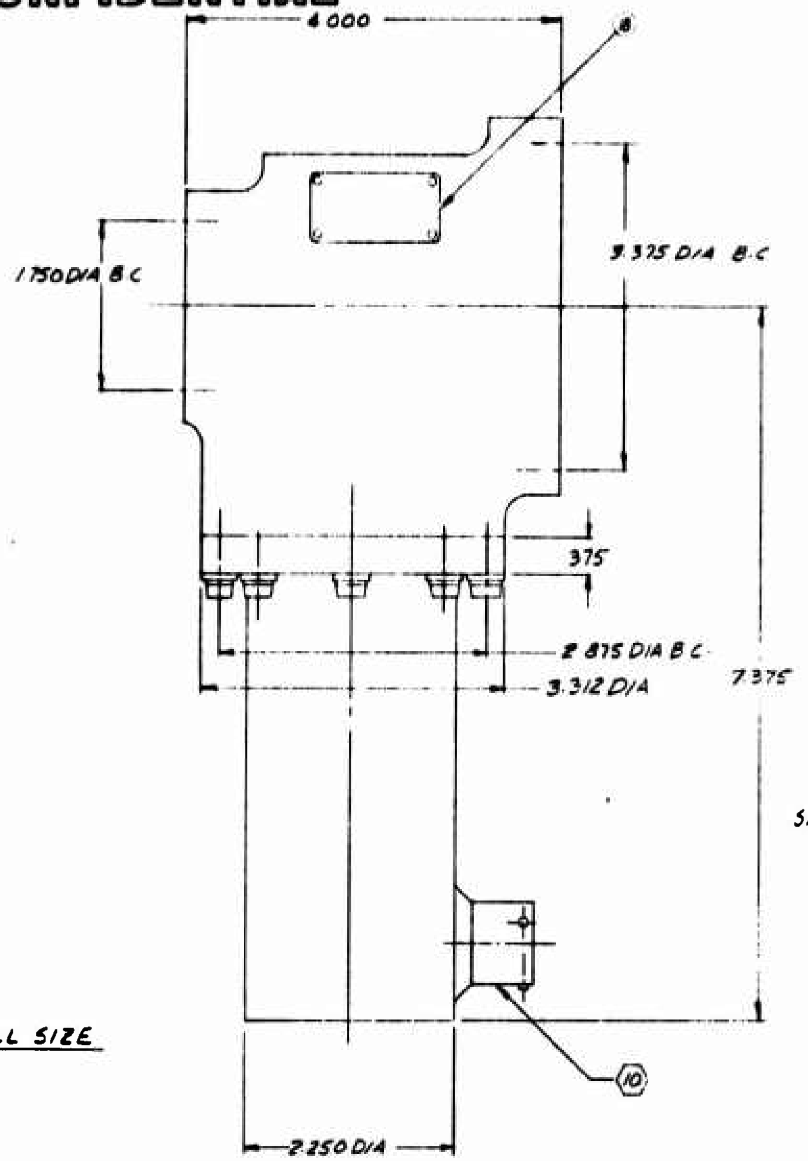

FULL SIZE

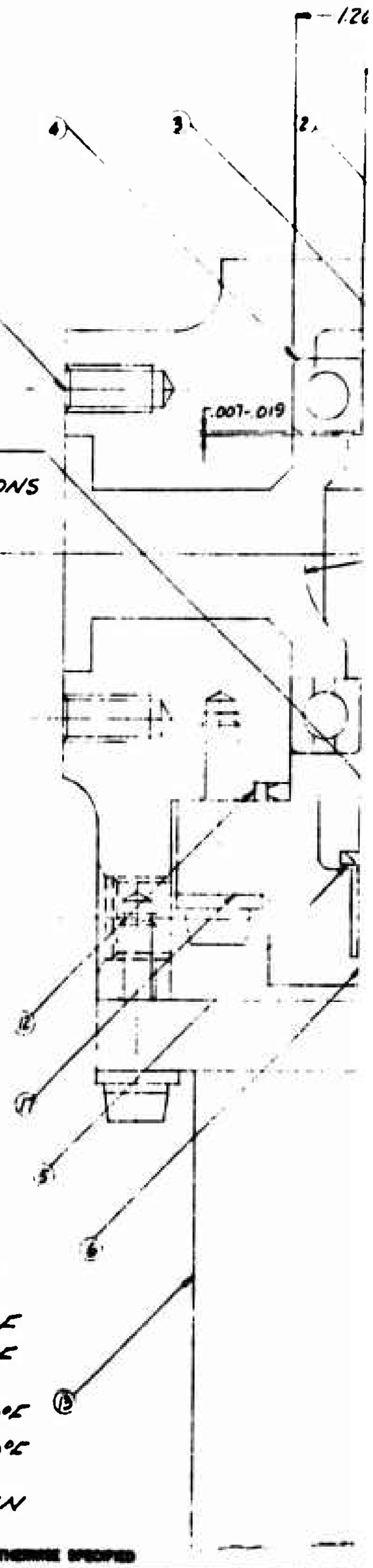

12. DESIGN PER DRS RY RS-17 L04-00003

(11) SIMILAR TO 550176

(10) SIMILAR TO RD 414-8003-1398
EXCEPT USE BRAZEABLE CONTACTS

(9) SIMILAR TO MRC 201-S

(8) HARRISON MFG CO. BURBANK, CALIF

(7) SIMILAR TO NAS 1102-08-10

(6) SIMILAR TO RD 111-3006-1014

(5) SIMILAR TO RD 111-3006-1013

4. ALLOWABLE SHAFT SEAL LEAKAGE-7SCIM
ALLOWABLE BALL SEAL LEAKAGE-5000SCIM

3. MAXIMUM INLET PRESS. 163 PSIA @ 1500°F
MAXIMUM OUTLET PRESS 14 PSIA @ 1500°F

2. MAXIMUM INLET PRESS. 1055 PSIA @ 650°F
MAXIMUM OUTLET PRESS. 300 PSIA @ 650°F

1. OPERATING MEDIUM - GASEOUS HYDROGEN

15. MAX. BALL TO MOTOR MISALIGNMENT
± 5°

14. BURST PRESS - PSIG

13. PROOF PRESS - PSIG

NOTE: UNLESS OTHERWISE SPECIFIED

ACTUATOR CHARACTERISTICS	
RUNNING TORQUE	15 IN-LBS
STALL TORQUE	60 IN-LBS
MAX TRAVEL	90°
SLEW RATE	1.0 SEC
HORSE POWER	.0036
DUAL POTENTIOMETER	
EACH POT.	0.3K TO 5K
FIXED PHASE VOLTAGE	110VAC 400~

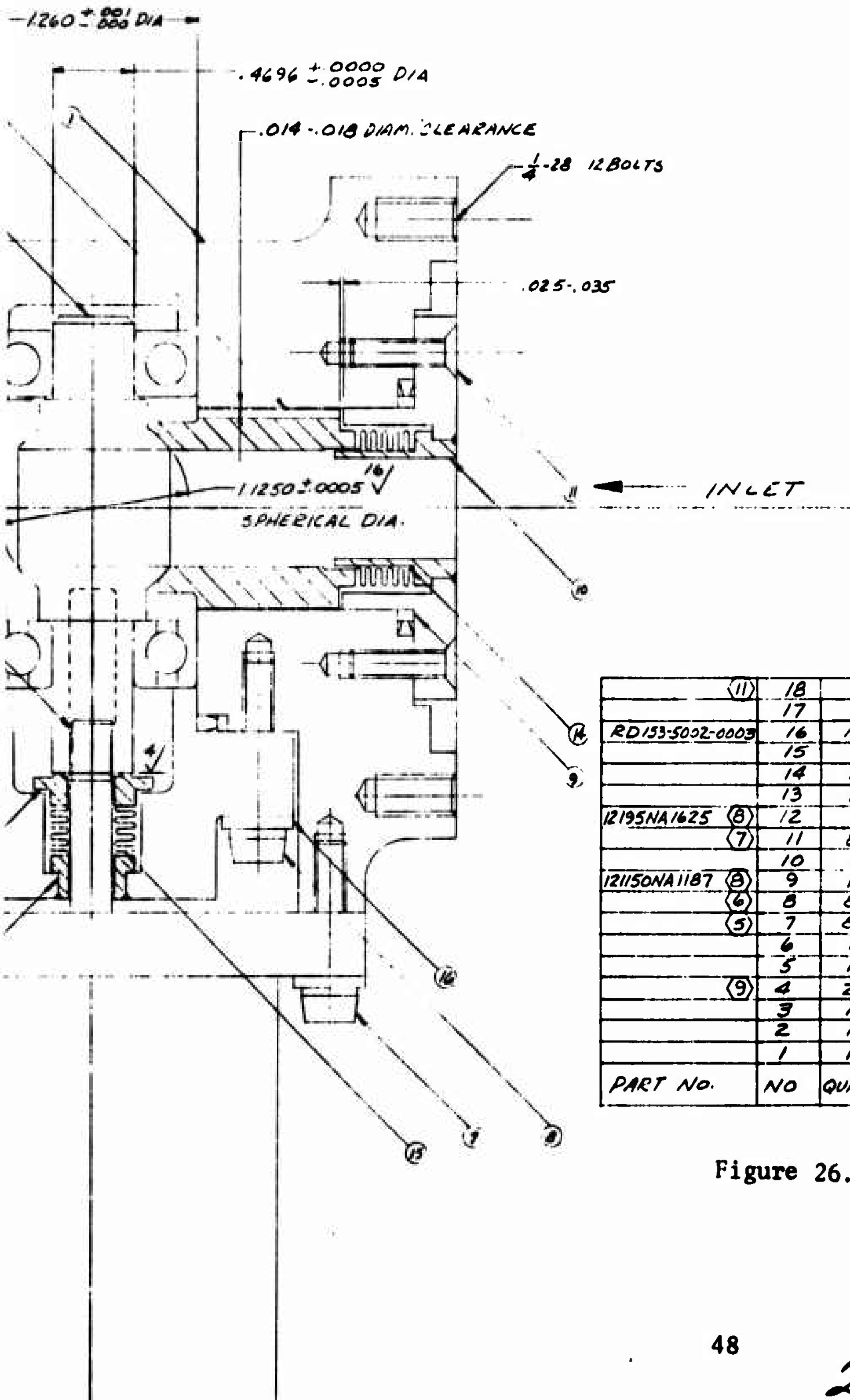

BELLOWS DATA		
PART NO.	(14)	(15)
OUTSIDE DIA	.930	.470
INSIDE DIA	.690	.310
WALL THICKNESS	.005	.005
ACTIVE CONV.	8	7
INST. LENGTH	.375	.281
LOAD @ INST LGTH (LBS)	10	30
RATE (LBS/IN)	250	400

BEARING LOADS (LBS)		
TEMPERATURE °F	650	1500
RADIAL	107	14
THRUST	36	2

PART NO.	NO	QUANT.	DESCRIPTION	MATERIAL	FINISH
(11)	18	1	NAMEPLATE	302 CRES	PASSIVATE
	17	1	CAP	INCO 718	PASSIVATE
RD153-5002-0003	16	16	WASHER	A 286	PASSIVATE
	15	1	FORMED BELLOWS	INCO 625	PASSIVATE
	14	1	FORMED BELLOWS	INCO 625	PASSIVATE
	13	1	AC ELECT. ACTUATOR	COMMERCIAL	——
12195NA1625 (8)	12	1	K SEAL 12195	INCONEL X 750	GOLD PLATED
(7)	11	8	SCREW (8-32)	RENE 41	PASSIVATE
	10	1	RETAINER	INCO 718	PASSIVATE
121150NA1187 (8)	9	1	K SEAL 121150	INCONEL X 750	GOLD PLATED
(6)	8	8	BOLT (10-32)	RENE 41	PASSIVATE
(5)	7	8	BOLT (10-32)	RENE 41	PASSIVATE
	6	1	RETAINER	INCO 718	PASSIVATE
	5	1	SEAL	INCO 718	FLAME PLATE
(9)	4	2	BALL BEARING	STELLITE	PASSIVATE
	3	1	SHAFT	RENE 41	PASSIVATE
	2	1	SEAL	INCO 718	FLAME PLATE
	1	1	HOUSING	INCO 718	PASSIVATE

Figure 26. Main Engine Fuel Turbine Throttle Valve (U)

2 CONFIDENTIAL

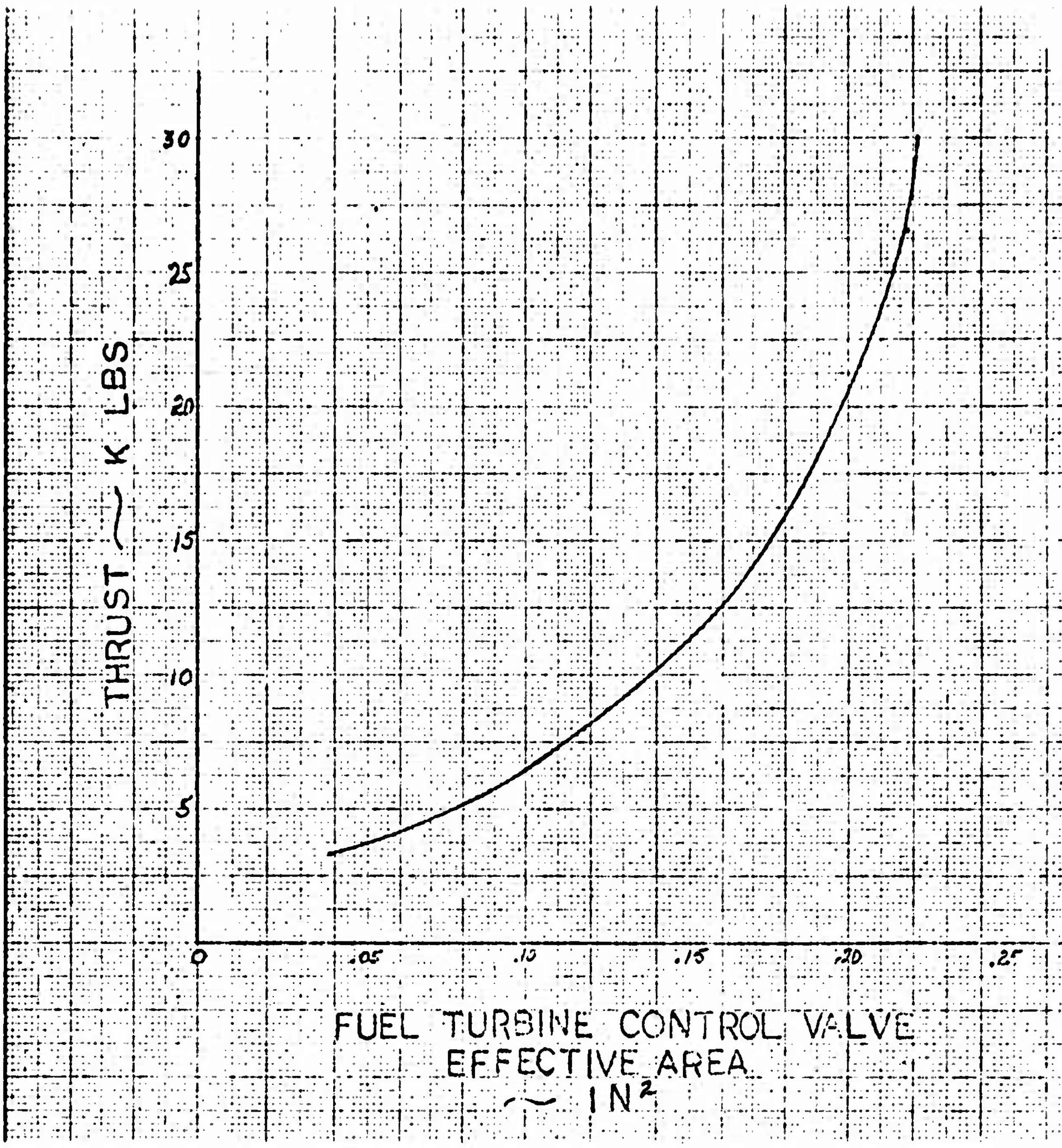

Figure 27. Main Engine Fuel Throttle Valve Area vs Thrust Level (U)

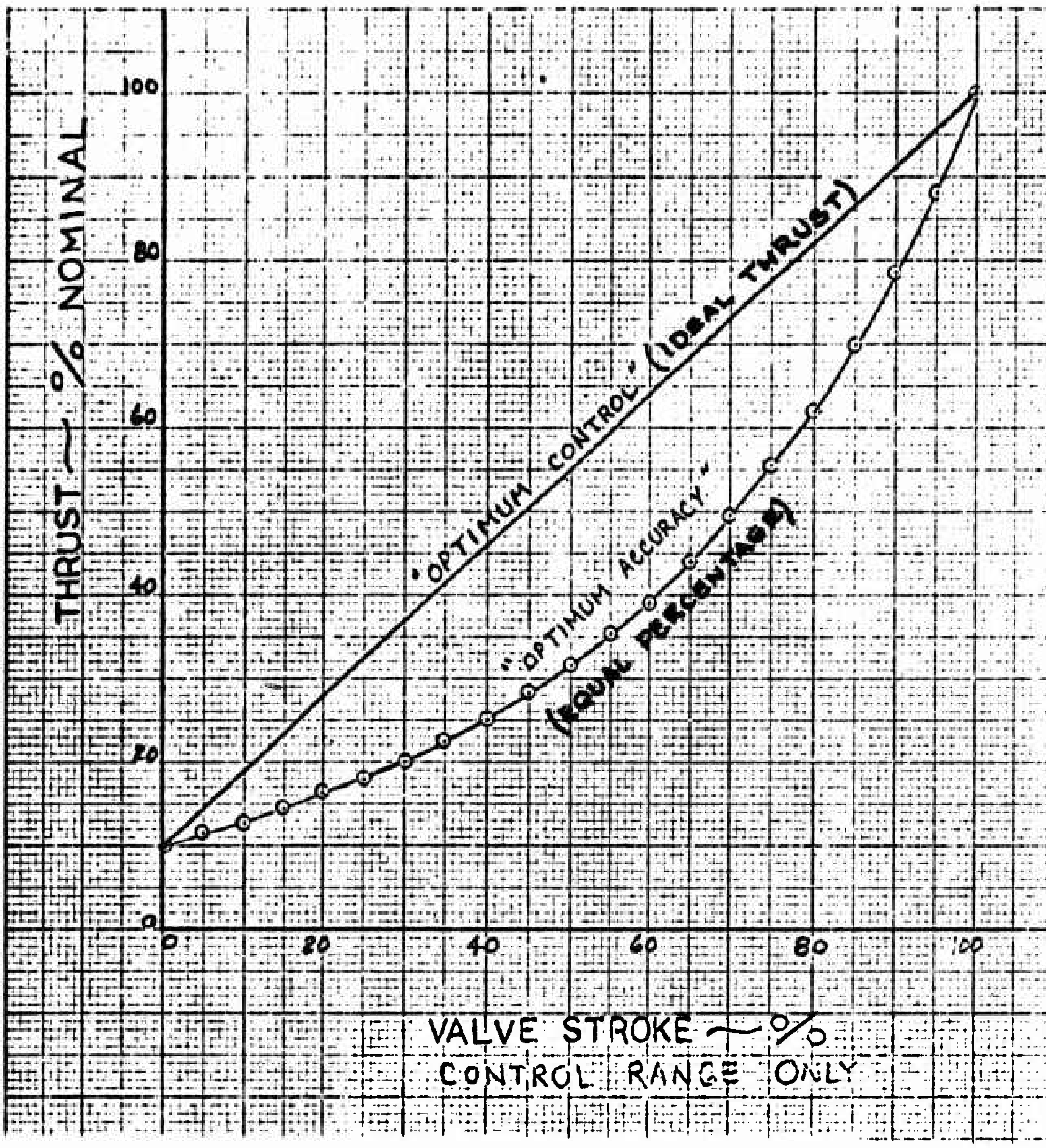

Figure 28. Ideal Thrust vs Valve Stroke Curves, Optimum Control and Equal Percentage Curves (U)

(U) 6. SECONDARY ENGINE CONTROL SYSTEM ANALYSIS AND DESIGN

(C) Similar controls for the thrust and mixture ratio control to those of the main engine were developed for the secondary engine. This was done by computing the turbomachinery time constants using the formula:

$$w = 60\ T/2\ \pi\ I\ N$$

where w is the turbomachinery lag frequency (radians per second). T is the torque at the operating level (in.-lb), π = 3.14159, I is the inertia of the rotating parts (in.-lb-sec^2), and N is the operating level speed (rpm). The following computed values of w were used in the analysis:

	Oxidizer Turbopump	Fuel Turbopump	Ratio
Primary Engine	9.08 rad/sec	3.18 rad/sec	2.86
Secondary Engine	4.00 rad/sec	1.70 rad/sec	2.35

(U) Therefore, it is to be expected that system gain figures and frequencies will be lower than those of the main engine.

(C) At this point, it was decided that available transient analysis data for the main engine should be analyzed as to frequency content and approximated Laplace rational functions. The reason behind this was to determine how the turbomachinery natural frequencies enter into the engine response characteristics required in the generation of a closed-loop design. The 30-percent thrust level was selected as representative.

(C) Two digital computer programs were utilized, a program to convert time response data to frequency response data (CONVOLUTION), and a program to fit frequency response data with rational Laplace functions (GOODFIT). There are four transfer functions to be determined: the change in chamber pressure with change in the fuel turbine valve area, the change in mixture ratio with change in the fuel turbine valve area, the change in

(C) chamber pressure with change in the oxidizer turbine valve area, and the change in mixture ratio with change in the oxidizer turbine valve area. The frequency response curves, together with the fitted transfer function curves, are shown in Fig. 29 and 30 for the fuel throttle valve, and in Fig. 31 and 32 for the oxidizer throttle valve.

(C) The four transfer functions determined were:

$$d\, P_c/dA_{FTV} = \frac{0.335\ (s - 0.143)}{s^2 + 1.7\ s + 1.2}$$

$$d\, MR/dA_{FTV} = \frac{-6.86}{s + 3.43}$$

$$d\, P_c/dA_{OTV} = \frac{1.42}{s + 1.28}$$

$$d\, MR/dA_{OTV} = \frac{8.39\ (s + 0.563)}{(s + 0.892)\ (s + 5.84)} = \frac{8.38}{(s + 9.25)}$$

where

FTV = fuel throttle valve
OTV = oxidizer throttle valve

(C) For the last transfer function listed, a first-order approximation to the function is made for comparison purposes. It can be seen that the response frequencies are related in the following way. The frequencies in the mixture ratio transfer functions are directly related to the turbomachinery time constants (9.08 as compared to 9.25 oxidizer, and 3.18 as compared to 3.43 fuel). The chamber pressure transfer function responses show frequencies slightly higher than the power level (30 percent) times the slower of the two turbopump frequencies (the fuel at 3.18 rad/sec).

(C) Based on these observations, the extrapolation can be made from the main engine to the secondary engine. Reference is made to the control schematic shown in Fig. 33. It is assumed that loop gains may stay the same to obtain equivalent response characteristics; this means that only those factors that have the dimension of time (or its reciprocal) need

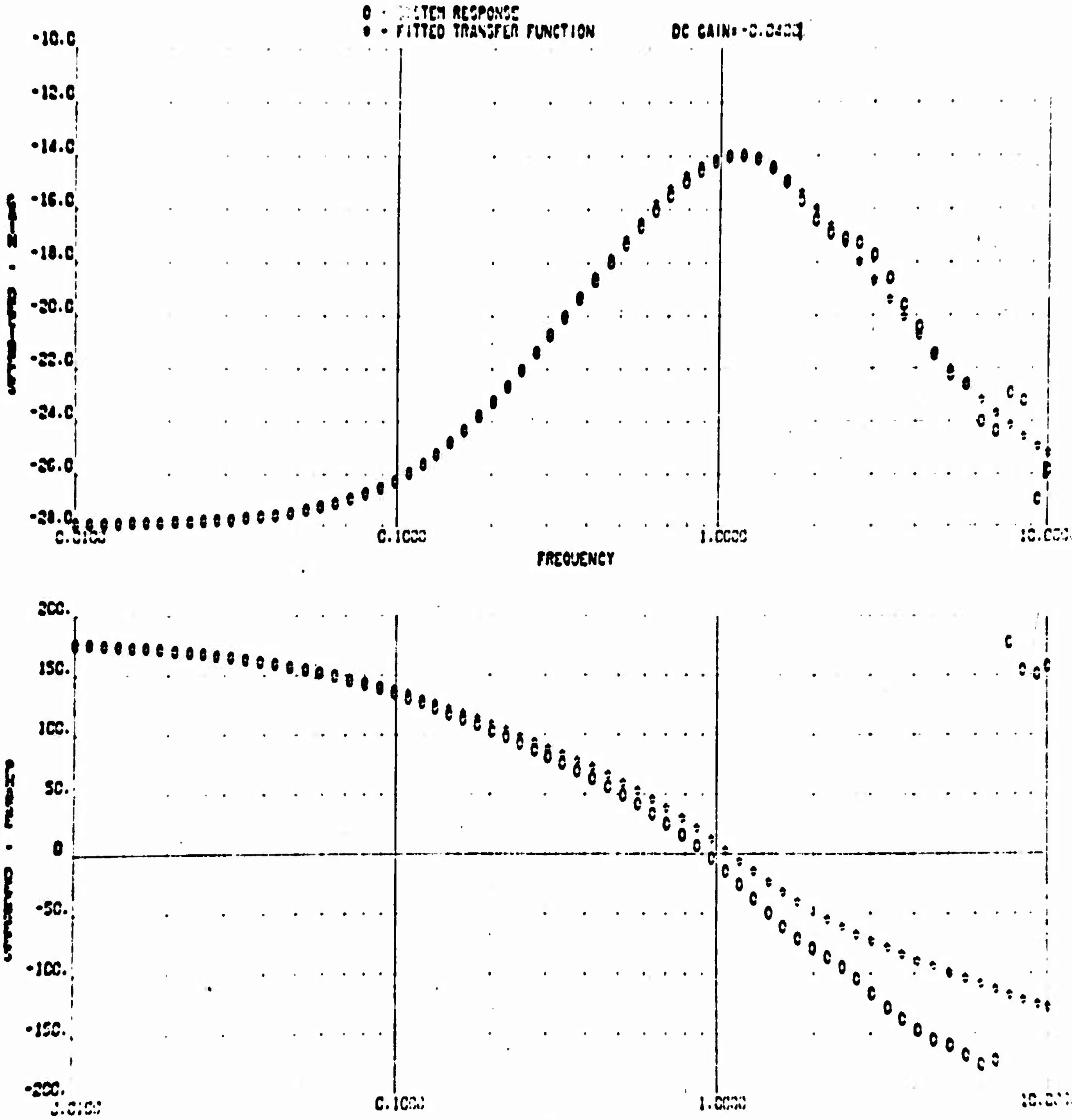

Figure 29. Chamber Pressure as a Function of Fuel Throttle Valve Area (U)

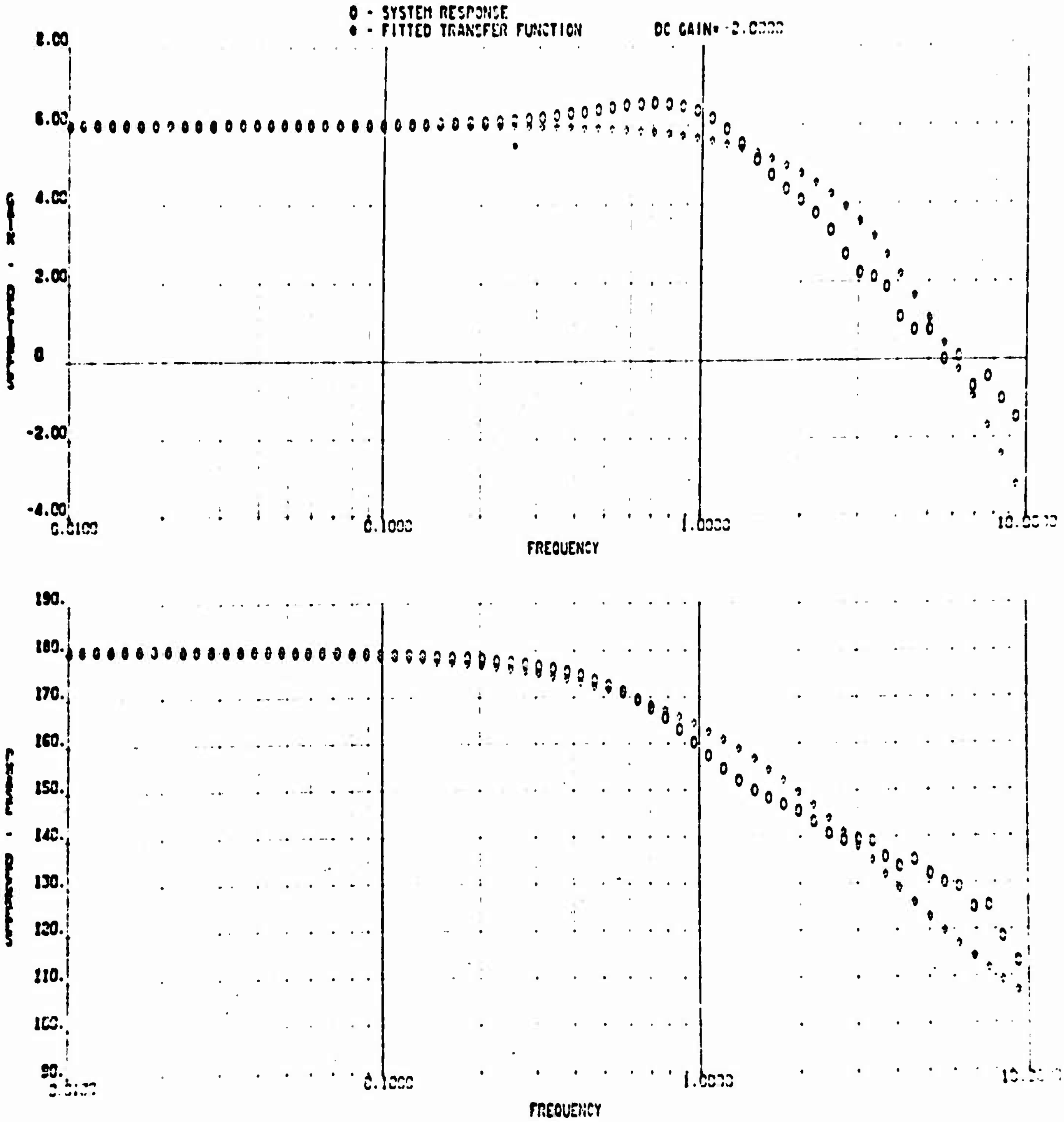

Figure 30. Mixture Ratio as a Function of Fuel Throttle Valve Area (U)

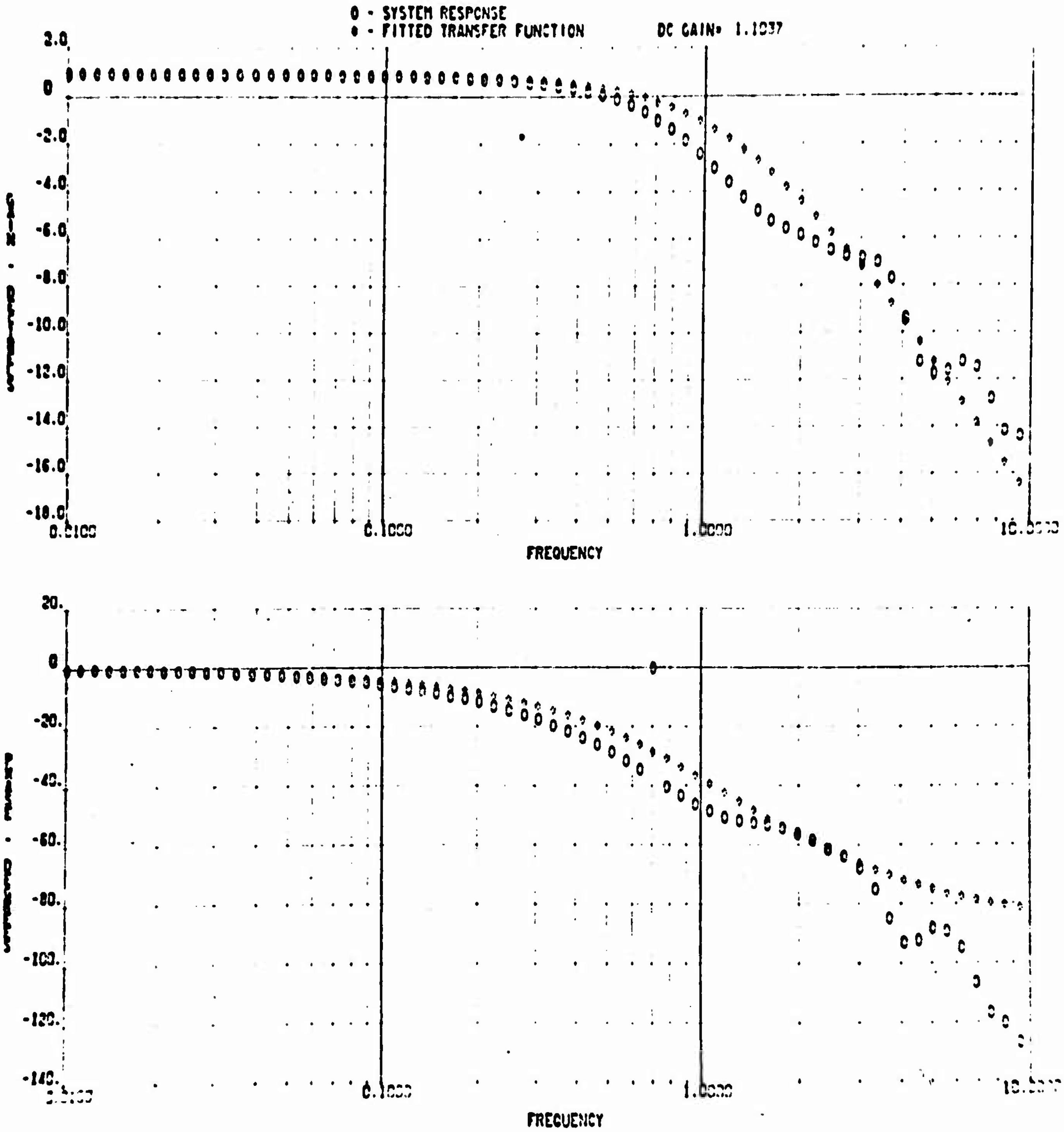

Figure 31. Chamber Pressure as a Function of Oxidizer Throttle Valve Area (U)

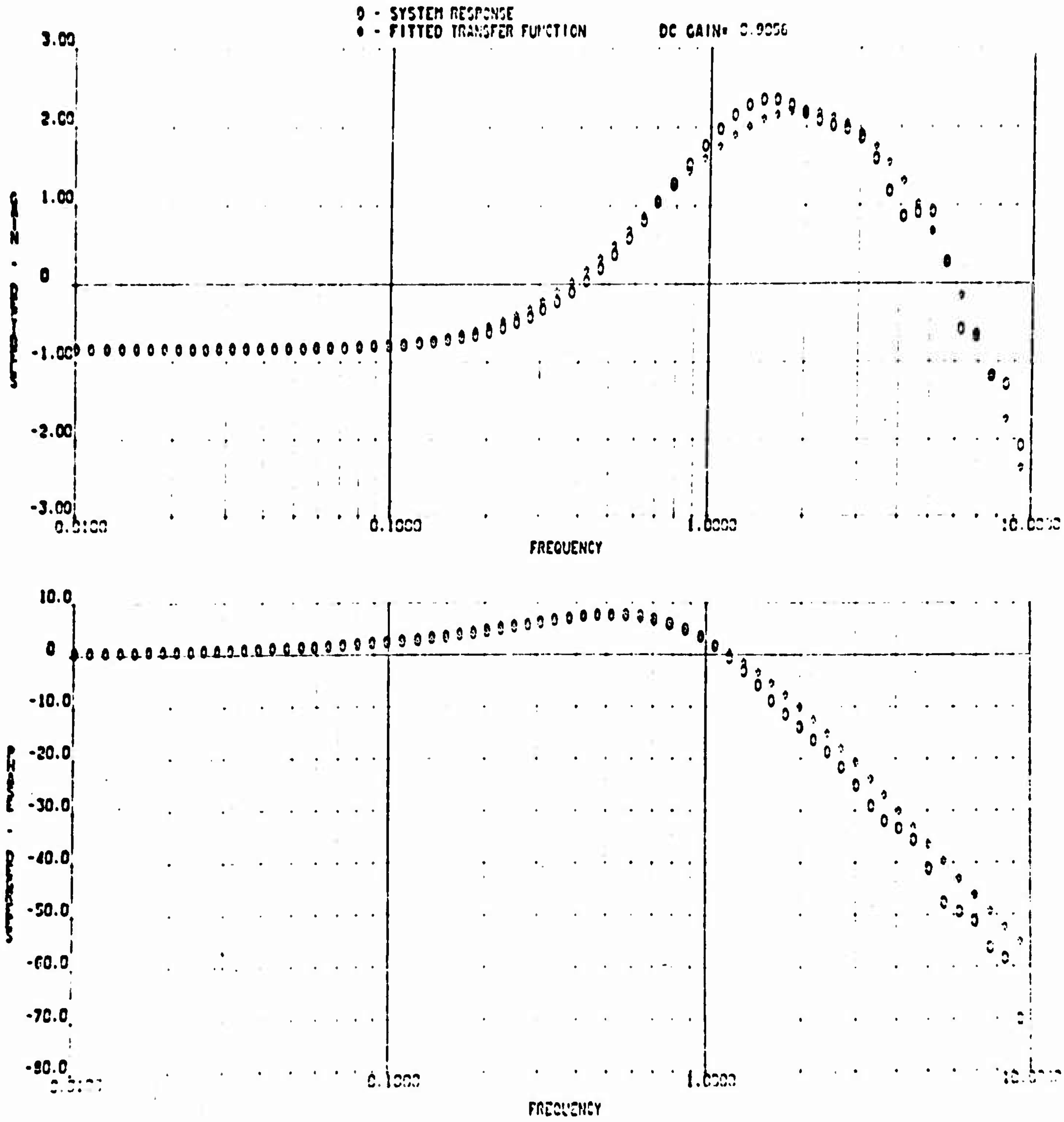

Figure 32. Mixture Ratio as a Function of Oxidizer Throttle Valve Area (U)

(C) be changed. By this reasoning, K_3 should be the same for both engines because the ratio of the turbomachinery time constants is approximately the same. The factors that will vary are K_2, K_5, and τ_2 and, of course, the numerator time constant of the cross-transfer function.

(C) The numerator time constant is the reciprocal of the oxidizer turbopump frequency or 1/4 (=0.25). The value for τ_2 and for K_2 will be directly related to the ratio of the fuel turbomachinery time constants for the main engine to the secondary engine (or 1.7/3.18) or about one-half the values for the main engine. The value for K_5 will be directly related to the ratio of the oxidizer turbomachinery time constants for the main engine to the secondary engine (or 4.00/9.08) or four-ninths the value for the main engine. These values are reflected in the schematic of Fig. 33 and the values of control constants of Fig. 34.

(U) Some corroboration of this extrapolation was made by comparing time constants observed in some preliminary analog computer model runs of the secondary engine to those in this control system. Correspondence was judged to be adequate.

(U) 7. CONTROLS SPECIFICATIONS AND REPORTS

(U) Preliminary specifications for components of the pneumatic control system for the main and secondary engine were revised to reflect refinements made to engine pneumatic requirements as a result of further analysis of system requirements. These revised specifications, together with the turbine spin valve design requirement specification, are in review prior to publication.

(U) The following reports were reviewed during this report period:

AFRPL-TR-68-32, "Wide Range Flow Control Program," F. Merritt, L. Dumont, December 1968.

AFRPL-TR-68-22, "Final Report on the Development of Analytical Techniques for Bellows and Diaphragm Design," T. M. Trainer, L. E. Hulbert, J. F. Lesting, R. E. Keith, March 1968.

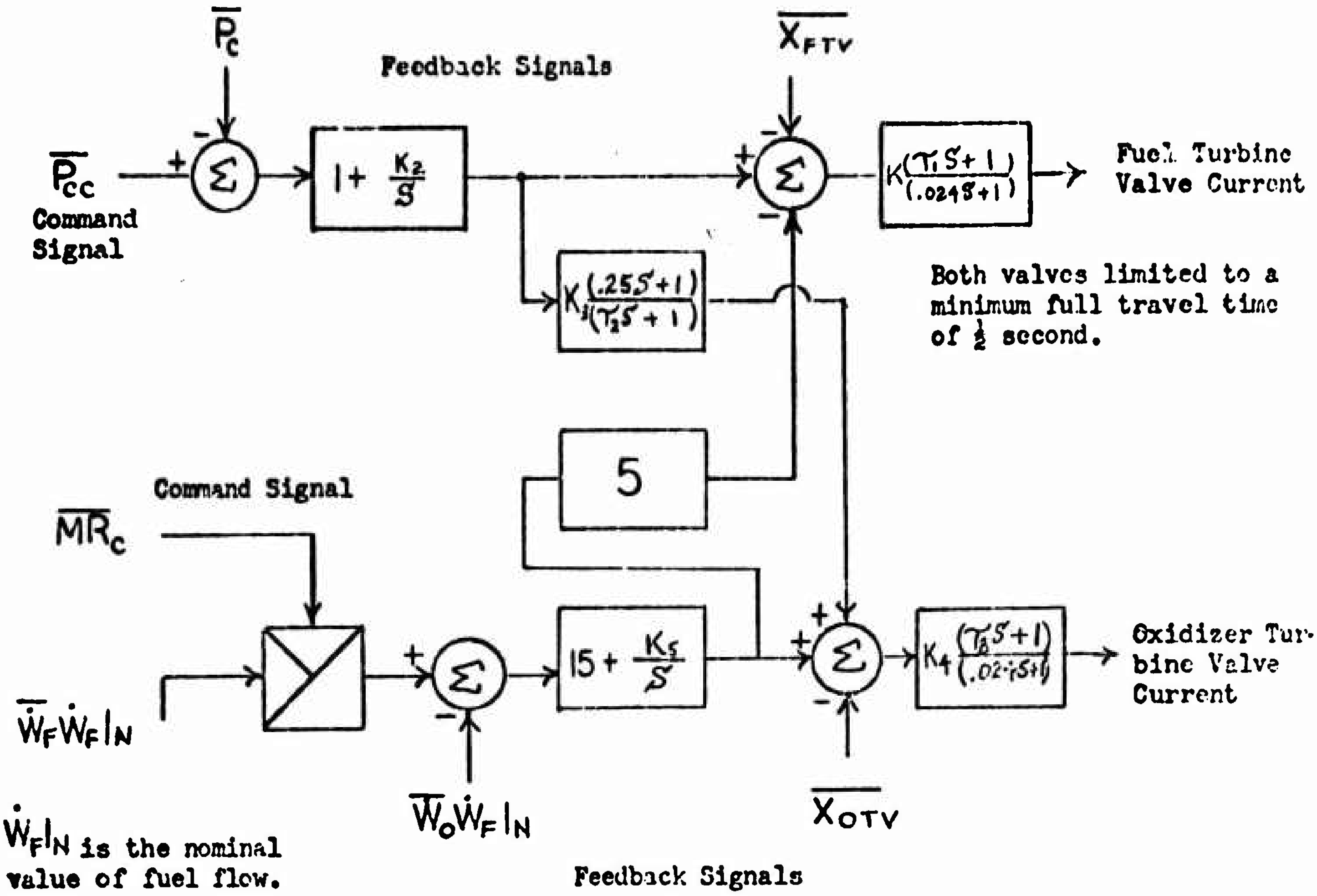

$$K_1 = \frac{21.6\ X_{FTV}|_N}{K_{FTV}}$$

$$K_4 = \frac{21.6\ X_{OTV}|_N}{K_{OTV}}$$

$$\boxed{\begin{array}{l} K_1 = K_4 = .216 \\ \tau_1 = \tau_3 = .024 \end{array}}$$

K_{FTV} = Fuel Turbine Valve Slew Rate Response to Current

τ_1 = First Order Approximation to Fuel Turbine Valve Time Constant (Small Signal)

K_{OTV} = Oxidizer Turbine Valve Slew Rate Response to Current

τ_3 = First Order Approximation to Oxidizer Turbine Valve Time Constant (Small Signal)

Note: Barred variables refer to decimal fractions of nominal value, as $\overline{P_c}$ may take on values from 0 to 1.0 (or more).
The $'_N$ designation means nominal value.

Figure 33. Control System Compensation for Secondary Engine (U)

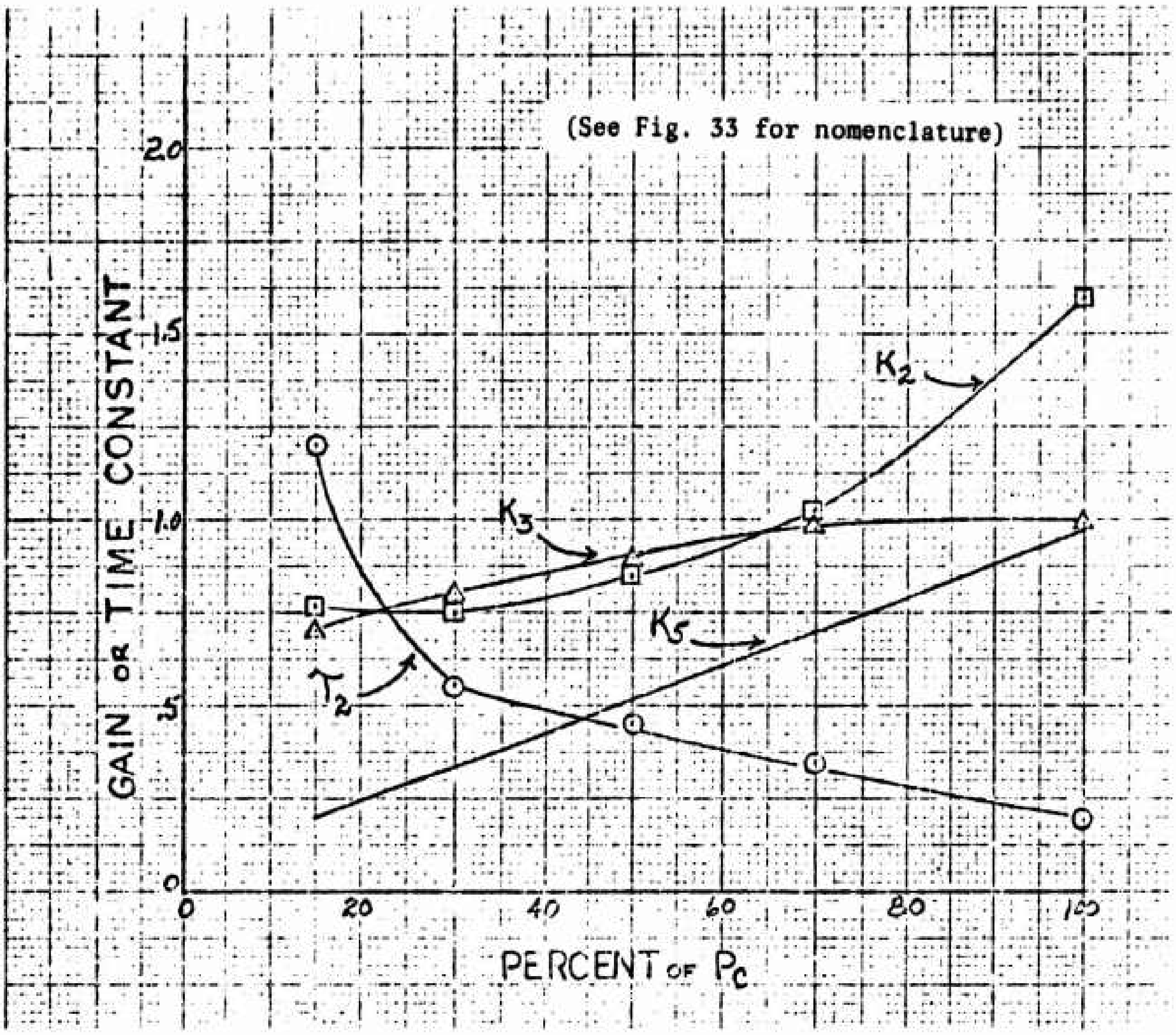

Figure 34. Compensation Parameters as a Function of Power Level (U)

(U) TASK II--CRITICAL COMPONENT DEMONSTRATION TESTING

(C) The objectives of this task are to design, fabricate, and test critical engine component hardware to determine performance and demonstrate solutions to potential design and fabrication problems. The critical components include segments of the main thrust chamber, complete main thrust chamber assembly, and seals and bearings for the LF_2 pumps. Progress was made in the following areas:

1. Design and fabrication of main thrust chamber assembly components
2. Design and fabrication of the nozzle extension and base closure that will contain a secondary thrust chamber simulation
3. Design and fabrication of a reduced size, 5-inch, water-cooled segment chamber and injector
4. Design and fabrication of the prototype, regeneratively cooled, 30-degree segment chamber and injector
5. Fabrication of the main and secondary, and test of the main, engine LF_2 pump bearing and seal testers

(U) 1. THRUST CHAMBER SEGMENT DESIGN AND FABRICATION

(C) Design and fabrication effort during this quarterly period was concentrated on the 30-degree, prototype segment and preliminary manufacturing effort on the 360-degree thrust chamber segments and injector segments. A complete summary of the segment hardware design, fabrication, and test status is presented in Table 4 .

(U) a. 30-Degree Prototype Segment Chamber Design

(C) The selected design for the 30-degree prototype thrust chamber segment consists of a channel-wall chamber utilizing a single-pass cooling circuit. The design has a 3.5-inch length, from injector face to throat plane, G_c contour combustion chamber.

TABLE 4

(U) AMPT PROGRAM TASK II THRUST CHAMBER DESIGN, FABRICATION, AND TEST STATUS

	Design	Fabrication	Test Status
5-Inch Water-Cooled Chamber Segment (G_c) U/N 1	Complete	Complete	46 tests, slight throat erosion; 8 additional tests, shortened combustion zone, throat erosion, nonrepairable
5-Inch Water-Cooled Chamber Segment (G_c) U/N 1	Complete	Complete	7 tests, throat melted (lack of coolant water)
5-Inch Water-Cooled Chamber Segment (K) U/N 1	Complete	Complete	17 tests, no damage
5-Inch Water-Cooled Chamber Segment (G) U/N 1 (Reduced Size)	80-percent Complete	50-percent Complete	No tests to date
5-Inch Triplet Injector Segment, U/N 1	Complete	Complete	3 tests, face overheated, nonrepairable
5-Inch Triplet Injector Segment, U/N 2	Complete	Complete	4 tests, face overheated, nonrepairable
5-Inch Triplet Injector Segment, U/N 3	Complete	Complete	10 tests, structural failure of injector, nonrepairable
5-Inch Fan Injector Segment, U/N 1	Complete	Complete	17 tests, face overheated, nonrepairable
5-Inch Fan Injector Segment, U/N 2	Complete	Complete	14 tests, damaged on test 051, nonrepairable
5-Inch Injector Segment, U/N 3	Complete	Complete	21 tests (8 of the tests in shortened chamber), vent-to-oxidizer braze joint leak, sectioned for metallography
5-Inch Fan Injector Segment, U/N 4	Complete	Complete	9 tests, face overheated, nonrepairable
5-Inch Fan Injector Segment, U/N 5 (Narrow Face)	80-percent Complete	30-percent Complete	No tests to date
5-Inch GF_2 Injector Segment, U/N 1	Complete	Complete	1 test, damaged on test 051, nonrepairable

TABLE 4

(U) (Concluded)

	Design	Fabrication	Test Status
30-Degree Water-Cooled Chamber Segment, U/N 1	Complete	Complete	14 tests, major repair completed
30-Degree Tube-Wall Chamber Segment, U/N 1	Complete	Complete	27 tests, some tube cracks at throat, repaired
30-Degree Tube-Wall Chamber Segment, U/N 2	Complete	Complete	1 test, slight damage at braze joint, repaired
30-Degree Channel-Wall Chamber Segment, U/N 1*	Complete	Complete	12 tests, cracking of hot-gas side skin, erosion in throat, sectioned for analysis
30-Degree Prototype Chamber Segment, U/N 3	Complete	90-percent Complete	No tests to date
30-Degree Injector Segment, U/N 1 (Brazed Face)	Complete	Complete	43 tests, slight body damage at third O-ring groove, vent-to-fuel-to oxidizer braze joint leak
30-Degree Injector Segment, U/N 2 (Integral Face)	Complete	Complete	2 tests, no damage
30-Degree Injector Segment, U/N 3 (Brazed Face)	Complete	Complete	8 tests (one test in the fuel biased) (SWTC), erosion damage on injector body and face, repaired
30-Degree Injector Segment, U/N 4 (Brazed Face)	Complete	Complete	No tests to date
Main Tube-Wall Nozzle Extension	Complete	Tube Tooling Complete, Material Ordered	No tests to date
Main Thrust Chamber and Injector	80-percent complete	20-percent complete	No tests to date
Base Manifold and Secondary Nozzle Simulator	50-percent Complete	Material Ordered	No tests to date
Thrust Mount Assembly	Complete	15-percent Complete	No tests to date

*Fabrication under company sponsorship

(C) The design layout of the prototype chamber segment was presented in Ref. 1, but detail designs were not completed at that time because selection of the hot-gas fabrication technique had not been completed. The evaluation program for selection of the thrust chamber hot-gas face has been completed. The following hot-gas face configuration was selected for the thrust chamber segments:

1. Inner Body: stretch-formed, wrought-nickel sheet that is furnace-braze attached to the electroformed nickel substrate into which the coolant passages have been machined

2. Outer Body: explosively formed, wrought-nickel sheet that is furnace-braze attached to the electroformed nickel substrate into which the coolant passages have been machined

3. Side Plates: (Baffles) Wrought-nickel sheet that is furnace-braze attached to the wrought-nickel plate into which the coolant passages have been machined

(C) All sample work previously detailed in Ref. 2 was completed, and a wrought-nickel face was determined to be superior to an electroformed nickel face because of reproducible sheet quality and mechanical properties. Although the improved electroform samples were successful, the inability to completely define the mechanism of electroform failure on the company-sponsored, 30-degree channel chamber was considered sufficient reason to relegate this process to a backup classification.

(C) The wrought-sheet braze samples No. 7 and No. 8 (presented in Ref. 2) will be discussed in detail because the decision to use wrought-nickel face sheets was, to a major degree, based on the success of these two samples.

(U) (1) Sample No. 8, Outer Body

(C) This sample, which represents the actual chamber segment outer body, was completed first and is shown in Fig. 35. The manufacturing procedure was as follows. The basic forging was machined to provide the contour surface

1EH32-6/2/69-C1E

Figure 35. 30-Degree Segment Outer Body With Brazed Sheet Hot-Gas Surface (Before Trimming Edges)(U)

(C) for the thick electroformed nickel substrate and all internal manifolds and feed passages. The thick nickel substrate was electroformed, and then machined to provide the hot-gas wall contour and coolant passages (slots). The braze alloy foil, 0.001-inch thick, was spot tacked to the lands with a stored-energy welder. Braze tooling and a pressure bag were used for face attachment. Visual inspection following brazing indicated a satisfactory assembly with no wrinkling of the face sheet or other damage or deformation. All coolant passages were rodded with a 0.014-inch-diameter wire and were found to be clear with no obstructions. The body was then machined at the forward and aft end for channel end TIG-braze closure. Following this operation, an attempt was made to rod the passages again to verify that all passages were open prior to closure of the channel ends. Twenty-six channels were found to be plugged with foreign material located in the throat region, which is the minimum flow area. Although this was primarily a braze test sample, the presence of foreign material plugging was significant because it could occur on subsequent segments and would present a serious problem. It was apparent that techniques should be developed to remove the plugs and changes made in manufacturing sequence, machining techniques, and the design to prevent plugging.

(U) Twenty-six coolant passages were plugged with a mixture of wax, CRES chips, nickel chips, and grinding dust. Removal methods included (nonconcurrent): pressurized injection of solvents and concentrated nitric acid; hypodermic injection of concentrated hydrochloric acid, concentrated nitric acid, and commercial nickel stripper; vibration on a 30K shaker table; and ultrasonic cleaning. This effort resulted in the unplugging of seven coolant passages, but was unsuccessful in the other 19, indicating that stringent preventative measures were required.

(U) When it became apparent that the foreign material could not be removed, closure of the channel ends for hydrostatic pressure test was completed. The segment was hydrostatic pressure tested at 2500 psig and satisfactory hot-gas face sheet braze attachment was demonstrated.

(U) (2) Sample No. 7, Inner Body

(U) This sample, which was completed after sample No. 8, represents the actual chamber inner body, and is shown in Fig. 36. The sample met all engineering requirements for the prototype thrust chamber inner body and, therefore, was scheduled to be used for the prototype thrust chamber segment assembly. The manufacturing sequence and operations for the sample were very similar to the outer body sample discussed previously, with the exception of the stringent contamination control procedures that had been instituted.

(C) The inner body sample was successfully hydrostatic pressure tested to 2750 psig at ambient temperature.

(U) b. Thirty-Degree Prototype Segment Fabrication

(U) The outer body detail design is shown in Fig. 37. It was originally planned that the outer body sample (No. 8) would be used for the prototype thrust chamber if it satisfactorily met all engineering requirements. As noted previously, segment coolant passages were inadvertently plugged during a manufacturing operation. Fabrication of a substitute segment body was immediately initiated.

(U) Fabrication of the outer body segment for the prototype segment has been completed satisfactorily. The completed segment is shown in Fig. 38 and 39, following furance brazing and channel-end closure, and immediately prior to alloying for the 30-degree prototype assembly braze cycle.

(U) (1) Inner Body

(U) The inner body detail design is shown in Fig. 40. The inner body segment that will be used for the 30-degree prototype was originally designated as sample No. 7. The sample satisfactorily met all engineering requirements, so was accepted for use in the 30-degree prototype assembly.

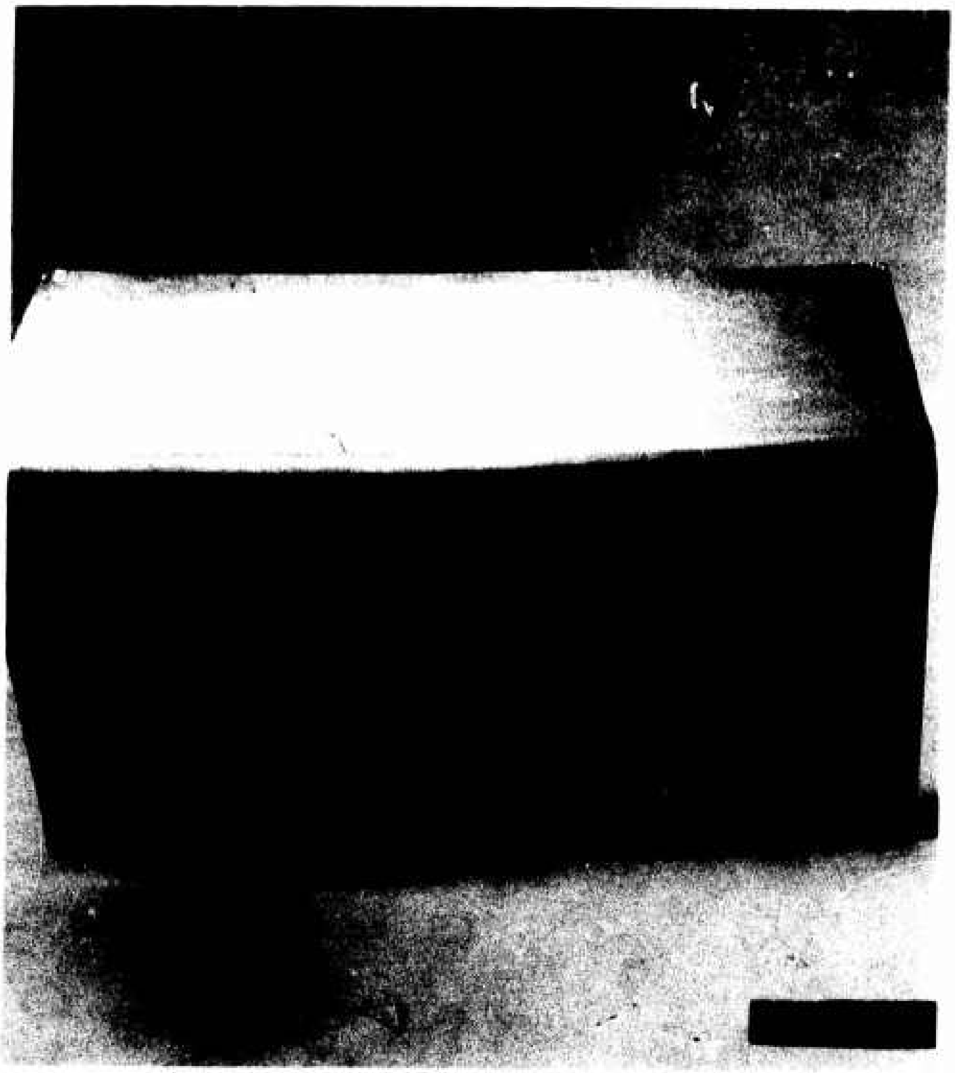

1EH82-6/16/69-C2A

Figure 36. 30-Degree Prototype Segment Inner Body (U)

CONFIDENTIAL

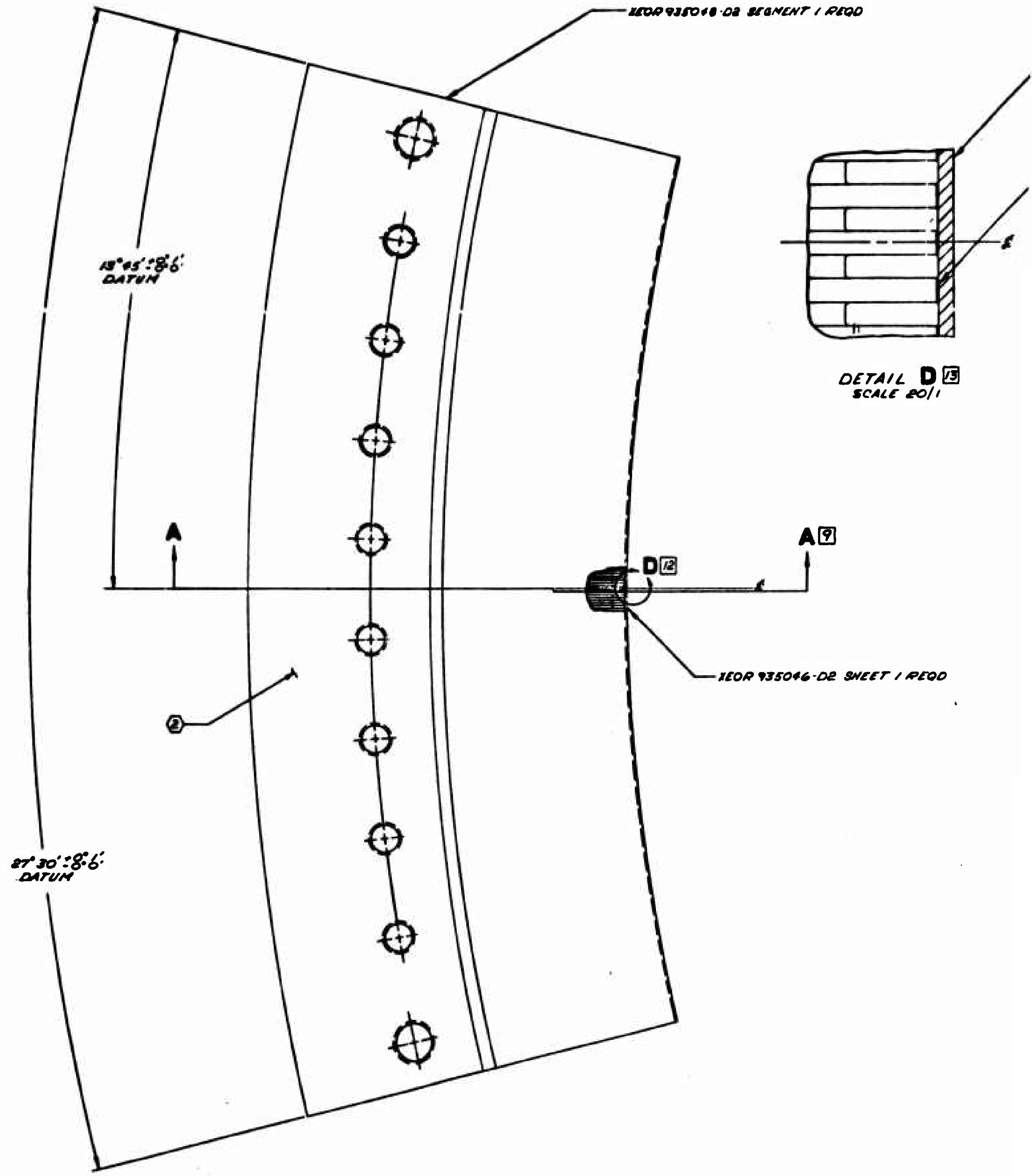

-02 SEGMENT 1 REQD

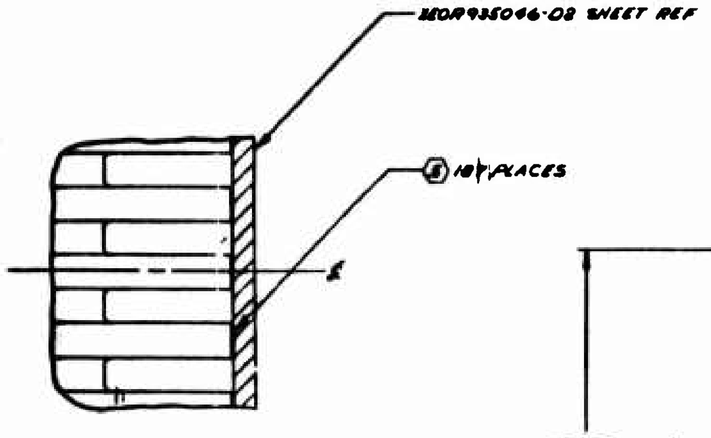

DETAIL D 13
SCALE 20/1

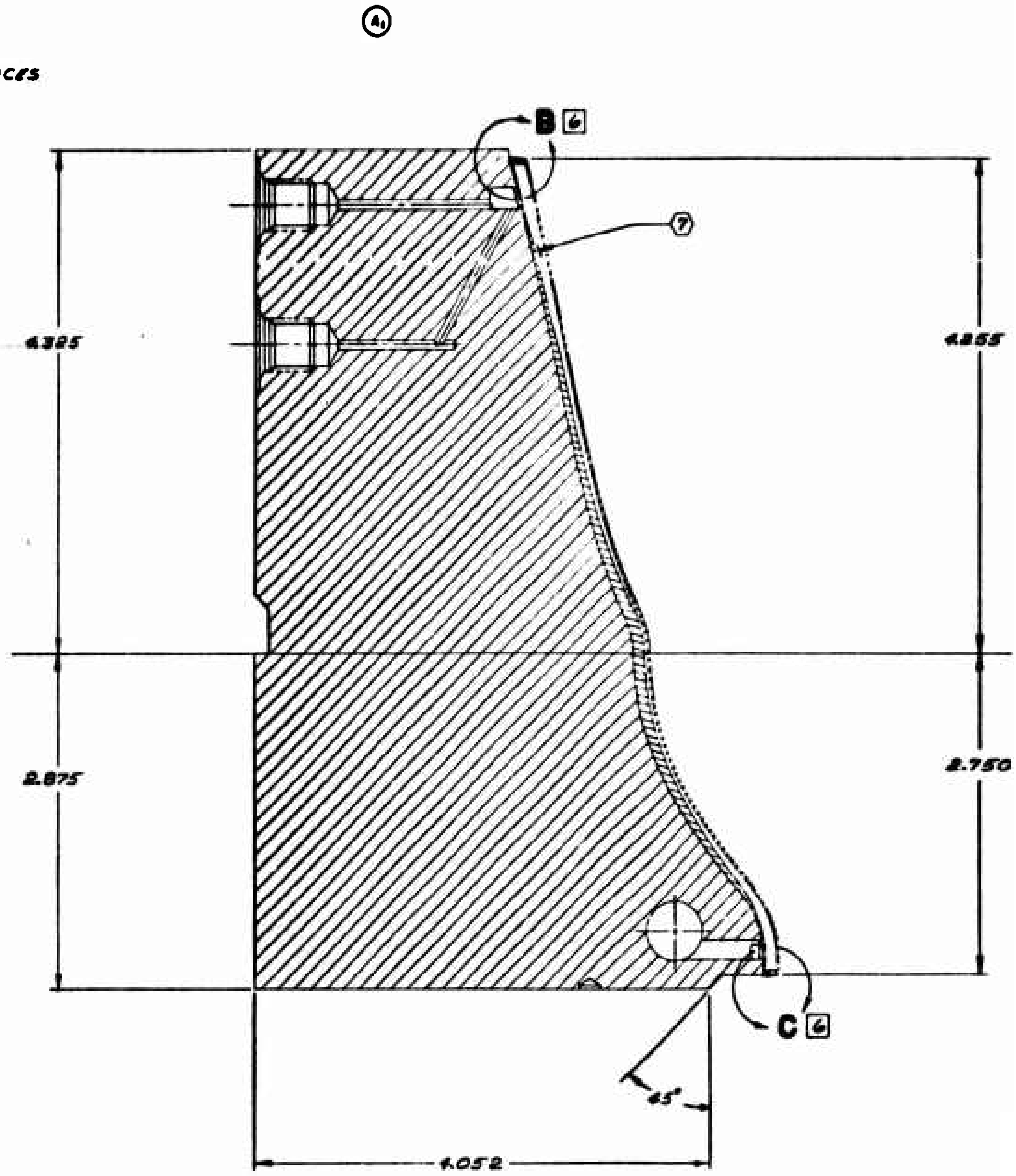

A 9

-XEOR 935046-D2 SHEET 1 REQD

SECTION A-A

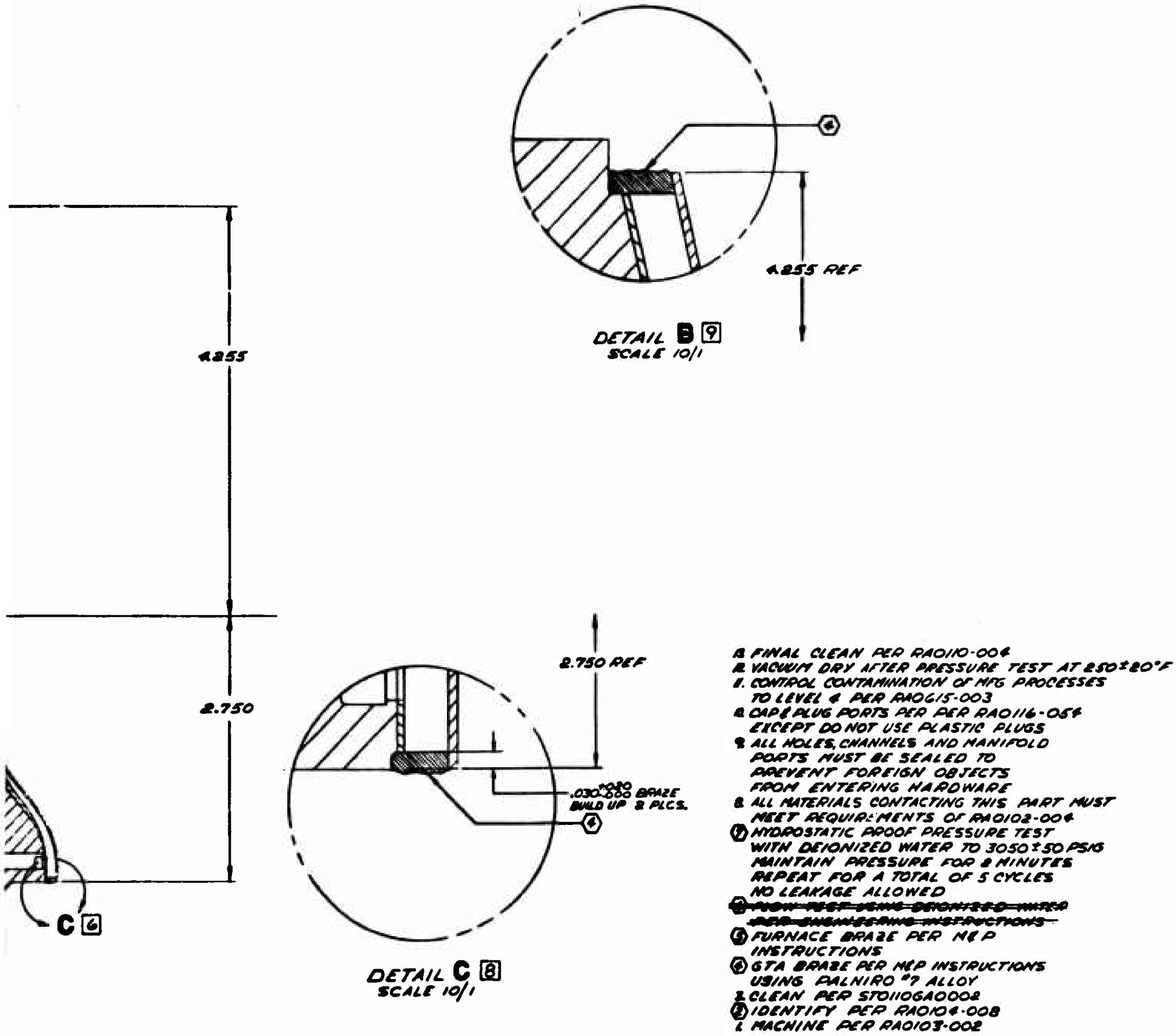

Figure 37. Outer Body Brazed Shell Segment (U)

1EH42-7/22/69-C1A

Figure 38. Prototype Segment Outer Body (before edge trimming) (U)

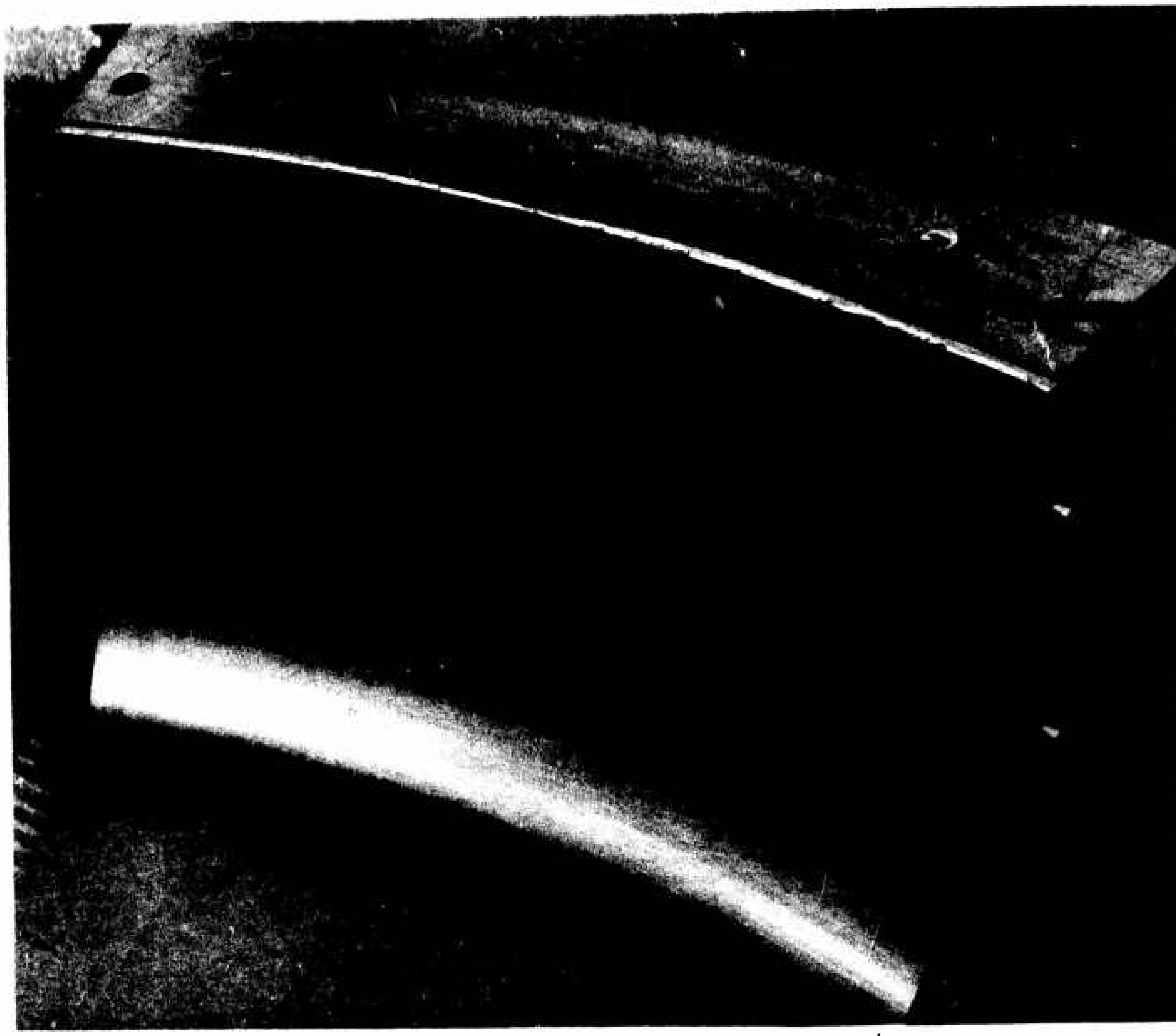

1EH32-7/31/69-C1B

Figure 39. Outer Body Prior to Final Segment Assembly (U)

CONFIDENTIAL

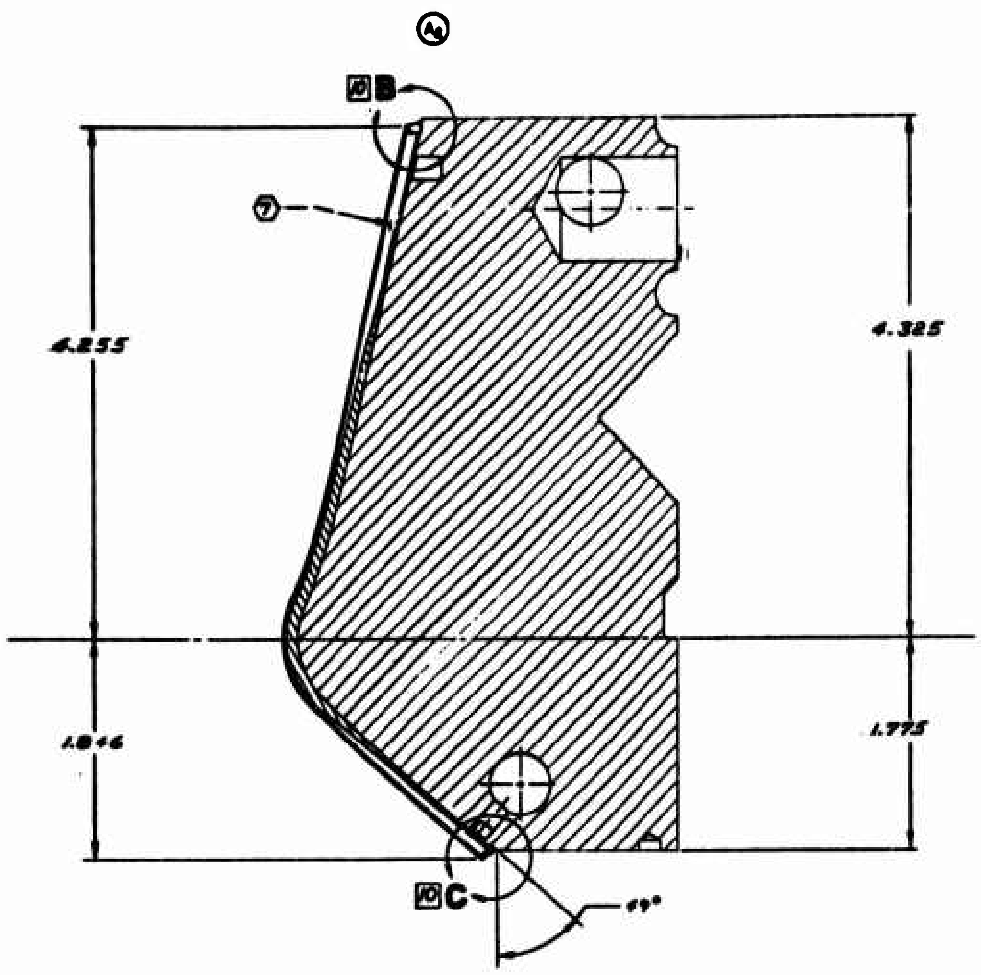

SECTION A-A

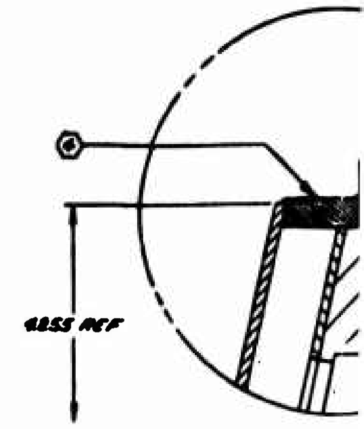

DETAIL
SCALE

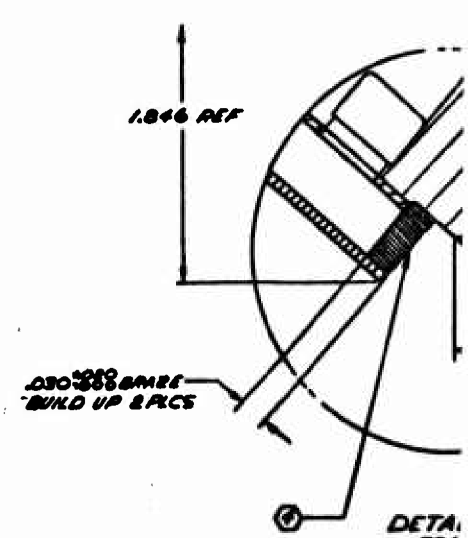

DETAI
SCA

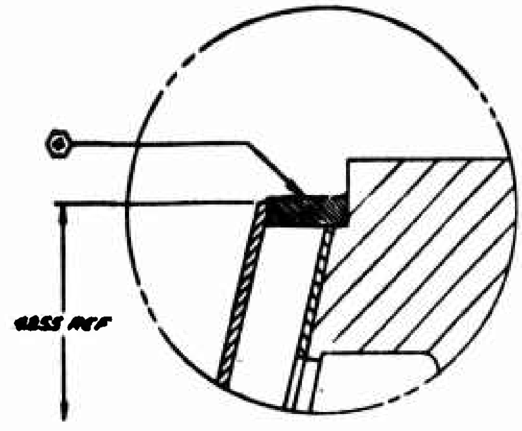

DETAIL B [13]
SCALE 10/1

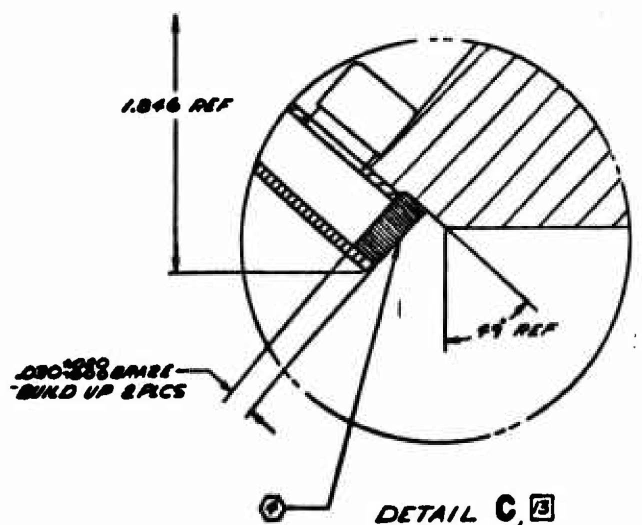

DETAIL C [13]
SCALE 10/1

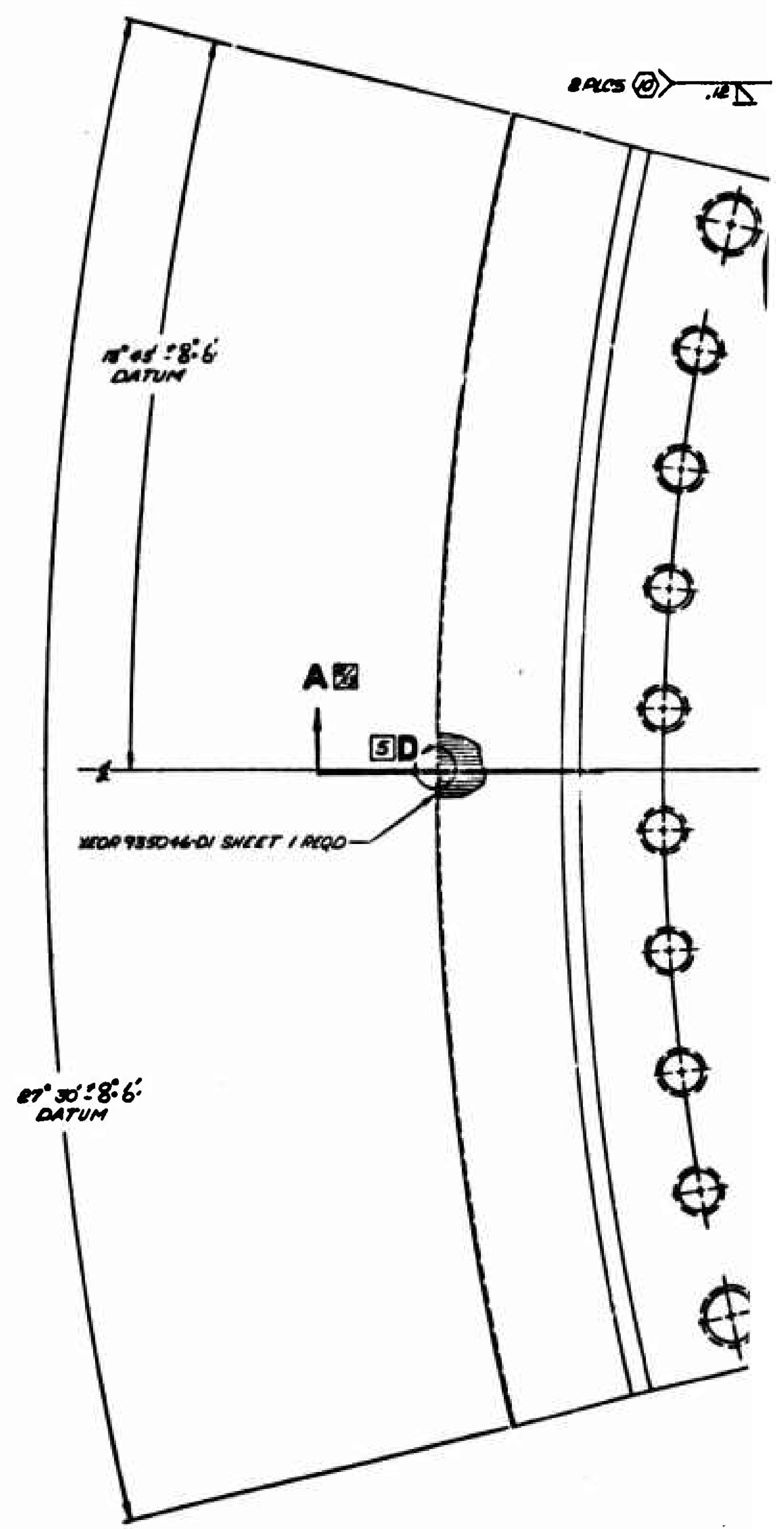

2

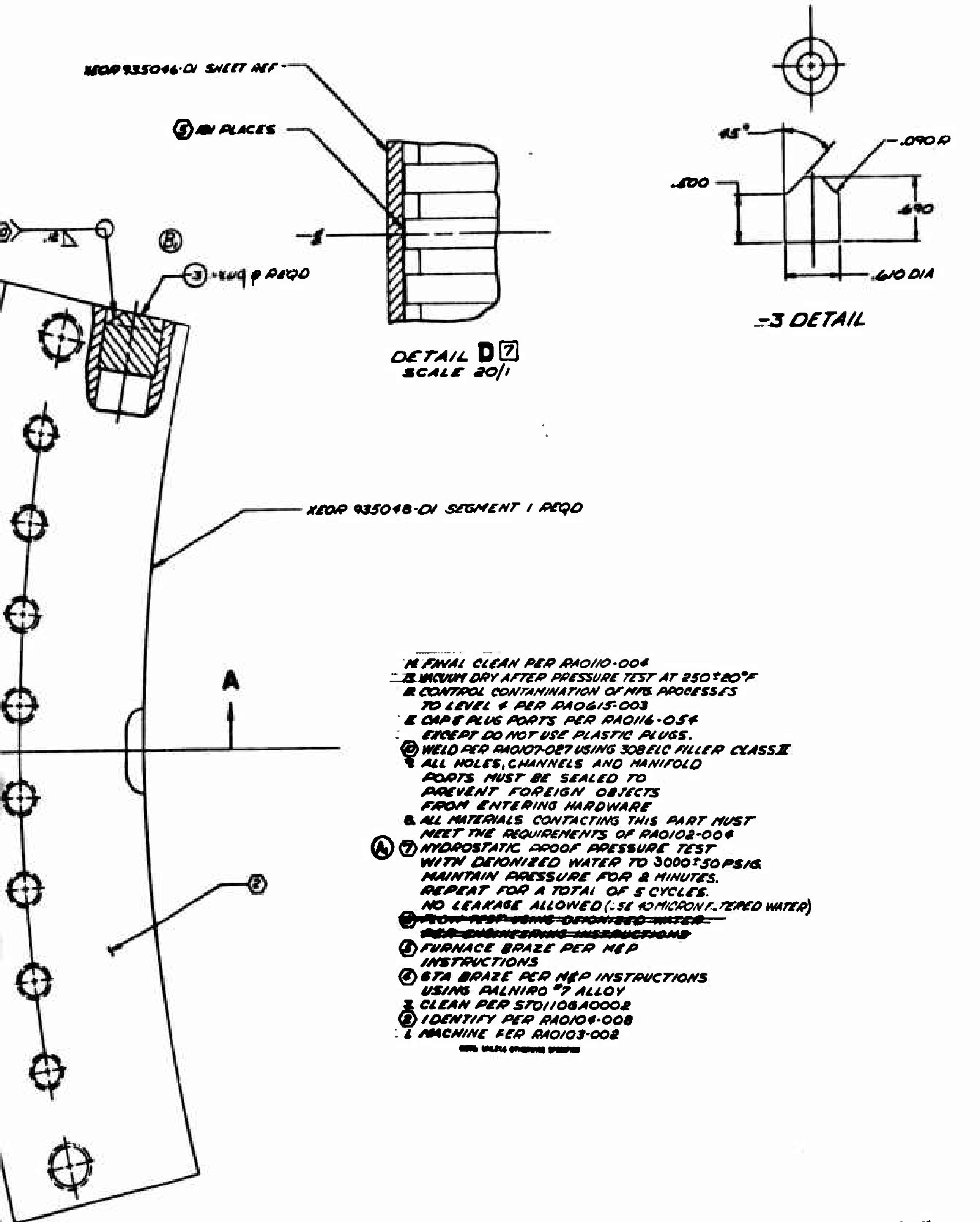

Figure 40. Inner Body Brazed Sheet Segment (U)

3

(U) Completion of fabrication of the inner body segment for the prototype segment was subsequently accomplished. The completed segment is shown in Fig. 41 and 42, immediately prior to alloying for the 30-degree prototype assembly braze cycle.

(U) (2) End Plates (Baffles)

(C) The baffle plates have been completed. The furnace braze attachment of the hot-gas face was satisfactorily accomplished and demonstrated by a 2750-psig hydrostatic pressure test at ambient temperature. The end plates are shown in Fig.43 through 45. Figure 43 shows the condition of the baffles following pressure test, prior to final machining, and Fig. 44, after final machining. Figure 45 shows the result of a radiographic inspection of the two baffles performed immediately prior to alloying for final assembly brazing of the prototype segment. The coolant passage details are readily discernible in Fig. 45.

(U) (3) Prototype Final Braze Assembly

(C) The prototype final braze assembly will consist of the:

1. Inner Body
2. Outer Body
3. Left- and Right-Hand Baffles

(C) The design is shown in Fig. 46. The inner and outer bodies were located on a special tooling plate for establishment of the 0.187-inch throat gap during final machining. The end plates were then located with respect to the bodies, and the four alignment pins transferred from each inner and outer body to the end plates.

(C) Alloying, brazing, final machining of the injector-to-segment joint and the O-ring seal groove machining will complete the fabrication processes of the assembly. The assembly is scheduled for completion 15 August 1969.

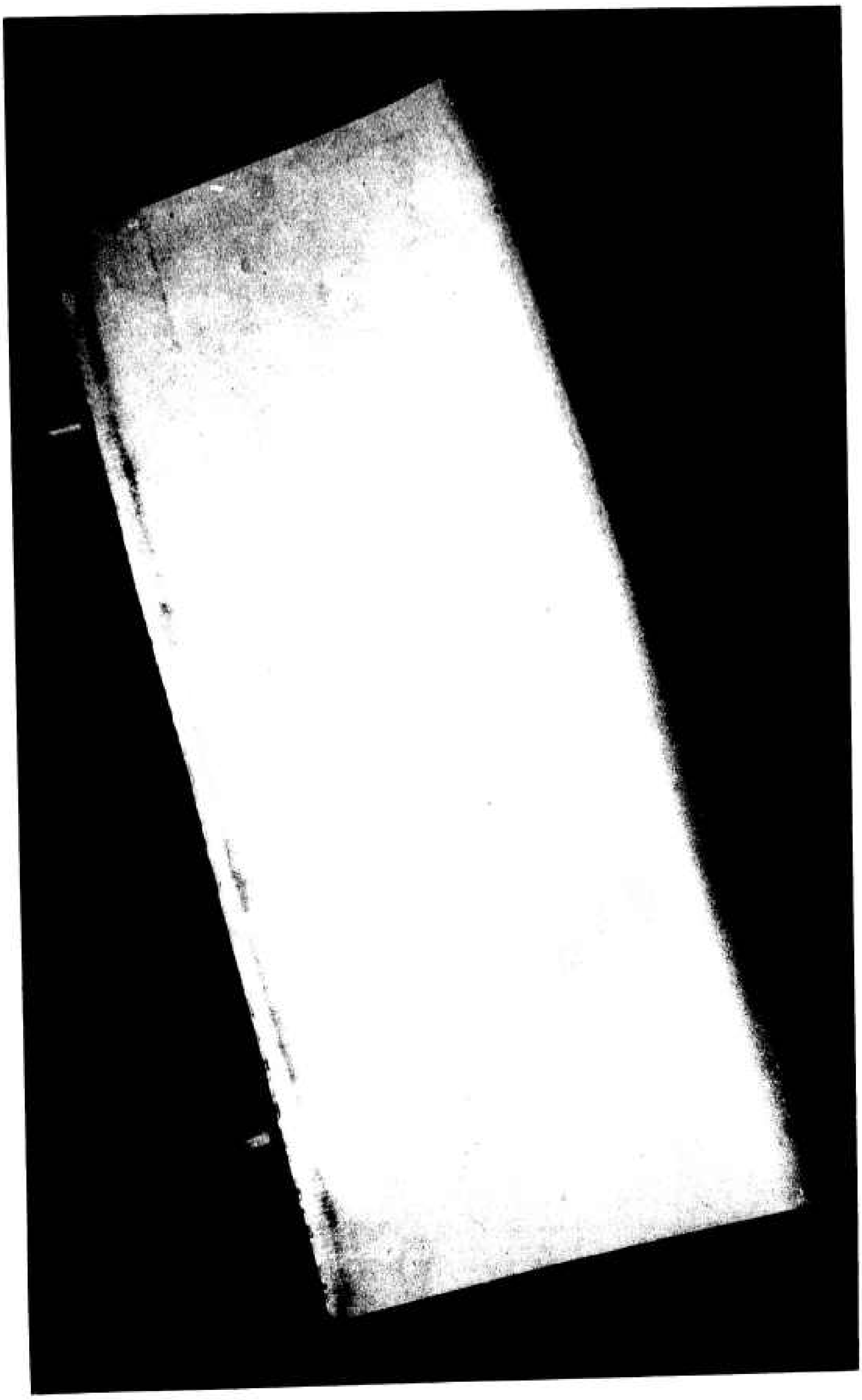

1EH32-7/31/69-C1F

Figure 41. Completed Inner Body Segment (View A) (U)

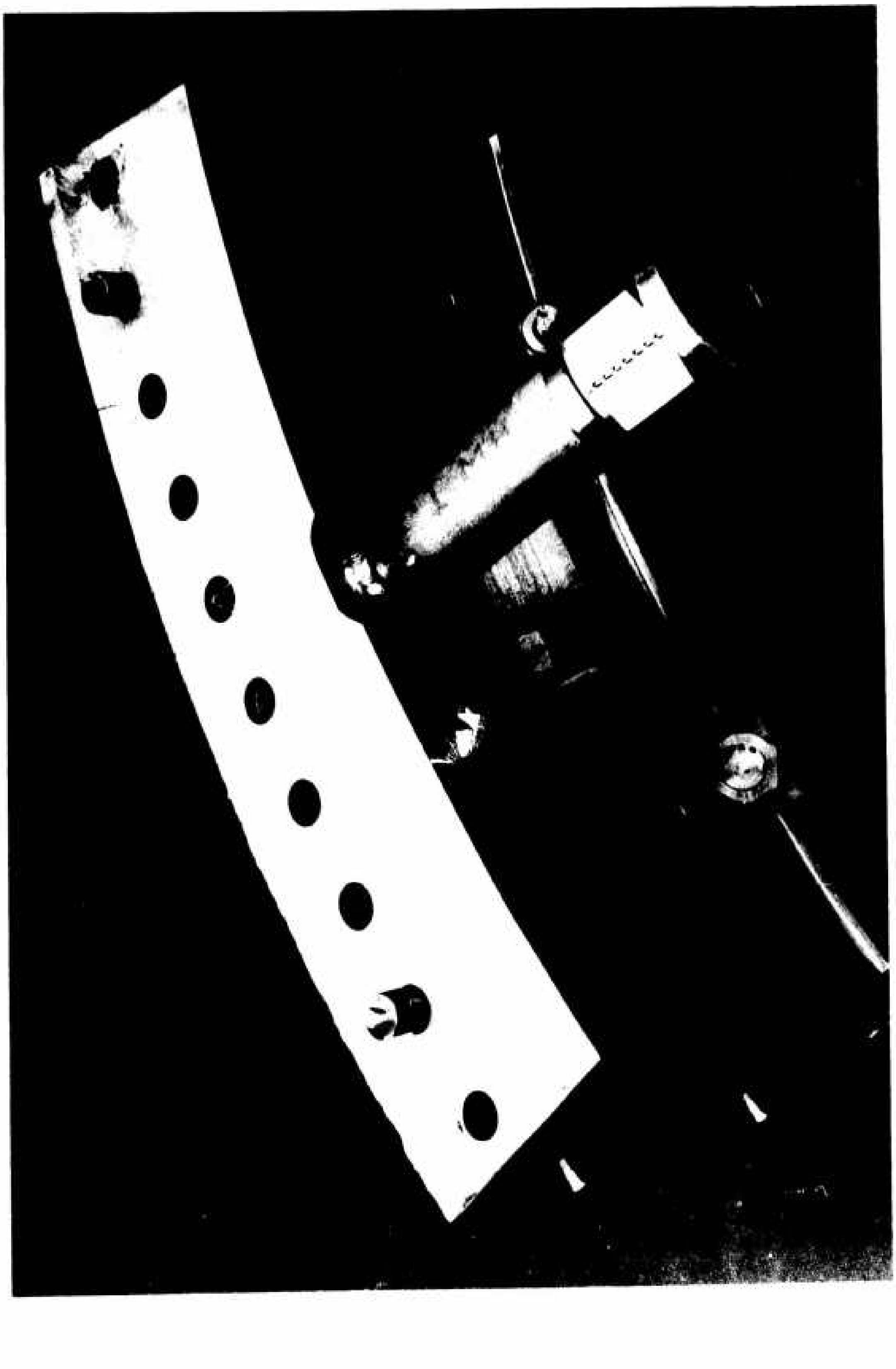

1EH32-7/31/69-C1A

Figure 42. Completed Inner Body Segment (View B) (U)

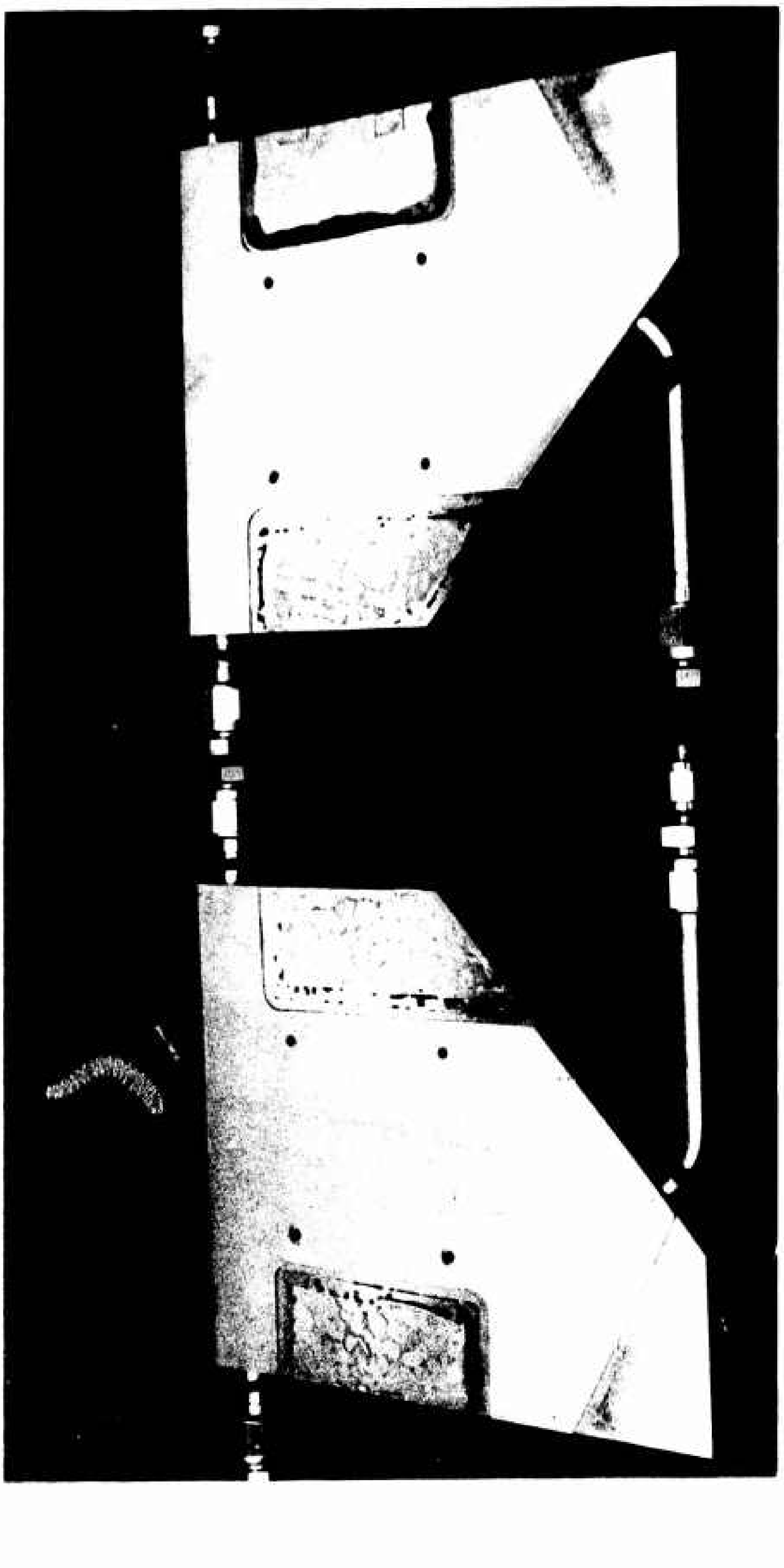

1EH52-7/14/69-C1C

Figure 43. Baffles Prior to Final Machining (U)

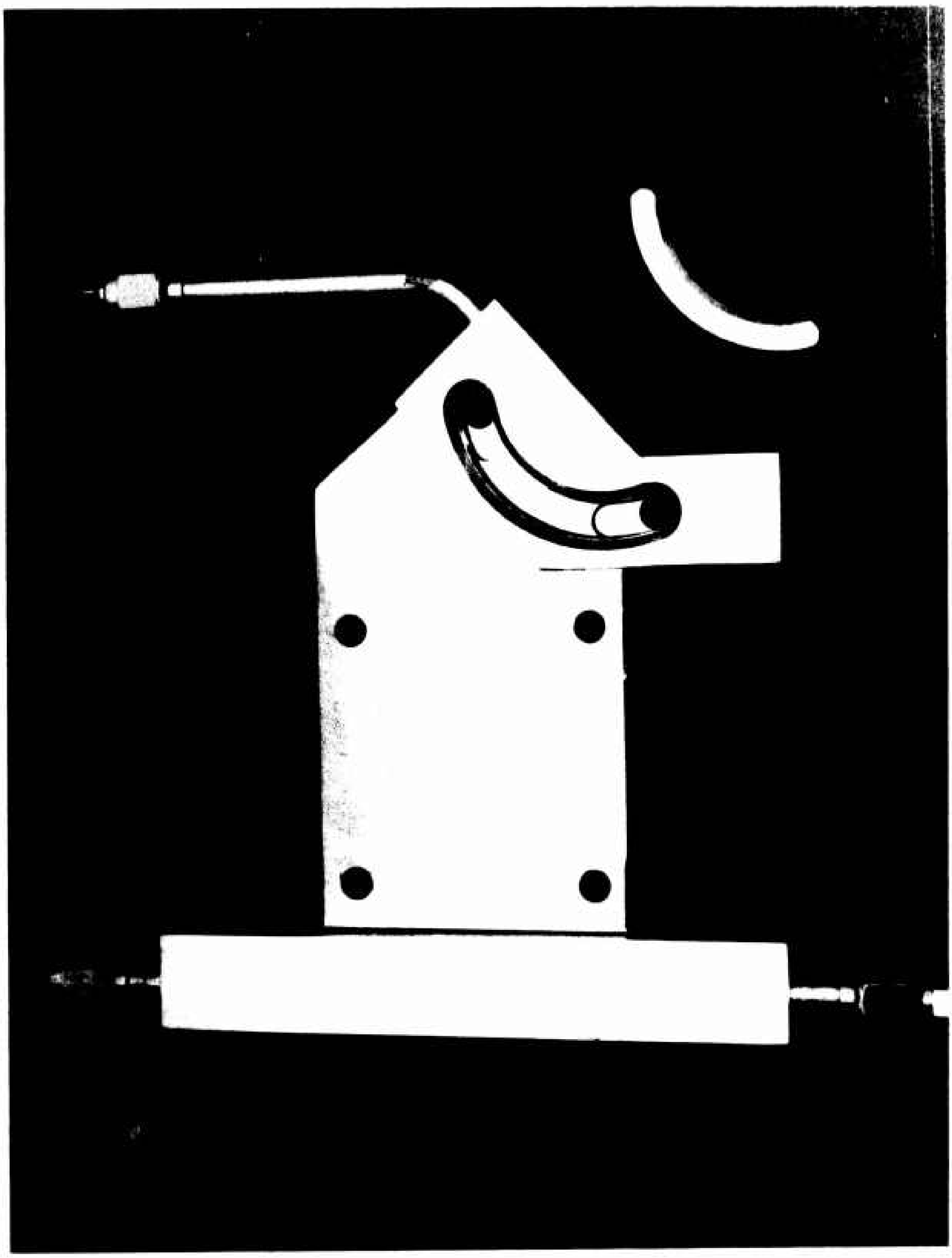

1EH32-7/31/69-C1G

Figure 44. Baffles After Final Machining (U)

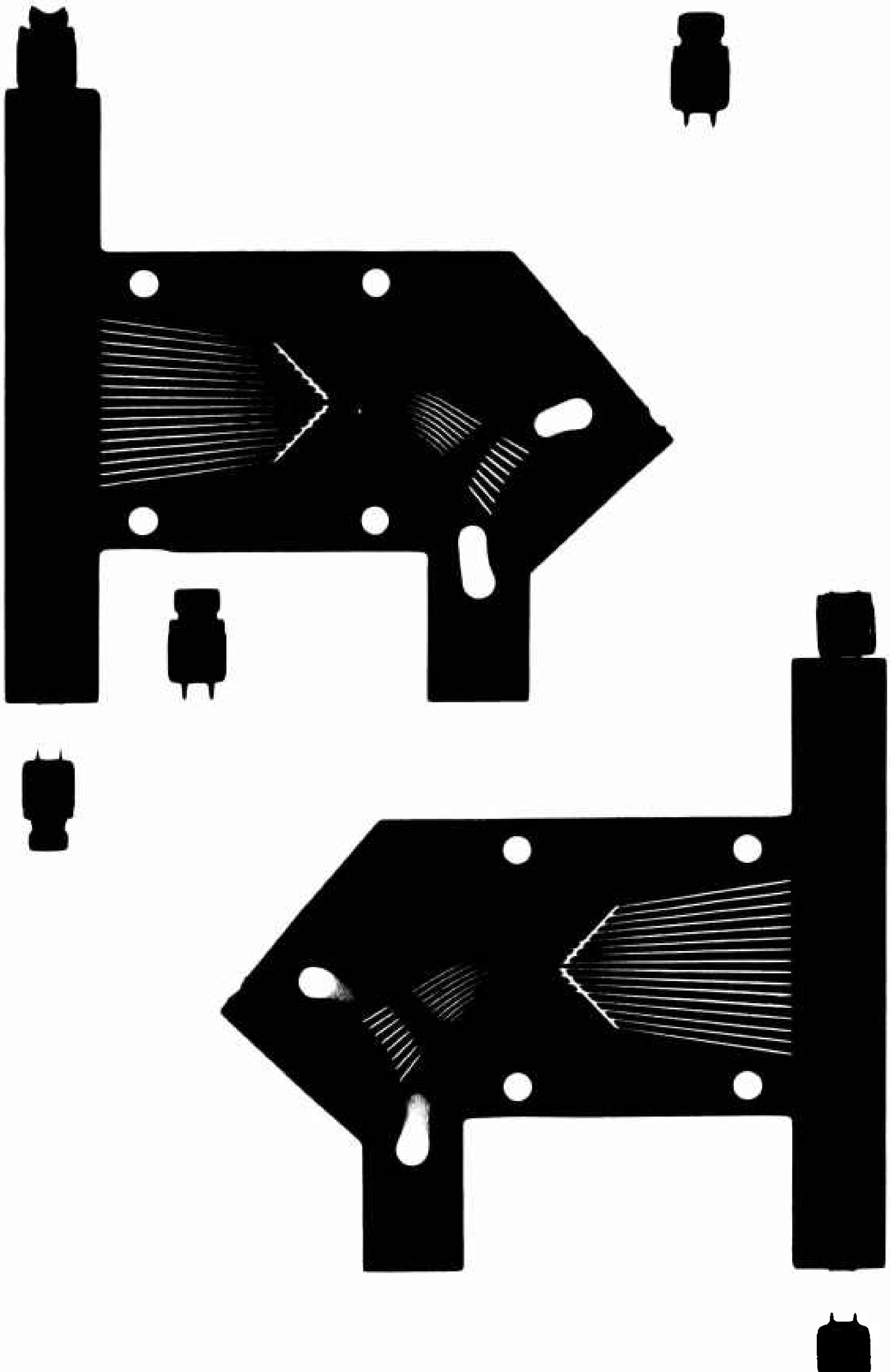

Figure 45. X-Ray of Baffle

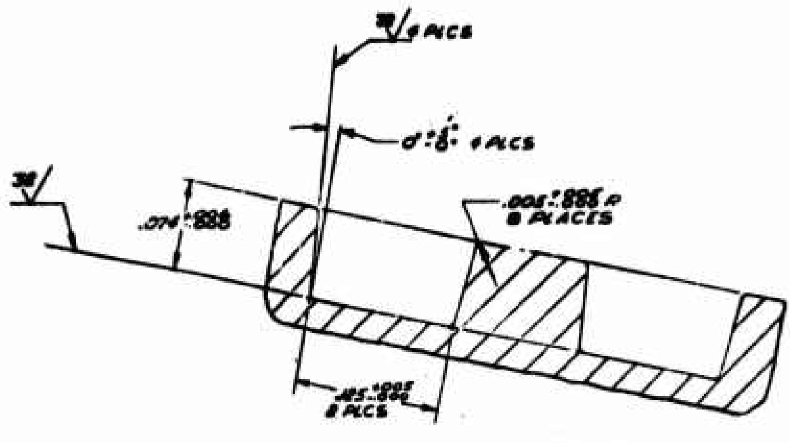

SECTION C-C
SCALE 20/1

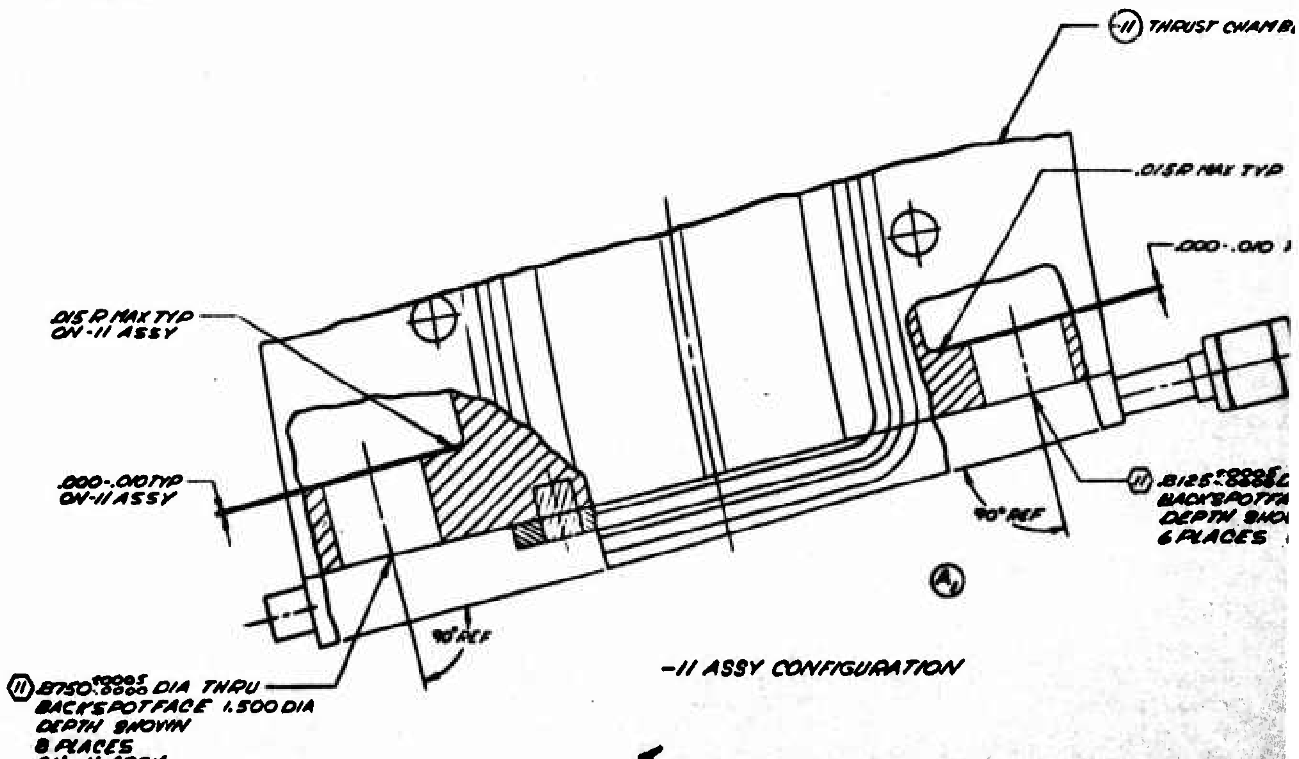

-11 ASSY CONFIGURATION

I

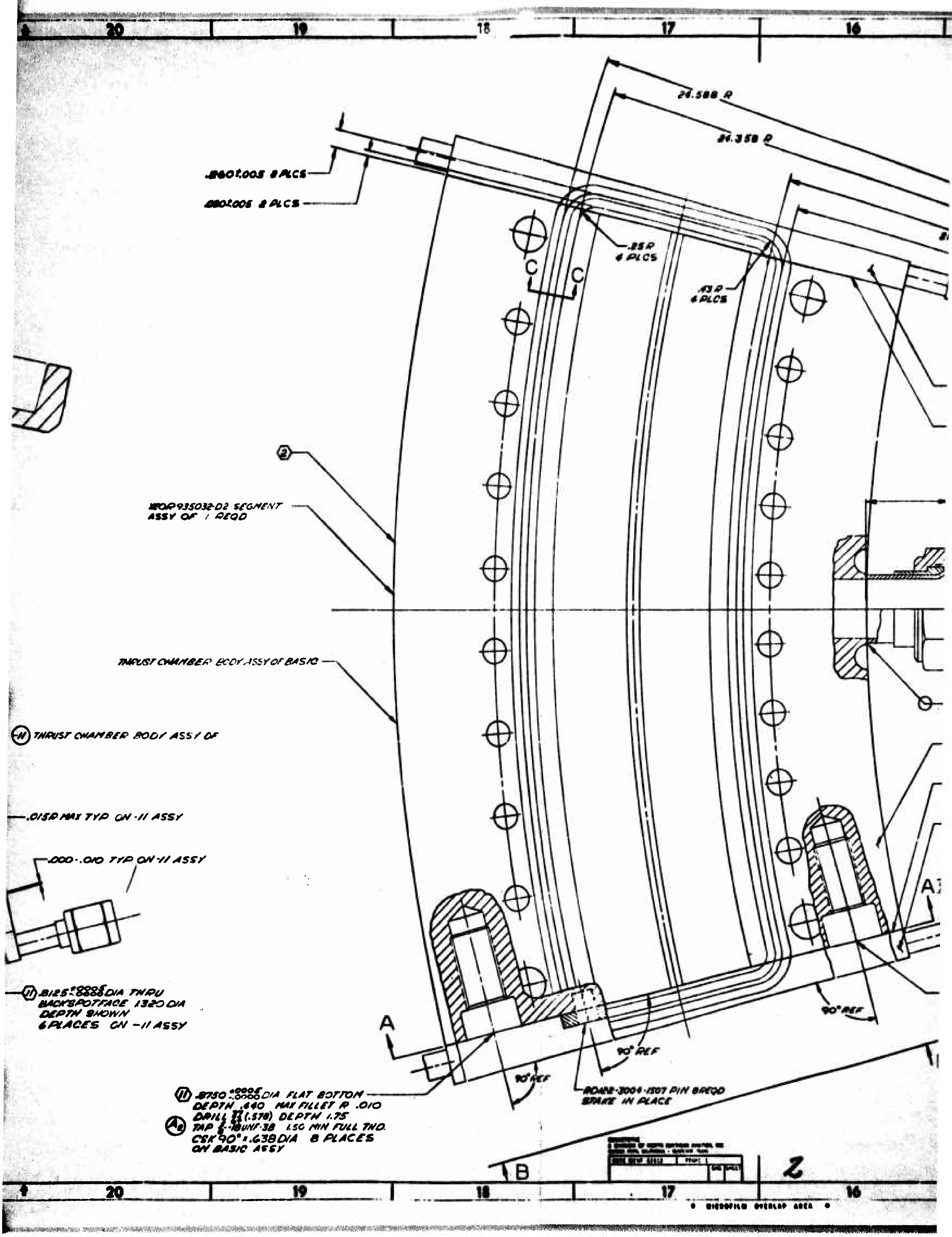

20
19
18
17
16
24.588 R
24.358 R
.260±.005 8 PLCS
.080±.005 8 PLCS
.25 R
4 PLCS
.13 R
4 PLCS
C
C
XEOP935032-D2 SEGMENT
ASSY OF 1 REQD
THRUST CHAMBER BODY ASSY OF BASIC
-11 THRUST CHAMBER BODY ASSY OF
.015 R MAX TYP ON -11 ASSY
.000-.010 TYP ON -11 ASSY
11 .8125 DIA THRU
BACKSPOTFACE 1.320 DIA
DEPTH SHOWN
6 PLACES ON -11 ASSY
A
11 .8750 +.0005 -.0000 DIA FLAT BOTTOM
DEPTH .440 MAX FILLET R .010
DRILL (.578) DEPTH 1.75
TAP UNF-3B 1.50 MIN FULL THD.
CSK 90° × .638 DIA 8 PLACES
ON BASIC ASSY
90° REF
90° REF
90° REF
PIN 8 REQD
STAKE IN PLACE
B
A
Z
20
19
18
17
16
MICROFILM OVERLAP AREA

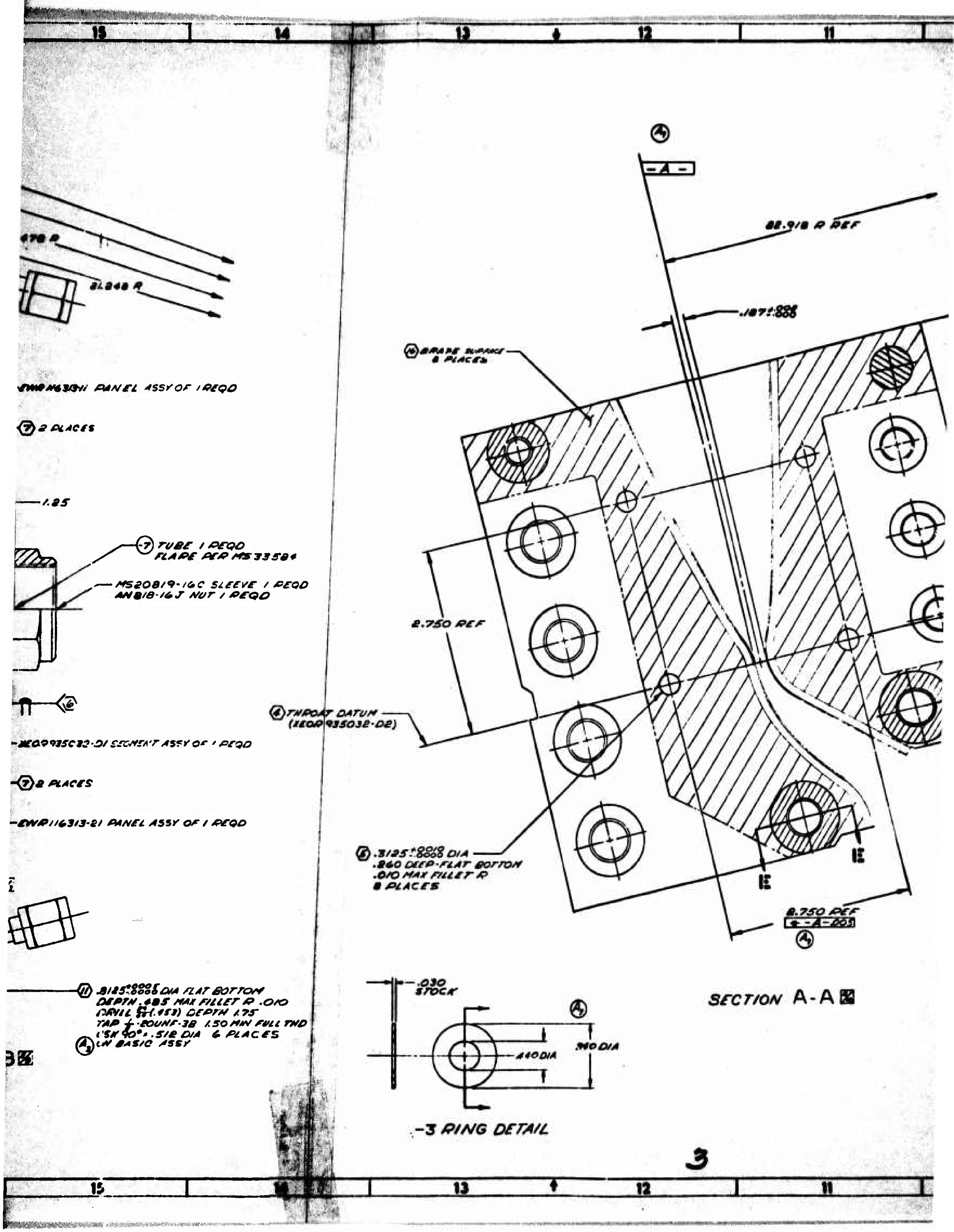

15
14
13
12
11
-A-
88.918 R REF
.187±.002
.000
31.248 R
(16) BRAZE SURFACE
8 PLACES
EWR116313-11 PANEL ASSY OF 1 REQD
(7) 2 PLACES
1.25
(7) TUBE 1 REQD
FLARE PER MS33584
MS20819-16C SLEEVE 1 REQD
AN818-16J NUT 1 REQD
2.750 REF
(4) THROAT DATUM
(XEOR935032-D2)
XEOR935C32-D1 SEGMENT ASSY OF 1 REQD
(7) 2 PLACES
EWR116313-21 PANEL ASSY OF 1 REQD
(5) .3125 +.0010 -.0000 DIA
.260 DEEP-FLAT BOTTOM
.010 MAX FILLET R
8 PLACES
E
E
2.750 REF
-A-.005
(11) .3125 +.0005 -.0000 DIA FLAT BOTTOM
DEPTH .485 MAX FILLET R .010
DRILL (.453) DEPTH 1.75
TAP 1/2-20UNF-3B 1.50 MIN FULL THD
CSK 90° x .512 DIA 6 PLACES
IN BASIC ASSY
.030
STOCK
.440 DIA
.960 DIA
-3 RING DETAIL
SECTION A-A
3

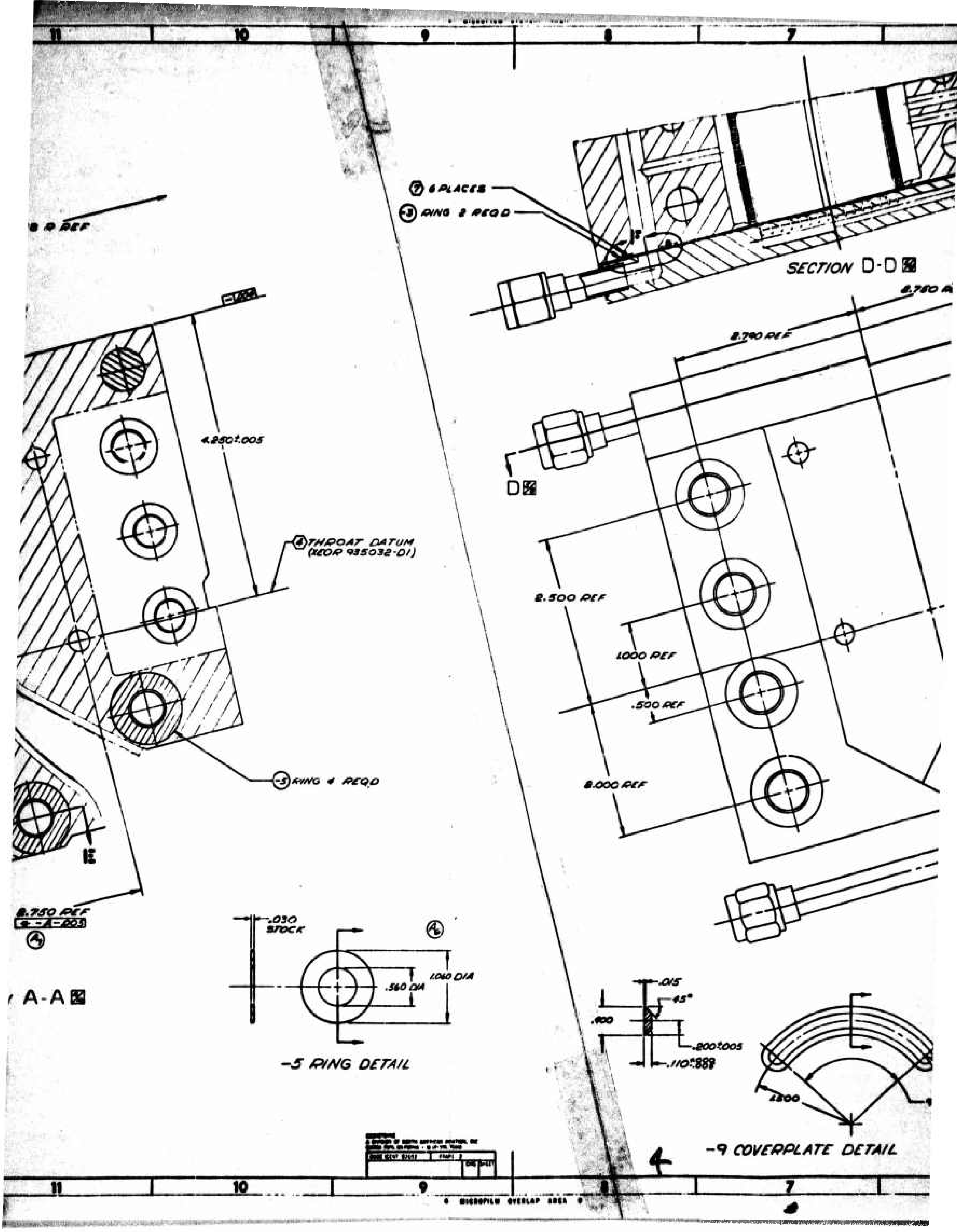

7 6 PLACES
-3 RING 2 REQ'D
SECTION D-D
8.790 REF
D
2.500 REF
1.000 REF
.500 REF
8.000 REF
4.250±.005
4 THROAT DATUM (XEOR 935032-D1)
-5 RING 4 REQ'D
E
8.750 REF
A-A
.030 STOCK
1.060 DIA
.560 DIA
-5 RING DETAIL
.015
45°
.100
.200±.005
-9 COVERPLATE DETAIL
4
MICROFILM OVERLAP AREA

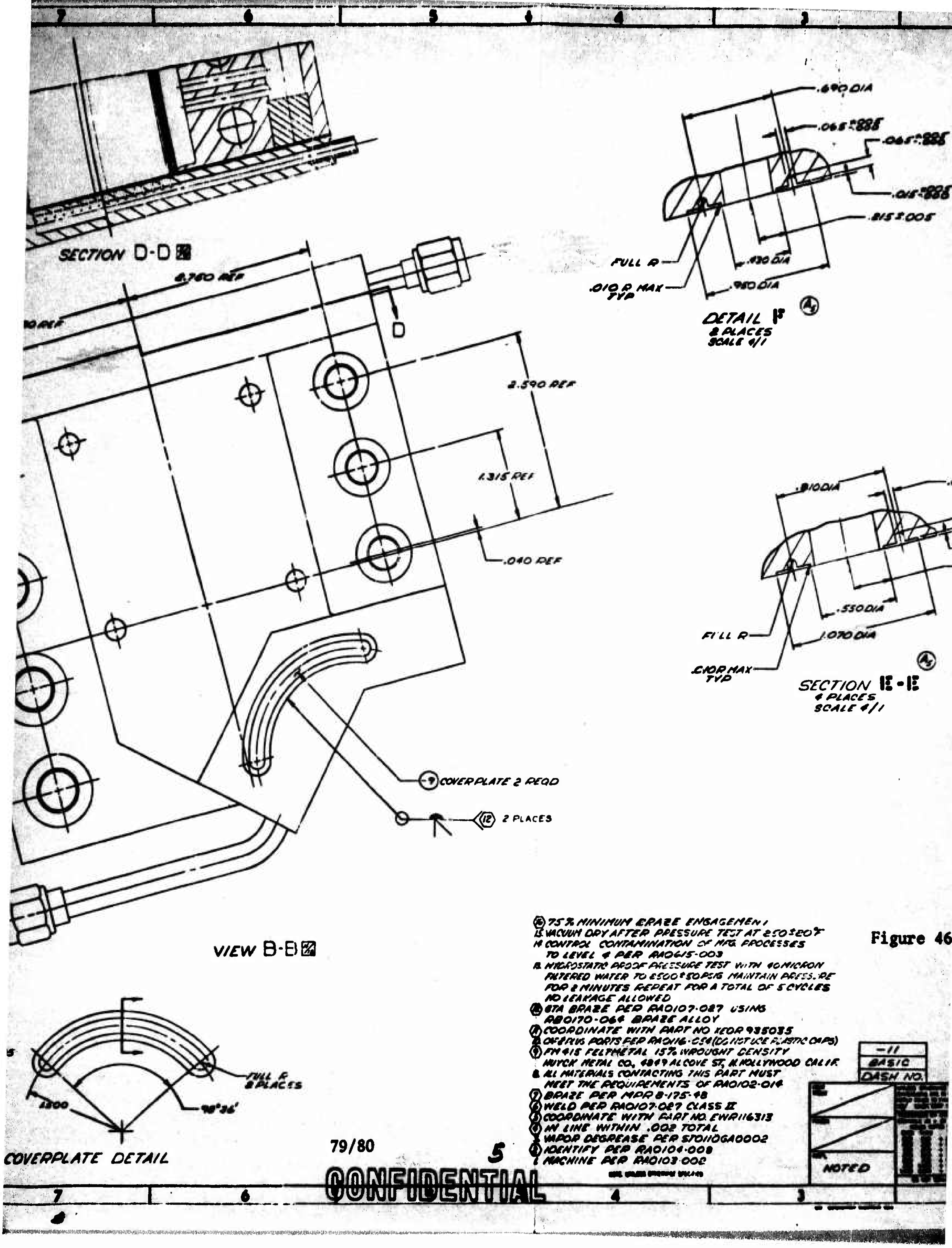

Figure 46

CONFIDENTIAL

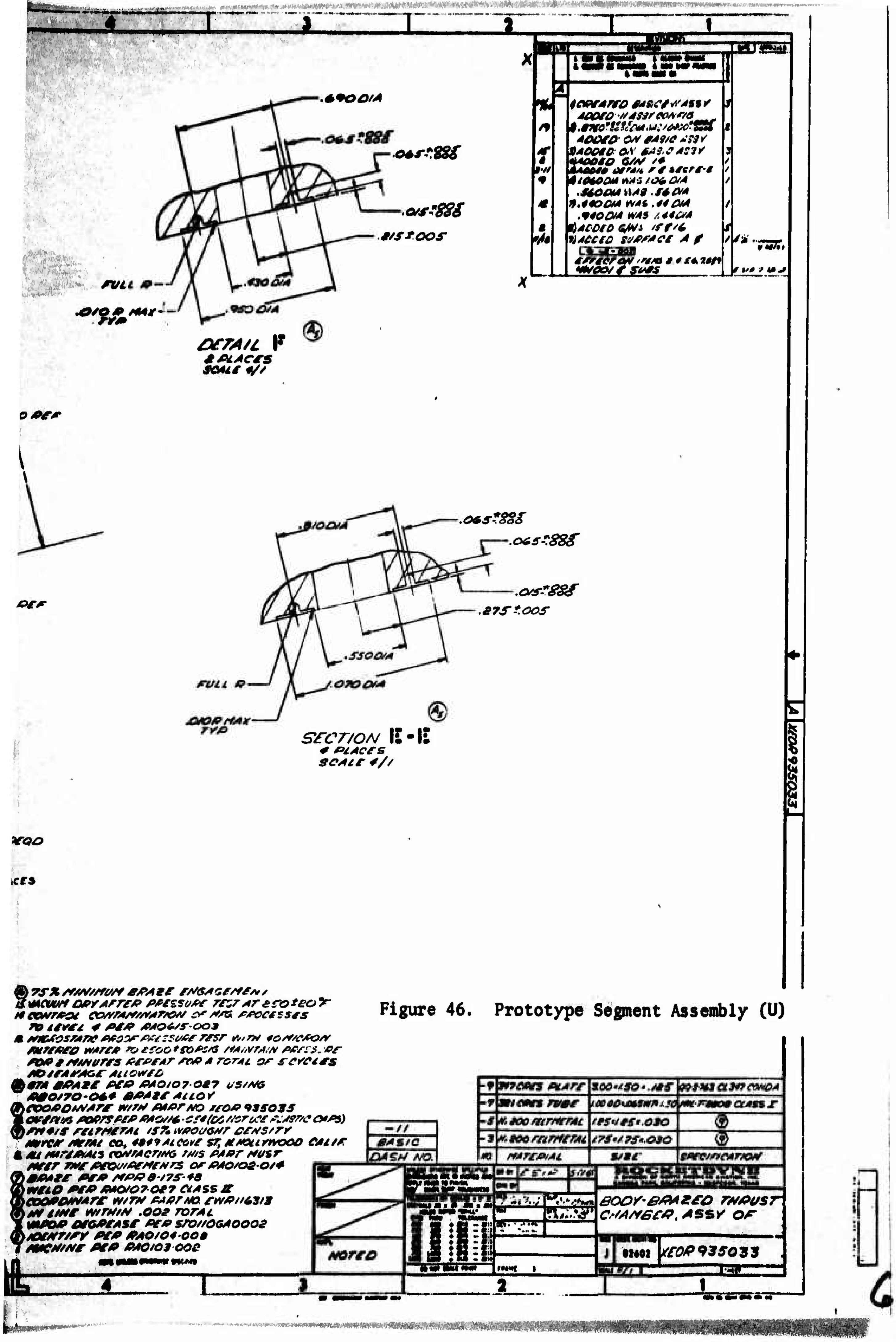

Figure 46. Prototype Segment Assembly (U)

(U) c. Thirty-Degree Prototype Injector Segment, U/N 4

(U) Fabrication of the prototype injector detail parts, consisting of the body and face, has been completed. Detail designs of these parts were presented in Ref. 1 . Detail design of the braze assembly is shown in Fig.47 .

(U) Fabrication of the prototype injector U/N 4 has been completed, and all engineering requirements have been completed. The injector assembly is shown in Fig. 48.

(U) d. Thirty-Degree Prototype Injector Segment, U/N 5

(C) Fabrication of a backup prototype injector, U/N 5, is presently in process. The injector design is identical to the prototype injector, U/N 4. Fabrication of the injector body has been completed, while the face is still in work.

(U) e. Nozzle Extension

(U) The detail design for the nozzle extension is almost complete, and is shown in Fig. 49.

(U) The tube-forming tooling is complete and is being proofed. The design layout and detail design drawings of a combination stacking, brazing, and machining fixture have been completed. The material for this fixture has been received. All forgings required for the part have been received.

(U) f. Main Thrust Chamber Segments

(U) The ring forgings for the main thrust chamber inner and outer bodies have all been received from the vendor. Preliminary machining of these forgings has been completed. The inner body rings have been parted into 30-degree segments, and one of the two outer body rings has been parted into segments. Preparation for electroforming of the nickel substrate is in process. The ring forgings for the injector body have been received from the vendor and are being machined. Figures 50 and 51 show a number of the segments in various stages of fabrication.

CONFIDENTIAL

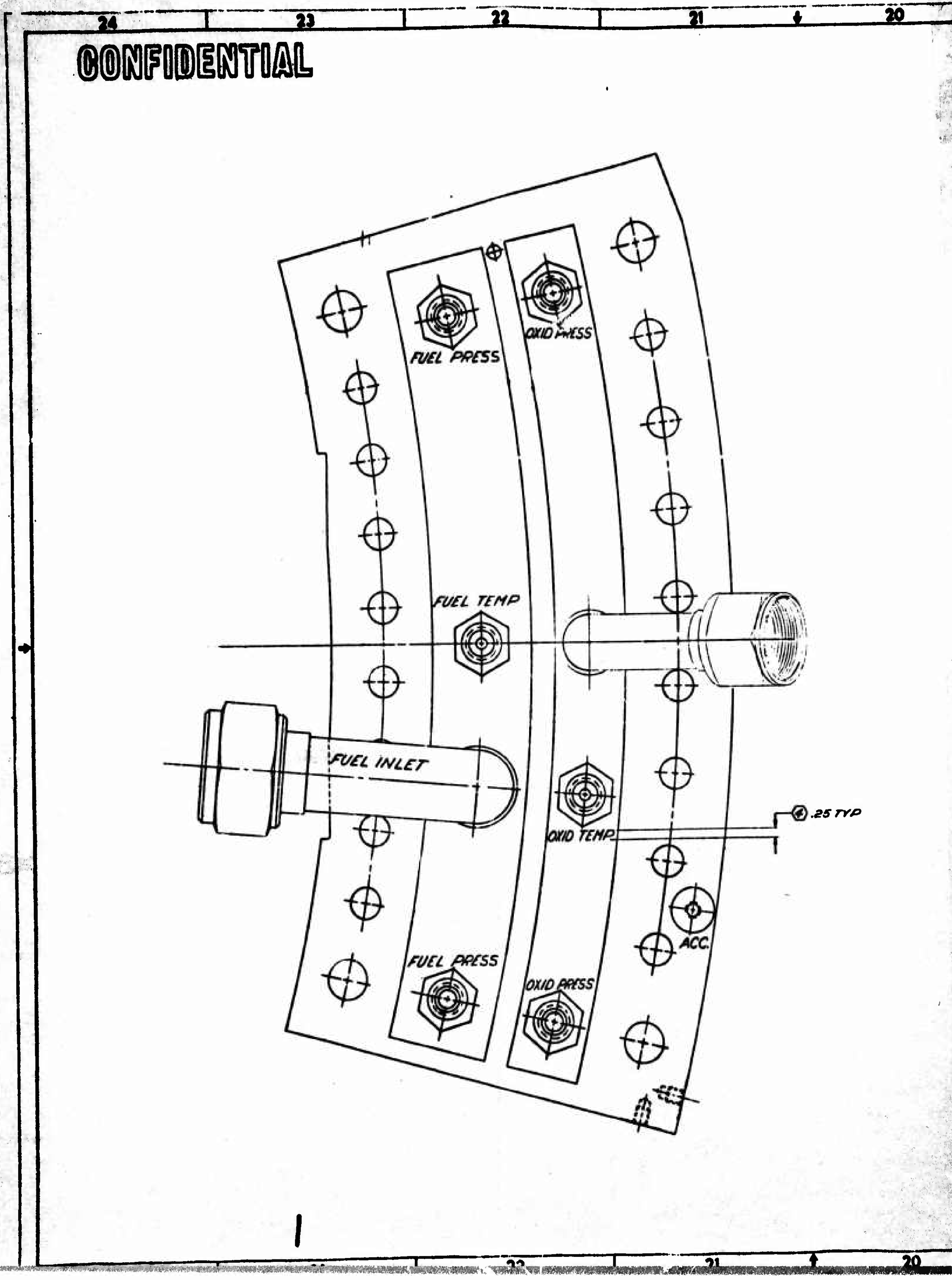

1

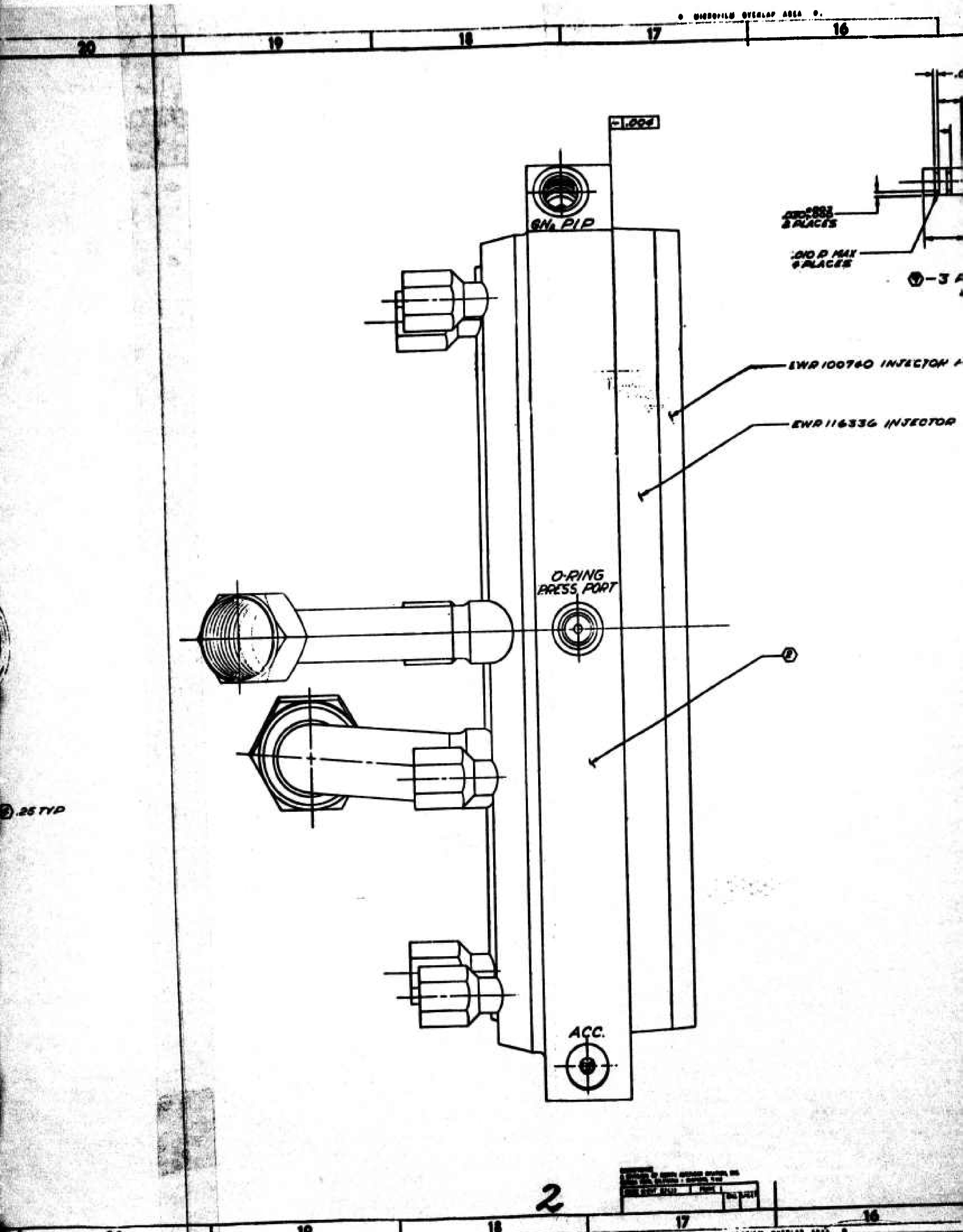
20
19
18
17
16
.004
GN_2 PIP
.030 +.003 -.000
2 PLACES
.010 R MAX
4 PLACES
-3
EWR 100760 INJECTOR
EWR 116336 INJECTOR
O-RING
PRESS PORT
.25 TYP
ACC.
2

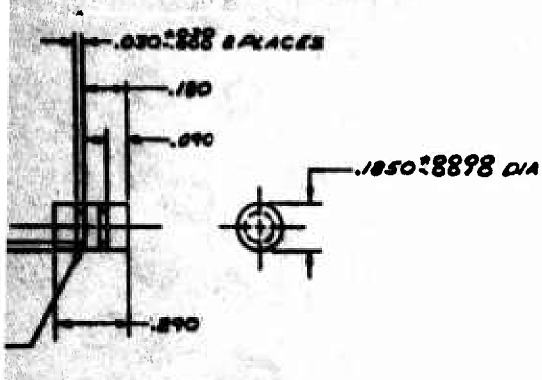

⑦-3 PLUG DETAIL
SCALE 4/1

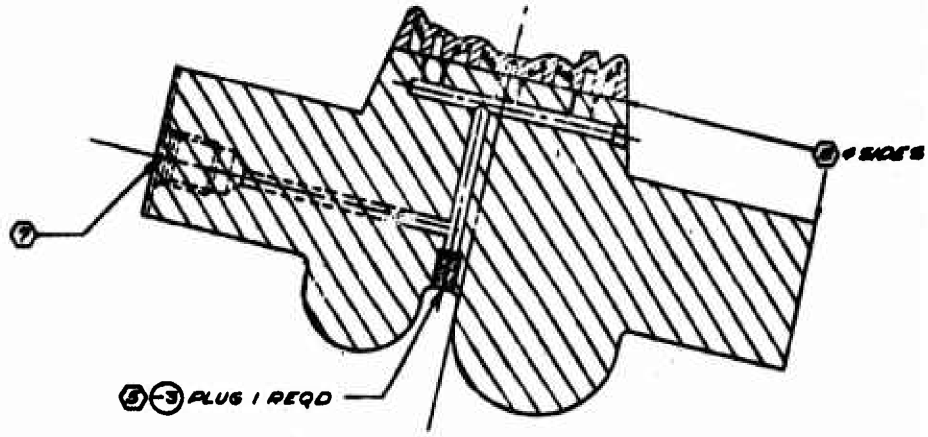

SECTION B-B

…JECTOR FACEPLATE 1 REQD

…JECTOR BODY 1 REQD

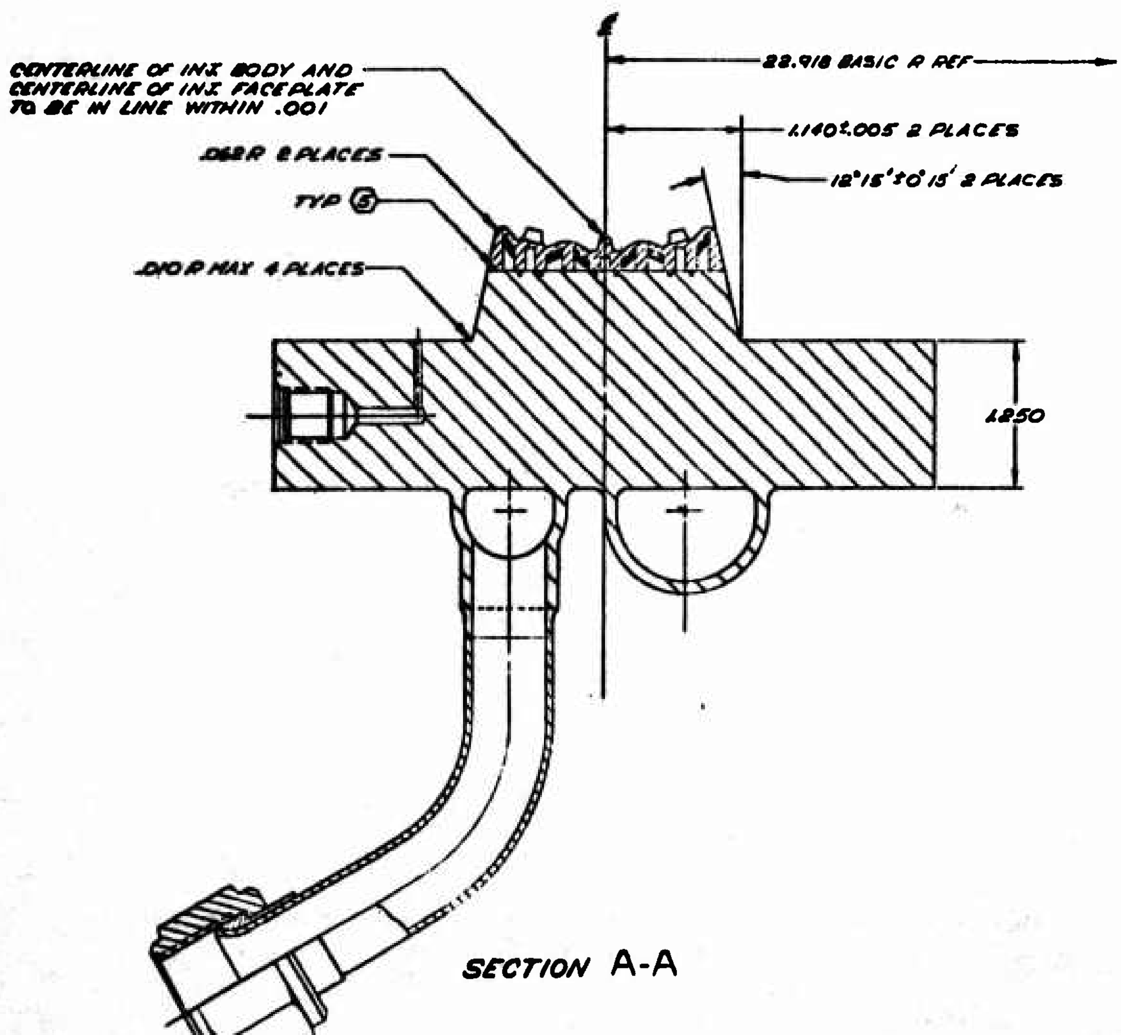

SECTION A-A

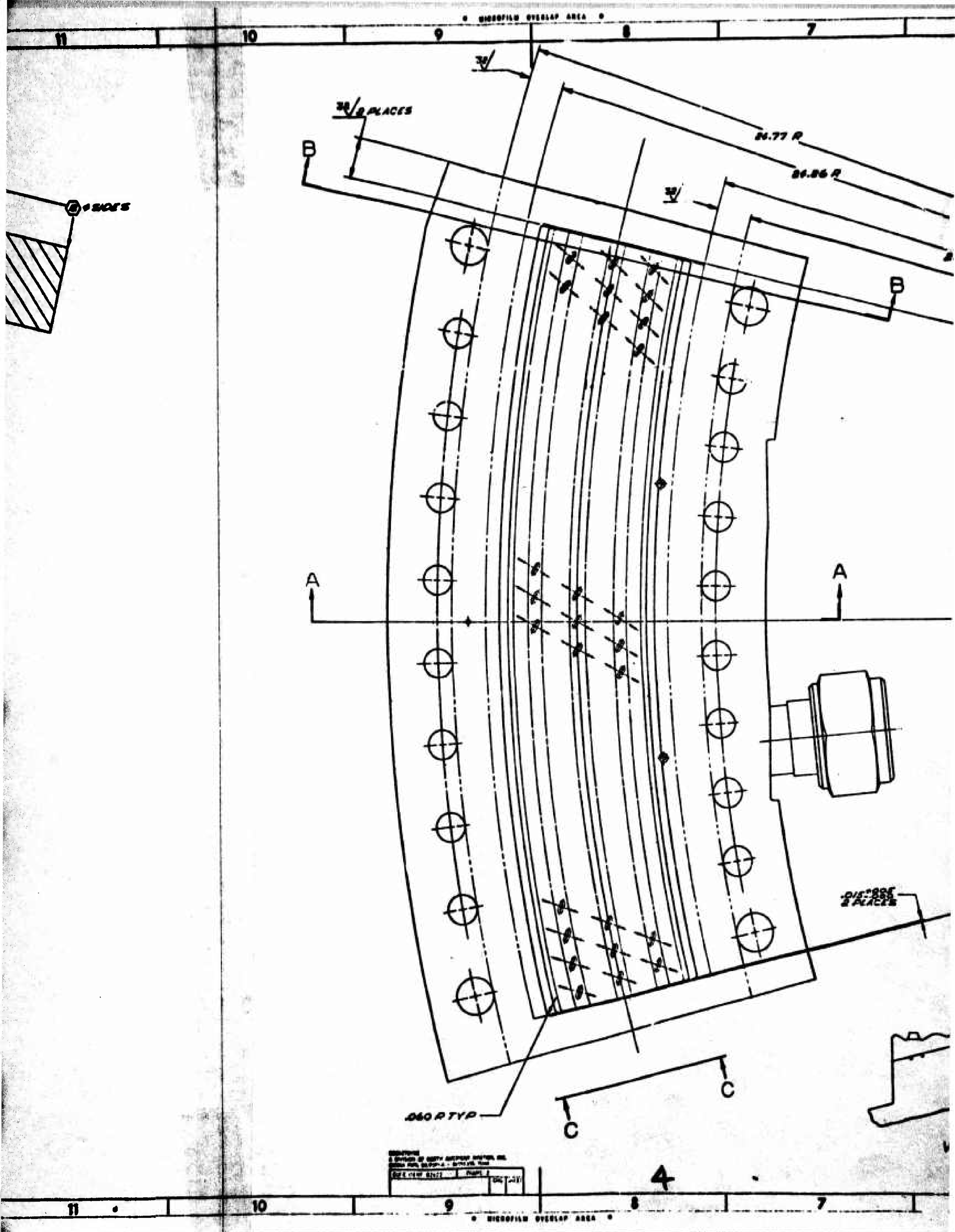
MICROFILM OVERLAP AREA
11
10
9
8
7
B
B
A
A
C
C
.060 R TYP
4

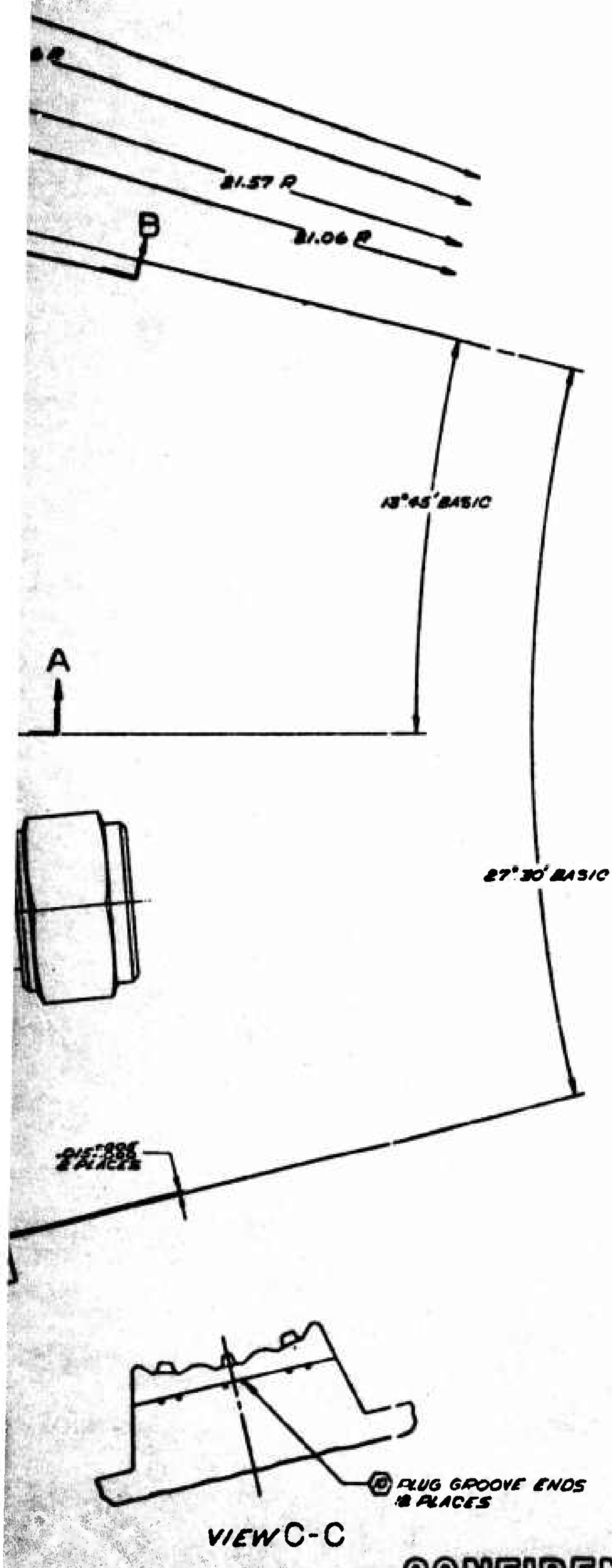

13. VACUUM LEAK TEST PER IL 9125-10
(12) DUCTILE NICKEL PLATE .0005±.0002 PER RA0109-006 PLATING ON ENTIRE PART OPTIONAL EXCEPT DO NOT PLATE INJECTOR FACEPLATE
11. CLEAN & STABILIZE PER ST0110RA0043
(10) GTA BRAZE PER RA0107-027 USING RB0170-064 BRAZE ALLOY
(9) DUCTILE NICKEL PLATE .0002-.0003 PER RA0109-005
8. CAP & PLUG PORTS PER RA0116-054
(7) HYDROSTATIC PROOF PRESSURE TEST PURGE PASSAGE TO 11,000±200 PSIG USING DEIONIZED WATER HOLD PRESS FOR ONE MIN. NO LEAKAGE ALLOWED
6. FLOW TEST PER IL 9125-10
(5) BRAZE PER MPR 8-175-47
(4) PRINT LETTERING AS SHOWN EXCEPT DO NOT IMPRESSION STAMP
3. USE SULPHUR FREE MATERIALS WHEN PROCESSING TO PREVENT EMBRITTLEMENT OF NICKEL MATERIAL AS DESCRIBED IN RA0103-014
(9) IDENTIFY PER RA0104-008
7. MACHINE PER RA0103-002

NOTED.

Figure 47. Prot

REVISIONS

CONFIDENTIAL
(LEGEND UNCLASSIFIED)

'LEAK TEST PER IL 9125-10
E NICKEL PLATE .0005±.0002 PER
9-005 PLATING ON ENTIRE
OPTIONAL EXCEPT DO NOT
INJECTOR FACEPLATE
STABILIZE PER STO110RA0043
AZE PER RA0107-027 USING
)-064 BRAZE ALLOY
NICKEL PLATE .0002-.0003
0109-005
LUG PORTS PER RA0116-054 ·
TATIC PROOF PRESSURE TEST PURGE
TO 11,000±200PSIG USING DEIONIZED WATER
SS FOR ONE MIN. NO LEAKAGE ALLOWED
ST PER IL 9125-10
PER MPR 8-175-47
ETTERING AS SHOWN EXCEPT
MPRESSION STAMP
PHUR FREE MATERIALS WHEN
SSING TO PREVENT
TTLEMENT OF NICKEL MATERIAL
CRIBED IN RA0102-014
TY PER RA0104-008
VE PER RA0103-002

Figure 47. Prototype Injector Assembly (U)

-3	304L CRES ROD	$\frac{1}{2}$ DIA × .37	304L QQ-S-763 CLASS 304L
NO	MATERIAL	SIZE	SPECIFICATION

ROCKETDYNE

INJECTOR - BRAZED
ASSY OF

J 02602 EWR 116346

NOTED.

FRAME 1

EWR 116346

S

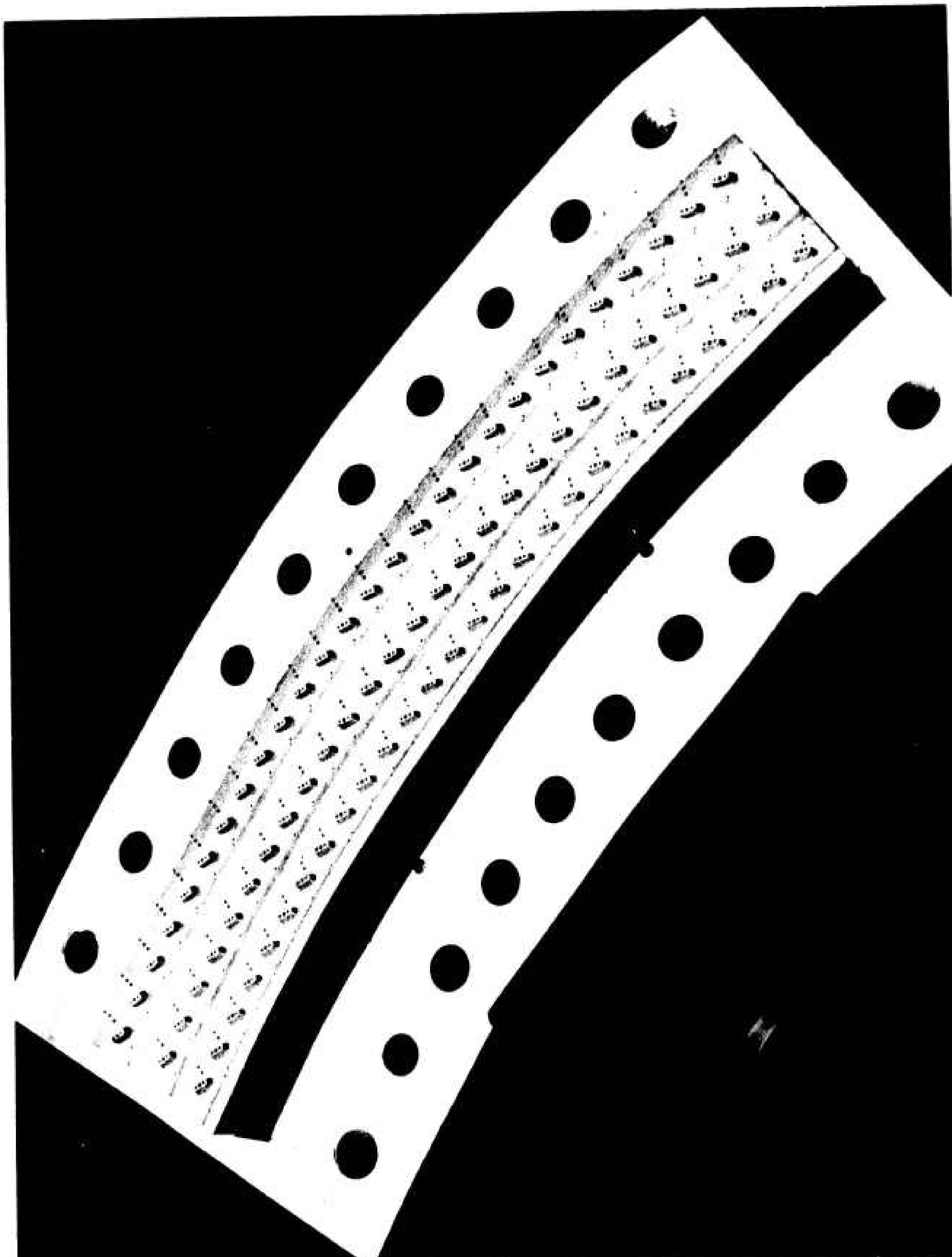

1EH42-7/22/69-C1C

Figure 48. U/N 4 30-Degree Brazed Injector (U)

CONFIDENTIAL

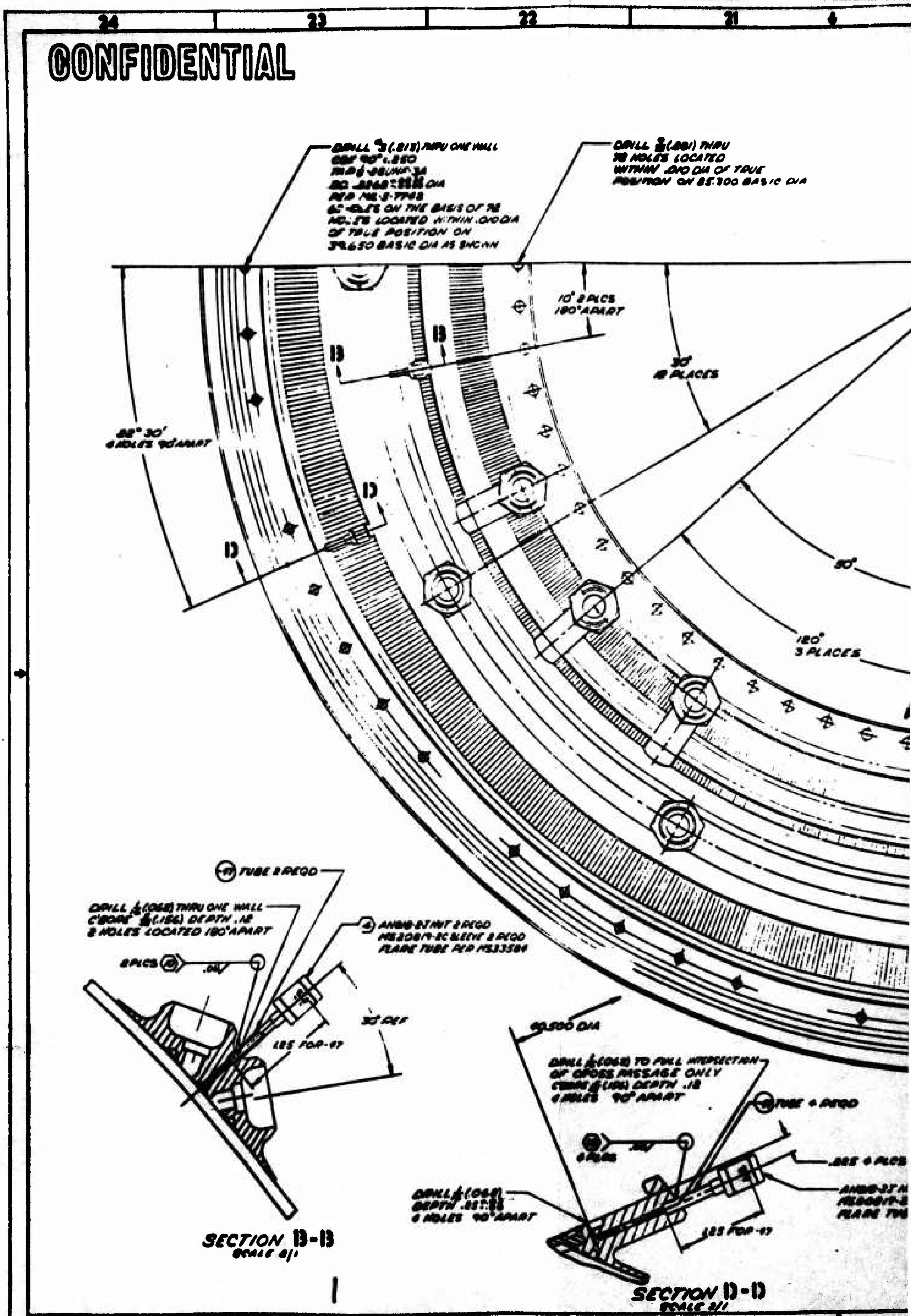

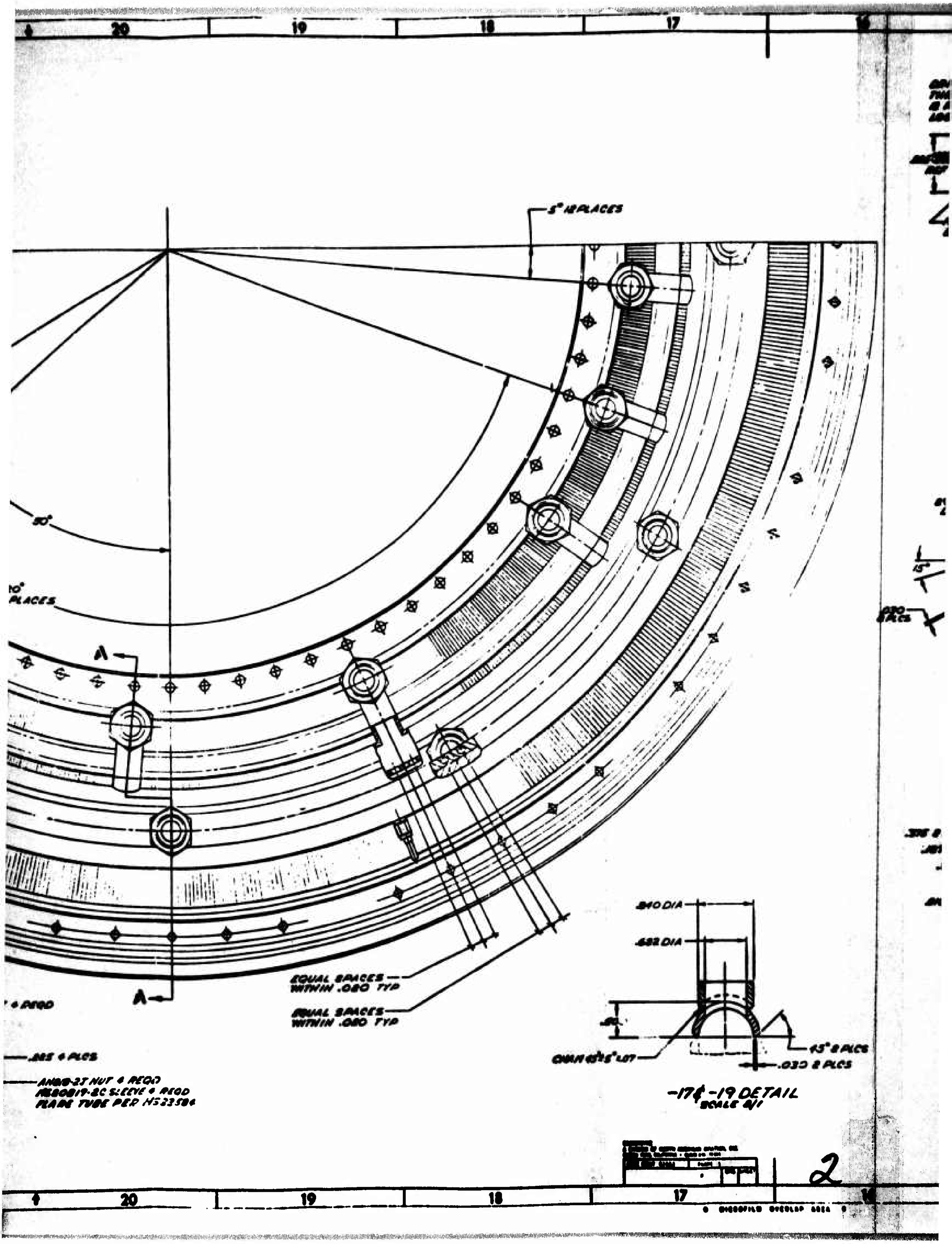

20
19
18
17
5° 12 PLACES
30°
10°
PLACES
A
A
EQUAL SPACES WITHIN .080 TYP
EQUAL SPACES WITHIN .080 TYP
.840 DIA
.682 DIA
45° 2 PLCS
.030 2 PLCS
-17 & -19 DETAIL
SCALE 8/1
AN818-2J NUT 4 REQD
MS20819-2C SLEEVE 4 REQD
FLARE TUBE PER MS33584
2

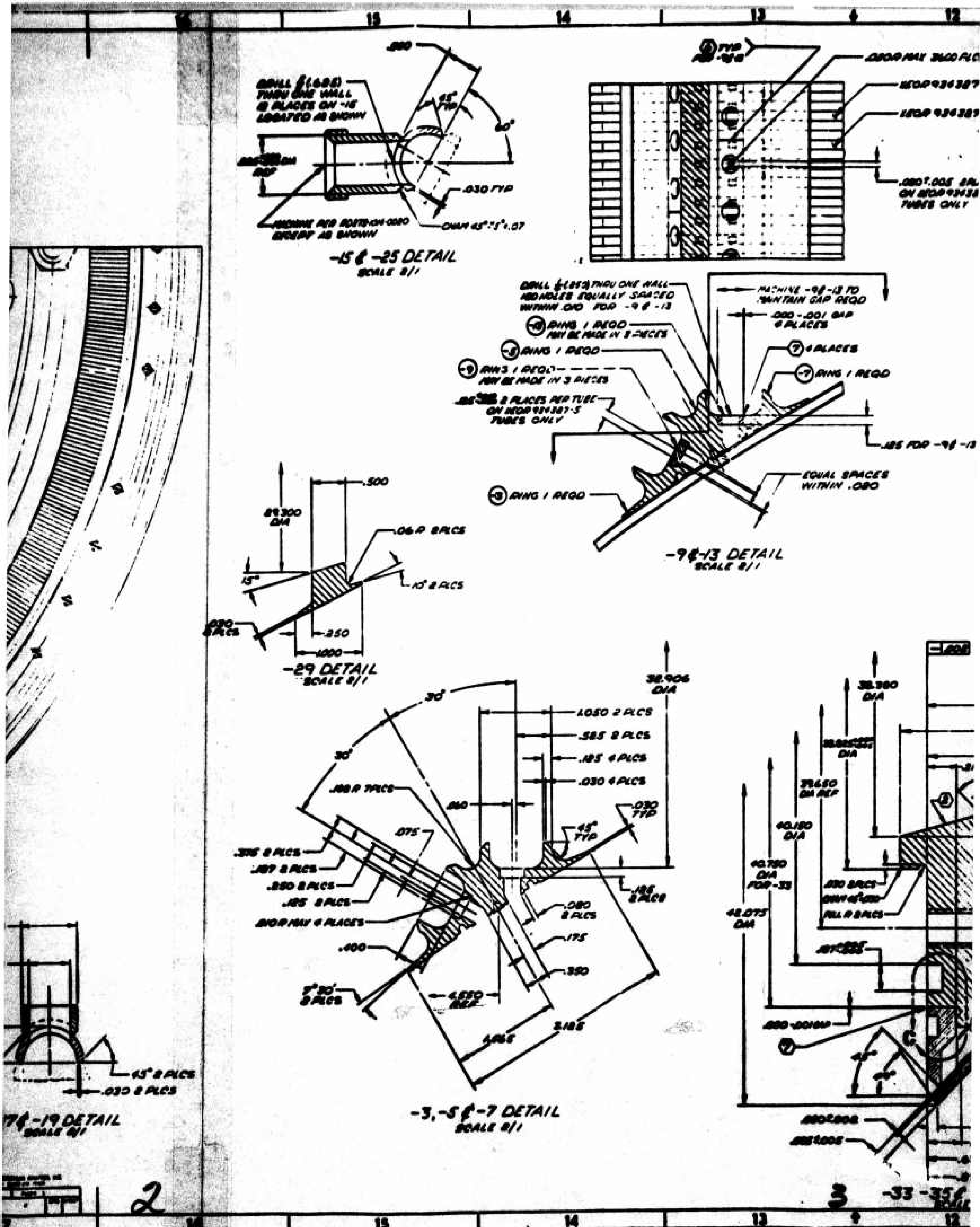

-15 & -25 DETAIL
SCALE 8/1
-9 & -13 DETAIL
SCALE 8/1
-29 DETAIL
SCALE 8/1
-3, -5 & -7 DETAIL
SCALE 8/1
-17 & -19 DETAIL
SCALE 8/1
.030 TYP
.500
.250
1.000
.06 R 2 PLCS
10° 2 PLCS
15°
45° 2 PLCS
.030 2 PLCS
1.050 2 PLCS
.585 2 PLCS
.185 4 PLCS
.030 4 PLCS
45° TYP
.316 2 PLCS
.187 2 PLCS
.250 2 PLCS
.185 2 PLCS
.080 2 PLCS
.175
.350
.400
4.650 REF
3.185
38.906 DIA
38.380 DIA
40.180 DIA
42.075 DIA
RING 1 REQD
EQUAL SPACES WITHIN .080
2
3
15
14
13
12

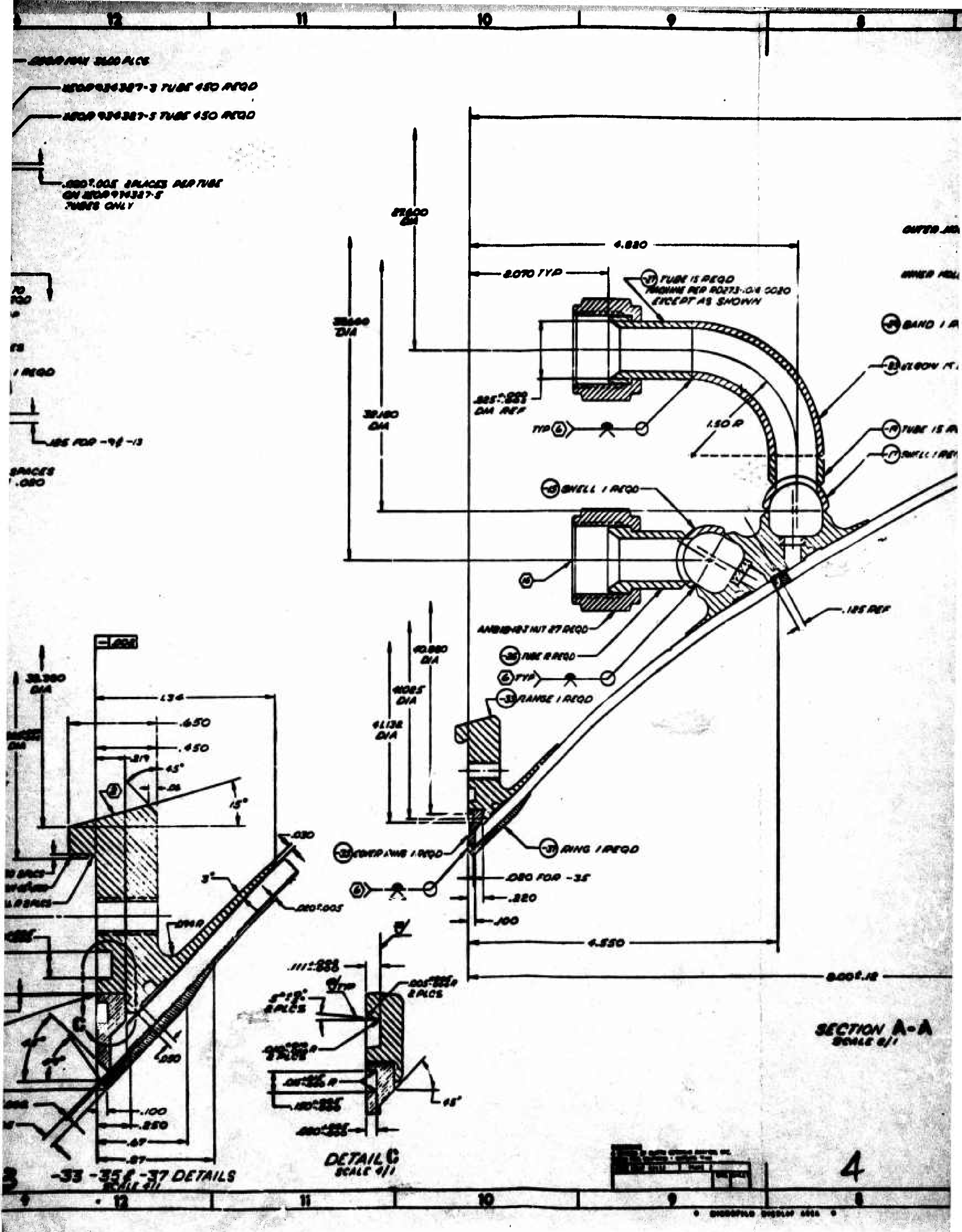
12
11
10
9
8
4.880
2.070 TYP
TUBE 1S REQD
EXCEPT AS SHOWN
BAND 1
1.50 R
SHELL 1 REQD
AN818-13 NUT 27 REQD
TUBE 8 REQD
FLANGE 1 REQD
RING 1 REQD
.125 REF
.080 FOR -35
.220
.100
4.550
.650
.450
45°
15°
.030
3°
.020±.005
.100
.250
SECTION A-A
DETAIL C
-33 -35 & -37 DETAILS
4

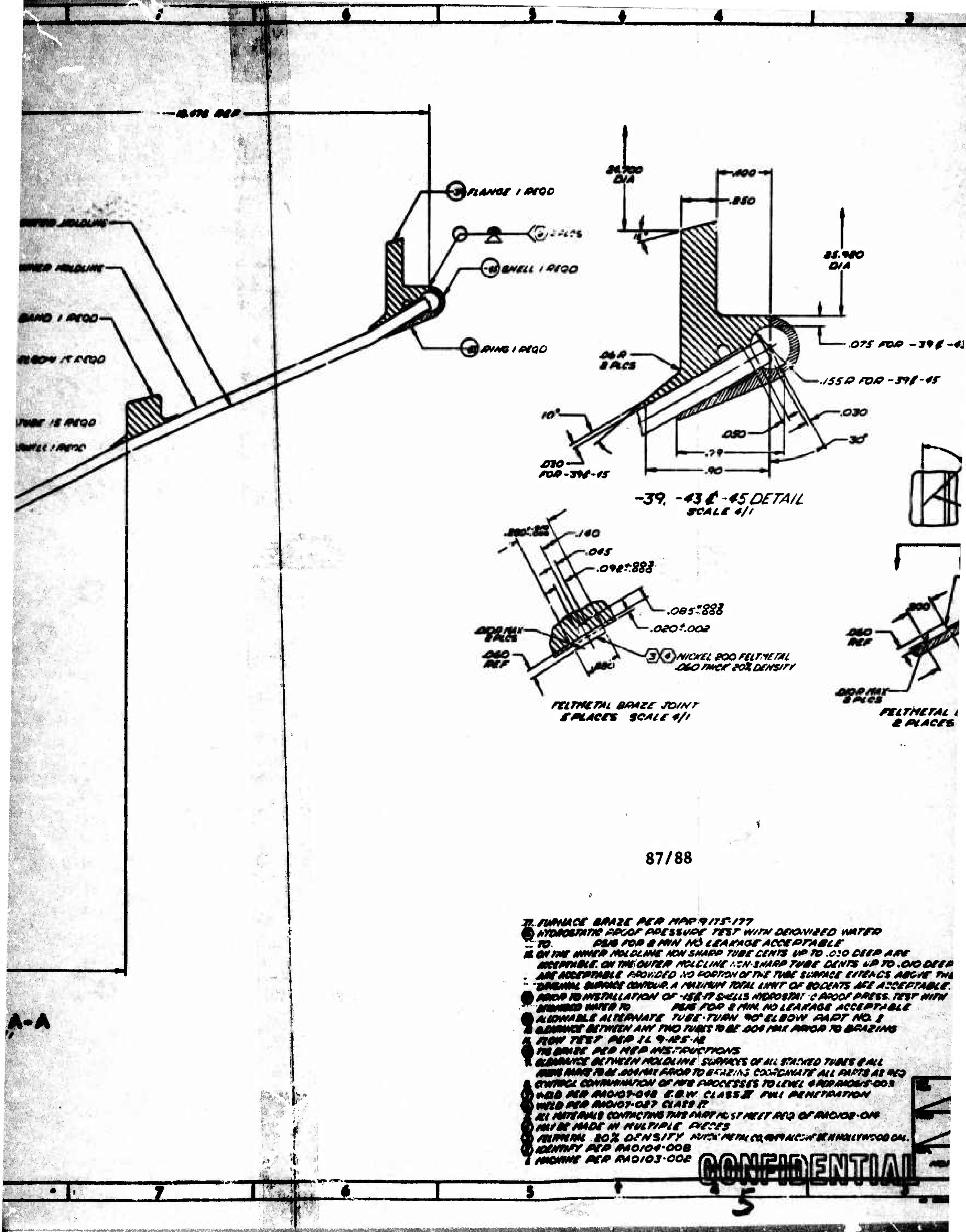
FLANGE 1 REQD
SHELL 1 REQD
RING 1 REQD
BAND 1 REQD
TUBE 12 REQD
-39, -43 & -45 DETAIL
SCALE 4/1
.075 FOR -39 & -45
.155 R FOR -39 & -45
.06 R
2 PLCS
NICKEL 200 FELTMETAL
.060 THICK 20% DENSITY
FELTMETAL BRAZE JOINT
2 PLACES SCALE 4/1
A-A
FURNACE BRAZE PER MPP 9175-177
HYDROSTATIC PROOF PRESSURE TEST WITH DEIONIZED WATER
TO PSIG FOR 2 MIN NO LEAKAGE ACCEPTABLE
PRIOR TO INSTALLATION OF -15 & -17 SHELLS HYDROSTATIC PROOF PRESS. TEST WITH
DEIONIZED WATER TO PSIG FOR 2 MIN. NO LEAKAGE ACCEPTABLE
ALLOWABLE ALTERNATE TUBE-TURN 90° ELBOW PART NO. 2
FLOW TEST PER IL 9-125-12
TIG BRAZE PER MEP INSTRUCTIONS
WELD PER RA0107-027 CLASS II
MAY BE MADE IN MULTIPLE PIECES
IDENTIFY PER RA0104-008
MACHINE PER RA0103-002
CONFIDENTIAL
5

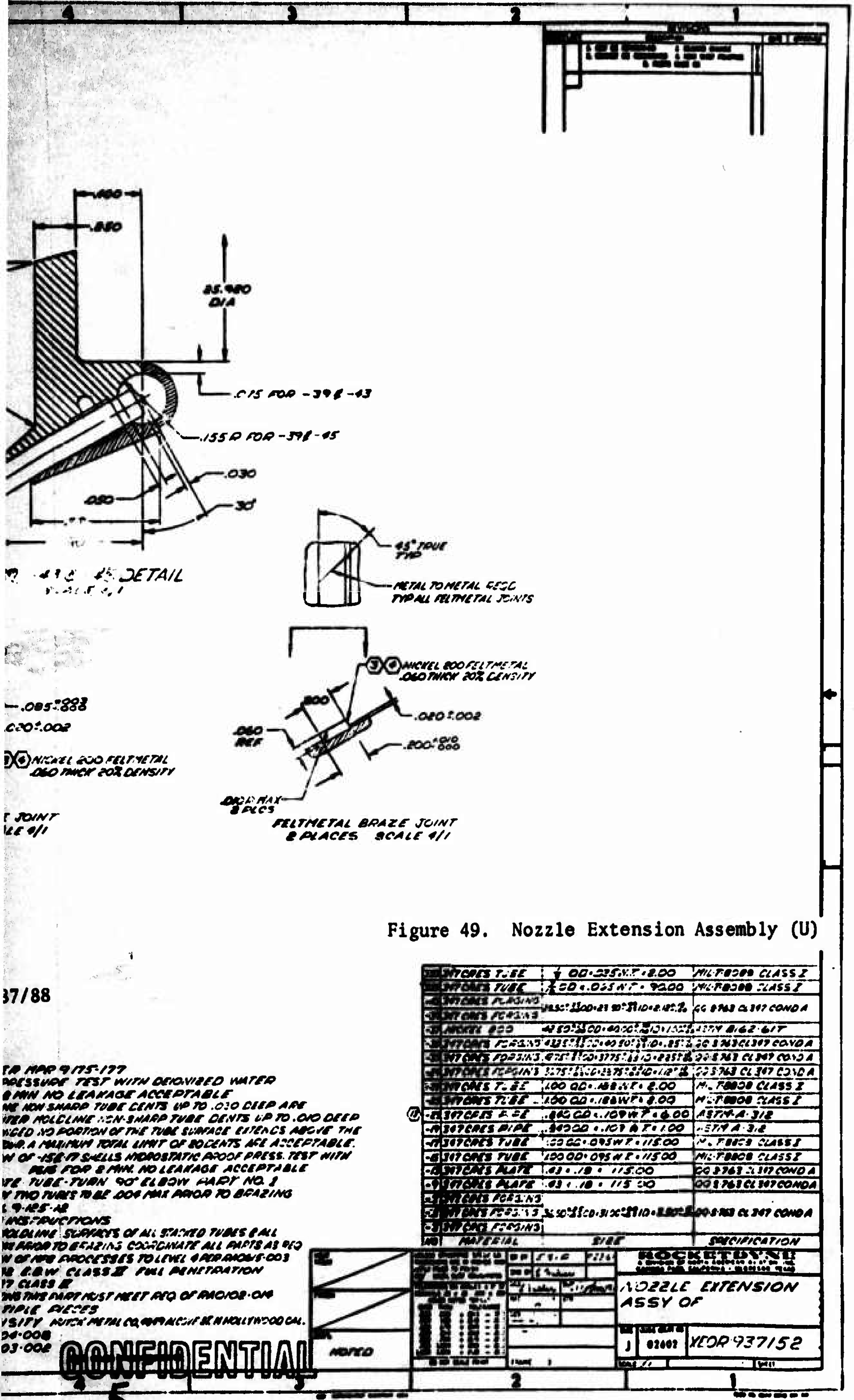

Figure 49. Nozzle Extension Assembly (U)

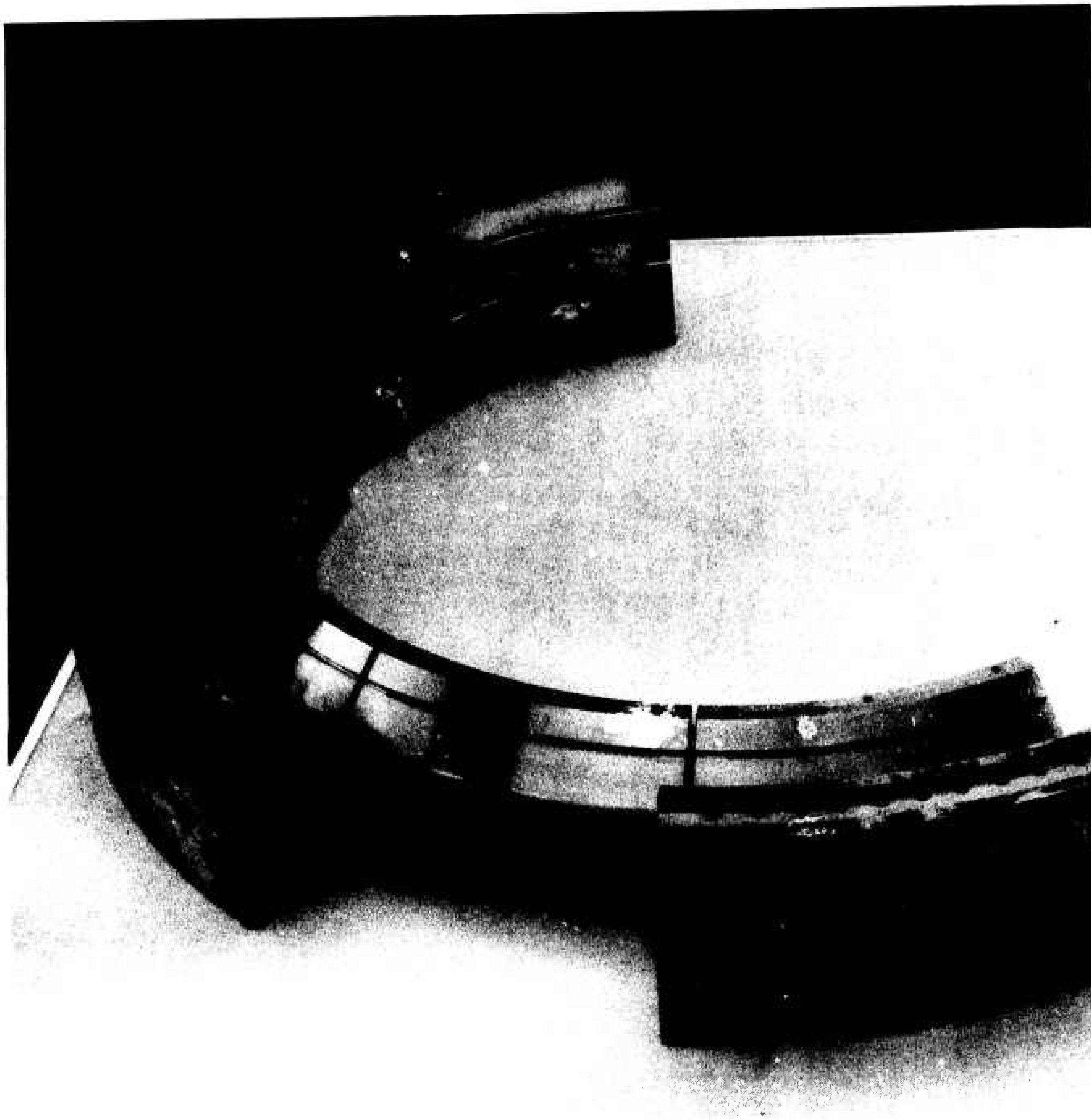

1EH22-8/13/69-C1M

Figure 50. Main Thrust Chamber Segments (View A) (U)

1EH22-8/13/69-C1N

Figure 51. Main Thrust Chamber Segments (View B) (U)

(U) g. Thirty-Degree Water-Cooled Chamber Segment

(U) Repair of the chamber segment by removal of the damaged throat section and furnace-braze attachment of a new section was completed. One checkout test was conducted and the repaired segment performed satisfactorily with no water leakage or damage.

(U) h. Thirty-Degree Injector (U/N 3) Modification

(C) The U/N 3 injector was scheduled to be used for combustion stability evaluations to be conducted in the 30-degree, water-cooled segment. To maintain a consistency of design, it was necessary to modify the injection pattern of the U/N 3 injector to the prototype injector pattern. This was a minor modification that consisted of the addition of 0.018-inch-diameter oxidizer bias orifices. The modification was completed and one satisfactory checkout test was conducted with the injector. No injector damage was noted during posttest inspection though the oxidizer side of the injector had been contaminated as a result of the failure of the facility oxidizer feed line. A discussion of the failure is presented subsequently.

(U) i. Five-Inch, Water-Cooled Thrust Chamber Segment

(C) The 5-inch, water-cooled thrust chamber segment has been described extensively in Ref. 1 . Fabrication of the segment was initiated and is approximately 50-percent complete, with completion scheduled for September 1969.

(C) Fabrication of the reduced-size injector also has been initiated and is scheduled for completion in September.

(U) 2. HEAT TRANSFER ANALYSIS

(U) a. Effect of Injector Oxidizer Bias on Coolant Circuit Operation

(C) A heat transfer study was performed to ascertain the effect of oxidizer film cooling on the operation of the prototype thrust chamber segment. It was concluded that no adverse effects would be sustained and that reductions in pressure drop and heat rejection would be realized throughout the throttle range.

(C) Three tests with oxidizer film cooling (oxidizer bias) were evaluated in this study. They were conducted at chamber pressures of 612, 222, and 74 psia. The data were obtained from water-cooled calorimeter thrust chamber hardware. These were superimposed on the prototype segment channel-wall configuration to determine operating parameters. The test mixture ratio, combustion temperature local gas-side heat transfer film coefficients, and chamber pressures were used to predict bulk temperature rise, chamber wall temperature, and pressure drop.

(C) The effect of the oxidizer bias was considered as follows. The gas-side heat transfer film coefficient was lowered throughout the combustion zone and in the throat. This covered the local heat flux in these areas and, also, the overall bulk temperature rise. The lowered bulk temperature rise and the local heat flux caused the maximum wall temperature to be lowered approximately 150 F from the runs without oxidizer bias.

(U) Table 5 presents a summary of the conditions used to analyze the oxidizer bias runs.

TABLE 5

(U) MAIN THRUST CHAMBER OXIDIZER BIAS INJECTOR ANALYSIS OF COOLANT CIRCUIT

Chamber Pressure, psia	Coolant Inlet Pressure, psia	Coolant Exit Pressure, psia	Coolant* Exit Bulk Temperature, F
650	1940	1405	474
222	760	508	782
78	360	263	1330

*Inlet temperature assumed to be -340 F

(U) Figure 52 compares the thrust chamber exit bulk temperature with and without injector oxidizer bias over the range of chamber pressure necessary for throttling.

(U) Figure 53 shows the inlet pressure as a function of chamber pressure. Also shown is the coolant exit pressure for the oxidizer bias and the no-oxidizer bias cases. Both outlet pressure curves are based on the same inlet pressure curve.

(U) b. Baffle and Nozzle Extension One-Dimensional Heat Transfer Analysis

(C) Calculations were carried out to determine pressure drops and peak temperatures in the nozzle extension and chamber segment end plates (baffles). Peak gas-side surface temperature of the baffles at 650-psia chamber pressure was estimated to be 1570 F, and pressure drop will be 136 psi for an inlet pressure of 2100 psia. The heat transfer study of the nozzle extension was performed at chamber pressures of 650, 222, and 90 psia. Pressure drops of 62, 32, and 20 psi resulted at the respective chamber pressures. A peak gas-side wall temperature of 1630 F was found to occur at a chamber pressure of 90 psia and was located at the leading edge.

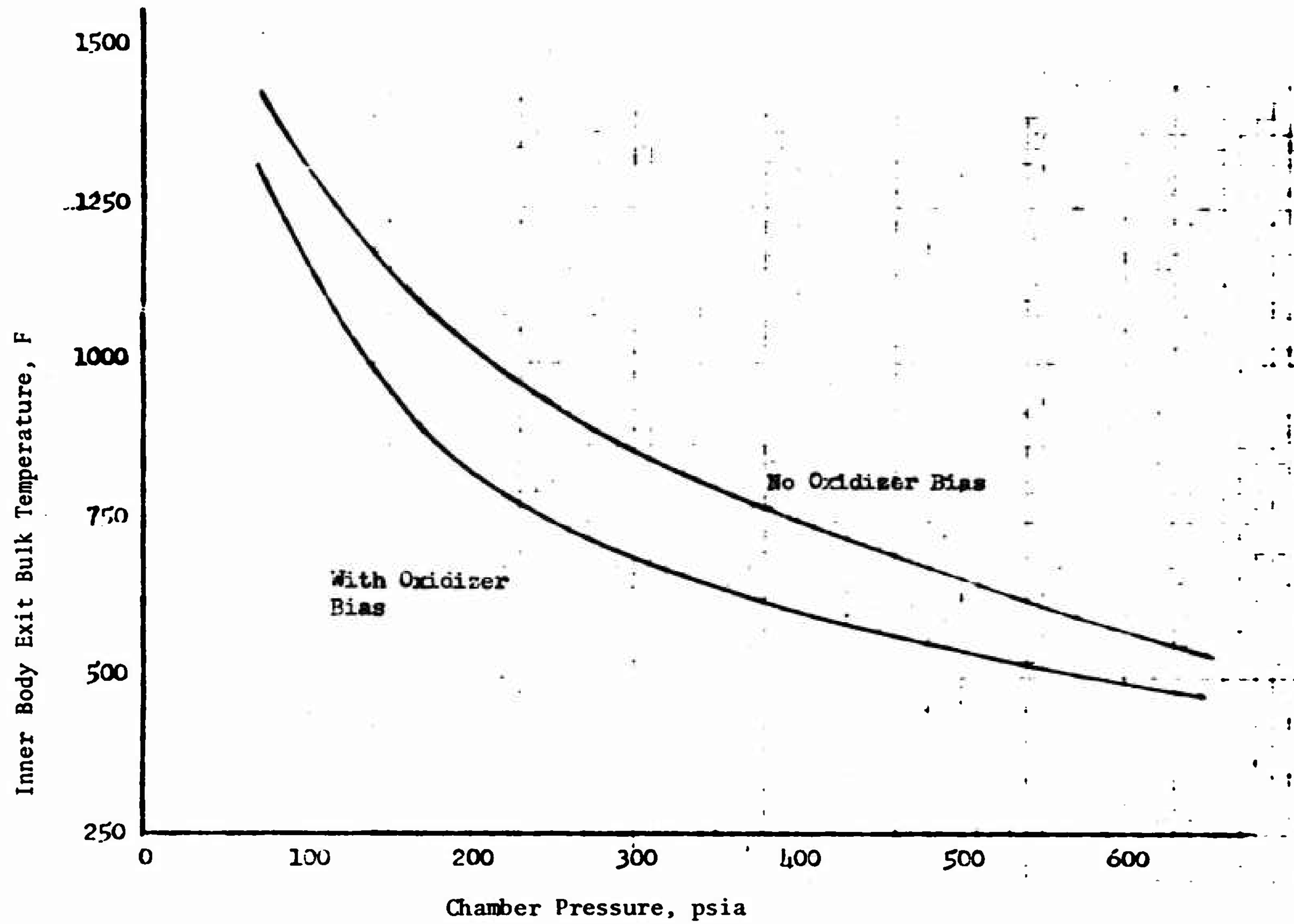

Figure 52. Main Thrust Chamber Segment Effect of Injector Oxidizer Bias on Inner Body Exit Bulk Temperature (U)

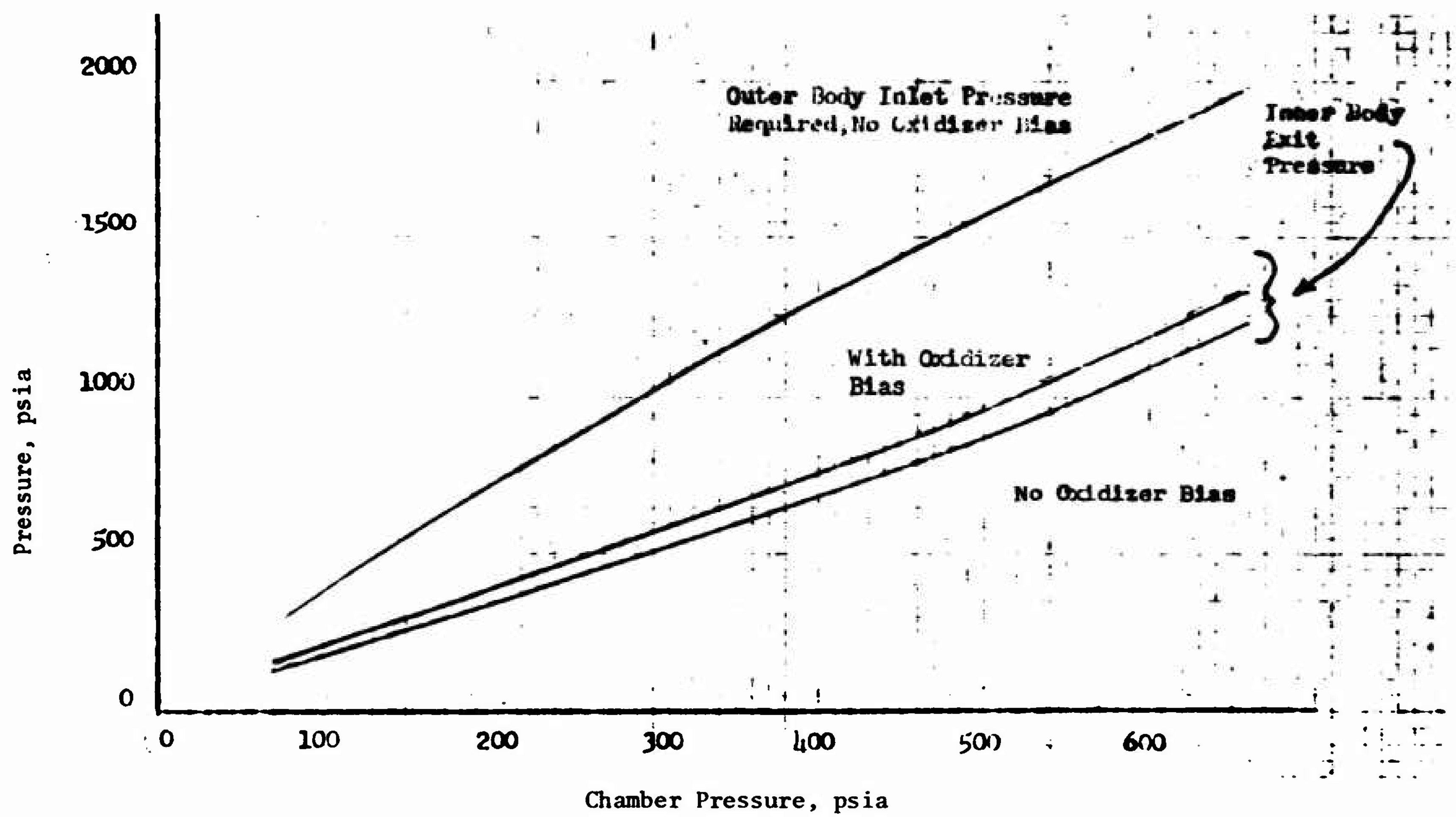

Figure 53. Main Chamber Segment Effect of Oxidizer Bias on Pressure Loss in Outer and Inner Body (U)

(U) (1) Description of Analysis

(U) Heat transfer and fluid flow calculations were made on both the nozzle extension and the baffle with the one-dimensional heat transfer digital computer program.

(U) In the program, the cooling circuit is divided into 42 increments. For each increment, iteration is made on the heat flux from the combustion gas to the coolant, the resulting temperature profile, and the coolant change of state until they are compatible with the friction and momentum pressure drop over the increment.

(U) (a) Baffle

(U) The gas-side surface heat transfer coefficients were determined from the solid-wall segment tests and are identical to the coefficients used in the design analysis for the main chamber segment. The coolant-side surface coefficient was determined by the equation of Hess and Kunz, modified by Miller et al., in Ref. 1 :

(U) $$Nu_{0.4} = 0.0204\ Re_{0.4}^{0.8}\ Pr_{0.4}^{0.4}\ (1 + 0.00983\ \frac{\nu_w}{\nu_b}) \qquad (1)$$

where

Nu = Nusselt number = $\frac{hd}{k}$, dimensionless

h = surface heat transfer coefficient, Btu/in.^{2}-sec-F

D = equivalent diameter of channel, in.

k = thermal conductivity of coolant, Btu/in.-sec-R

Re = Reynolds number = $\frac{\rho VD}{\mu}$, dimensionless

ρ = coolant density, lbm/in.^{3}

V = coolant velocity, in./sec

μ = coolant viscosity, lbm/in.-sec

Pr = Prandtl number = $C_p\mu/k$, dimensionless

C_p = coolant constant pressure specific heat, Btu/lbm-R

ν = $\frac{\mu}{\rho}$, in.^{2}/sec

Subscripts w and b indicate coolant properties are to be evaluated at wall and bulk temperatures, respectively, and subscript 0.4 indicates coolant properties are to be evaluated at $T_{0.4}$ where

$$T_{0.4} = T_b + 0.4\ (T_w - T_b)$$

(U) Equation 1 was found to have an absolute average deviation of 16.2 percent when correlated with 1961 experimental data points taken at pressures of 455 and 2450 psia, coolant bulk temperatures of 150 R and less, and wall temperatures of -100 F to 1400 F.

(U) (b) Nozzle Extension

(U) Gas-side heat transfer coefficients were computed using a General Electric computer program to solve the equation:

$$\frac{h}{\rho V C_p} = St \qquad (2)$$

where St = Stanton number (dimensionless) and h, ρ, V, and C_p are as previously defined. The method used to solve Eq. 2 is explained in detail in Appendix A. The results are shown in Fig. 54 through 56.

(U) The coolant surface heat transfer coefficient was determined by:

$$Nu_b = 0.025 \, Re_b^{0.8} \, Pr_b^{0.4} \left(\frac{T_b}{T_w}\right)^{0.55}$$

where subscripts b and w indicate properties are evaluated at bulk coolant temperature and wall temperature, respectively. McCarthy and Wolf (Ref. 1) found the above equation to have an average absolute deviation of 10 percent when correlated with experimentally determined values taken at pressures of 190 to 1354 psia, bulk temperatures of 215 to 734 R, heat fluxes from 0.98 to 14.7 Btu/in.^{2}-sec, and Reynolds numbers from 12,000 to 1,670,000.

(U) (2) Calculated Results

(U) (a) Baffle

(U) Flowrates in the individual channels were selected to satisfy the requirement of equal pressure at the intersection of the channels and at the rear collection manifold. The pressure drops (coolant temperatures that accompany flow distribution) are presented in Table 6. Figure 57 shows the baffle configuration and the channel numbering system referenced in Table 6.

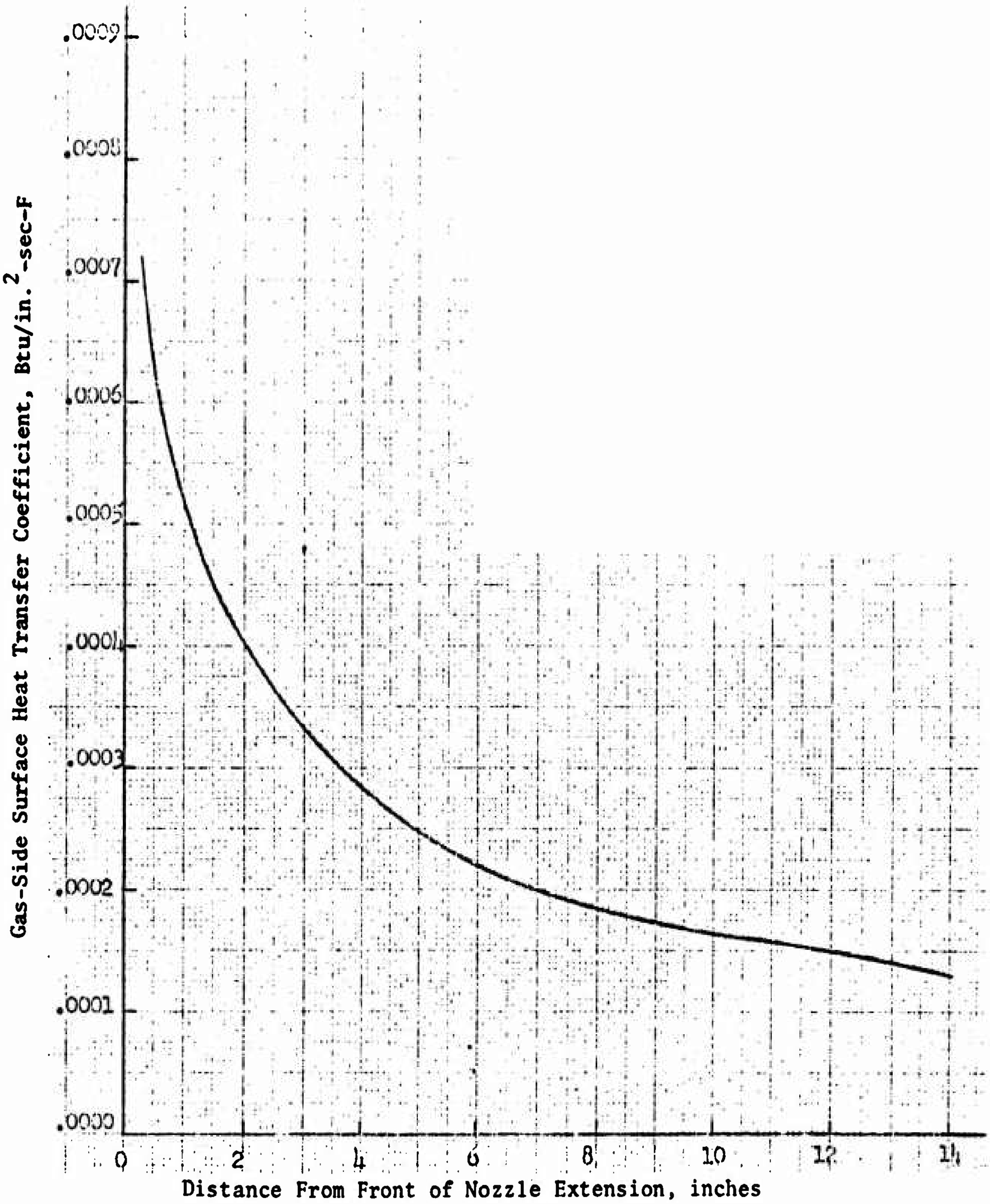

Figure 54. Nozzle Extension Gas-Side Surface Heat Transfer Coefficient vs Distance Along Surface From Leading Edge (650-psia chamber pressure) (C)

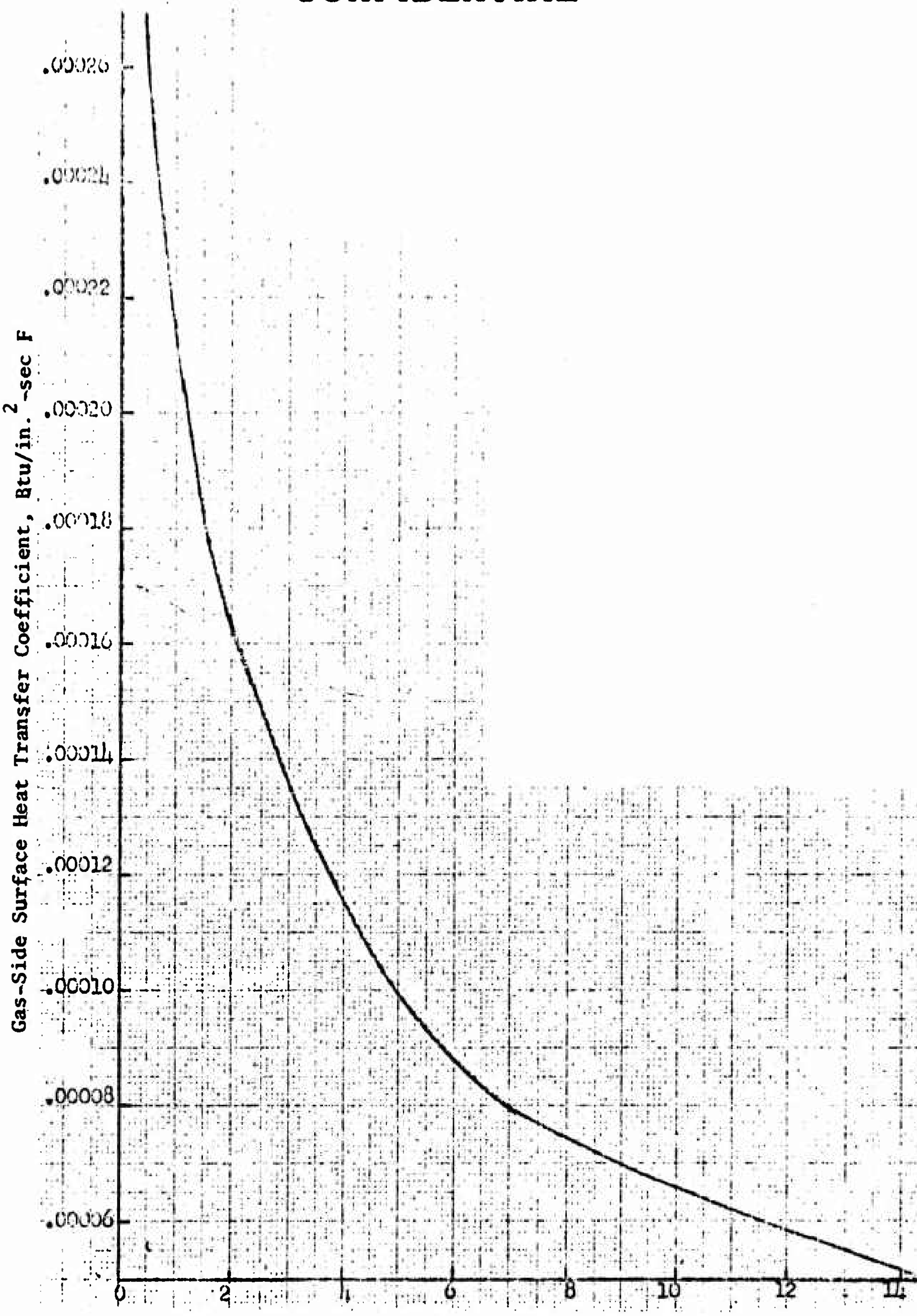

Figure 55. Nozzle Extension Gas-Side Surface Heat Transfer Coefficient vs Distance Along Surface From Leading Edge (222-psia chamber pressure) (C)

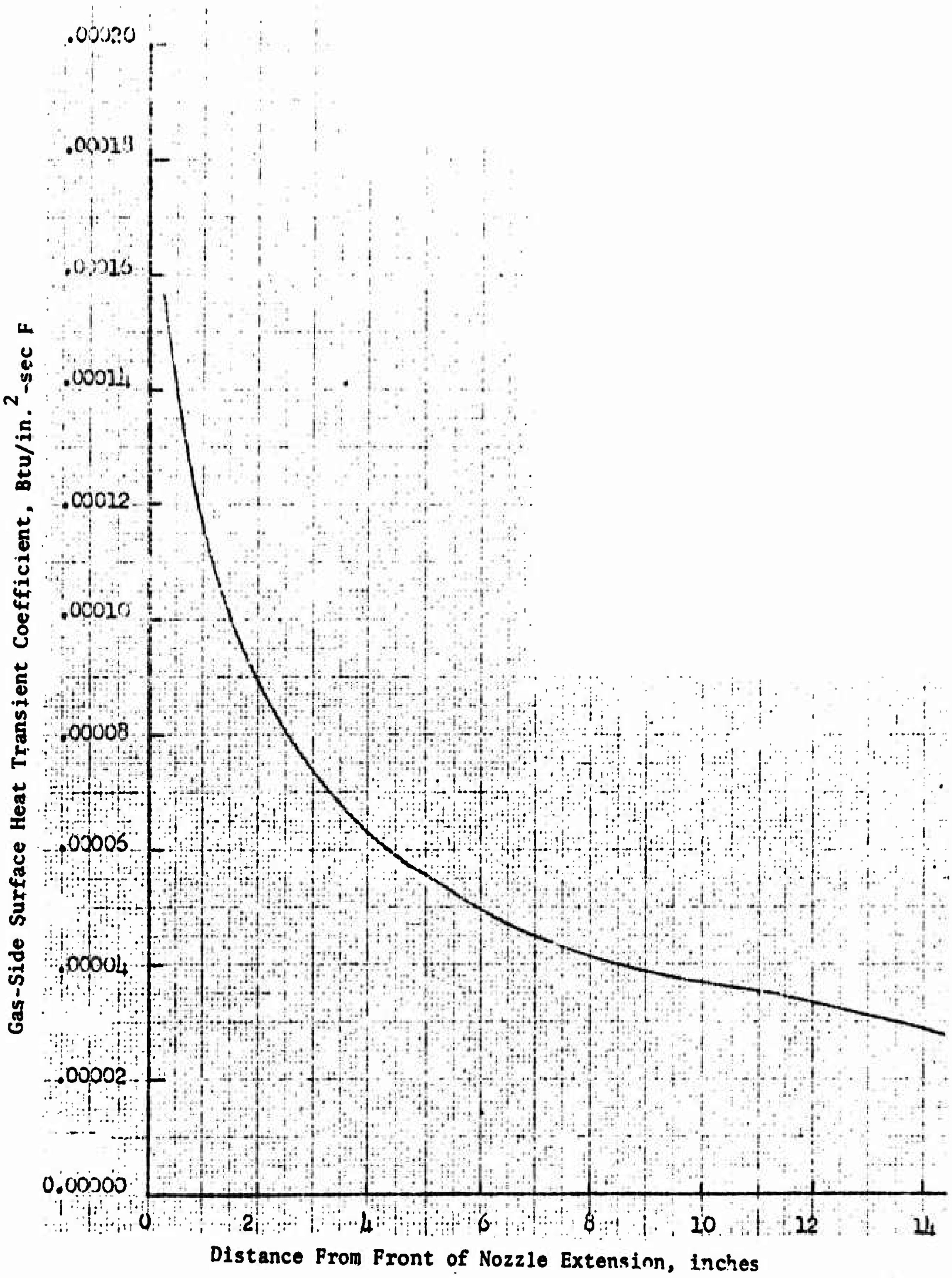

Figure 56. Nozzle Extension Gas-Side Surface Heat Transfer Coefficient vs Distance Along Surface From Leading Edge (90-psia chamber pressure) (C)

TABLE 6

(C) BAFFLE CALCULATED RESULTS (P_C = 650 PSIA)

	Front Section					Rear Section				
Channel No.	Flow-rate, lbm/sec	Inlet Pressure, psia	Intersect Pressure, psia	Intersect Pressure Loss, psi	Coolant Temperature at Inter-sect, R	Flow-rate, lbm/sec	Inlet Pressure, psia	Exit Pressure, psia	Coolant Exit Temperature, R	Maximum Gas-Side Surface Temperature, F
1	0.0135	2100	2070	14	110	0.0228	2056	1964	146	1567
2	0.0125	2100	2070	15	110	0.0243	2055	1964	136	1529
3	0.0125	2100	2070	19	110	0.0272	2051	1964	119	1318
4	0.0125	2100	2070	22	110	0.0289	2048	1964	109	1318
5	0.0116	2100	2070		122					1500
6	0.0129	2100	2070		95					928
7	0.0139	2100	2070		75					-25
8	0.0148	2100	2070		57					-400

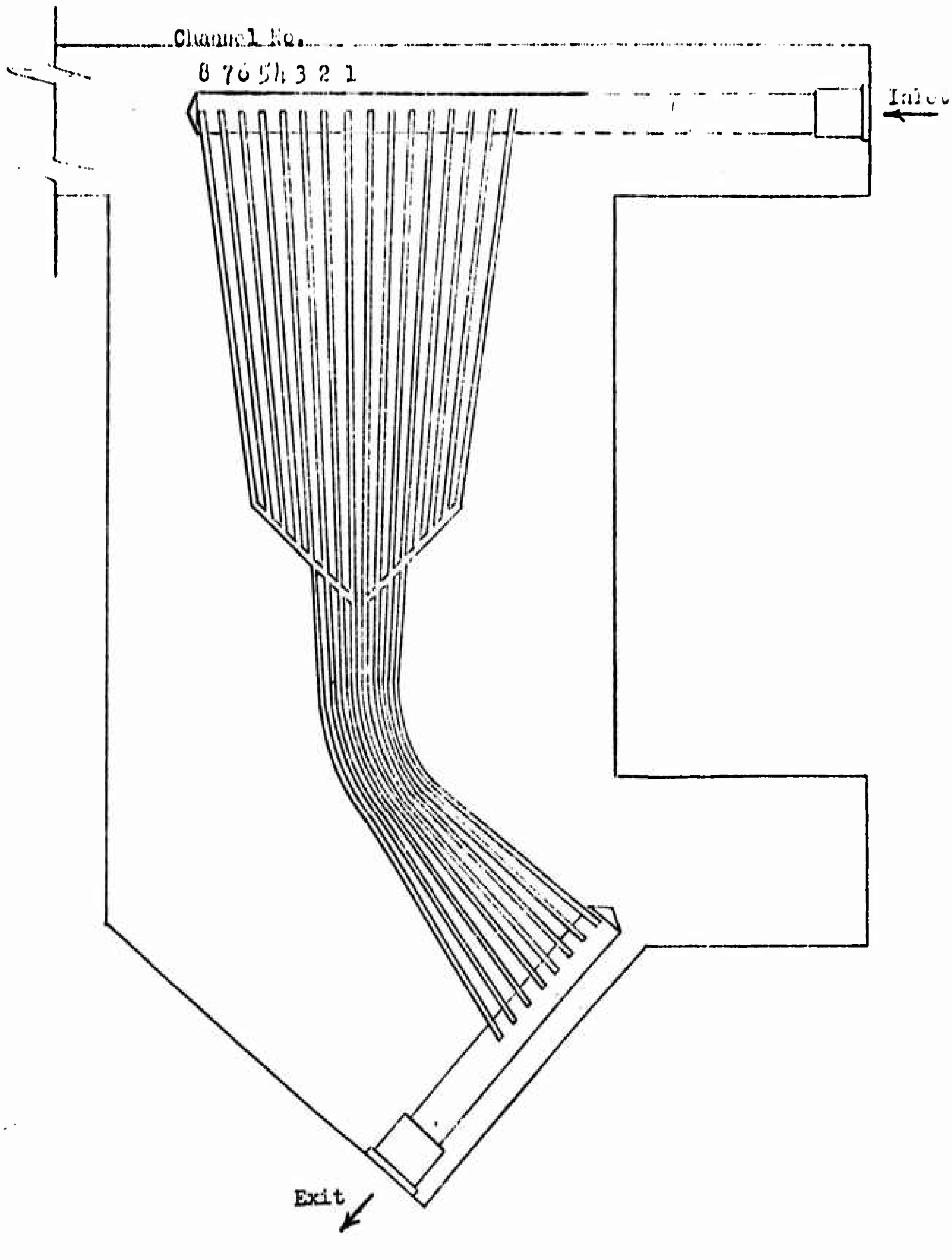

Figure 57. Prototype Segment Baffle (U)

(C) It must be noted that the maximum gas-side surface temperature in channel 1 is determined by a one-dimensional heat flow analysis, as are all the temperatures. Because the maximum value in channel 1 occurred at 0.2 inch upstream of the throat, where heat flux is at its highest, a two-dimensional calculation would yield a value higher than 1567 F at that location. Based on previous studies, the effect will be less than 50 F.

(U) (b) Nozzle Extension

(C) With the coolant entering the tube assembly in the upstream direction, at a location 6 inches (measured axially) from the leading edge of the nozzle extension and following the two-pass circuit illustrated in Fig. 58, the conditions calculated to exist in the nozzle extension are as shown in Table 2. These results also are presented in Fig. 59 and 60 in graphic form.

(U) 3. SEGMENT THRUST CHAMBER/INJECTOR TESTING

(U) Thrust chamber test activity to date has consisted of 5-inch and 30-degree thrust chamber/injector segments. A summary of this testing through the present quarter is presented in Table 8 for the 5-inch hardware and the 30-degree hardware. The table presents the total tests, and accumulated test time at the end of testing a particular thrust chamber/injector combination. For reference purposes, the test numbers associated with the tests are included. More detail of particular tests can be obtained from previous quarterly reports (Ref. 1 through 7).

(C) The testing conducted during this quarterly period consisted of one facility checkout test conducted prior to the combustion stability evaluation program. The test, 021-69, was conducted with the 30-degree water-cooled calorimetry chamber and the 30-degree injector (U/N 3).

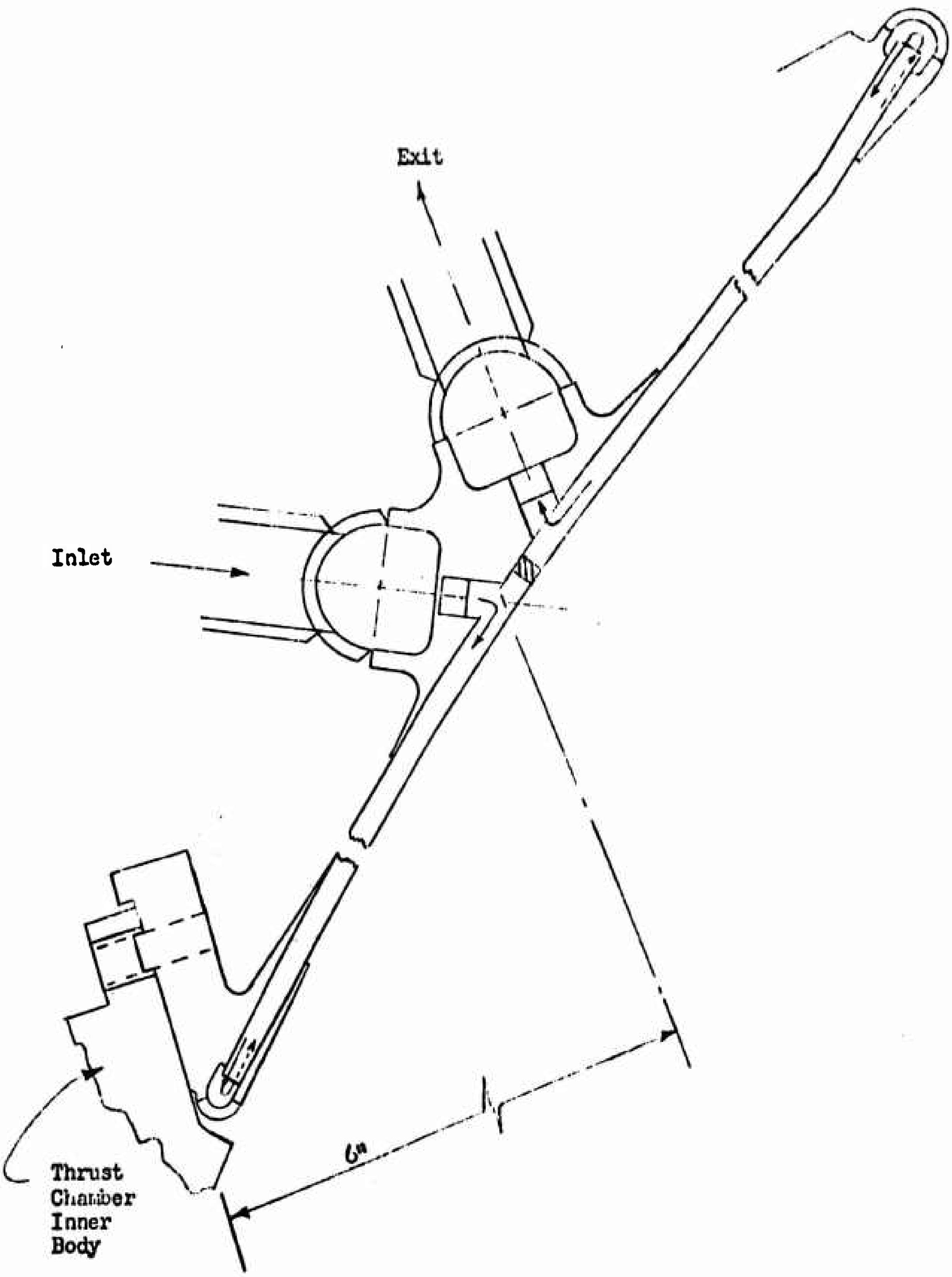

Figure 58. Two-Pass Nozzle Extension With Manifold Located 6 Inches (Axially) Downstream of Rear of Thrust Chamber Inner Body (C)

TABLE 7

(U) NOZZLE EXTENSION COMPUTED RESULTS

Chamber Pressure, psia	650	222	90
Maximum Gas-Side Surface Temperature, F	1254	1469	1632
Pressure Drop, psi	62	34	20
Hydrogen Inlet Temperature, F	474	781	1223
Hydrogen Exit Temperature, F	663	893	1452
Hydrogen Temperature Rise, R	194	209	232
Inlet Pressure, psia	1200	448	198

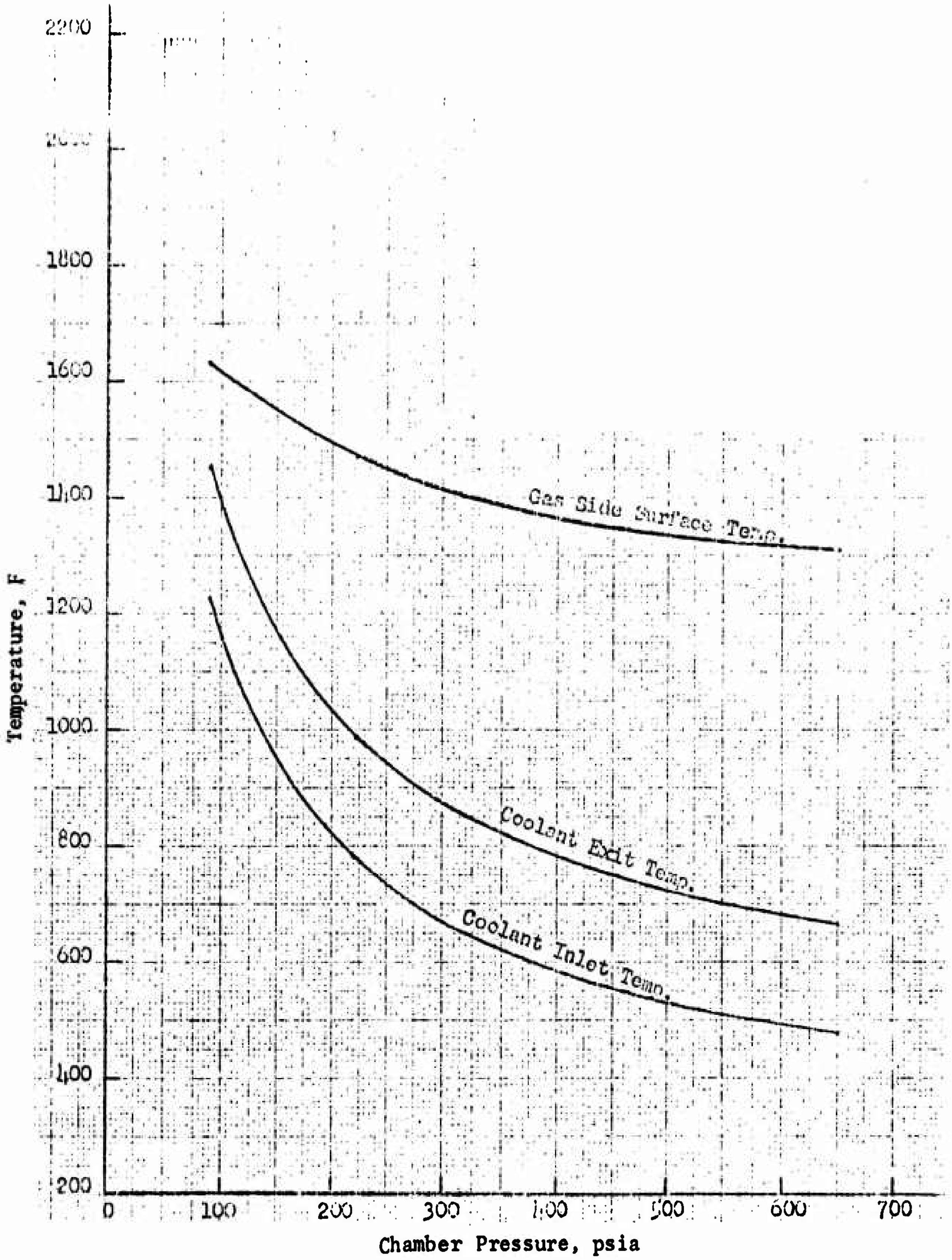

Figure 59. Nozzle Extension Gas-Side Surface Temperature and Coolant Inlet and Exit Temperature (U)

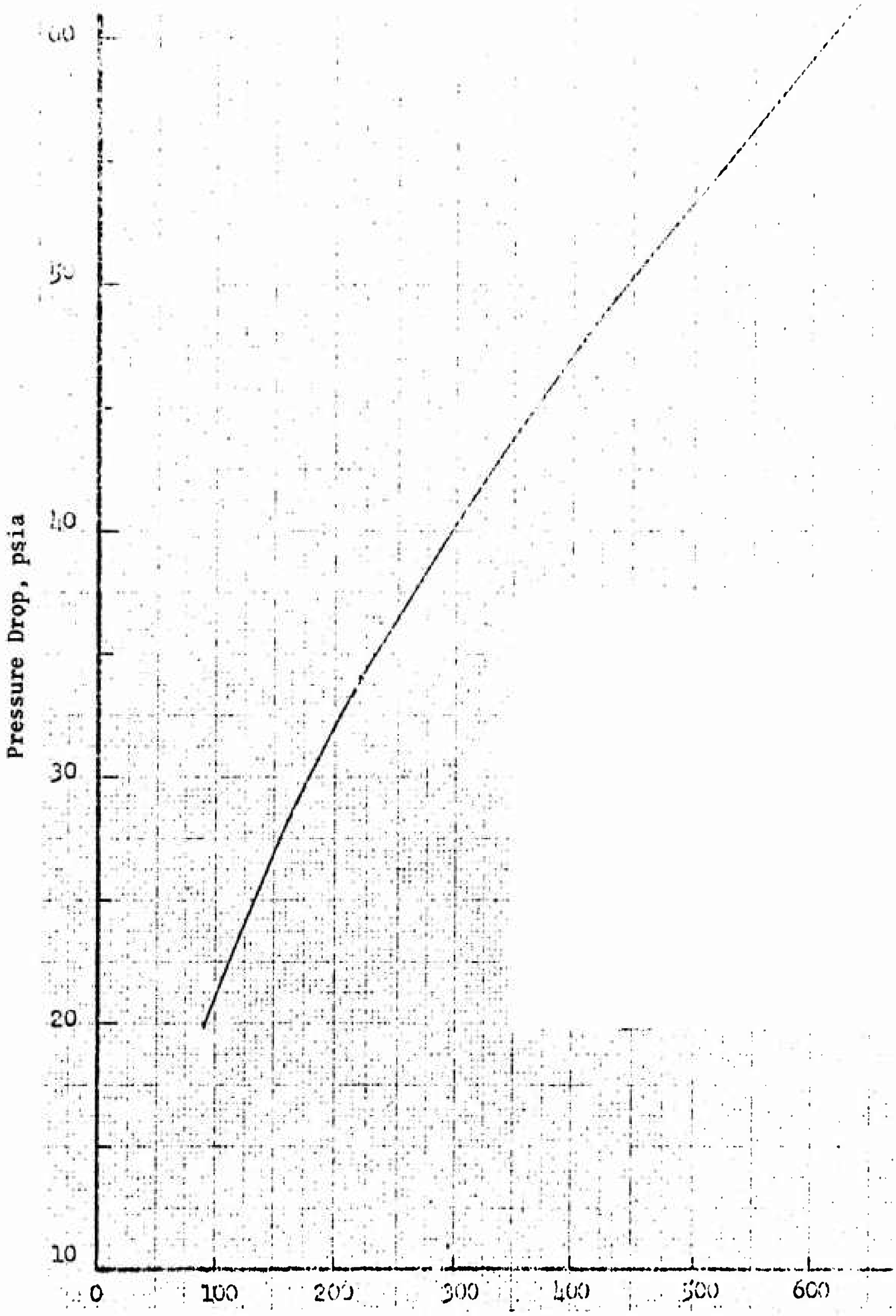

Figure 60. Nozzle Extension Tube Assembly Pressure Drop (U)

TABLE 8

(U) THRUST CHAMBER TEST SUMMARY

Hardware Configuration		Testing*	
Thrust Chamber	Injector	No. of Tests	Duration, seconds
5-Inch Segment**			
G_c Contour, Water-Cooled, U/N 1 (3.5-inch combustion zone, 46 tests, 263 seconds)	Triplet, U/N 1	3	4.4
	Triplet, U/N 2	4	4.3
	Fan, U/N 1	7	8.7
	Triplet, U/N 3	5	19.8
	Fan, U/N 2	13	96.3
	Fan, U/N 3	14	129.5
G_c Contour, Water-Cooled, U/N 1 Mod (2.68-inch combustion zone)	Fan, U/N 3	8	103.1
K Contour, Water-Cooled	Fan, U/N 1	8	38.8
	Fan, U/N 4	9	23.1
G_c Contour, Water-Cooled, U/N 2	Fan, U/N 1	2	12.5
	Triplet, U/N 3	5	10.8
Tube Wall, U/N 1	Fan, U/N 2	1	0.3
30-Degree Segment***			
Water-Cooled	Integral Fan, U/N 2	2	5
	Brazed-Face Fan, U/N 1	9	100.9
	Brazed-Face Fan, U/N 3	3	67.2
Tube Wall, U/N 1	Brazed-Face Fan, U/N 1	22	196.8
	Brazed-Face Fan, U/N 3	5	27.7
Tube Wall, U/N 2	Brazed-Face Fan, U/N 1	1	10.0
Channel-Wall, U/N 1	Brazed-Face Fan, U/N 1	11	103.1
	Brazed-Face Fan, U/N 3	1	4.9

*Refer to Table 4 for final hardware condition
**Test Series: 001-68 through 074-68, 103-68 through 107-68 (107-68 final test in 1968), 009-69 through 011-69
***Test Series: 076-68 through 102-68, 001-69 through 008-69, 012-69 through 021-69, 1001 through 1008

(C) Test 021 was scheduled for 5.0 seconds mainstage duration at a chamber pressure of 350 psia and mixture ratio of 14.0 (o/f). One pulse gun was sequenced to provide a stability rating pulse at 4.8 seconds into mainstage. The pulse gun was loaded with 15 grains of Bullseye powder in a 0.38-caliber cartridge with a 7500-psi burst diaphragm located between the cartridge and the combustion zone. The test was terminated at 3.05 seconds of mainstage by a test observer because of burnout of the oxidizer main line. Figure 61 shows the test in progress prior to the fire. Analysis of the test records and test films indicates that the fire originated in the oxidizer main valve and burned out the oxidizer main line downstream of the oxidizer main valve. The oxidizer flowmeter section of line upstream of the main valve also was burned out; however, the films reveal that burnout of the flowmeter line section was a consequence of the fire and not the cause.

(U) The pulse gun charge was removed from the chamber intact. Cutoff was initiated prior to firing of the pulse gun.

(U) Facility repair is in process and will require approximately 1 week, after which the stability test program will be resumed.

(U) 4. OXIDIZER PUMP BEARINGS AND SEALS

(C) During this report period, the bearing and seal effort was primarily devoted to the fabrication of the main and secondary oxidizer bearing and seal testers and the testing of the main engine bearings and seals. Diagrams of the main bearing and seal tester and the complete assembly including the turbine drive are presented in Fig. 62 and 63. A malfunction occurred during the second test in this quarter and the fourth test on the main bearing and seal tester. In addition, other operational problems necessitated rescheduling of the test program, ordering replacements for the damaged hardware, and incorporation of some design improvements. A detail discussion of the malfunction and corrective action in process is presented later in this report.

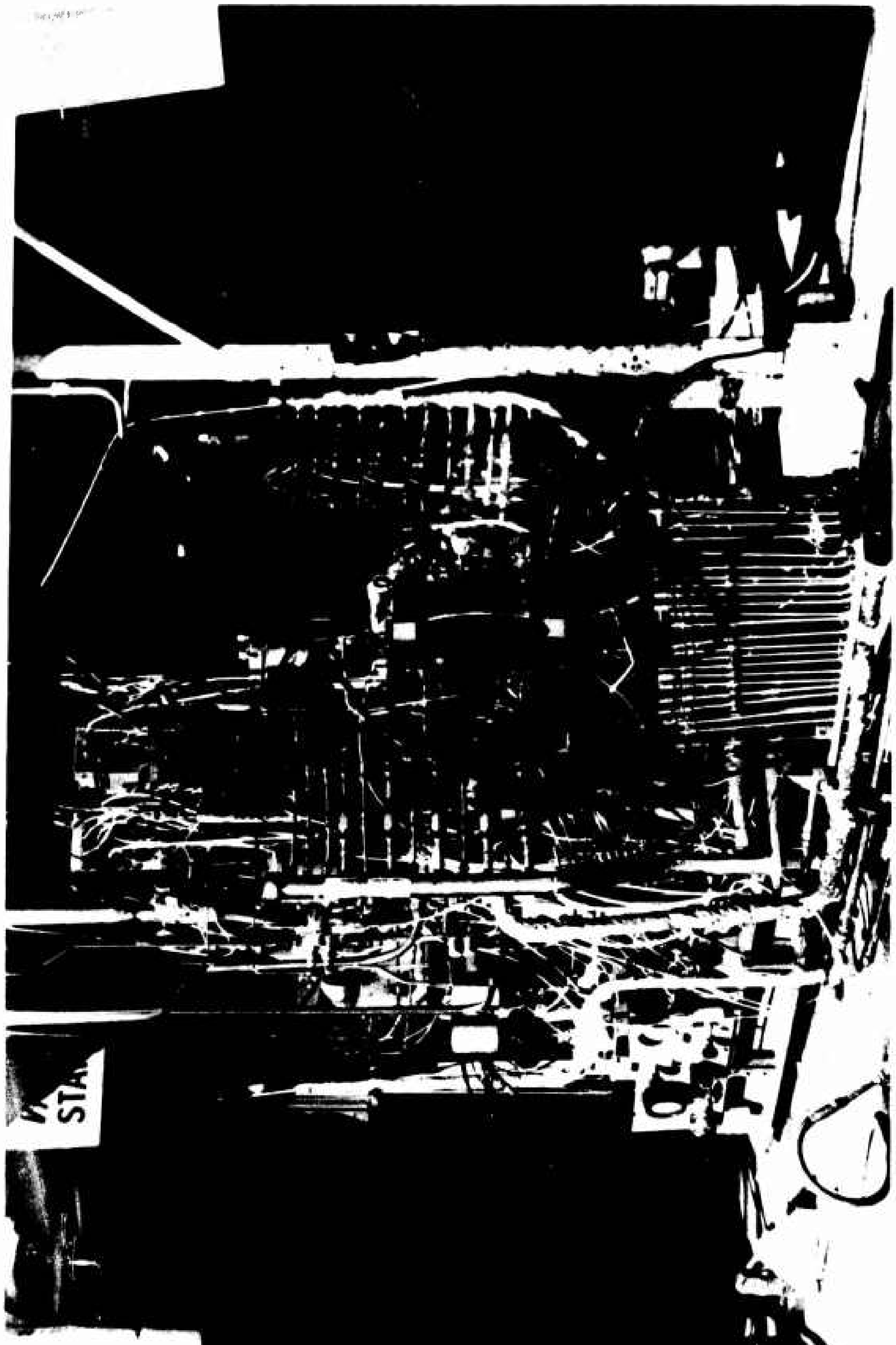

5WJ25-7/28/69-S1

Figure 61. Facility Checkout Test 021, Mainstage (U)

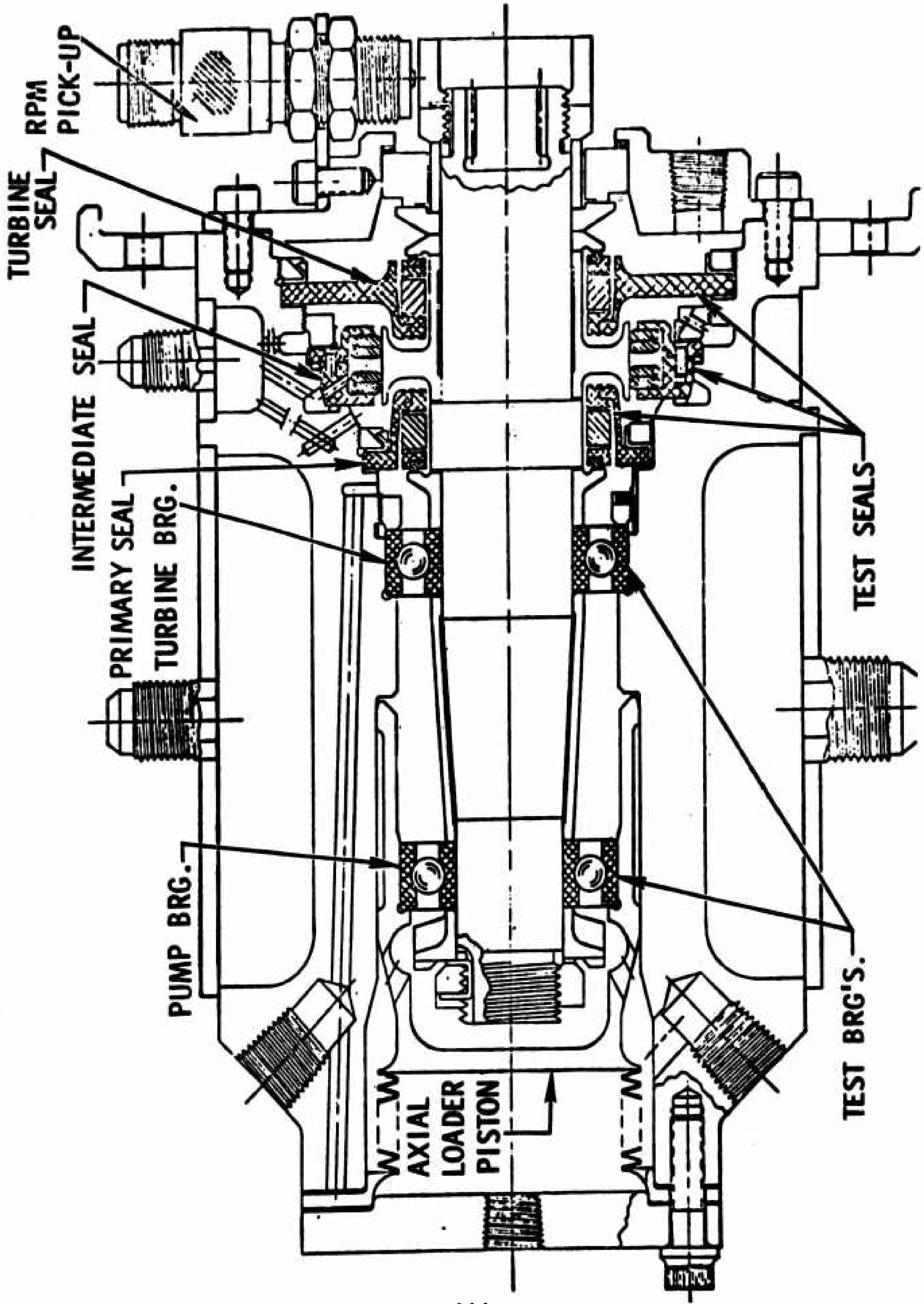

Figure 62. Main Bearing and Seal Tester (U)

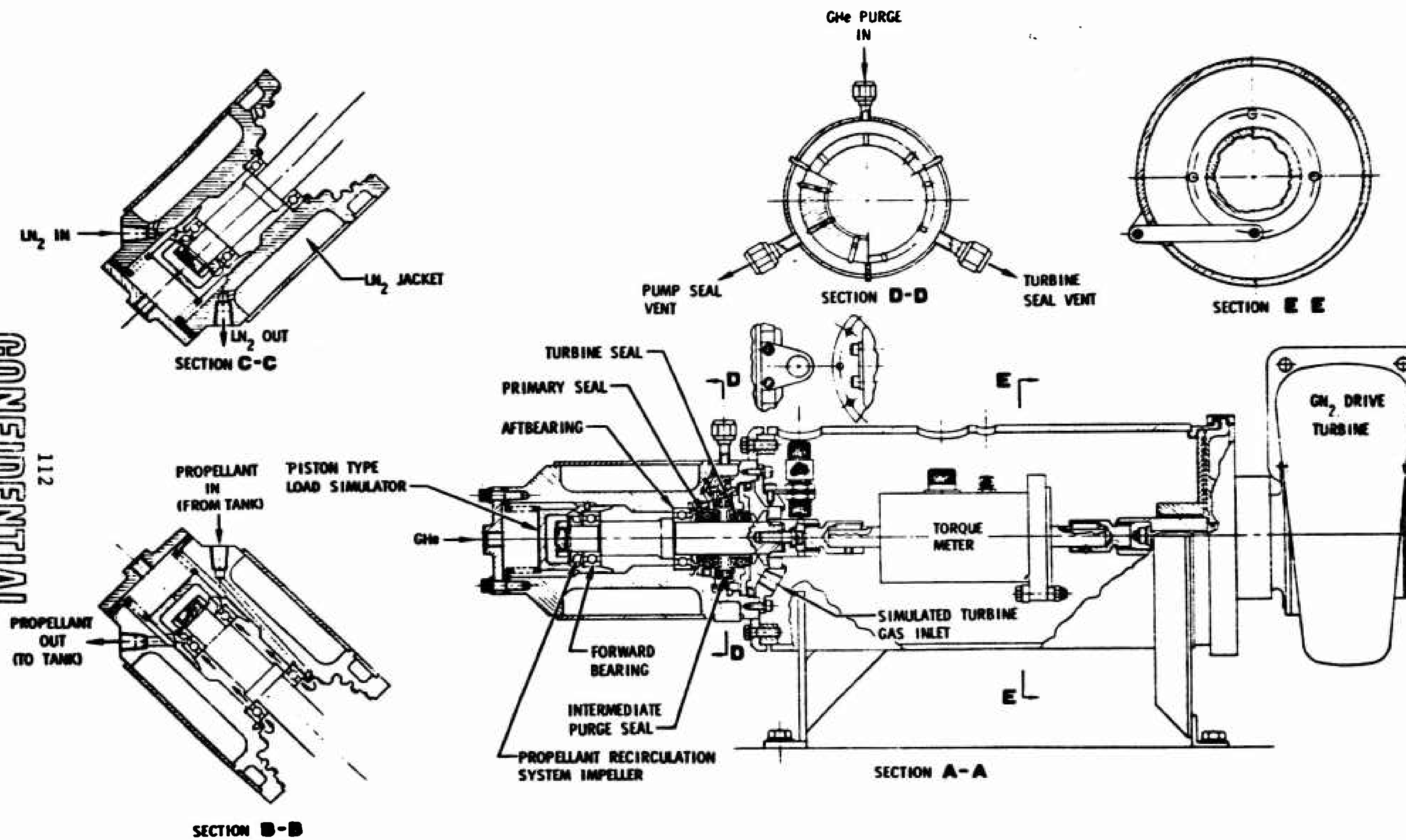

Figure 63. Main Oxidizer Bearing and Seal Tester and Drive Assembly (U)

(U) a. Main Tester Design and Fabrication

(U) Fabrication of all tester hardware was completed during the last report period; however, as a result of the test malfunction, replacement hardware is required. The following replacement hardware is scheduled to be completed 22 August 1969:

Shaft	Nut, primary seal
Housing	Nut, turbine seal
Nut, rear	Nut, inner seal
Spacer	Bracket, rpm pickup
Nut, bearing	Carrier, auxiliary seal

(C) The damaged tester housing was reworked by welding a sleeve in place of the seal portion and using the outboard slave seal to allow performance testing on the oxidizer recirculation impeller using an oil-water solution in lieu of LF_2 prior to the resumption of the main bearing and seal test program. The housing rework has been completed and all hardware is available for the performance tests.

(C) A new LF_2 recirculation impeller (slinger) has been designed and fabricated to improve the LF_2 flow through the tester. The new slinger is designed for 5-gpm LF_2 flow and 100-psi differential pressure.

(C) The LF_2 flow through the tester also has been improved by increasing the size of the inlet port and flow passage. This will provide more assurance that the fluorine remains at liquid condition as it flows through the tester.

(C) The air fan blower used on the turbine shaft to absorb torque for speed control was redesigned to increase the torque from 6 in.-lb to 14 in.-lb at 28,000 rpm. This change was required for additional speed control. The new blower has been fabricated and is available tor test.

(U) The primary seal drain flow area in the tester housing was increased on the new replacement housing to reduce the seal drain backpressure caused by seal leakage. The helium purge gas flow into the primary drain will be significantly higher with the new floating ring intermediate seal.

(U) The torquemeter which seized on test 002 has been repaired by the manufacturer and returned to Rocketdyne. The seizure occurred between the shaft on the turbine end and the bearing retainer.

(U) b. Main Seal Design and Fabrication

(U) All of the seal hardware from the original order has been received. A status of the main seal hardware and a list of the seal design values are presented in Tables 9 and 10, respectively.

(C) The segmented intermediate seal design was changed to a purged, solid, double floating ring-type design, the same as the secondary pump seal (Fig. 64) because of the high drag torque and the torque variation of the segmented-type seal. The floating ring design has negligible drag torque but slightly higher leakage. The rings are free to be centered by the shaft and are designed to maintain a clearance on the mating ring OD. Four seals have been ordered with 0.002-inch-diametral clearance and two seals with 0.005-inch-diametral clearance. The floating ring seal material is AmCerMet 701-65 composite (sintered Inconel 600 with BaF_2-CaF_2 filler), which has approximately the same contraction rate as the Inconel 718 shaft, to maintain a constant clearance as the temperature changes.

(C) Six additional Al_2O_3-NiCr spray nose piece primary seals and three additional turbine seals have been ordered to support the main tester program. Also, three additional turbine seal mating rings and three additional BaF_2-CaF_2 coated Inconel 718 intermediate seal mating rings have been ordered.

TABLE 9

(U) MAIN BEARING AND SEAL HARDWARE STATUS

Hardware	Quantity Ordered	Quantity Received	Status
Primary Seal			
Seals			
Kentanium K162B Insert	2	2	Not tested
AL_2O_3 Insert	1	1	Insert broken
AL_2O_3 Spray (INCO shoulder)	2	2	Two damaged, LN_2 and test 004
AL_2O_3-NiCr Spray	2	0	Returned to Chicago Rawhide for rework, due 1 September 1969
AL_2O_3-NiCr (new order)	6	0	Due 1 October 1969
Without Insert	2	0	Hold at Chicago Rawhide pending selection
Nose Piece Inserts			
Kentanium K162B	5	5	Not tested
AL_2O_3 Solid	5	5	Not tested
Mating Rings			
Kentanium K162B	8	8	Two damaged, LN_2 and test 004
AL_2O_3 Coated INCO 718	8	8	One damaged, test 002
Intermediate Seal			
Seals			
Segmented Kentanium	3	3	Not tested
Segmented Bearium	3	3	Two damaged, test 002 and 004
Segmented BaF_2-CaF_2	3	3	Not tested
Floating Ring BaF_2-CaF_2	6	0	Due 1 October 1969

TABLE 9

(U) (Concluded)

Hardware	Quantity Ordered	Quantity Received	Status
Mating Ring			
INCO 718	3	3	Two damaged, test 002 and 004
BaF_2-CaF_2-Coated Inconel	3	3	Not tested
BaF_2-CaF_2 (new order)	3	0	Due 1 September 1969
AL_2O_3 -Coated Inconel	3	3	Not tested
Turbine Seal			
Seals			
Carbon P5N	3	3	One destroyed, test 004
Carbon P5N (new order)	3	0	Due 1 October 1969
Mating Ring			
Chrome-Plated INCO 718	3	3	Two damaged, test 002 and 004
Chrome-Inconel (new order)	3	0	Two damaged, test 002 and 004
Bearings			
25 MM	10	10	Three damaged, LN_2, test 002, 004
30 MM	10	10	Three damaged, LN_2, test 002, 004

TABLE 10

(U) OXIDIZER TURBOPUMP SEAL DESIGN VALUES

Design Value	Main Turbopump Seals			Secondary Turbopump Seals		
	Primary	Intermediate	Turbine	Primary	Intermediate	Turbine
NA5 Specification No.	NA5-260265	NA5-260266	NA5-260267	NA5-260306	NA5-260307	NA5-260308
Seal Type	Bellows Face	Purged Floating Gap	Bellows Face	Bellows Face	Purged Floating Gap	Bellows Face
Fluid Pressures, psia	200	50	50	200	50	50
Spring Load, pounds	5/26	---	5.8/19.4	1.4/3.7	---	1.4/3.7
Pressure Balance Ratio	0.6	---	0.6	0.6	---	0.6
Hydraulic Load, pounds	10.5/14.0	---	0/3.6	0.8/1.1	---	0.2/0.27
Total Load, pounds	15.5/40.0	---	5.8/23.0	2.2/4.8	---	1.6/4
Surface Speed, ft/sec	173	244	173	205	125	205
Unit Load, psi	34/88	---	13/51	30/76	---	22/64
PV Factor, psi x fps	5900/15300	---	2260/8850	5780/12500	---	4150/12000
Materials Seal Face	AL_2O_3 Spray K162B Insert	BaF_2-CaF_2 Composite	Carbon P5N	AL_2O_3 Spray	BaF_2-CaF_2 Composite	Carbon P5N
Mating Ring	K162B Solid AL_2O_3 Spray	BaF_2-CaF_2 Spray	Chrome Plate	AL_2O_3 Spray	BaF_2-CaF_2 Spray	Chrome Plate
Bellows	Inconel-X	---	Inconel-X	INCO 718	---	INCO 718

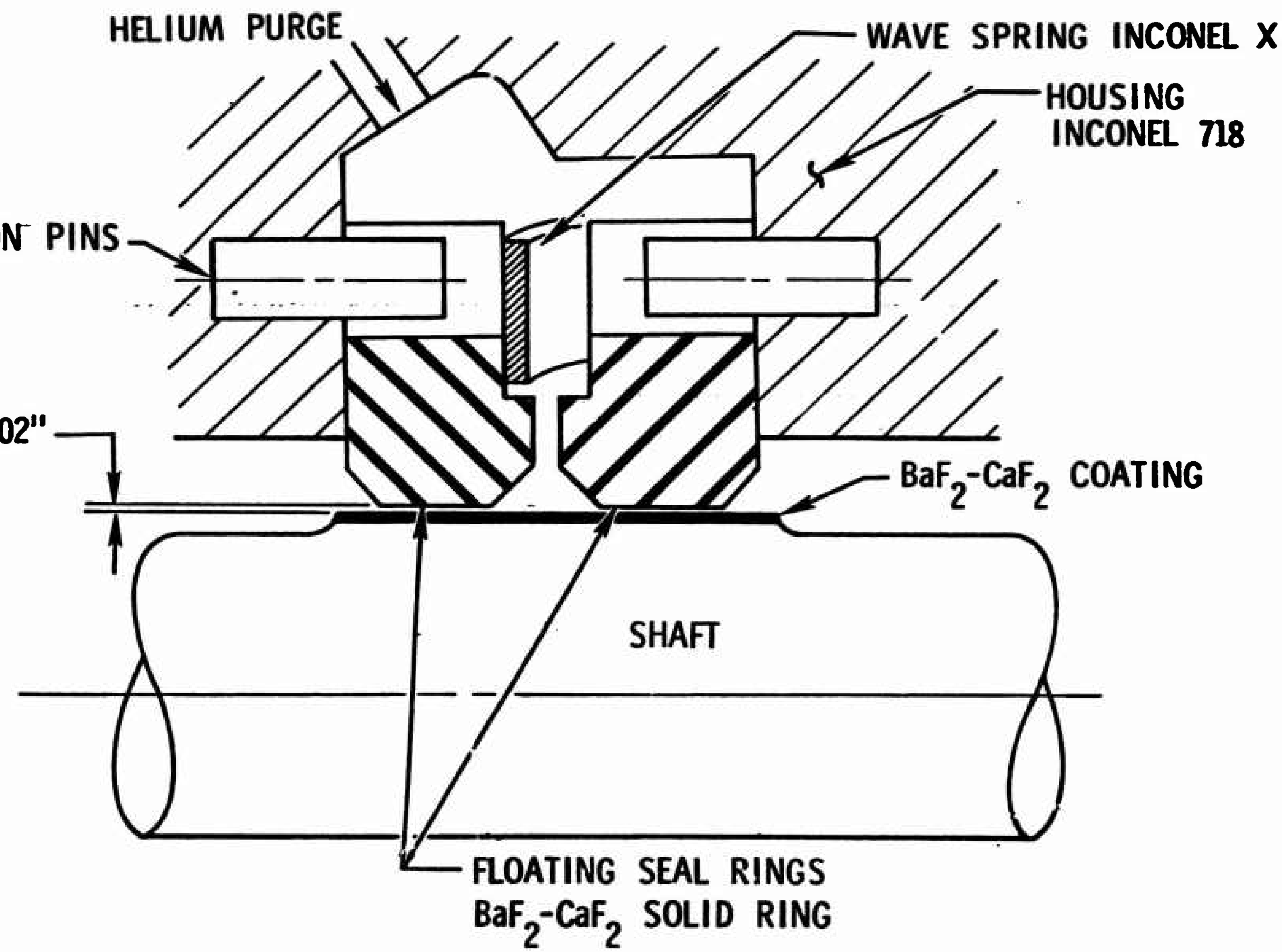

Figure 64. Secondary Oxidizer Turbopump Intermediate Floating Gap Low-Friction-Type Seal Detail (NA5-260307) (U)

(C) The two AL_2O_3-NiCr spray primary seals, which were received on the original order, have been returned to Chicago Rawhide for recoating of the AL_2O_3 because of edge roughness on the seal nose.

(U) c. Main Bearing Design and Fabrication

(U) The tester bearings have been received. Three sets of bearings have been damaged during testing and seven new sets are available in stock.

(U) d. Secondary Tester Design and Fabrication

(C) The torquemeter mount was changed from suspension by the turbine and tester shafts to a rigid mount with spline couplings to provide a greater safety margin for critical speed. The calculated critical speeds were 62,000 and 96,000 rpm for the suspended system and 32,000 and 165,000 rpm for the rigid mount. The operating speed is 75,000 rpm.

(C) The LF_2 recirculation impeller was redesigned to add a shroud for higher efficiency to ensure adequate HQ characteristics to maintain LF_2 flow through the tester.

(C) An air fan blower has been designed for installation on the turbine shaft to absorb 7 in.-lb torque at 75,000 rpm to improve speed control. Fabrication of the blower is scheduled to be complete 15 August 1969.

(U) e. Secondary Seal Design and Fabrication

(C) The seal design was completed and six sets of seals were ordered during the last report period. The scheduled seal delivery date is 15 August 1969.

(U) A list of seal design values and status of the secondary seal hardware are presented in Tables 10 and 11, respectively.

TABLE 11

(U) SECONDARY BEARING AND SEAL HARDWARE STATUS

Hardware	Quantity Ordered	Quantity Received	Status
Primary Seal			
AL_2O_3-NiCr Spray	6	0	Due 15 August 1969
Primary Mating Ring			
AL_2O_3 Spray on Bearing Race	6 bearings	0	Due 15 August 1969; to be coated at Rocketdyne
Intermediate Seal			
BaF_2-CaF_2 Composite	6	6	Due 15 August 1969
Intermediate Mating			
BaF_2-CaF_2 Coating on Shaft	2 shafts	0	Due 15 August 1969
Turbine Seal			
Carbon P5N	6	0	Due 15 August 1969
Turbine Mating Ring Chrome-plated INCO 718	6	6	Not tested
Bearings			
10 MM	6	0	Due 15 August 1969
6 MM	6	0	Due 15 August 1969

(U) f. Secondary Bearing Design and Fabrication

(C) The bearing design was completed and six sets of bearings were ordered during the last report period. The scheduled delivery date is 15 August 1969.

(U) The bearing hardware status and a summary of the bearing design values are presented in Tables 11 and 12, respectively.

(U) g. Main Tester Assembly and Static Tests

(C) The tester was assembled three times (two overhauls) during this report period. The second overhaul was required because of damage to the bearings and primary seal caused by lack of lubrication from running with LN_2 in the bearing cavity. The following hardware was installed:

Primary Seal
    Seal--AL_2O_3 Spray (INCO Shoulders) 80-5329 CR2
    Mating Ring--Kentanium K162B solid ring SN2

Intermediate Seal
    Seal--Bearium B-10 segmented 80-5292 CR1
    Mating Ring--INCO 718 (no plating) SN1

Turbine Seal
    Seal--Carbon P5N (lapped) 80-5314 CR4
    Mating Ring--INCO 718 chrome-plated SN2

Bearings
    NA5-260268 SN I009
    NA5-260269 SN I005

(C) The static seal helium leakage rates on the second overhaul were as follows:

Primary Seal
    2 scim at 30 psid
Intermediate Seal
    1500 scim at 50 psid
Turbine Seal
    1 scim at 30 psid

TABLE 12

(U) OXIDIZER TURBOPUMP BEARING DESIGN SUMMARY

NA5 SPEC NO.	MAIN TURBOPUMP		SECONDARY TURBOPUMP	
	260268	260269	260311	260310
ITEM	POSITION		POSITION	
	TURBINE	PUMP	TURBINE	PUMP
TYPE	ANGULAR CONTACT BALL BEARING	ANGULAR CONTACT BALL BEARING	SPLIT INNER RING BALL BRG	ANGULAR CONTACT BALL BEARING
BORE, mm	25	20	8	8
OD, mm	47	42	27	22
WIDTH, mm	12	12	8	7
CLASS, ABEC	5	5	7	7
BALL COMPLEMENT				
NUMBER OF BALLS	13	11	8	7
BALL DIAMETER, INCH	1/4	1/4	3/16	5/32
PITCH DIAMETER, INCH	1.42	1.22	.755	.591
INITIAL CONTACT ANGLE, DEGREES	25	25	25	25
RACE CURVATURES				
INNER	.52	.52	.52	.52
OUTER	.53	.53	.53	.53
CAGE				
O.D. CLEARANCE	.015-.020	.015-.020	.055-.010	.005-.010
POCKET CLEARANCE	.020-.025	.020-.025	.015-.020	.015-.020
MATERIALS				
BALLS	440-C	440-C	440-C	440-C
RACES	440-C	440-C	440-C	440-C
CAGE	K-MONEL	K-MONEL	K-MONEL	K-MONEL
DN @ SPEED	$.7 \times 10^6$	$.56 \times 10^6$	$.6 \times 10^6$	$.6 \times 10^6$

(C) A static test was performed to measure the primary seal drain cavity pressure versus helium flow through the drain to determine the backpressure caused by seal leakage. The data indicated that the drain passages should be increased to prevent excessive backpressure if the seal leakage is high. The measured backpressure at 8000-scim drain flow was 15 psig (see Fig. 65). The drain flow passage was increased approximately 2.5 times on the new replacement housing.

(U) h. Main Bearing and Seal Dynamic Tests

(C) Two dynamic bearing and seal tests with liquid fluorine were performed at the Santa Susana Propulsion Research Area, Mike stand, for a total duration of 574 seconds during this report period.

(C) The following summary shows the total dynamic testing on the main bearing and seal program:

Test No.	Date, 1969	No. of Starts	Time, seconds	Speed, rpm	Remarks
001 (LF_2)	4-2	0	0	0	No rotation; turbine valve not open
002 (LF_2)	4-3	1	3	42,500	Torquemeter seized; rebuilt tester with new bearings and seals; used solid shaft in place of torquemeter and added air fan for speed control
LN_2 Starts	4-25	5	61	6,400-53,700	Speed control erratic; damaged bearings and seals due to LN_2; rebuilt tester and added bigger air fan
003 (LF_2)	5-10	8	56	33,000	Speed control erratic; suspect intermediate seal torque variation
004 (LF_2)	5-12	5	518	16,700-47,000	Fire started at intermediate seal and burned through housing

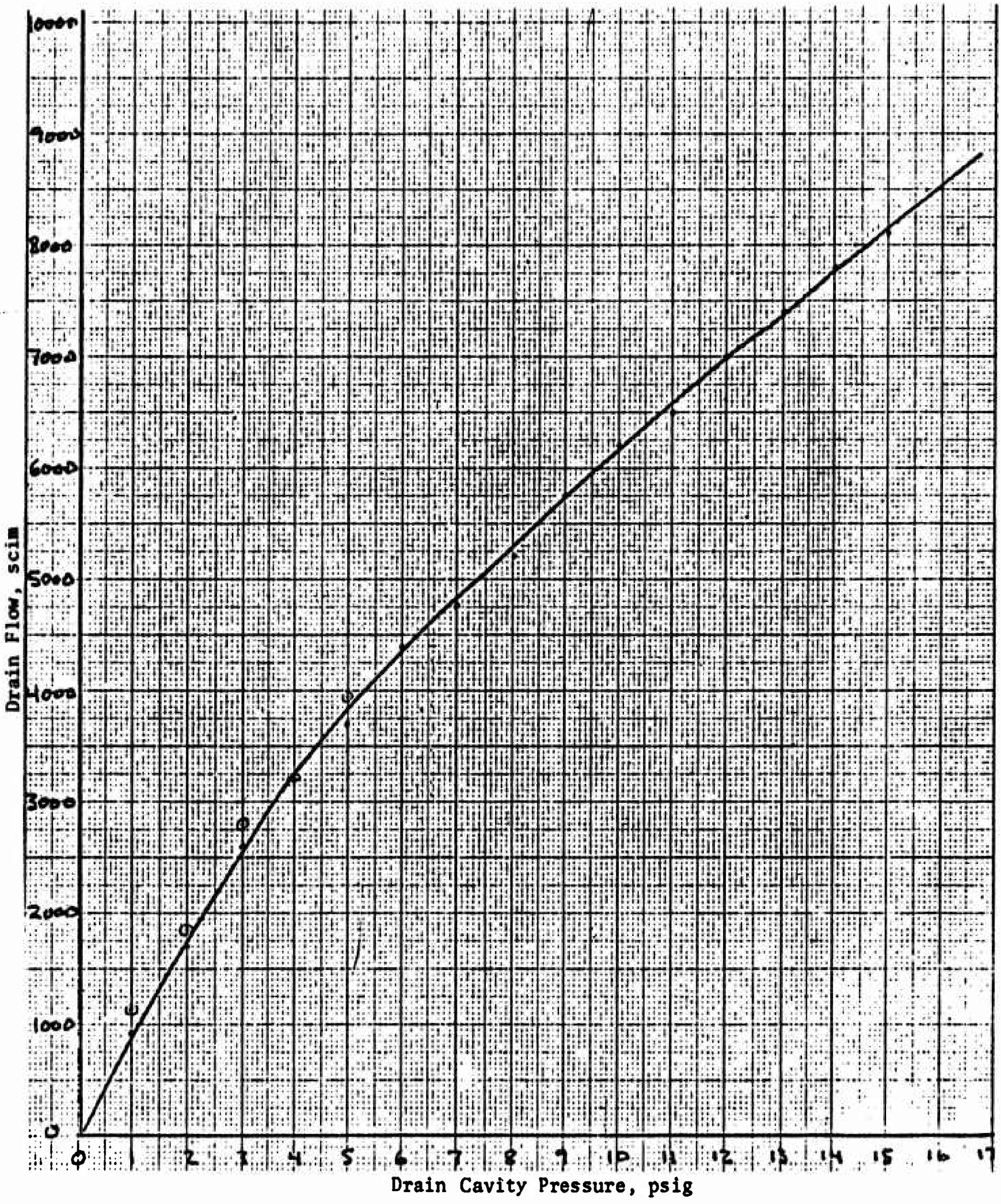

Figure 65. Main Tester Seal Drain Flow (He) vs Drain Cavity Pressure (primary and turbine ≈ same) (U)

(U) The following dynamic testing was conducted during this report period.

(C) (1) Test 003 (5-10-69)--8 Starts for 56 Seconds

(C) The tester was chilled down with liquid fluorine and the turbine inlet pressure was increased to 64 psig when the speed suddenly spiked to 33,000 rpm. The pressure was vented to 45 psig and the speed dropped to 15,000 rpm, then decayed to zero with no change in pressure. The pressure was increased again to 77 psig and the speed spiked to 33,000 rpm, then dropped to zero when the pressure was vented to 66 psig. The speed spiked from zero to approximately 30,000 rpm six more times with the turbine pressure constant at approximately 90 psig. The test was terminated because of erratic speed control.

(C) The intermediate seal purge pressure decayed from approximately 50 to approximately 45 psig at the same time the speed increased, then gradually recovered to approximately 50 psig at the same time the speed dropped to zero (Fig. 66).

(C) It was determined that the erratic speed control was caused by a variation in the tester torque caused by the segmented intermediate seal drag torque changing from the loading caused by the purge pressure.

(C) The purge pressure, which loads the segments against the shaft, decayed gradually, reducing the seal drag and allowing the turbine to start rotation. The seal leakage increased as rotation starts, which further reduced the purge pressure because of the slow response of the pressure regulator and allowed a progressive speed increase until the pressure regulator responded and started to build up the purge pressure. The speed then decreased and stopped after repressurization because of the additional seal drag.

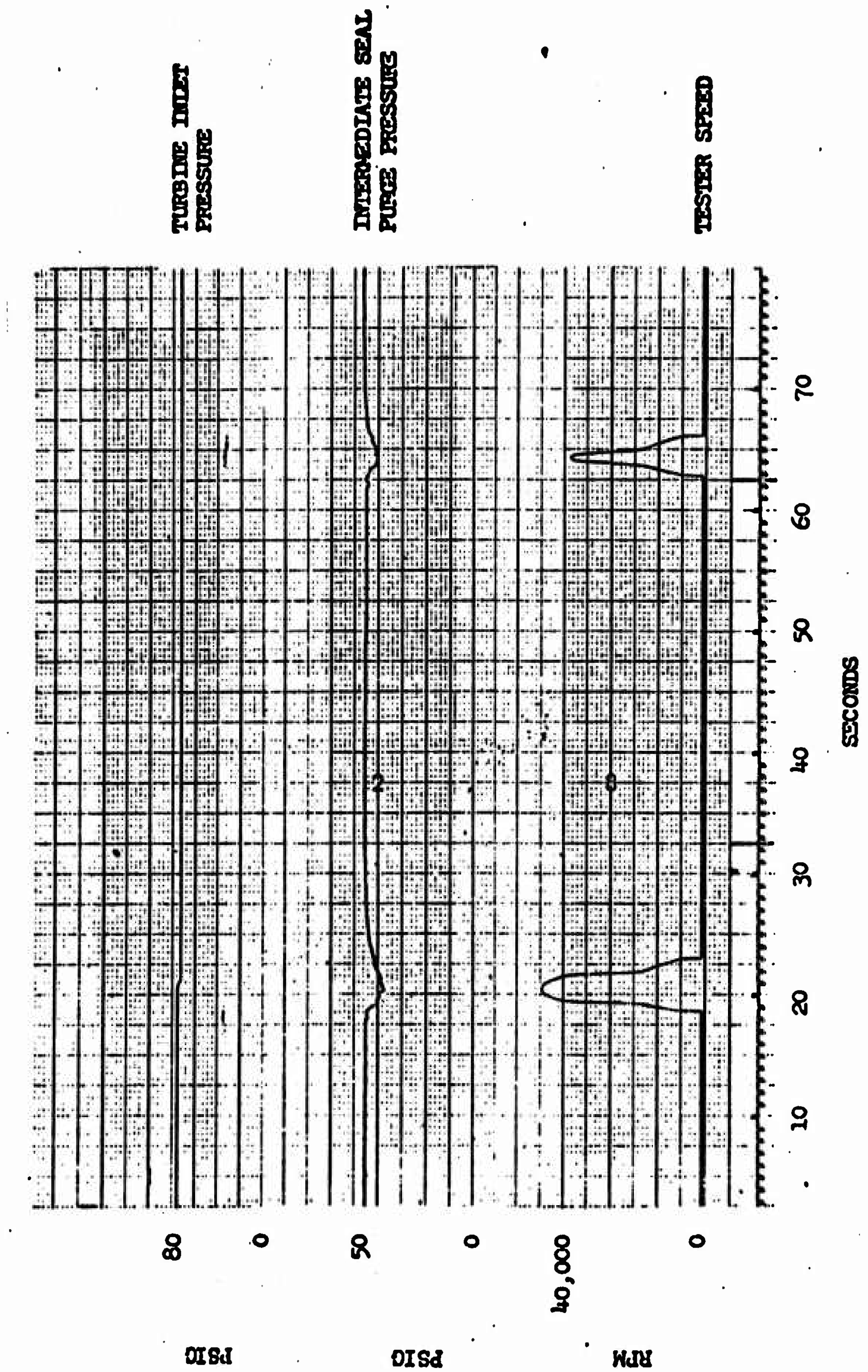

Figure 66. Segmented Intermediate Seal Stability (U)

(C) Because it was determined that part of the speed control problem was related to variation of the intermediate seal drag torque from the loading caused by the purge pressure, it was decided to run the initial portion of test 004 with no purge pressure to eliminate that variable. This was not considered to be a hazard because the main function of the purge is to provide a pressure barrier between the oxidizer and fuel-rich drain cavities to maintain separation, and there was no combustible gas in the tester. The purge also provides some cooling and lubrication for the rubbing segments; however, the load decrease with no purge pressure would probably compensate for the lack of cooling.

(C) (2) Test 004 (5-12-69)--5 Starts for 518 Seconds

(C) Test 004 consisted of the following five starts for a total rotation time of 518 seconds (Fig. 67). The total elapsed time from start to cut was 982 seconds.

(C) (a) First Start (56 Seconds)

(C) The turbine inlet GN_2 pressure was increased gradually with no intermediate seal purge pressure and the bearing cavity pressure set at 95 psig. The turbine broke loose at 40-psig inlet pressure and spiked up to 29,000 rpm, then leveled off at 28,000 rpm when the turbine pressure was vented to 38 psig, and gradually dropped to 21,000 rpm while the turbine pressure was constant at 38 psig. The speed was relatively steady, but there was no oxidizer flow through the bearings; therefore, the turbine pressure was vented to stop rotation until the cause of no flow was determined.

(C) It was suspected that the recirculation impeller on the tester shaft was not pumping because of cavitation or vapor lock of the oxidizer at the impeller inlet. The bearing cavity pressure was increased to 114 psig to improve the NPSH at the impeller inlet.

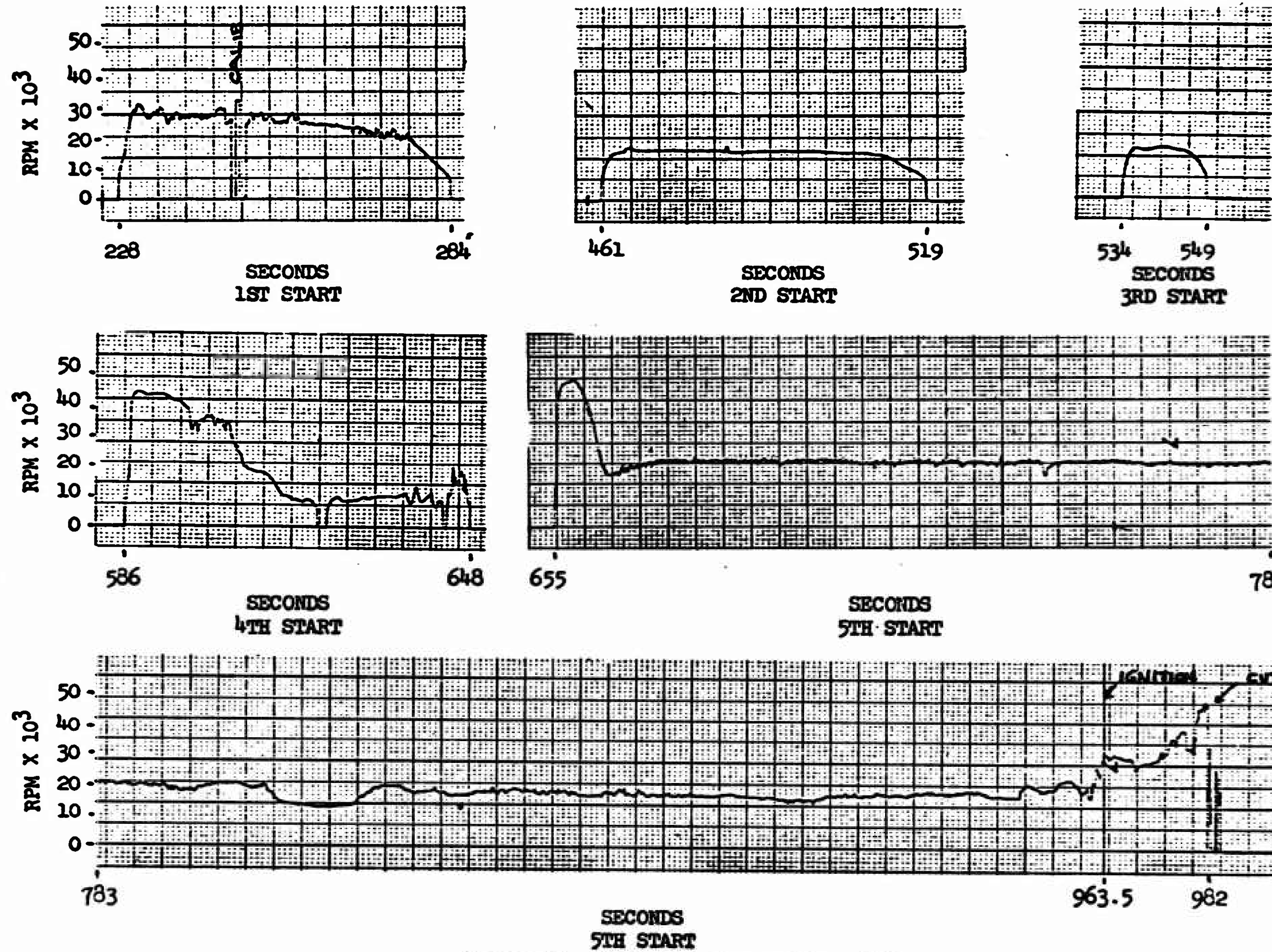

Figure 67. Test 004, rpm vs Time (U)

(C) (b) Second Start (58 Seconds)

(C) Turbine rotation started at an inlet pressure of 34 psig and leveled off at 17,000 rpm for 58 seconds, then dropped to zero at a constant inlet pressure of 34 psig. The oxidizer flow was intermittent and the bearing cavity pressure was increased again to 132 psig approximately 20 seconds before the speed dropped to zero.

(C) (c) Third Start (15 Seconds)

(C) The turbine inlet pressure was increased from 34 to 37.5 psig and the turbine restarted and leveled off at 17,000 rpm for 15 seconds, then dropped to zero again with no change in turbine inlet pressure.

(U) The oxidizer flow was initiated by cycling the bleed valve open, which vents the oxidizer return line to atmospheric pressure and causes flow because of the pressure differential from the oxidizer tank.

(C) (d) Fourth Start (62 Seconds)

(C) The turbine inlet pressure was increased gradually from 37.5 to 52 psig and the speed spiked up to 43,000 rpm and gradually decayed to zero as the inlet pressure was gradually vented to 42 psig, then restarted and increased to 10,000 rpm as the turbine inlet was repressurized to 53 psig. The inlet pressure was increased to 58.5 psig and the speed increased to 11,000 rpm, then dropped to zero. The bearing cavity pressure was increased from 130 to 163 psig at the same time. Oxidizer flow was maintained intermittently by cycling the bleed valve open.

(C) (e) Fifth Start (327 Seconds)

(C) The turbine suddenly restarted and spiked to 48,000 rpm at a constant inlet pressure of 58 psig, then dropped to 21,000 rpm when the inlet pressure was vented to 34 psig and remained relatively steady for 300 seconds with a gradual decay to 18,000 rpm while the inlet pressure was constant at 34 psig.

(C) Oxidizer flow was maintained intermittently by cycling the bleed valve open. The bearing cavity pressure was vented to 105 and then to 75 psig because of the oxidizer flow out the bleed.

(C) It was decided to increase the speed to 28,000 rpm, leave the oxidizer bleed open to maintain flow, and gradually increase the intermediate seal purge pressure to determine the effect of seal drag on speed.

(C) The turbine inlet pressure was increased from 34 to 38 psig and the speed responded with an increase to 21,000 rpm. The pressure was increased again from 38 to 42 psig and there was no change in speed. Another pressure increase from 42 to 47 psig resulted in a speed increase to 23,000 rpm. The pressure gradually decayed to 45.5 psig and the speed followed with a decrease to 17,000 rpm. Then the speed suddenly increased to 31,000 rpm while the pressure was constant at 45.5 psig. Also, at approximately the same time, the Bently scope showed excessive shaft deflection. Because it was suspected that the deflection was caused by running at a critical speed, an attempt was made to change the speed; however, before any adjustment to the pressure could be made, the speed increased again to 40,000 rpm. The pressure was vented from 45.5 to 43.5 psig and the speed dropped to 33,000 rpm, then spiked to 48,000 rpm. At this time, the window observer saw fire and sparks coming from the tester and the test was terminated.

(C) Posttest inspection of the tester revealed a hole burned through the tester housing in the area of the primary seal drain. There also was a secondary fire caused by ignition of lubricating oil that had leaked from the turbine and collected in the torquemeter housing. There was some minor fire damage to the test stand instrumentation.

(U) The turbine and tester turned freely and was only slightly rough with approximately 2 to 4 in.-lb torque.

(C) Disassembly and inspection of the tester hardware revealed the following (see Fig. 68 and 69).

1. The major portion of the burning was centered in the primary seal drain and intermediate seal area, indicating that the origin of the fire was on the primary side of the intermediate seal.

2. There was no burning in the intermediate seal purge cavity area of the tester housing, indicating that the fire did not start inside of the intermediate seal.

3. There was no burning in the turbine seal drain area of the tester housing, indicating that the fire did not start at the turbine seal.

4. The primary seal drain cavity portion of the tester housing was completely burned out through the housing, indicating that combustion was supported by oxidizer leakage through the primary seal.

5. The seal portion of the tester housing was partially burned and covered with molten metal and slag.

6. The bearing cavity portion of the tester housing was not damaged by the fire and appeared to be completely isolated from the burning in the seal area by the primary seal.

7. The primary seal housing was partially burned away from the drain side, but the sealing face was in good condition and the seal was still functional enough to maintain adequate sealing of the oxidizer. The burned-away portion of the seal housing was covered with molten metal and slag.

8. The tester bearings were slightly rough, but were not damaged by the fire and appeared to be in reasonably good condition. The roughness was probably caused by the high speed and high loads from the excessive shaft deflection during the failure.

9. The tester shaft was slightly damaged by slag deposits on the seal end, but would probably be reusable after rework.

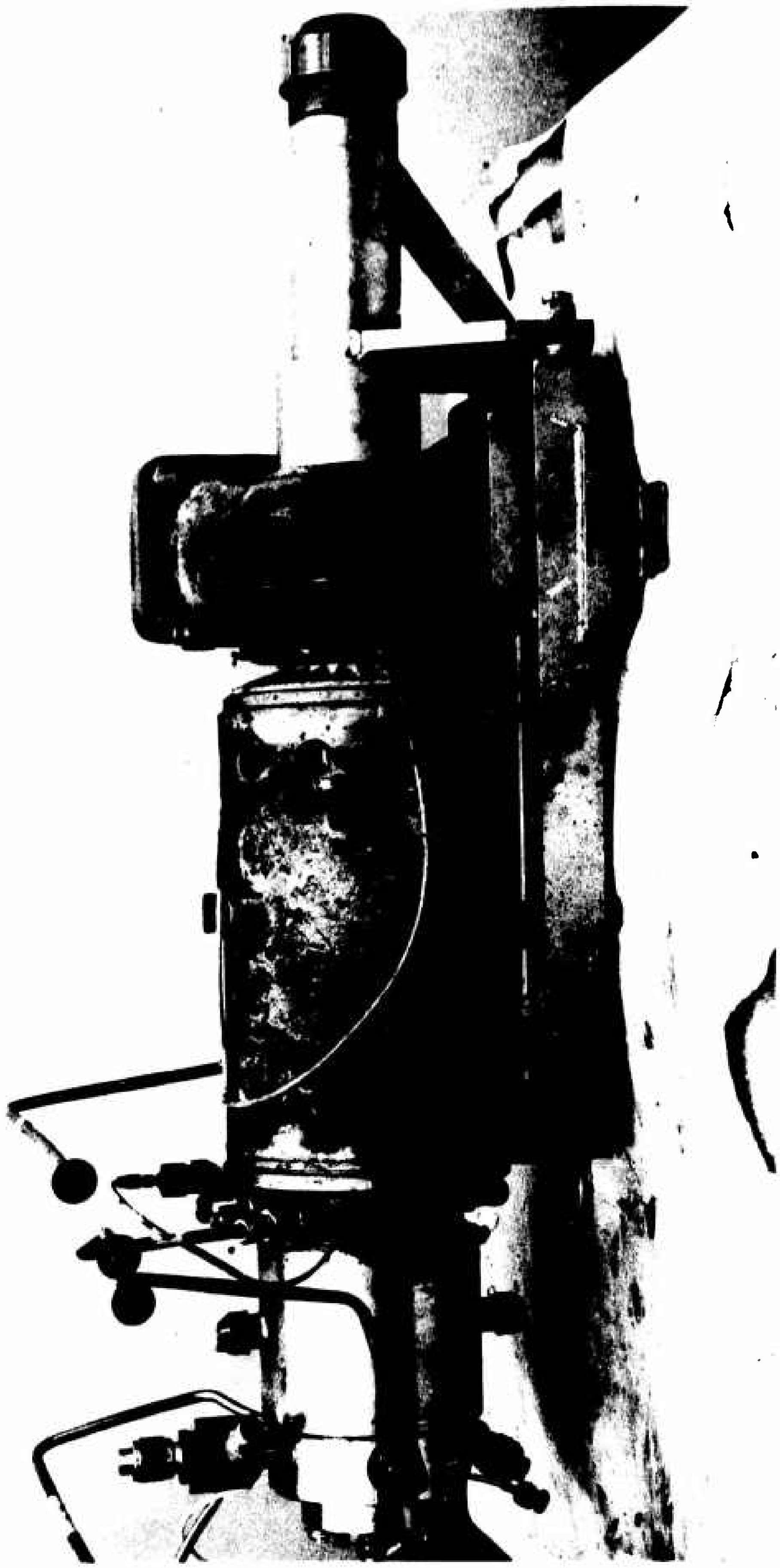

Figure 68. Tester and Drive Assembly (Posttest 004) (U)

1EH95-5/13/69-C1A

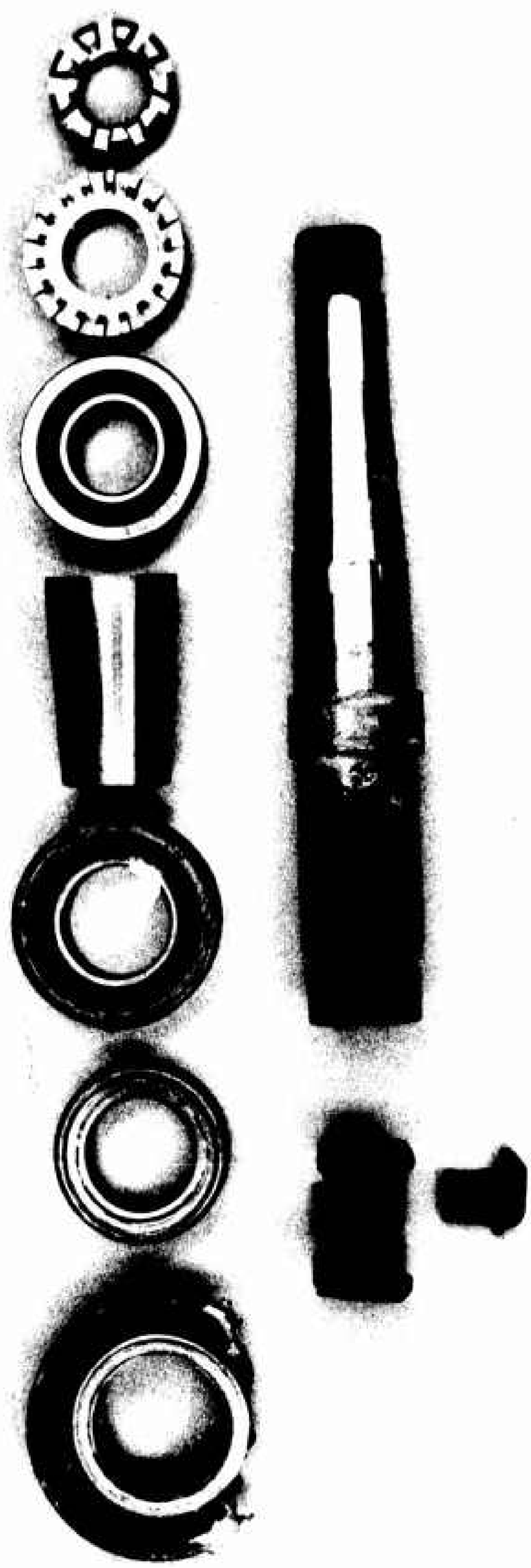

1EH95-5/15/69-C1B

Figure 69. Seals, Bearings, and Shaft (Posttest 004) (U)

(C) 10. The Bently distance detector on the quill shaft coupling at the tester contacted slightly, indicating a radial deflection of 0.025 inch at that location.

11. There was no rubbing on the primary seal ID, indicating that the radial deflection at that location was less than approximately 0.030 inch.

12. The tester shaft nut had burned through and spun off, hitting the air fan and bending the blades.

(C) The test data indicate that the fire started in the primary seal drain cavity at 963.5 seconds, which was 18.5 seconds before the test was cut at 982 seconds (see Fig. 66 and 67, 70 through 73, and Table 13).

(C) The first indication of the fire was a pressure and temperature increase in the primary seal drain. The pressure spiked to 3.0 psig and the temperature spiked off-scale and went erratic, apparently from the temperature bulk burning out. There was a temperature and pressure increase in the turbine seal drain at about the same time, but the pressure only reached 1.0 psig, indicating the origin of the pressure source was in the primary drain. The turbine drain temperature bulb did not burn out, indicating lower temperature than the primary drain.

(C) There was a second ignition in the primary seal drain approximately 1 second later at 964.7 seconds, which caused a pressure spike of 11.5 psig in the primary drain, 2.7 psig in the intermediate purge cavity, and 0.7 psig in the turbine drain. The progressive decrease in the pressure levels indicates that the pressure source originated in the primary drain.

(C) The data show that the tester speed had increased from 17,000 to approximately 30,000 rpm when the first indication of the fire occurred (Fig. 70). The only explanation for the speed increase is a decrease in tester torque because the turbine inlet pressure was constant at 45.5 psig. It is theorized that this speed increase, and the other speed changes which occurred at a constant turbine inlet pressure, were a result of the segmented intermediate seal drag torque variation.

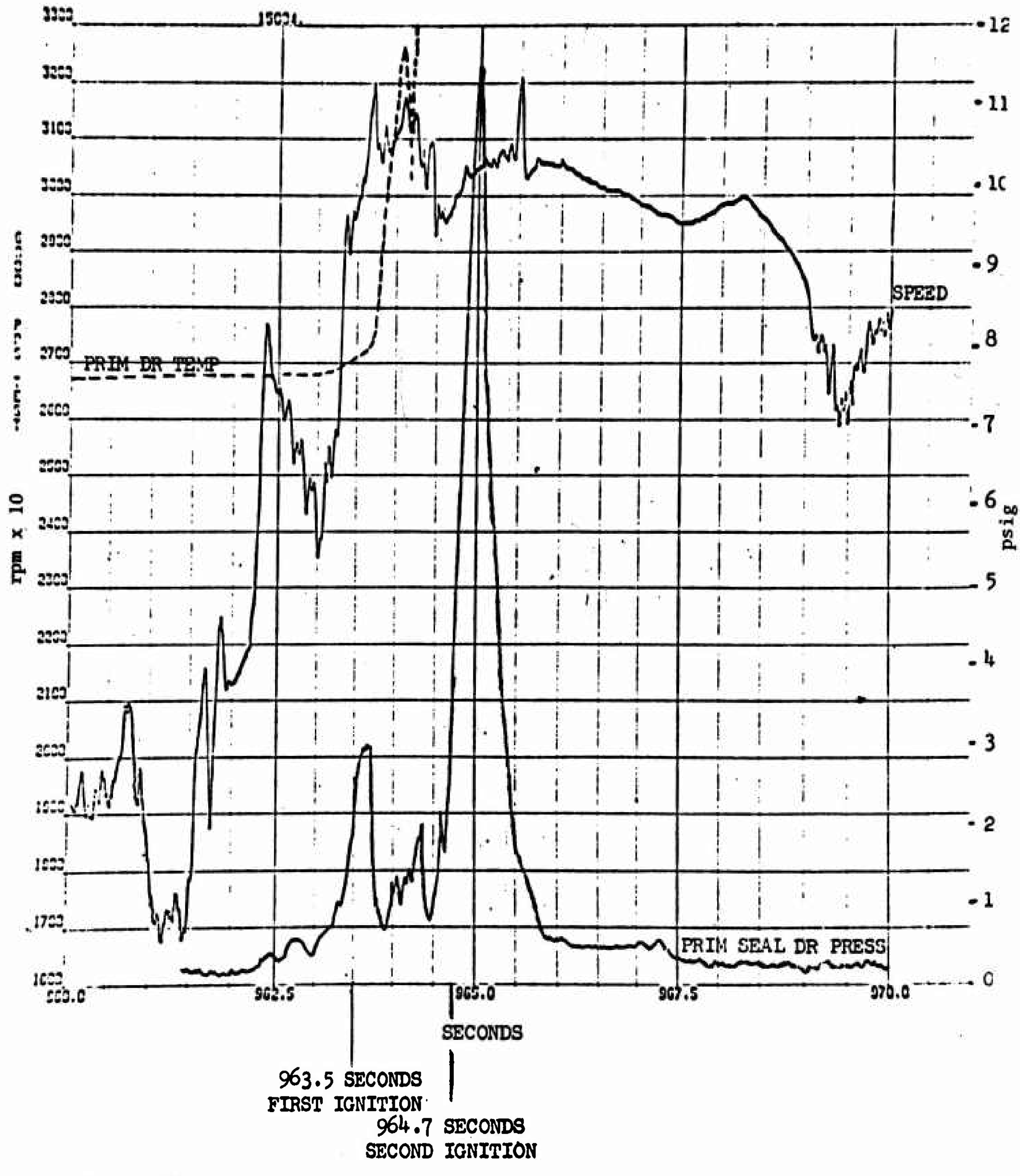

Figure 70. Test 004 Failure, Primary Drain Temperature and Primary Drain Pressure Tester Speed vs Time (U)

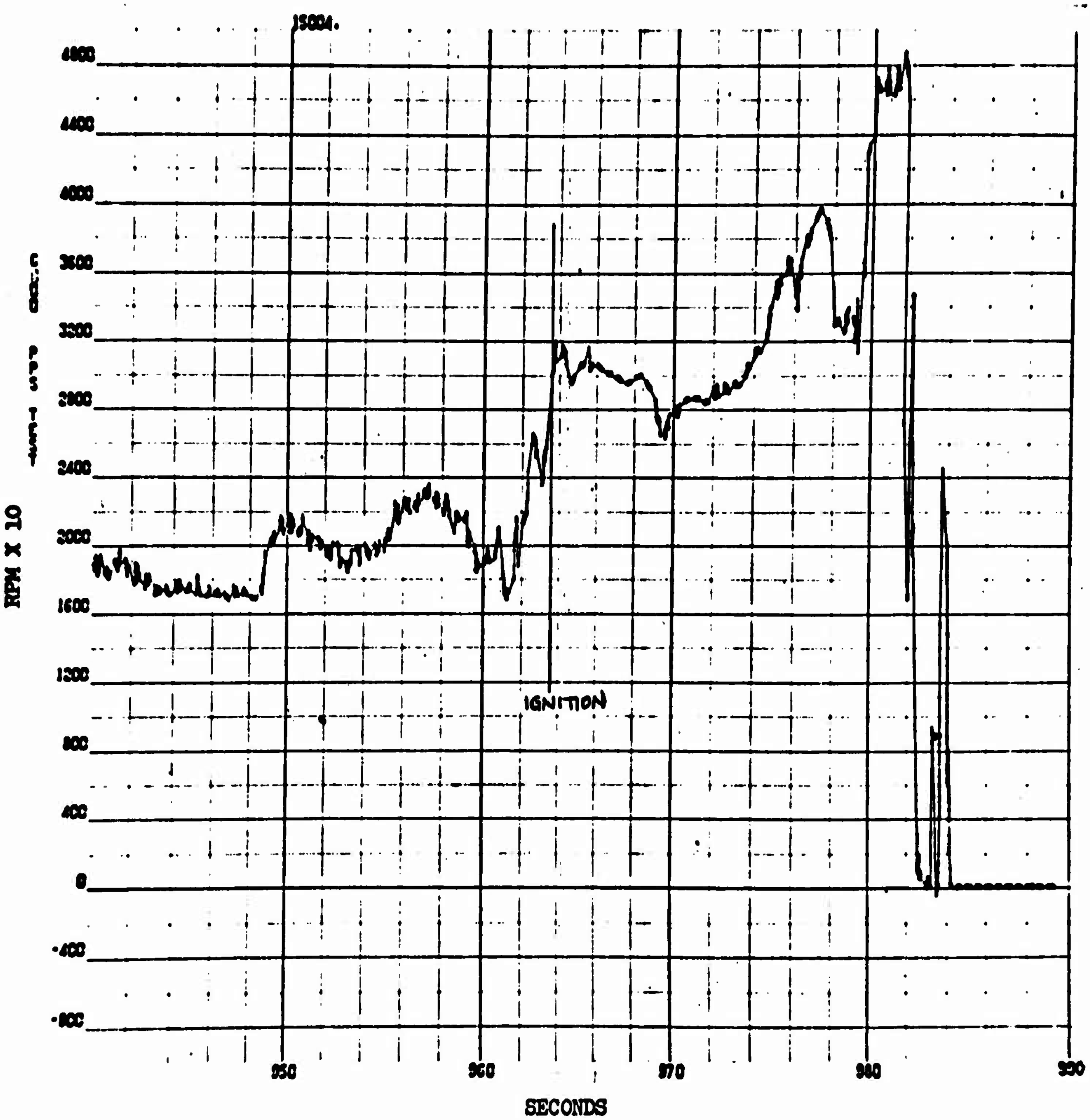

Figure 71. Test 004: 940 to 990 Seconds, Last 50 Seconds; Tester Speed (C)

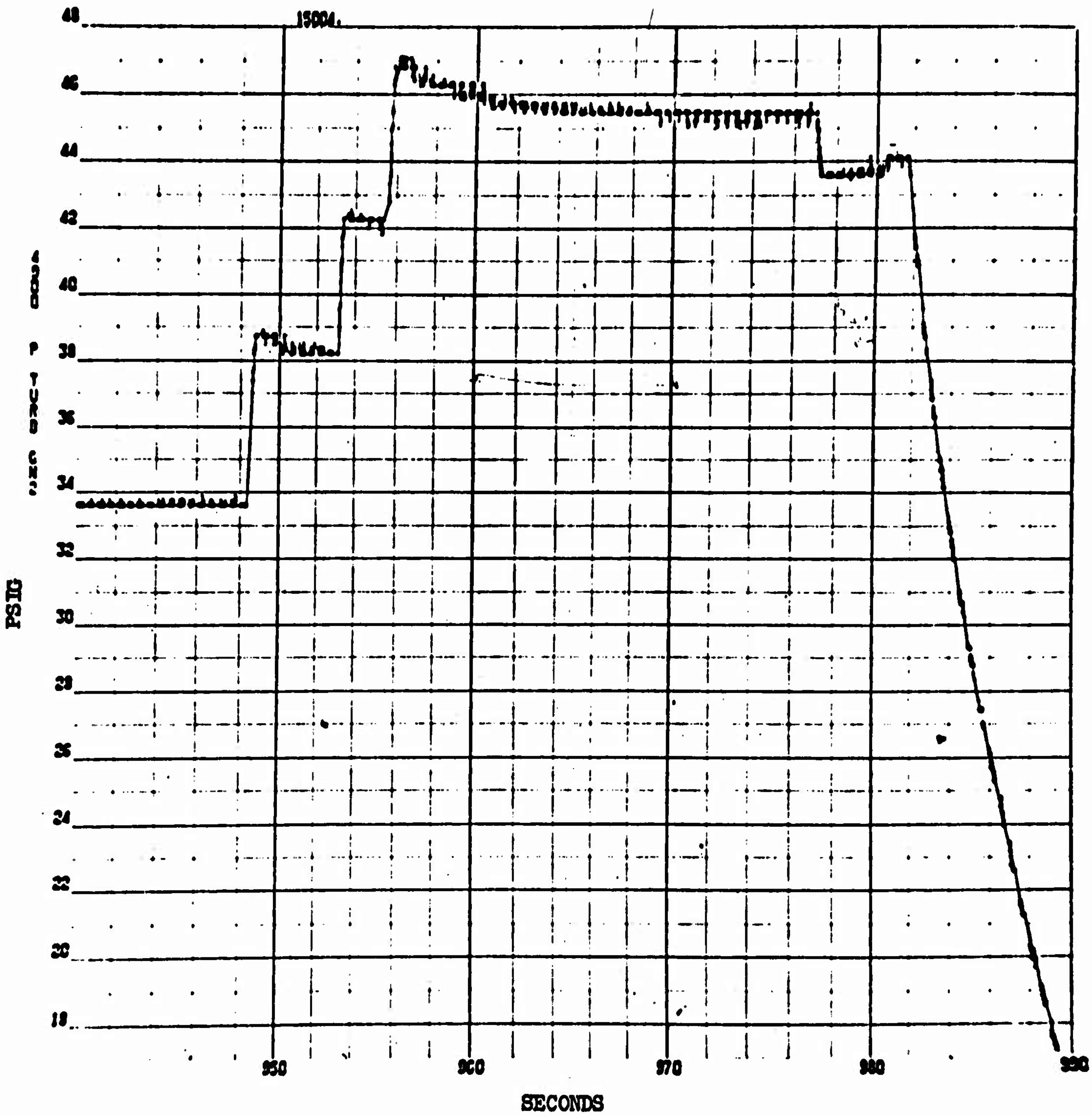

Figure 72. Test 004: 940 to 990 Seconds, Last 50 Seconds; Turbine Inlet Pressure (C)

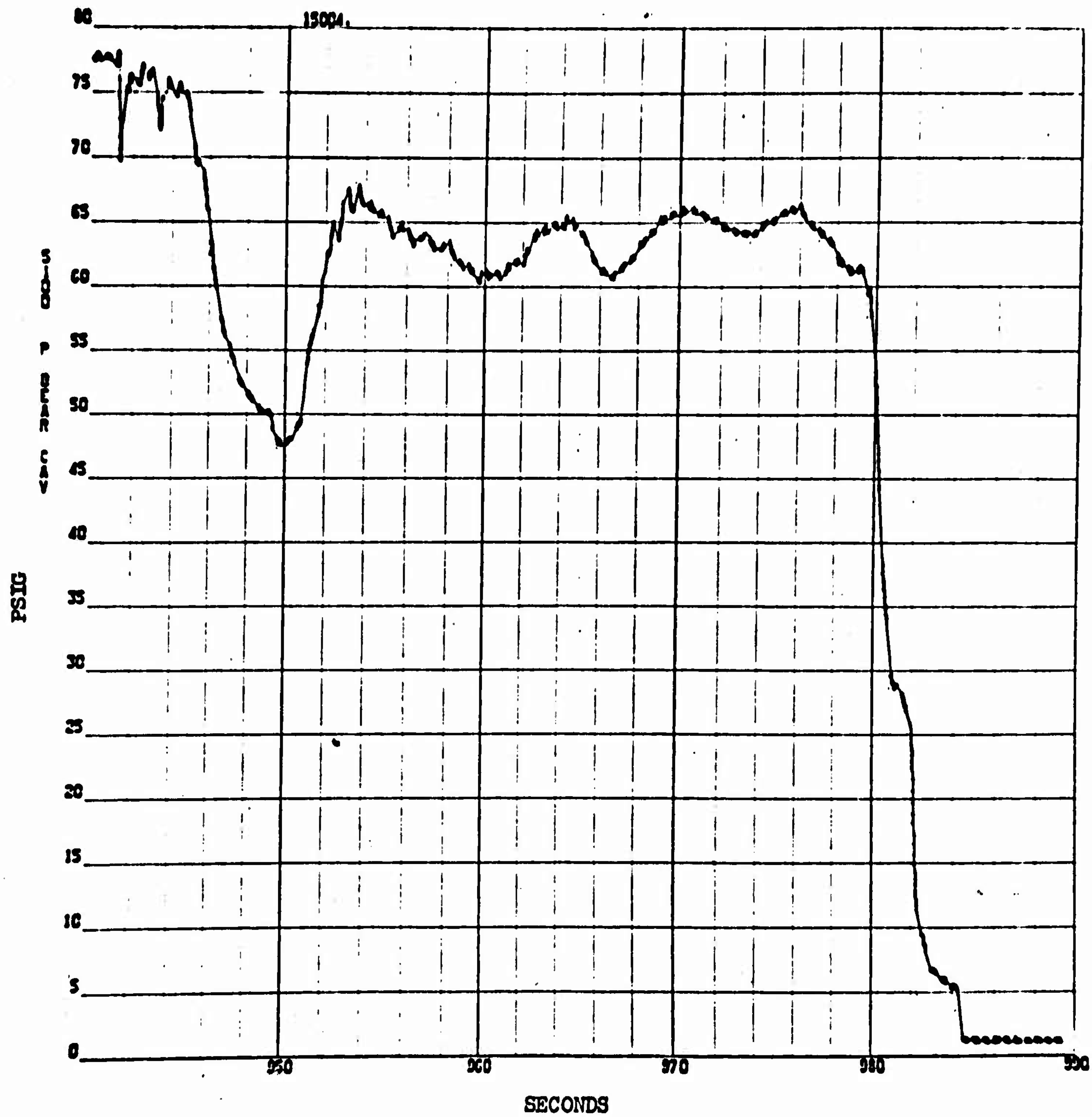

Figure 73. Test 004: 940 to 990 Seconds, Last 50 Seconds; Bearing Cavity Pressure (C)

TABLE 13

(U) MARK 34 TESTER DATA SUMMARY, TEST 004

Parameter	Time Slice, seconds								
	First Start	Second Start	Third Start	Fourth Start		Fifth Start			
	230	470	540	590	635	660	675	963.5	980.5
Oxidizer Inlet Temperature, F	-267	-240	-260	-277	>-200	-255	-255	-279	-277
Oxidizer Outlet Temperature, F	-269	-266	-261	-261	-259	-226	-216	-273	-282
Primary Seal Drain Temperature, F	-217	-174	-126	-164	-140	- 91	- 70	-164	**
Turbine Seal Drain Temperature, F	*-304	*-140	*-114	*-100	*-106	*-80	*-55	*+165	**
Internal Seal Purge Temperature, F	-142	-122	-114	-116	-110	-110	-108	- 55	+ 85
Oxidizer Inlet Pressure, psig	93.5	114.9	131.0	132.5	132.0	161.9	162.1	70.2	66.8
Internal Seal Purge Pressure, psig	6.9	4.7	5.4	40.4	0.17	17.5	10.9	0.46	0.8
Primary Seal Drain Pressure, psig	7.2	5.7	6.5	41.5	0.21	17.8	11.6	1.5	0.77
Turbine Seal Drain Pressure, psig	6.5	3.1	1.6	28.5	0.32	14.6	7.9	0.7	i.8
Oxidizer Outlet Pressure, psig	95.2	116.4	132.4	134.3	133.7	162.9	163.2	70.4	36.5
Load Bellows Pressure, psig	104.1	132.5	132.4	152.0	151.6	151.5	151.4	151.3	151.3
Turbine Inlet Pressure, psig	39.5	33.4	37.0	50.3	58.4	46.8	33.6	45.5	44.1
Bearing Cavity Pressure, psig	94.9	116.2	132.3	134.7	132.8	163.2	163.1	64.9	35.7
Tester Speed, rpm	28,889	16,952	17,329	43,255	10,788	43,669	22,314	29,640	46,993
Oxidizer Flow, gpm	<0.1	<0.1	0.7	0.4	<0.1	0.3	<0.1	<0.1	1.4

*Questionable measurement
**Pegged off-scale

(C) The data indicate that the most probable cause of the failure was ignition of the Bearium B-10 intermediate seal segments on the primary drain side, followed by complete combustion of the intermediate and turbine seals with the gaseous oxidizer which had leaked through the primary seal and accumulated throughout the seal area. The greater amount of burning in the primary drain was caused by the fire starting in that area and from the combustion being supported by the additional oxidizer which was leaking through the primary seal. The fire apparently burned out after approximately 10 seconds because of depletion of the oxidizer in the seal drain area. The primary seal was effectively containing the oxidizer to the bearing cavity. The speed increased to 40,000 rpm, then to 48,000 rpm because of the lower seal drag torque.

(C) Ignition of the Bearium B-10 segments in a highly oxidizing atmosphere is possible because of the heat generation between the rubbing surface of the segments and the rotating mating ring. The segments are loaded against the mating ring with a garter spring which is stretched around the OD of the segments. The garter spring load is low (1.0 pound) compared to the load caused by the purge pressure (40 pounds). Because there was no purge pressure on test 004, the only static load was from the garter springs; however, the additional dynamic load imposed on the rubbing surface of the segments, if the shaft was rotating with the deflection (indicated by the Bently measurements and the critical speed calculations), could be much higher because of the inertia and friction hysteresis of the segments as they try to follow the eccentric motion of the shaft. Therefore, it is believed that the excessive shaft deflection caused a high load on the rubbing surface of the segments, which resulted in a surface temperature sufficiently high to ignite the Bearium in the oxidizing atmosphere.

(C) The effect of the seal purge on the resultant surface temperature would probably be negligible because the load decrease with no purge would compensate for the lack of cooling and lubrication. However, the inert gas barrier provided by the purge might have prevented the oxidizer from reacting with the hot rubbing surface of the segments.

(C) Another less likely possible cause of the failure is rubbing between the primary side of the intermediate seal housing ID and the mating ring OD from excessive shaft deflection. However, this is not very probable because the shaft should not have deflected as much at that location as the housing clearance. The housing clearance should have been between 0.015 to 0.030 inch, and the maximum shaft deflection, obtained from the calculated deflection mode and the known deflection at the Bently, is approximately 0.010 inch.

(C) It is possible, also, that the carbon nose piece on the turbine seal could have ignited in the oxidizer atmosphere; however, the data and the condition of the hardware indicate that the fire started in the primary drain. The turbine seal is not normally exposed to the oxidizer, because the intermediate seal purge maintains a barrier between the primary and turbine seal drains.

(C) Because it was concluded that the Bearium B-10 segmented intermediate seal was the cause of the failure, and also because of the high drag torque and the torque variation of the segmented-type seal, the intermediate seal design was changed to a floating ring-type design fabricated from AmCerMet 701-65 composite material (see discussion in Main Seal Design and Fabrication section of this report).

(C) Analysis of the test results revealed the following problems with the tester and test facility operation:

1. Turbine speed control and speed adjustment sensitivity
2. Turbine lube oil drainage
3. Quality of liquid fluorine at tester (liquid condition not maintained)

(U) i. Tester and Drive Problems

(C) The following problems are discussed in the Main Tester Design and Fabrication sections of this report:

1. Turbine performance and erratic speed
2. LF_2 recirculation impeller (slinger) performance (inadequate LF_2 flow through tester)
3. Tester and drive system critical speed evaluation

(C) The test facility modifications required to correct the above problems have been completed. The following changes were incorporated:

1. Added venturi in the turbine GN_2 line to maintain linear back-pressure on the regulator
2. Increased the turbine inlet GN_2 line size to reduce the GN_2 velocity
3. Reorificed GN_2 pressure regulator to increase sensitivity of adjustment
4. Moved GN_2 pressure regulator control next to pressure chart to allow direct control
5. Added scavenge pump to turbine oil drain to prevent oil accumulation in turbine
6. Added flow restrictor and bypass to prevent excessive oil flow to turbine
7. Insulated LF_2 tank LN_2 jacket to maintain colder LN_2 around the LF_2, which will allow subcooling the LF_2 in the tank
8. Increased the LN_2 insulation jacket flow by adding another supply line in parallel from the LN_2 tank

(C) The corrective action for the turbine performance and erratic speed problem consisted , redesigning the air fan, which is installed on the turbine shaft to absoro torque, to increase the torque required at operating speed. The additional crag of the larger air fan and the improved control of the turbine GN_2 pressure should eliminate the erratic speed variation caused by the turbine drive and reduce the sensitivity of the turbine speed to tester torque variation. The performance of the improved facility GN_2 pressure controls and the turbine and air fan will be measured, using a spare turbine to absorb torque in place of the tester, prior to resumption of bearing and seal testing with fluorine.

(C) The problem of inadequate liquid fluorine flow through the tester for proper bearing lubrication and liquid quality is caused by the recirculation impeller on the tester shaft not pumping. A new, redesigned impeller with improved HQ characteristics has been fabricated and the tester housing fluorine inlet passage size has been increased. These changes, along with the facility changes to improve the liquid quality at the tester, should provide sufficient fluorine recirculation. The performance of the redesigned impeller will be measured, using the repaired tester housing with an oil-water solution, prior to resumption of the bearing and seal testing with fluorine.

(C) The tester and drive system critical speed is considered to be a problem on the main tester only if the operating speed of 28,000 rpm is exceeded; therefore, no change has been made to the main tester drive to alter the critical speed. It is considered that the improved turbine speed controls will prevent overspeed operation. The shaft deflection will be monitored with Bently distance detectors during the dynamic bearing and seal testing. Also, the shaft deflection will be measured during the turbine performance tests, prior to the bearing and seal testing, to determine if there is a critical speed problem at speeds up to 30,000 rpm.

(C) The status of the performance testing is as follows:

1. Turbine nozzle blowdown and stall torque testing completed; nozzle area and stall torque characteristics determined
2. Turbine performance mapping at 28,000 rpm; air fan performance and critical speed evaluation testing completed
3. LF_2 recirculation impeller HQ performance testing scheduled to be completed in early August
4. Turbine performance mapping at 75,000 rpm; air fan performance and critical speed evaluation testing scheduled to be complete in late August

(U) j. Bearing and Seal Test Program Plan

(C) It is planned to resume bearing and seal dynamic testing with liquid fluorine using the secondary tester on 1 September 1969. The secondary testing is scheduled to continue through October 1969 and the main bearing and seal testing is scheduled for November and December 1969 (see test schedule, Fig. 74).

(C) The secondary testing will be conducted at 75,000 rpm with liquid fluorine at 150 psig using one material combination for the seals and bearings. The seals will then be run at the limits of speed, fluid pressure, and installed compressions to determine the effect on leakage and wear.

(C) The main testing will be conducted at 28,000 rpm with liquid fluorine at 150 psig to evaluate the leakage and wear life of the AL_2O_3 spray nose-K162B mating ring primary seal material combination. The other backup material combinations will be tested if the first choice is unsatisfactory. The final material combination will be tested at the limits of speed, fluid pressure, and installed compression.

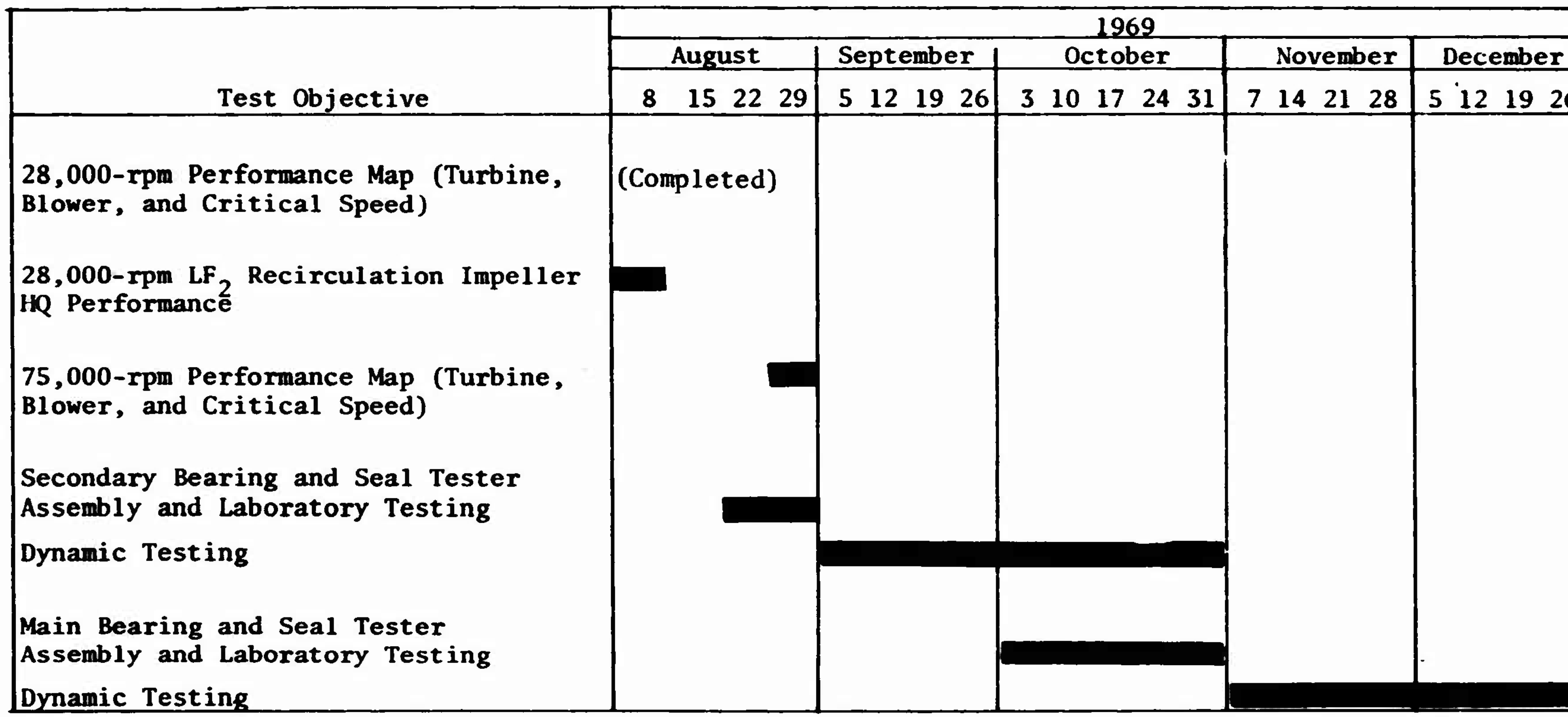

Figure 74. Turbopump Bearing and Seal Test Schedule (U)

(U) 5. FACILITY PREPARATION AND OPERATION

(U) a. Victor Test Stand

(C) There was no AMPT contract activity at this facility during May and June. During July, testing was resumed with the 30-degree, water-cooled segment stability test program. A section of the facility oxidizer feed line, flowmeters, and main valve was damaged during test 021. Repair will be completed and testing resumed by early August.

(U) b. Mike Test Stand

(C) Modifications to the test stand, which included LF_2 tank insulation and insulation of the LN_2-jacketed LF_2 lines, were completed. Performance testing of the bearing and seal tester drive turbine was initiated the last week in July.

(U) c. NFL Facility

(C) The contract award for the facility buildup has been made. Construction began 24 June 1969, and completion is scheduled for 7 November 1969. Installation of the diffuser water system and altitude chamber penetrations is in progress. Electrical installations have started. Shop fabrication of piping components and structure was begun.

REFERENCES

1. AFRPL-TR-69-132, Advanced Maneuvering Propulsion Technology Program (Sixth Quarterly Report), Rocketdyne, a division of North American Rockwell Corporation, Canoga Park, California, CONFIDENTIAL.

2. AFRPL-TR-69-47, Advanced Maneuvering Propulsion Technology Program (Fifth Quarterly Report), Rocketdyne, a division of North American Rockwell Corporation, Canoga Park, California, CONFIDENTIAL.

3. AFRPL-TR-68-221, Advanced Maneuvering Propulsion Technology Program (Fourth Quarterly Report), Rocketdyne, a division of North American Rockwell Corporation, Canoga Park, California, CONFIDENTIAL.

4. AFRPL-TR-68-154, Advanced Maneuvering Propulsion Technology Program (Third Quarterly Report), Rocketdyne, a division of North American Rockwell Corporation, Canoga Park, California, CONFIDENTIAL.

5. AFRPL-TR-68-20, Advanced Maneuvering Propulsion Technology Program (Second Quarterly Report), Rocketdyne, a division of North American Rockwell Corporation, Canoga Park, California, CONFIDENTIAL.

6. AFRPL-TR-68-17, Advanced Maneuvering Propulsion Technology Program (First Quarterly Report), Rocketdyne, a division of North American Rockwell Corporation, Canoga Park, California, CONFIDENTIAL.

7. AFRPL-TR-67-214, Advanced Thrust Chamber for Space Maneuvering Propulsion, Rocketdyne, a division of North American Rockwell Corporation, Canoga Park, California, 1 July 1967, CONFIDENTIAL.

8. R-6529, Investigation of Cooling Problems at High Chamber Pressures, Final Report, Rocketdyne, a division of North American Rockwell Corporation, Canoga Park, California, 15 September 1966. (U)

9. AFRPL-TR-66-147, Poppet and Seat Design Data for Aerospace Valve, Rocketdyne, a division of North American Rockwell Corporation, Canoga Park, California, July 1966. (U)

10. RPL-TDR-64-68, Rocket Engine Valve Poppet and Seal Design Data, Rocketdyne, a division of North American Rockwell Corporation, Canoga Park, California, May 1964. (U)

11. Miller, W. S., et al., Forced Convection Heat Transfer to Liquid Hydrogen at Supercritical Pressures, p. 5, Rocketdyne, a division of North American Rockwell Corporation, Canoga Park, California, 1965.

12. Kutateladze, S. S., Turbulent Boundary Layers in Compressible Gases, Academic Press Co., New York, N. Y., 1964.

13. Shapiro, A. H., The Dynamics and Thermodynamics of Compressible Fluid Flow, Vol. I, Ronald Press Co., New York, N. Y., 1953.

14. McCarthy, J. R., and H. Wolf, The Heat Transfer Characteristics of Gaseous Hydrogen and Helium, Research Report RR60, 12 December 1960.

APPENDIX A

The nozzle extension gas side surface heat transfer coefficient was calculated by the equation:

1a) $$\frac{h}{\rho V C_p} = St$$

where

2a) $$V = \frac{V}{V_{max}} V_{max} = \left(1 - \frac{1}{1 + \frac{\gamma - 1}{2} M^2}\right)^{.5} \left(2 g_c C_p T_{st}\right)^{.5}$$

3a) $$\rho C_p = \frac{\rho}{\rho_{max}} \frac{\rho_{max}}{\mu_{max}} \left(\frac{\mu C_p}{k}\right)_{max} k_{max} = \left(\frac{1}{1 + \frac{\gamma - 1}{2} M^2}\right)^{\frac{1}{\gamma - 1}} \frac{1}{\nu_{st}} P_{r_{st}} k_{st}$$

4a) $$ST = \Upsilon_{\Delta_2} \frac{E}{2} P_r^{-.75} \left(\frac{\mu}{\mu_{st}}\right)^m Re_{\Delta_2}^{-m}$$

where

V = Gas velocity --- (in/sec)

γ = Ratio of C_p/C_v --- (dimensionless)

C_p = Constant pressure specific heat --- (BTU/lbm-R)

C_v = Constant volume specific heat --- (BTU/lbm-R)

T = Temperature --- (^oR)

g_c = Gravitational constant --- (32.2 lbm-ft/lbf-sec^2)

ρ = Density --- (lbm/in^3)

μ = Viscosity --- (lbm/in-sec)

k = Thermal conductivity --- (BTU/in-sec-^oR)

ν = Kinematic viscosity = $\frac{\mu}{\rho}$ ---- $\frac{in^2}{sec}$

M = Mach number = $\frac{V}{a}$ --- (dimensionless)

a = Acoustic velocity --- (in/sec)

Pr = Prandtl No. = $\frac{C_p \mu}{k}$ --- (dimensionless)

St = Stanton Number --- (dimensionless)

Υ_{Δ_2} = Ratio of actual St to St

Calculated with Re_{Δ_2} and ignoring the effects of density variation, pressure gradient and mass transfer. --- (dimensionless)

Re_{Δ_2} = Reynolds Number based on enthalpy deficit thickness of boundary layer --- (dimensionless)

m = .25

E = .0256

Subscripts St and max refer respectively to stagnation and maximum.

Equation 1a) is the definition of Stanton number. Equation 2a) is obtained by combining the relation

4a) $$\frac{\rho}{\rho_{max}} = \left(1 - \left(\frac{V}{V_{max}}\right)^2\right)^{\frac{1}{\gamma - 1}}$$

(Equation 6.21 of reference d) with

5a) $$\frac{\rho_{st}}{\rho} = \left(1 + \frac{\gamma - 1}{2} M^2\right)^{\frac{1}{\gamma - 1}} = \frac{\rho_{max}}{\rho}$$

(Equation 4.14c of reference e)

Equation 3a) is obtained by substituting equation 5a) for ρ/ρ_{max}. The value of Re_{Δ_2} is gotten using Kutateladze's solution (Equation 5.73 reference d).

UNCLASSIFIED

Security Classification

DOCUMENT CONTROL DATA - R & D

(Security classification of title, body of abstract and indexing annotation must be entered when the overall report is classified)

1. ORIGINATING ACTIVITY (Corporate author) Rocketdyne, a Division of North American Rockwell Corporation, 6633 Canoga Avenue, Canoga Park, California 91304	2a. REPORT SECURITY CLASSIFICATION CONFIDENTIAL 2b. GROUP 4

3. REPORT TITLE

ADVANCED MANEUVERING PROPULSION TECHNOLOGY PROGRAM (Seventh Quarterly Progress Report)

4. DESCRIPTIVE NOTES (Type of report and inclusive dates)

Quarterly Progress Report, 1 May 1969 to 31 July 1969

5. AUTHOR(S) (First name, middle initial, last name)

6. REPORT DATE September 1969	7a. TOTAL NO. OF PAGES 160	7b. NO. OF REFS 14
8a. CONTRACT OR GRANT NO. F04611-67-C-0116 b. PROJECT NO. Part I, Item 1AB c. Sequence No. B008 of Exhibit B d.	9a. ORIGINATOR'S REPORT NUMBER(S) R-7380-7 9b. OTHER REPORT NO(S) (Any other numbers that may be assigned this report) AFRPL-TR-69-189	

10. DISTRIBUTION STATEMENT

Qualified users may obtain copies of this report from the Defense Documentation Center

11. SUPPLEMENTARY NOTES	12. SPONSORING MILITARY ACTIVITY AFRPL, Edwards, California

13. ABSTRACT

(U) The engine design and analysis task was continued with a detailed parametric analysis of thrust chamber temperature and pressure drop characteristics, the revision of the engine balance, and continued main oxidizer and turbine control valve design activity.

(U) The engine critical component task effort was primarily directed toward the completion of fabrication of the prototype channel-wall thrust chamber segment. Design of the main thrust chamber nozzle has been completed and design of the base closure and second engine nozzle simulator is nearing completion.

(U) Though testing of the main engine bearings and seals was initiated during the previous quarter, the effort was stopped temporarily because of operational problems and has been rescheduled to start September 1969.

(U) The basic analysis and design of the propellant feed system was completed during the previous quarter by both General Dynamics/Convair and Lockheed Missiles and Space Company.

UNCLASSIFIED
Security Classification

14 KEY WORDS	LINK A		LINK B		LINK C	
	ROLE	WT	ROLE	WT	ROLE	WT
Propellant System						
Advanced Engines						
System Performance						
Propellant Storage						

UNCLASSIFIED
Security Classification